Curved Amphipathic Oligothiophenes:

Curvature directed S.A. with applications in energy transfer systems and membrane curvature detection in living cells

Patrick Van Rijn

Curved Amphipathic Oligothiophenes:

Curvature directed S.A. with applications in energy transfer systems and membrane curvature detection in living cells

Proefschrift

ter verkrijging van de graad van doctor

aan de Technische Universiteit Delft,

op gezag van de Rector Magnificus Prof.ir. K.C.A.M. Luyben,

voorzitter van het College voor Promoties

in het openbaar te verdedigen op maandag 7 juni 2010 om 10.00 uur

door

Patrick Van Rijn

doctorandus in de scheikunde

geboren te Delfzijl

Dit proefschrift is goedgekeurd door de promotor:

Prof.dr. J.H. van Esch

Samenstelling promotiecommissie:

Rector Magnificus, Technische Universiteit Delft, voorzitter

Prof.dr. J.H. van Esch, Technische Universiteit Delft, promotor

Prof.dr. E.J.R. Sudhölter, Technische Universiteit Delft

Prof.dr. S.J. Picken, Technische Universiteit Delft

Prof.dr. L.D.A. Siebbeles, Technische Universiteit Delft

Prof.dr. B.J. Ravoo, Westfälische Wilhelms-Universität Münster

Dr. T.J. Savenije, Technische Universiteit Delft

Dr. E.A.J. Reits, Universiteit van Amsterdam

nait soez'n, deur broez'n......

Contents

Chapter 5

Amphiphilic conjugated thiophenes for self-assembling antenna systems in water

Chapter 6

Highly efficient Energy Transfer in water-soluble mixed aggregated oligothiophenes

Chapter 7

Photo-induced charge separation in self-assembled PCBM/amphipathic oligothiophene aggregates in water

Chapter 8

Amphipathic curved oligothiophenes as a tool for detecting membrane curvatures and imaging of membranes in living cells

Abbreviations

Chemicals

DMF	Dimethylformamide
DMSO	Dimethylsulphoxide
NBS	N-bromosuccinimide
THF	Tetrahydrofuran
DCM	Dichloromethane
EtOH	ethanol
MeOH	methanol
EtOAc	ethyl acetate
Et$_2$O	diethyl ether
PET	mixed petroleum fractions
TMS	trimethylsilyl
NR	Nile Red
TBAF	tetrabutylammonium fluoride
TPP	tetraphenylporphyrin
DOPC	*1,2*-Dioleoyl-*sn*-glycero-*3*-phosphocholine
DOPS	*1,2*-Dioleoyl-*sn*-glycero-*3*-phosphoserine
DMPC	*1,2*-Dimyristoyl-*sn*-glycero-*3*-phosphocholine

Technical terms

Cryo-TEM	Cryo-transmission electron microscopy
DLS	Dynamic Light Scattering
MALDI-ToF	Matrix-assisted laser desorption ionization time-of-flight
MS	Mass spectrometry
UV-Vis	Ultraviolet-visible
cmc	critical micelle concentration
cac	critical aggregation concentration
ITC	Isothermal Titration Calorimetry
l.m.w.	low molecular weight
S.A.	self-assembly
ET	energy transfer
FRET	Förster Resonance Energy Transfer
DSC	Differential Scanning Calorimetry
NMR	Nuclear Magnetic Resonance
APT	Attached Proton Test

Abbreviations

GPC	gel permeation chromatography
LC	liquid chromatography
ESI	electron spray impact
D	energy donor
A	energy acceptor

Physical symbols

R	molar gas constant
N_A	Avogadro number
P	packing parameter
λ	wavelength (nm)
ε	molar extincion coefficient (L mol^{-1}cm^{-1})
Φ_F	fluorescence quantum yield
τ	fluorescence lifetime (s)
φ	energy transfer efficiency
k_{ET}	rate constant for energy transfer (s^{-1})
k_{NR}	rate constant for non-radiative decay (s^{-1})
k_{LUM}	rate constant for luminescence decay (s^{-1})
k_{CT}	rate constant for charge transfer (s^{-1})
K_{SV}	association constant from Stern-Volmer (M^{-1})

Chapter 1
A more transparent molecular structure-aggregate shape approach: curved amphiphilic systems

1.1 Control of shape and size in nature

Nature acts as a source of inspiration for many fields of chemical research, including supramolecular chemistry[1] because it provides many systems with different scaling (cells, organelles, liposomes/micelles, proteins and DNA). These structures are formed by self-assembly of small molecular components or intra-molecular folding and are also able to control the spatial positioning of functional groups required for complex functions like catalysis, replication, energy storage etc.[2,3]

The control of size, spatial positioning and shape is directly correlated to the function.[3] The size is controlled over length scales ranging from 1 nm in small peptide fragments to 100 μm for the arrangement of living cells. Small amphiphilic molecules like bile acids are able to self-assemble into micellar structures based on hydrophobic interactions.[4] Due to a different molecular structures, phospholipids, also amphiphilic, are able to form bilayers (Figure 1).[3c] Proteins consist of a linear chain of covalently linked amino-acids, and the nature of the amino acid residues and the particular sequence dictate the overall shape with specific secondary structural features like helices and β-sheets (Figure 1) and allows for the formation of reactive sites inside the protein.[3b] Proteins are also found in multi-component self-assembled structures that are formed by templating e.g. in viral particles like the tobacco mosaic virus (TMV).[5] The structures mentioned here are in the order of 1-300 nm in size but extend well into the micrometer regime when looking at organelles and cells which consist of a complex mixture of entirely self-assembled (macro-)molecules (Figure 1).[3c] Especially the shape of organelles is quite

interesting. Most of them have a membrane with many different curvatures and since their dimensions are conserved over species, this conservation indicates that the shape is probably important for their function e.g. to aid in membrane budding, fission or fusion processes.[6] Since the main components of cell membranes are phospholipids which are amphiphiles, the aggregate morphology is based on its molecular structure. In cells, similar phospholipid membranes can display several different curvatures along the bilayer surface. For this curvature, proteins are used which influence the surface and directs the shape of the lipid membrane.[6]
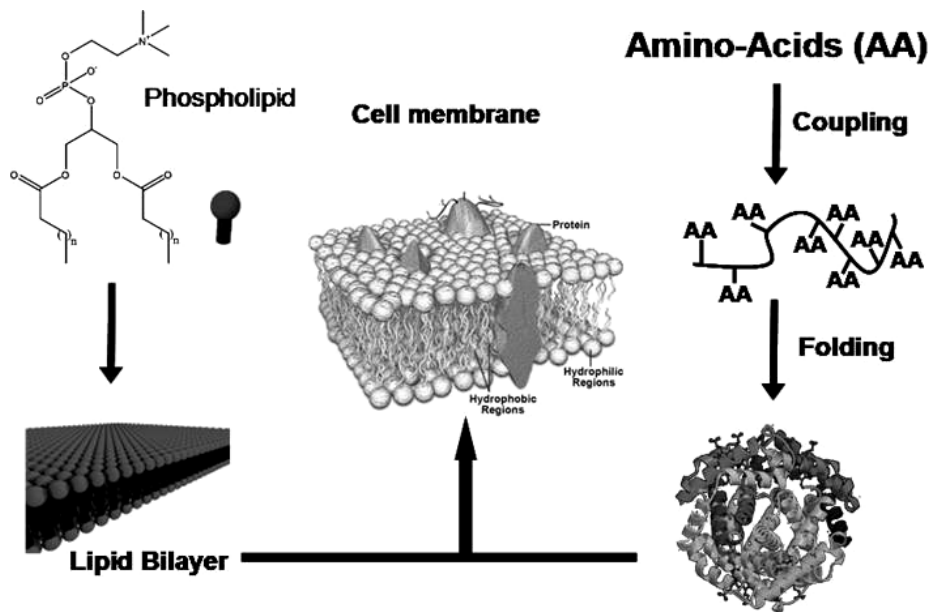

Figure 1: Phospholipids are able to form bilayers. Amino-acids can be connected via peptide bonds and are able to adopt functional secondary structures which form proteins. These combine in the cell membrane to form a highly complex, yet ordered structure.

1.2 The synthetic approach to control aggregate morphology and precise positioning of functional moieties

Mimicing the molecular assemblies and structural features seen in nature have been very successful up to a certain extend.[7] Molecular parameters which control the morphology of aggregates, composed of small molecules that interact by hydrophobic interactions, are the same in synthetic and natural systems. The molecular structure dictates the packing of amphiphiles inside the aggregate and induces the shape of the supramolecular assembly. A well-know theory describing the relation between molecular and aggregate structure is the structure-shape concept, as formulated by Israelachvili.[8] This theory correlates the relationship between the area of the hydrophilic head group and the volume and length of the aliphatic tail to the packing of the amphiphiles inside the aggregate which in turn relates to the curvature of the polar-apolar interface. Such a structure-shape relationship gives very useful insights in the behaviour of linear amphiphilic molecules and the supramolecular structures they form. However, the relationship between molecular structure (or molecular curvature) and the assembled structure is rather circumstantial and not well applicable to more complex systems. Therefore it would be an advantage to have a more direct relationship to predict the morphology or dimensions of a self-assembled structure.

To a certain extend this prediction can be made for covalently connected structural motifs like helices and sheets which have been synthetically prepared by relatively simple macromolecules *e.g.* foldamers.[9] However, to create more complicated systems, especially with a programmable design with respect to aggregate morphology and molecular orientation, a new approach in molecular design is necessary.

1.3 A new more transparent approach to address structure and shape

For utilisation of self-assembled systems, a more direct and transparent approach towards the relation between molecular structure and aggregate morphology needs to be developed. One such approach is by using curved amphiphiles, where the molecular curvature influences the shape instead of playing on the relative ratios between hydrophilic and hydrophobic groups on the amphiphile. These curved amphiphiles are expected to self-assemble like surfactants in which aggregate morphologies are dictated by the direct molecular curvature instead of the ratio of hydrophilic and hydrophobic groups. The curvature creation is achieved by using e.g. substituted 5-membered heterocyclic rings, fluorenes and basically any monomeric unit which creates a curvature (non-linear array) using reorientation of the side groups and is preferably conjugated along the backbone (Figure 2A).
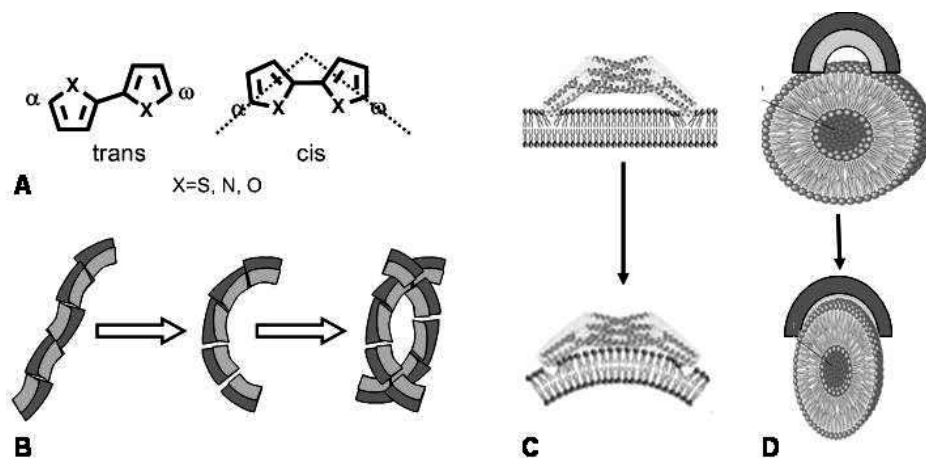

Figure 2: A) Aromatic 5-membered hetero-cycles which can adopt a curved conformation when in the cis-conformation. B) When designed as an amphiphile, it can aggregate based on hydrophobic effects. C and D represent a protein and a curved amphiphile, respectively depicting the possible interactions with lipid bilayers.

In an oligomeric array of *5*-membered rings, the *cis*-conformation provides a curved system. If the structure is designed like an amphiphile, then this structure will self-assemble in water in which the molecular curvature dictates the aggregate morphology (Figure 2B). A more clear relationship between molecular curvature and aggregate morphology allows for more efficient design of new materials with a high degree of control over its self-assembly properties and spatial arrangements of the molecules inside these aggregates.

Also we want to investigate if it is possible to utilise the molecular curvature for recognition of specific curved species e.g. curved molecules, small vesicles and other polar-apolar interfaces, as it is also found in nature with protein-membrane recognition and protein-protein interactions (Figure 2C and D). This allows for the creation of materials with not only programmable aggregation behaviour and aggregate morphology, but also containing new sensing capabilities.

1.4 Thesis outline

The different design elements needed and desired to create curved amphiphilic molecules will be discussed in **chapter 2** according to a literature survey. From a relative simple monomer design with minor variations, different self-assembling systems could be achieved based on an approach much like the structure-shape concept and gives a good idea about the behaviour of potentially interesting monomers which can be used to prepare curved oligomers and is presented in **chapter 3**. In order to express the curvature, the longer oligomers are synthesised and the dimer and tetramer are studied in **chapter 4** with respect to synthesis and aggregation behaviour. With extended knowledge about the aggregation behaviour of the different oligomers in water, interactions were investigated between the oligomers and various molecules and aggregates. This topic is divided into two sections: light harvesting systems and interaction with lipid bilayer surfaces. The thiophenes are electronically active and can be used in different ways e.g. in light-harvesting/antenna systems and will be discussed in **chapters 5, 6** and **7**. In the last

chapter (**8**) interactions with both synthetic lipid bilayers as well as biological ones (cells) were investigated. This thesis will end with a discussion and some concluding remarks on the developed systems.

1.5 References

1   I. W. Hamley, *Angew. Chem. Int. Ed.*, **2003**, *42*, 1692 –1712.
2   G. M. Whitesides and B. Grzybowski, *Science*, **2002**, *295*, 2418-2421.
3   a) I. W. Hamley and V. Castelletto, *Angew. Chem. Int. Ed.*, **2007**, *46*, 4442 – 4455; b) L. Stryer, *Biochemistry*, **1995**, *4th ed.*, W. H. Freeman and Company; c) B. Alberts, D. Bray, J. Lewis, M. Raff, K. Roberts and J. D. Watson, *Molecular Biology of the cell*, **1994**, *3rd ed.*, Garland Publishing, Inc.
4   A. F. Hofmann and A. Rods, *J. Lip. Research*, **1984**, *25*, 1477-1489.
5   R. W. Doms, R. A. Lamb, J. H. Rose and A. Helenius, *Virology*, **1993**, *193*, 545-562.
6   a) G. K. Voeltz and W. A. Prinz, *Nature Reviews Molecular Cell Biology*, **2007**, *8*, 258-264; b) C. A. Mannella, *Biochimica et Biophysica Acta*, **2006**, *1763*, 542–548; c) M. A. De Matteis and A. Godi, *Biochimica et Biophysica Acta*, **2004**, *1666*, 264– 274.
7   a) G. M. Whitesides, J. P. Mathias and C. T. Seto, *Science*, **1991**, *254*, 1312-1319; b) J.-M. Lehn, *Angew. Chem. Int. Ed.*, **1990**, *29*, 1304-1319.
8   J. Israelachvili, *Intermolecular & Surface Forces*, **1991**, *2nd ed.*, Academic Press.
9   a) R. Breslow and S. D. Dong, *Chem. Rev.*, **1998**, *98*, 1997-2011; b) D. J. Hill, M. J. Mio, R. B. Prince, T. S. Hughes and J. S. Moore, *Chem. Rev.*, **2001**, *101*, 3893-4011.

Chapter 2
Implemented structural designs: Amphipathicity, Foldamers and Conjugation

Abstract

In this chapter the basics of amphiphiles, amphipathic molecules, foldamers and water soluble conjugated oligomers and polymers will be discussed. These concepts are relevant to the design, aggregation behaviour and properties of the amphipathic conjugated oligothiophenes presented in this thesis.

2.1 Introduction

In this chapter a comprehensive introduction will be given about the various topics which form the foundation of the research described in this thesis. The chapter will start with a brief overview of the basic concepts of amphiphiles (2.2), and will then continue with an introduction on the less familiar amphipaths, an interesting class of amphiphilic molecules with distinct properties and a variety of important functions in nature (2.3). Many attempts have been made to mimic amphipaths and hence some examples of synthetic amphipaths will be given as well.

Finally two additional integrated topics in the research will be discussed. In paragraph 2.4 an overview of the properties, types, and applications of foldamers is given and in paragraph 2.5, conjugated water soluble polymers will be discussed.

2.2 Amphiphiles

Amphiphiles are an important class of molecules in both nature and technology as well as in everyday life. In nature, amphiphiles (phospholipids) are used to build the cell membranes, a supramolecular structure that consists of a double layer (or bilayer) of amphiphilic molecules that separate two aqueous environments from each other. The primary function of the lipid bilayer membrane is to keep the cell contents together and act as a semi-permeable barrier towards the environment (Figure 1A). In our everyday life amphiphiles are used as surfactants, detergents or emulsifiers in for instance soap, lotions, and creams (Figure 1B). The common function of these amphiphiles is to enable the dispersion of fatty substances like grease and oil in water, which are used to clean dishes, clothes and hands, but also to prepare emulsion sauces like mayonnaise. Amphiphiles like phospholipids and common surfactants have very different chemical structures, however the basic molecular architecture and the principle of how they work are the same.
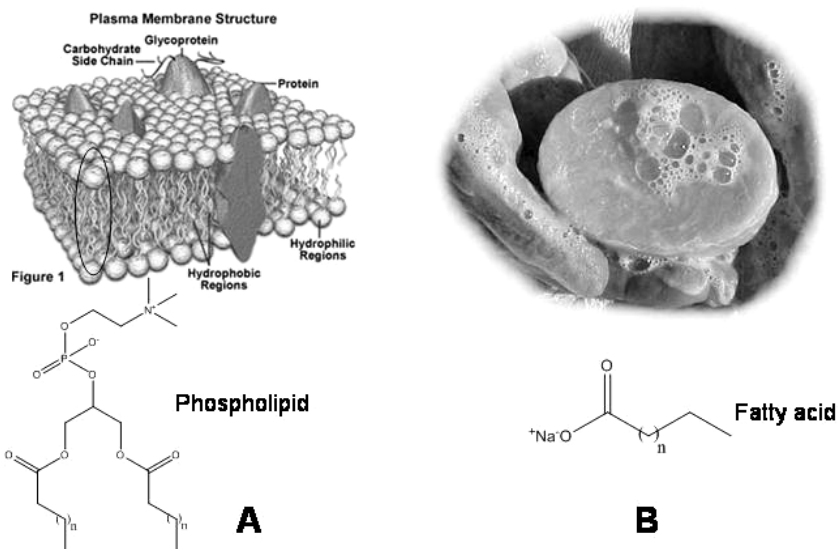
*Figure 1: **A)** Cell membrane composed of phospholipids that account for the bilayer formation separating the cell contents from the outside medium; **B)** a fatty acid in its alkaline form is the basic ingredient for many household detergents and soaps.*

Amphiphiles (*Amphi = on both sides*) are molecules that contain a hydrophilic and a hydrophobic group in the same molecule. In general, the hydrophilic group is a polar or even ionic group which is well soluble in water but poorly in apolar solvents, whereas the hydrophobic group is an apolar moiety which is poorly soluble in water due to the hydrophobic effect.[1] At higher concentrations the hydrophobic group and the water would phase separate, like oil and water. However, with amphiphiles such complete phase separation of the hydrophobic group is not possible as the covalently attached hydrophilic group prefers to reside in the aqueous phase. As a result, in water the amphiphile assembles into small aggregates, on which the hydrophobic groups form the interior, and the hydrophilic groups occupy the interfacial area between the aggregate and the aqueous phase, thereby minimising and maximising their exposure to the aqueous phase, respectively (Figure 2A). This aggregation process starts at a certain concentration which is called the critical micelle

concentration (cmc) (also known as critical aggregation concentration (cac) when the aggregate in question is not a micelle). Any molecules in excess of the cmc will take part in the aggregation process and therefore the molecularly dissolved (monomeric) amphiphile concentration will remain constant even at high concentrations. The concentration of monomeric amphiphiles and aggregates with increasing concentration is schematically drawn and shown in Figure 2A. At first the concentration of molecularly dissolved amphiphiles increases linearly with increasing total amphiphile concentration. At the cmc, this concentration remains constant and the concentration of aggregates starts to increase.

Aggregation in general increases the stability of the system. However, with surfactants this gained stability only with a limited number of molecules inside the aggregate due to the repulsion of the head group which is a destabilising factor. Because of this destabilisation, surfactant aggregates have a certain aggregation number at which the system is at its thermodynamic minimum. According to the pseudo-phase approximation, the chemical potential of monomers in aggregate and in solution at equilibrium is given by eq. **1** and can be expressed as the chemical potential difference between the monomers in aggregate and the monomers in solution, with the notation that the pseudo-phase approximation assumes that the concentration of monomer in the aggregate is 1. Here, R is the molar gas constant, T the temperature and it depends on the concentration of amphiphiles in solution [*Amph*]. The Gibbs free energy of the systems is given by eq. **2**.

$$\mu^{\theta}{}_{aggregate} = \mu^{\theta}{}_{solution} + RT \ln[Amph]_{solution} \qquad (\mathbf{1})$$

$$\Delta G^{\theta}{}_{aggregate} = \mu^{\theta}{}_{aggregate} - \mu^{\theta}{}_{solvent} = RT \ln[cmc] \qquad (\mathbf{2})$$

Considering the Gibbs free energy of the aggregates, which is favourable when largely negative, it becomes more negative with decreasing cmc. Therefore, a low

cmc yields a more thermodynamically stable aggregate with a high association constant resulting in a higher cooperativity. This overall relationship is known as the pseudo-phase model.[2]
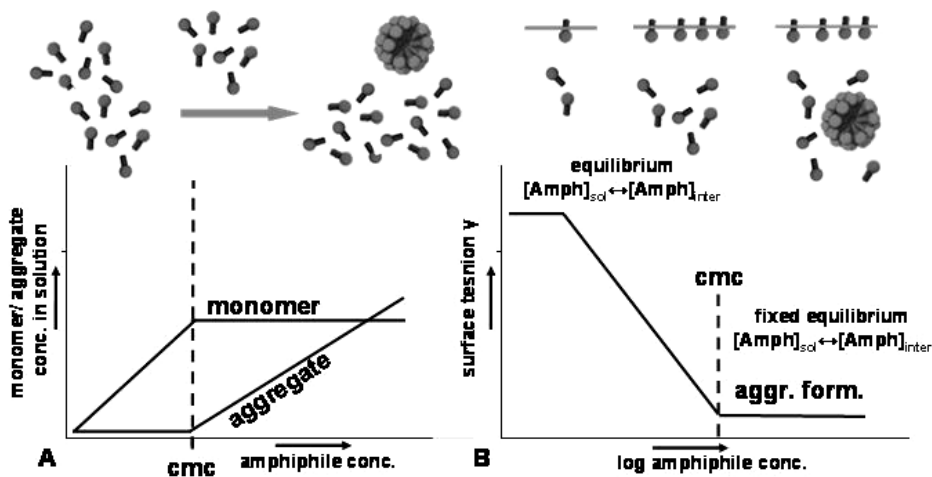
*Figure 2: **A)** Amphiphiles are molecularly dissolved up to a certain concentration. Any excess amphiphiles form aggregates with increasing concentration (at the cmc) at which the concentration molecularly dissolved amphiphiles remains constant. **B)** Changes in surface tension with increasing concentration. The concentration at the interface and bulk solution is always in equilibrium, changing the surface tension until the cmc is reached, then the concentration in the bulk remains the same and hence also the surface tension.*

The low aqueous solubility of the hydrophobic group also leads to the accumulation of amphiphiles at the water-air interface as well as at other interfaces between water and apolar phases. Also here the hydrophobic groups stick into the other phase whereas the hydrophilic groups occupy the aqueous side of the interface and are always in equilibrium. This equilibrium is described by the Gibbs adsorption isotherm which gives the free energy of transferring an amphiphile from solution to the surface.[2] Generally, it describes how the amphiphile concentrations in the bulk and at the interface, relate to each other. Changing the concentration in the bulk will affect the concentration at the surface.

This property is known as surface activity which is why amphiphiles are also named surfactants. Surface activity is measured in the form of surface tension. By assembly

of the amphiphiles on the surface, the surface tension (N/m) changes with increasing concentration since the bulk and the surface are in equilibrium with each other. When the cmc is reached, the amphiphile concentration in solution, as stated before, remains constant and so does the equilibrium between solution and interface as well, keeping the surface tension constant (Figure 2B).[2] This is a way to determine the cmc and is based on molecules directly influencing a measurable parameter. Other techniques that make use of such a parameter are Dynamic Light Scattering[3] (DLS), where the formation of aggregates changes the scattering behaviour of the incoming light, conductivity measurements for charged amphiphiles and fluorescence where formation of hydrophobic domains inside aggregates change the emission properties of a molecular probe[4]. Another way to determine the cmc is making use of enthalpy effects associated with the formation or break-up of aggregates and is used in Isothermal Titration Calorimetry (ITC).

Amphiphiles can contain hydrophilic groups ranging from sulfonates (anionic), quaternary amines (cationic), ethylene glycol groups (neutral) or zwitter-ionic groups in combination with various hydrophobic groups, usually aliphatic groups which differ in length, saturation and number of aliphatic chains (Figure 3A).[5] The morphology of the aggregates formed by amphiphiles depends on the molecular architecture of these amphiphiles.

Despite the large structural diversity, it has long been realised that in general amphiphiles with a single head group and a single chain tend to form micelles (Figure 3B). Upon changing the molecular structure towards two hydrophobic tails, the tendency is that bilayer structures are formed. In general such double chained amphiphiles have a lower cmc due to the larger hydrophobic groups. These lower cmc values indicate, as mentioned before, that the aggregates are more stable and that the association constants are higher. When even larger or more hydrophobic fragments are added, the amphiphiles precipitate in water. However, they are then likely to act as stabiliser in water-in-oil emulsions forming so called inverted

structures. The different morphologies that are obtained by amphiphiles in water are shown in Figure 3B.[6]
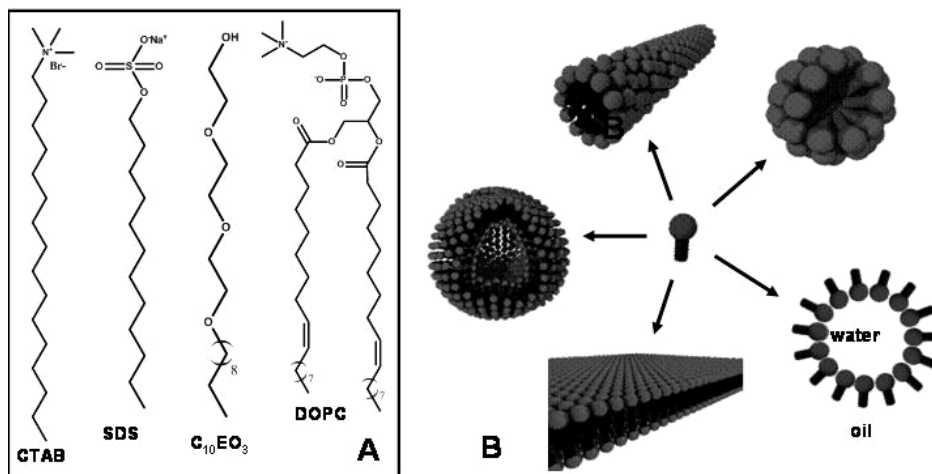
*Figure 3: **A)** Examples of different types of surfactants: cetyl trimethyl ammonium bromide (cationic), sodium dodecyl sulphate (anionic), triethylene glycol mono-n-decyl ether (neutral) and 1,2-Dioleoyl-sn-Glycero-3-phosphocholine (zwitterionic phospholipid). **B)** The different aggregate morphologies that surfactants can form depending on their molecular structure.*

The structures that are formed are dependent on different properties of the surfactant *i.e.* size and charge of the head-group, counter-ion, length and number of the aliphatic chains. These structural properties influence the molecular packing inside an aggregate and hence the overall morphology. In order to quantify such self-assembling systems, Israelachvili *et. al.* were successful in creating a general theory which describes the amphiphile structure/aggregate morphology relationship quite well. In this model the molecular structure was related to the packing parameter (P) which can be derived from the molecular structure according to eq. **3**:

$$P = \frac{V}{a_0 l_c} \qquad (3)$$

Here V is the volume of the hydrophobic segment, a_0 is the mean cross-section of the hydrophilic head group and l_C is the length of the aliphatic chain. The packing

parameter notes the shape of the molecules and as a rule the following values dictate the molecular structures to be: $P < 1/3$ cones; $1/3 < P < 1/2$ truncated cone; $1/2 < P < 1$ truncated cone and cylinders (spherical and lamellar) and for $P > 1$ inverted truncated. The different molecular structures dictate the aggregate morphology when in a closed packing to be spherical micelles (cone), elongated micelles (truncated cone), spherical and lamellar bilayers (truncated cone and cylinders) and inverted micelles (inverted truncated cone). The structure-shape model is applicable for many surfactant systems.

The structure-shape model uses a relatively simple method to describe the relationship between molecular structure and packing of the amphiphiles and relates that packing to aggregate morphology. However, the model is at best semi-quantitative because the parameters are affected by various conditions like temperature[7], molecular conformation, hydration and ionic strength of counter-ions[8] or aqueous media, making it difficult to know what the exact value for P and overall structures is. Other models described for amphiphilic assemblies do not relate the molecular structure with aggregate morphology or are a slightly more elaborate form of the model proposed by Israelachvili.[9,10] Preparing a system from which it is directly clear what kind of morphology will be formed with what kind of dimensions is to date not found. Some structures which are more elaborate and exotic behave in some cases as normal surfactants and others do not (Figure 4).[11] Even amphiphilic structures designed in a systematical fashion, as seen in Figure 4D,[12] lead to aggregate morphologies that are not expected beforehand by just looking at the molecular structure (they form *e.g.* helical elongated micelles).
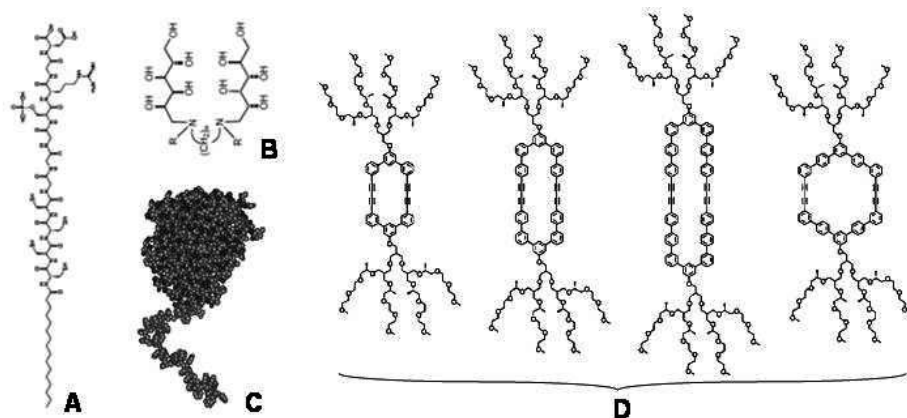
*Figure 4: Different exotic amphiphiles with; **A**) aliphatic tail with peptide head group; **B**) bola-amphiphile; **C**) a polymer hydrophobic segment attached to a protein head group and **D**) a circular aromatic moiety of various shapes and sizes with ethylene oxide head groups.*

2.3 Amphipathic Molecules

2.3.1 Amphiphilic vs. Amphipathic

A distinct class of amphiphilic molecules are amphipathic compounds which distinguish themselves from amphiphiles by the distribution of their hydrophobic and hydrophilic groups.[14] In "normal" amphiphiles the hydrophilic and hydrophobic groups are separated along the short molecular axis leading to the typical head-tail architecture (Figure 5A), but in amphipathic molecules the hydrophobic and hydrophilic segments are both located along the long axis of the molecule (Figure 5B). This leads to the typical amphipathic molecular structure with a distinct hydrophobic and a hydrophilic face, and therefore amphipathics are also referred to as *facial amphiphiles*.[13]
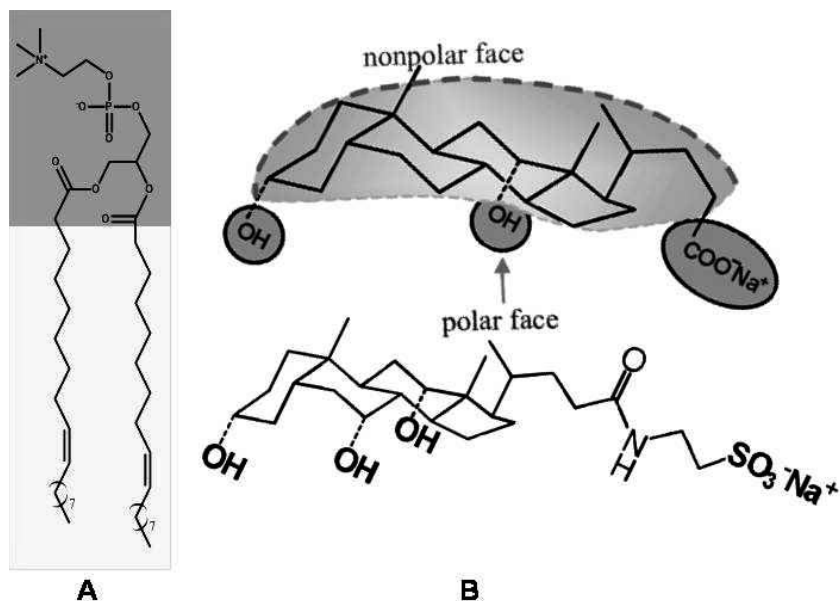
*Figure 5: **A)** Amphipathic molecule with distribution of hydrophobic and hydrophilic groups along the length axis of the molecule and **B)** showing a phospholipid with a head-tail distribution along the length axis of the molecule. The hydrophilic and hydrophobic segments are depicted light and dark grey, respectively.*

The distinct molecular architecture of amphipathic molecules led to different self-assembly behaviour but also to different functions.[16-18] For instance, in nature, amphipathic molecules are used to dissolve hydrophobic compounds. Moreover, they are also used as a bilayer penetrating structure, either to form trans-membrane channels or killing infected cells or alien cells like bacteria. Also amphipathic moieties are an important part of certain proteins which are responsible for reshaping membranes. Chemists are now seeing the potential of this class of compounds and are inspired to use these molecules in synthetic systems.

As the definition of this class of molecules is not always used in literature or named differently, several examples of amphipathic molecules will be described in the next section. Examples of how they are used in nature will be given but the main focus will be on the synthetic examples produced either by mimicking natural compounds or completely new structures with this amphipathic property.

2.3.2 Natural Amphipathic Compounds

<u>Amphipathic molecules</u>

One of the main functions of small amphipathic molecules in nature is to solubilise hydrophobic molecules by micellisation. Bile acids, steroid-type structures, for instance, are biologically the most important detergent-like molecules in many mammals. They are made in the liver by oxidation of cholesterol and are an important component in bile.[14] After the bile is released into the small intestines, the main function of the bile acids is dissolving fatty acids and assisting in the transport and digestion of triglycerides.[15] These amphipathic molecules are based on the flat and rigid steroid skeleton, of which one face has become hydrophilic due to the presence of three hydroxyl groups (Figure 6).[16]
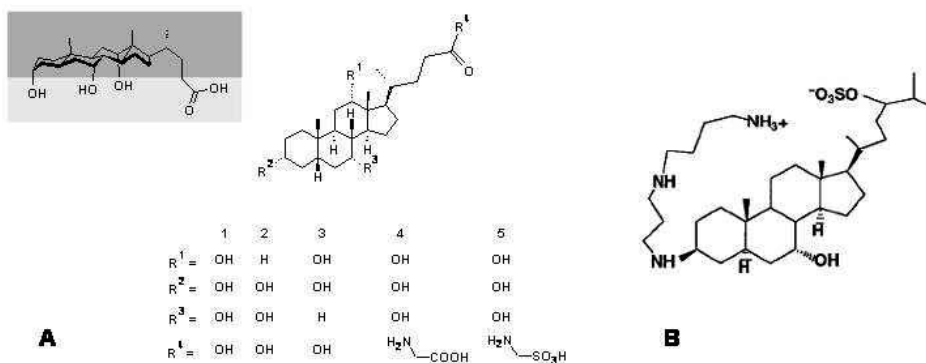
Figure 6: Structure of amphipathic cholic acids with its hydrophobic and hydrophilic face depicted dark and light grey, respectively. (b) Various natural bile acid derivatives 1 cholic acid, 2 chenodeoxycholic acid, 3 deoxycholic acid, 4 glycocholic acid, 5 taurocholic acid.

One of the cholic acid derivatives is named squalamine and it has two hydrophilic tails which fold over one face of the steroid-structure, making it amphipathic (Figure 6B). Squalamine is known to be a natural antibiotic because it interacts efficiently with cell membranes, leading to openings in the membrane and thereby killing it.[17]

Several squalamine derivatives have been synthesised to enhance its antibiotic properties, for instance by exchanging the positions of the polyamine and sulfonate groups on the steroid moiety[18] or by reducing the length of the alkyl sulfonate chain.[19] Both derivatives display greater antibacterial activities compared to squalamine. Over the years numerous new semi-synthetic antibiotics have been prepared as cholic acid derivatives,[20,21,22] but also molecules like porphyrins have been used.[23]

<u>Amphipathic Peptides</u>

Another important class of naturally occurring amphipaths consists of peptides, which obtain their amphipathic character from folding of the peptide into either an *α*-helix or *β*-sheet with a hydrophilic and a hydrophobic face. Many amphipathic peptides act as antibiotics. For example, natural antibiotics based on amphipathic *α*-helices are cecropins[24] and magainins[25] and antibiotic *β*-sheets are gramicidin S, polymyxin B and the tyrocidines.[26]

Folding of a linear peptide strand into its secondary structure such as an *α*-helix or *β*-sheet can result in an amphipathic molecule with the *α*-helical structure stabilised by hydrogen bonding. The helix has 3.6 residues per turn and therefore residue 1 and 19 are on the same position (5 turns per repeating cycle). The rest of the residues are located in different quadrants (Figure 7A) of which 5, 9, 12 and 16 are in the first quadrant, 2, 6 13, 17 in the second quadrant, 3, 7, 14, 18 in the third quadrant and 4, 8, 11, 15 in the fourth quadrant. When hydrophilic or hydrophobic amino acid residues are placed appropriately along the backbone of the helix, one side (quadrant or several quadrants) of the helix will become hydrophilic or hydrophobic, respectively, and the resulting *α*-helical peptide strand will be amphipathic (Figure 7A/B). The relation between primary structure and interfacial properties of the *α*-helix is more easily seen in a helical wheel representation (Figure 7B). An example of a natural amphipathic *α*-helix is the 23 sequence peptide magainin 2.[27] In this natural antibiotic the hydrophobic regions are formed by the hydrophobic amino

acids phenyl alanine (F), alanin (A), leucine (L), isoleucine (I), glycine (G), methionine (M) and valine (V). The hydrophilic amino-acids in magainin 2 are serine (S), lysine (K), glutamic acid (E), asparagines (N) and histidine (H). The positions of the amino-acids in the strand make one face hydrophilic and the other hydrophobic, giving it the amphipathic structure which in turn gives Magainin 2 its antibiotic properties.
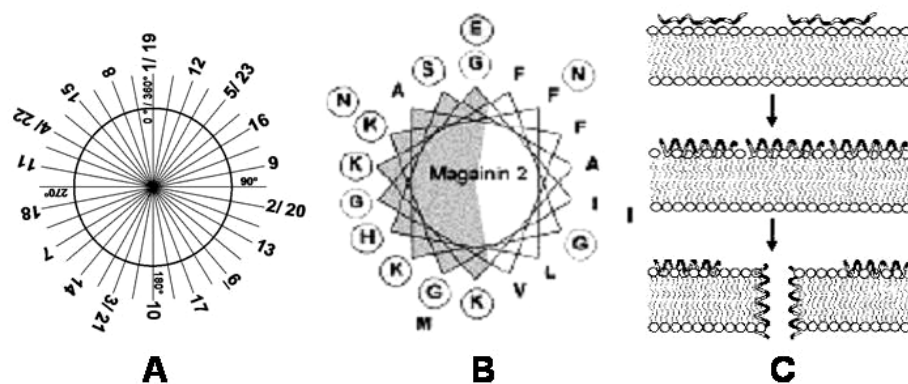
*Figure 7: **A)** The position of the amino-acid related to the position inside the sequence when folded into a helical shape with 3.6 amino-acids per turn. **B)** Helical wheel presentation of magainin 2; due to the amino-acid sequence the α-helix becomes an amphipathic structure. **C)** A schematic representation of a proposed mechanism of bilayer penetration by an amphipathic helical structure.*

These antibiotic properties come from its ability to penetrate the cell membrane. In Figure 7C a simplified representation is given of how an antibiotic like magainin 2, disturbs a membrane in such a way that the contents of the cell flow out of it. First adsorption of the strand onto the surface of the membrane takes place before the folded structure interacts with the membrane by insertion of the hydrophobic part into the hydrophobic region of the membrane. When enough amphipathic structures have accumulated, a small channel is formed which is stabilised by the long elongated hydrophobic domains of the amphipathic helix while the hydrophilic domains are in contact with the polar medium.[27]

The amphipathic structures are not only used as antibiotics but also play a role in other biological functions and the amphipathic structures are then an integrated part of a protein. Proteins, like for instance amphiphysin and endophilin-A1 (shape-altering proteins), are able to deform lipid bilayers in a very elegant manner.[35] Such a shape-altering protein contains two domains consisting of amphipathic helices. The amphipathic domains are positioned under an angle and when interacting with a lamellar lipid bilayer (Figure 8A) the membrane is directed in a curvature due to the overall curved structure of the protein.[28,29] Organelles like the mitochondria, lysosomes etc. take their shape because of these proteins.[30,31]
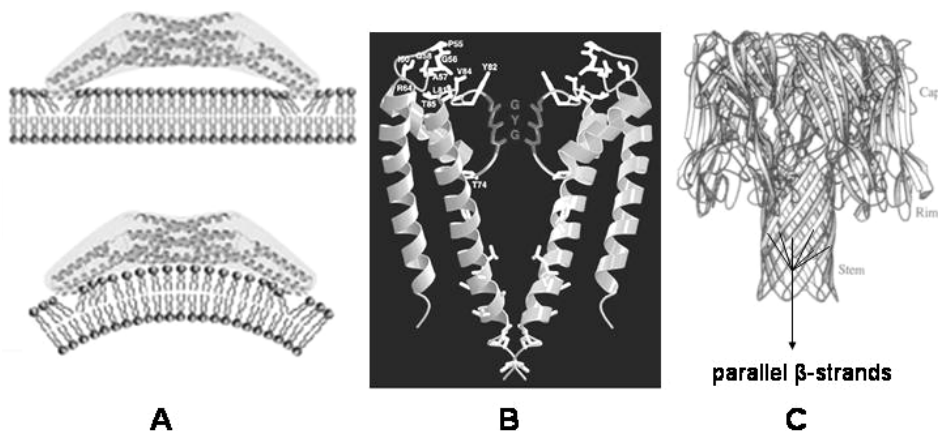
Figure 8: ***A)*** *A protein containing two amphipathic helices interacts with a bilayer and the curved overall structure of the protein forces a change in bilayer shape.* ***B)*** *α-type channel proteins of a potassium channel from Streptomyces lividans.* ***C)*** *A heptameric structure of α-HL composed of β-strands forming a cap (top of the pore), a rim (which interacts with phospholipids and receptors) and the stem (the actual pore that spans the membrane).*

Amphipathic helices are also found as part of trans-membrane pores like ion-channels and are used to stabilise the channel.[32] There are five different types of trans-membrane channels.[33] Of these types, the most relevant based on a helical structure are the *α*-type channel proteins; they form channels that cross the

membrane lined by α-helices which are amphipathic (Figure 8B). These are found in the cytoplasmic membranes of prokaryotes and eukaryotes, as well as in the eukaryotic organelle membranes.

The α-type channel proteins are particular useful in transporting ionic species and they are very specific[34] because of a delicate interplay of electrostatic repulsive and attractive forces. This was seen in the potassium channel from *Streptomyces lividans*.

Amphipathic β-strands are also known to form channels across membranes and are named β-barrels.[35] They are found in the outer membranes of chloroplasts, mitochondria and Gram-negative bacteria. In β-barrels all the hydrophobic parts are embedded in the membrane interior and the hydrophilic regions point into the pore interior.[36] In Figure 8C an example is shown how a pore is formed from β-strands.

It is clear that amphipathic molecules play an important part in biological systems. This is one of the reasons that chemists take interest in these types of molecules. Synthetic amphipathic molecules are discussed in the following paragraph.

2.3.3 Synthetic Amphipathic Compounds

The main focus of researchers on amphipathic molecules in natural systems has been set on exploration of their uses, structures and mechanisms. However, inspired by nature, researchers have also used amphipathic molecules for the creation of novel molecular- and nano-structures and for application as antibiotics.

Synthetic Molecules

Both low molecular weight (l.m.w.) amphipathic molecules and amphipathic α-helices have been synthetically prepared in order to develop new antibiotics and self-assembling systems.

L.m.w. amphipathic molecules self-assemble in a surfactant-like manner, which means that supramolecular structures (mostly micelles), based on hydrophobic

interactions, are being formed. However, by designing new types of l.m.w. amphipathic molecules, these architectures were extended and new interesting self-assembled structures were discovered.

One of the first groups of synthetic amphipathic compounds are based on the natural bile acid cholic acid, which has been synthetically modified with for instance quaternary amines[37], sugars[38], carboxylates[39], amines[40], amino acids[41] and sulfonates.[42] Various morphologies were obtained depending on the substitution. Highly ordered sheets[43] or fibers are examples of these structures.[44,45]

One interesting non-natural example of an amphipathic building block is based on a rigid-flexible macro-cycle. Amphipathicity is induced by the hydrophobic and rigid poly-aromatic domain and the flexible oligo(ethylene glycol) segment (Figure 9). In absence of a solvent these macro-cycles tend to aggregate forming highly ordered bilayers with the rigid hydrophobic aromatic domains in the core due to π-π stacking.[46] In aqueous solution these macromolecules assemble into a bilayer strap. This bilayer in turn folds into a helix, giving a novel helical tubular structure with a hydrophilic interior and exterior (Figure 9).[47]
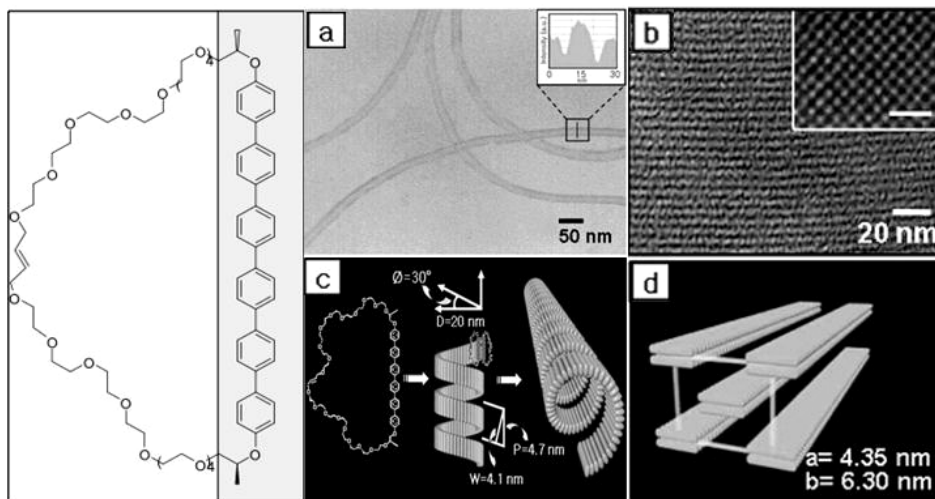
Figure 9: Rigid-flexible macrocycle assemble in well-defined structures like (a/c) tubular structures and (b/d) lamellar structures.

Not only the construction of self-assembling systems with the use of amphipathic molecules, but also the preparation of new medicines is a popular topic. Bacteriochlorins, which contain a central porphyrin-moiety, are envisioned to be attractive candidates for photodynamic therapy (PDT). Porphyrins have similar rigidity as the choline ring-system and with specific substitution on the different sides with hydrophilic and hydrophobic groups, amphiphilic and amphipathic properties have been introduced. The amphipathic properties increase interactions with membranes and together with the photo-physical properties of the porphyrins they could be of interest in PDT.[24]

The general trend is that l.m.w. amphipathic compounds form aggregates similar to architectures formed by common amphiphiles only with lower aggregation numbers due to the larger hydrophilic and hydrophobic surface area. Next to that also novel architectures are formed not seen with conventional surfactants.

Amphipathic Oligo- and Polymers

So far only inter-molecular self-assembling of discretely sized molecules has been discussed. In the case of amphipathic oligo- and polymers, aggregation has been found to take place both intra- and inter-molecular (folding and aggregation, respectively). Generally the structure and conformation of polymers are less predictable than in the case of l.m.w. molecules.

An example of an amphipathic system which assembles intra- and inter-molecularly is given by McCullough *et. al.*[48] These amphipathic regio-regular polythiophenes consist of alternating substituted thiophenes with a hydrophilic ethylene glycol and a hydrophobic alkyl chain (Figure 10). This polymer is build from an amphiphilic *bis*-thiophene. In a good solvent the polymer takes a random conformation, whereas between a hydrophilic and hydrophobic phase at the interface, the side chains orient and create an amphipathic structure. This in turn self-assembles inter-molecularly

into crystalline monolayers at the air-water interface due to both hydrophobic interactions as well as π-π interactions between the thiophene moieties.
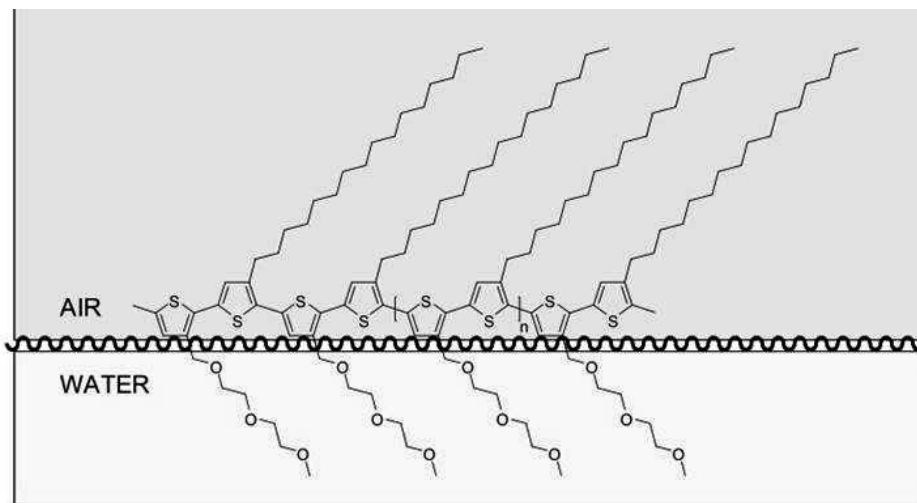
Figure 10: Amphipathic poly-thiophenes pack into highly ordered monolayers at water-air interfaces.

Another system also based on rigidity is the oligo-phenylene ethynylenes designed by Moore. The original design was meant to create a foldamer which folds into a helical structure due to solvophobic effects (*also see 2.4*).[49]
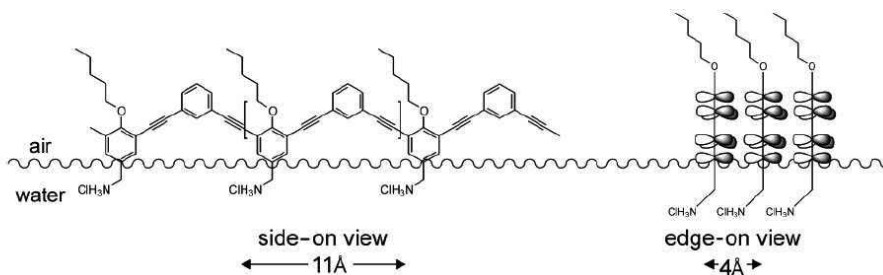
Figure 11: Due to hydrophobic interactions and π-π-stacking oligo meta-phenylene ethynylenes form ordered structures at a water-air interface.

Here every phenyl was substituted with a hydrophilic group and, when dissolved in a polar solvent, they orientate outward. However, when the substitution pattern was slightly modified by placing a hydrophobic and hydrophilic group opposite of each

other on the phenyl, it was found that a linear amphipathic structure was obtained (Figure 11). These amphipaths were found to stabilise oil-water emulsions and self-assemble in aqueous solution to form ordered layers.[50] Next to that, these amphipaths were found to be highly organised at water-air interfaces, due to patterning of the hydrophobic and hydrophilic segments and π-π-stacking.[51]

Polymers and oligomers, as displayed here, self-assemble at an interface. This interfacial activity is one of the reasons why previously discussed examples from natural systems display high antimicrobial activity. The idea that some of these compounds display similar characteristics and properties is quite well imaginable and indeed antimicrobial activity was also found for oligomers based on the meta-phenylene ethynylenes[52,53] as well as many other systems.[54,55,56,57,58]

Dendrimers are a special kind of polymers with well defined globular structures making them ideal candidates for supramolecular chemistry.[59] There are numerous examples of amphiphilic dendrimers giving rise to various architectures upon self-assembly and which are promising for creating functional materials.[60]

In case of amphipathic dendrimers, the amphipathicity is not always obvious. In the following case for instance, the amphipathicity is induced when the dendrimer is placed in an aqueous solution (Figure 12A) and it was found that it self-assembles into micellar aggregates of 10–40 nm in diameter.[61]

Another example is a 'star'-polymer created by Genson *et.al.* (Figure 12B).[62] These dendrimers with alternating hydrophobic/hydrophilic arms do not appear amphipathic at all. At the air-water interface, the arms show micro-phase separation: the hydrophobic arms directing into the air and the hydrophilic arms into the water. As a consequence the polymer becomes amphipathic and forms an ordered monolaye*r*.

The previous examples illustrate that amphipathic dendrimers, due to their globular structure, tend to aggregate in spherical and elongated micelles or form monolayers at air/water interfaces and, even if it is not obvious at first, in solution the system

redirects in such a way that the hydrophobic interactions are maximised and as a whole it becomes amphipathic.
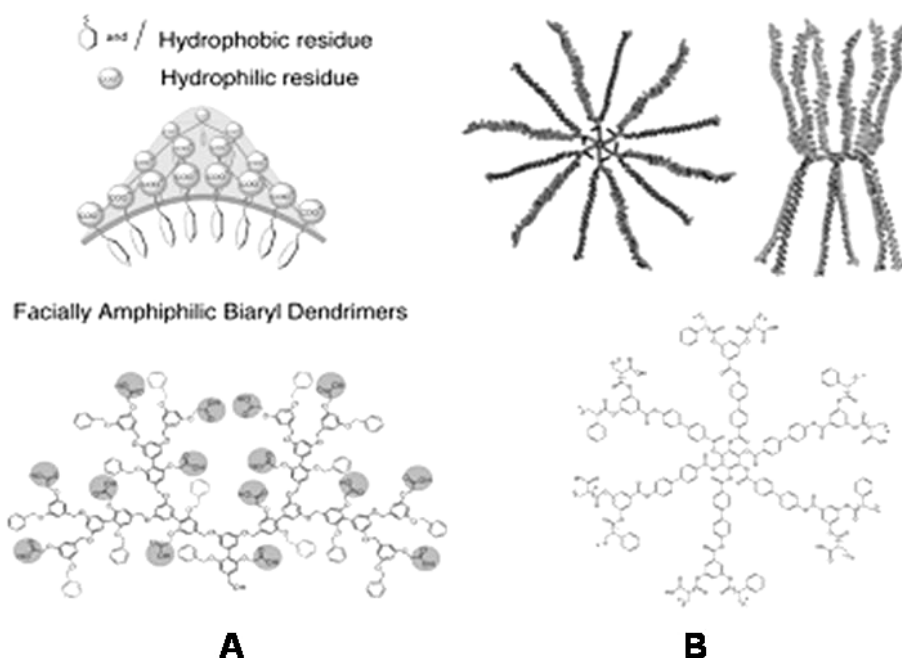
*Figure 12: **A**) Molecular structure of a dendrimer described by Thayumanavan et. al. (bottom). Amphipathicity of the molecule becomes clear in aqueous solution (top). **B**) Molecular structure of a dendrimer with alternating hydrophobic/ hydrophilic arms (bottom), which forms two dimensional structures at water/air interfaces (top).*

Polymer chains in the form of non-natural poly-peptides, which upon folding form amphipathic *α*-helices (relevant examples of *β*-sheets not found), are also known. This was found to occur either with a non-natural sequencing of natural amino-acids or by using non-natural amino-acids. The use of amino-acids makes it possible to rely on the intra-molecular H-bonding for their folding properties.

In 2005 Chmielewski and co-workers developed an amphipathic helix, based on a poly-proline scaffold which, as a result of hydrogen bonding, folds in a helix spontaneously with three residues per turn. By functionalising these residues with

hydrophobic and hydrophilic side chains an amphipathic helix was obtained (Figure 13A).[63] To visualise the cell penetrating effect, the helices were functionalised with a fluorescein group. According to circular dichroism, both functionalisations have little effect on the helical structure of the polyproline scaffold. Non-amphipathic poly-proline helices where also synthesised as a control experiment and showed little uptake in breast cancer cells (MCF-7) whereas amphipathic helices show uptake in these cells by fluorescence microscopy.
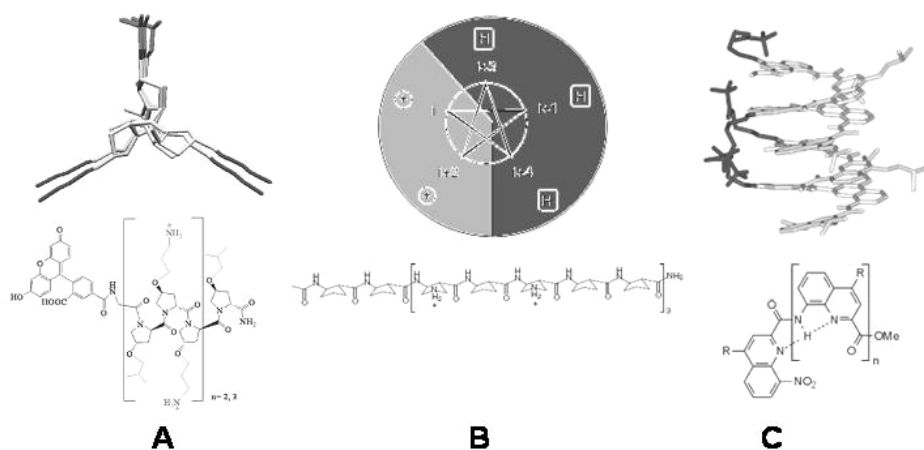
*Figure 13: **A)** Sequence of polyproline backbone, which, upon self-assembly, forms an amphipathic helix **B)** a β-amino acid oligomer forming a helical structure and **C)** quinoline based amino acid helical amphipathic structure.*

Instead of α-amino acids, for creation of synthetic amphipathic α-helices, also β-amino acids have been used. These are in general less susceptible for attack and destruction by proteins. This reduced destruction is convenient when used in the body for possible medicinal applications.[64,65] The helix has five residues per two turns, for the first and the third residue of the helix hydrophilic amono-acids were used and for the others hydrophobic ones. Upon folding the peptide structure creates an amphipathic helical structure (Figure 13B).

Also non-natural aromatic amino-acids were used, like the group of Huc did. By using a quinoline based amino acid (Figure 13C); the folding behaviour is better visualised because of the sensitivity of the conjugated moieties towards changing environments like folding and aggregation.[66]

Many different strategies have been followed and substitution patterns varied, not even to mention the many different types of functionalities that have been introduced. Whether based on *β*-amino acids[67] or with sulfide[68] and crown-ether[69] functionalities added, the numerous variations make this approach of using polymers, very powerful for finding new applications and medicinal active agents.

2.4 Foldamers

2.4.1 Introduction

Surfactant systems give well defined discrete sized structures, based on inter-molecular interactions. A well defined shape and size can also result from intra-molecular interactions, as is applied in the field of foldamers. This field is one of the cornerstones of the research shown in this thesis. Nature is also a source of inspiration for foldamers. Natural systems like DNA and proteins of all sorts get their ability of data storage and catalytic- and responsive behaviour from the precise *3*-dimensional structure which is obtained by precise positioning and folding of base-pairs (DNA/RNA) and amino-acids (proteins). The design and synthesis of new macromolecules with defined size, structure, and behaviour will help to understand how structures in nature are formed but will also lead to new materials. One approach to new macromolecules with well defined structure and function is the design and synthesis of foldamers, *i.e.* oligomers build from structurally defined monomers that fold in a conformational defined ordered state in solution.[70] These states are stabilised by non-covalent interaction between non-adjacent monomer units or by bulk-solvent. The forces that play a role are hydrogen bonding,[71,72]

ionic/molecular-interactions,[73,74,] hydrophobicity/hydrophilicity,[68] steric restrictions/favourable conformations[75] and π-π stacking.[68] Often combinations of multiple forces contribute to the folding process. Some examples of possible folding motives are shown in Figure 14.
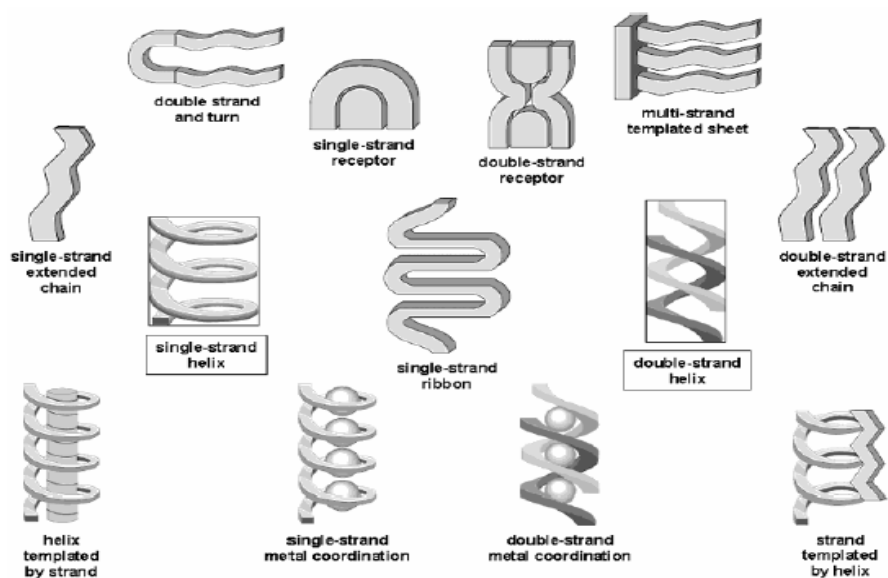
Figure 14: Different folding motives of foldamers.

Foldamers give various structures like sheet-like structures, ribbons and helices. In the original idea of the research presented in this thesis, the helix plays an important role, and therefore this discussion on foldamers is primarily focussing on helices.

For designing helical structures one or more of the previously mentioned forces are used to stabilise the folded structure. This thermodynamically stable situation is vital in the folding process and cooperativity is an important factor in reaching this situation. Folding is interplay between entropy and enthalpy. A folded state **F** must have a lower Gibb's free energy than an unfolded state **U**. Folding thermodynamics is controlled by two main factors. The unfolded state must lose the *conformational entropy* present in **U** in order to realise the *enthalpic gain* present in **F**. The initiation (nucleation) of folding is not favourable because the loss of entropy is not yet

balanced by the gain in enthalpy. However, when the first turn is formed, the propagation, which is a cooperative process, will make the enthalpy gain more favourable than the unfavourable loss of entropy.[68] So the better the cooperativity, the better the structure will fold, only when the cooperativity is too high, then the structure will only fold once before it remains permanent in its folded conformation. Usually the initiation of folding uses a different force (e.g. solvophobic effects) than the one that is used for the propagation of folding (the stabilising force *e.g.* hydrogen bonding, ionic interactions, preferable conformations but also bulk solvent).

The overview given in the next few paragraphs is mostly limited to the solvophobically driven systems in combination with π-π stacking (with a few exceptions) because these systems are most related to the topic in this thesis. For a complete overview on foldamers the reader is referred to ref. 68 as a general review and to the other references given above.

2.4.2 Foldamers by solvophobic/solvophilic effects in combination with π-π stacking and/or hydrogen bonding

The design of many foldamers is, just like the design of the compounds in this thesis, based on unfavourable solvent interactions. When a monomeric unit of a foldamer is designed more or less like an amphiphile, it is expected that similar driving forces for aggregation (be it inter- or intra-molecular) play a role. As mentioned in paragraph **2.2**, hydrophobic and hydrophilic interactions are able to orient molecules at the polar/apolar interface. This orientation also occurs when the molecules/amphiphiles are covalently connected.

The best known and most frequently used foldamer is the *m*-phenylene ethynylene based foldamer (Figure 15) which was also briefly discussed in **2.3.3**.[76] This is a *meta*-substituted phenyl and each phenyl is connected via an ethynylene-unit. On the other *meta*-position different groups have been be attached, tetraethylene glycol chains, but also amine-functionalities and aliphatic chains have been reported.[77]
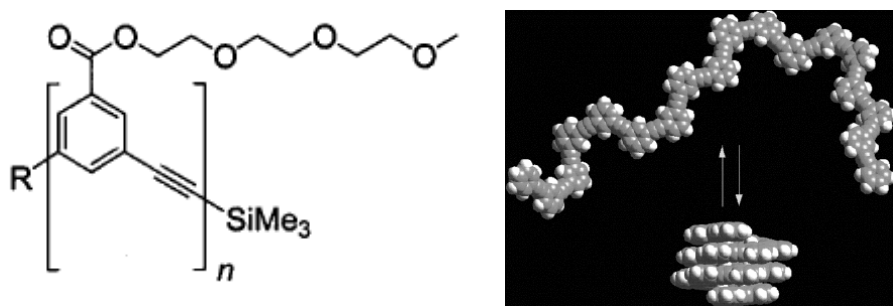
Figure 15: A phenylene-ethynylene-based foldamer that transforms from a random coiled state into a defined structure dependent on bulk solvent.

The folding of this system is very well defined. The angle of a *meta*-substituted phenyl has an internal angle of 120°. This means that six monomers are needed to create one turn and that phenyl-*7* is placed directly on top of the first. The overall folded structure was altered with respect to the diameter by replacing the ethynylene-spacer for a single bond.[78] In order to change the number of monomers per turn, the *ortho*-substituted compound was prepared which resulted in an internal angle of 60° and therefore only three monomers per turn were necessary.[79]

Responsiveness to external stimuli was introduced by adding hetero-atoms into the backbone or onto the side-chains, which can coordinate to different ions or interact with complementary guests (Figure 16).[80] Another possibility is to introduce elements in the backbone that induce conformational changes for instance by introducing azo-groups in order to obtain photo-chromism.[81]

One possible application of these foldamers is as a reactive sieving agent. A sieving system was prepared by using phenylene-ethynylenes which where differently modified at both ends of the foldamer with different sized groups in order to make the entrance of the cavity of the foldamer different in size and also the phenyl moiety in the middle of the strand was exchanged for a pyridine as the reactive site. By introducing different methyl sulfonates of different shapes and sizes, the pyridine nitrogen was methylated and the rate of methylation differed with shape and size of the methyl sulfonate that was introduced.[82] Similar reactive sieving sites are known

to be present also in enzymes.[83] Though the foldamer sieves are not nearly as good as the sieving cavities found in the enzymes.
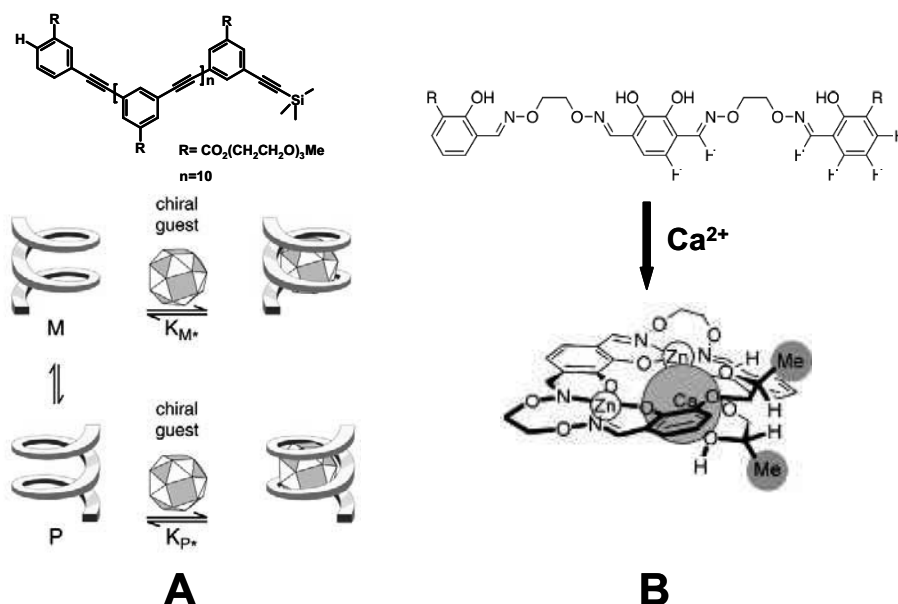
*Figure 16: Foldamers as host for molecules and ions; **A**) phenylene-ethynylene-based foldamer that is able to host different chiral hydrophobic species which dictate the chiral twist of the helix and **B**) a foldamer that wraps around a metal-ion in which induces the folding.*

The examples given so far are all single helical strands. However, there are also examples of in nature of double stranded (DNA) and triple stranded (collagen) helical structures. Several synthetic multi-stranded structures have been prepared, only these structures were not stabilised by solvophobic effects but rather by hydrogen bonding. It was shown that synthetic oligo-peptide strands also are able to form multi-stranded architectures by intertwining of single strands. This intertwining occurs because the main strand extends like a spring and the loss of energy associated with it is compensated by direct non-covalent inter-chain interactions (Figure 17A).[84] Also other foldamer structures have been made with various

structural properties like double handedness in a single strand[85] and even changing the direction of the folded structure by 90º due to coordination of two strands to a central metal-ion[86]. Even though these structures are quite sophisticated already, it remains a challenge to make more complex variations and introduce responsiveness.
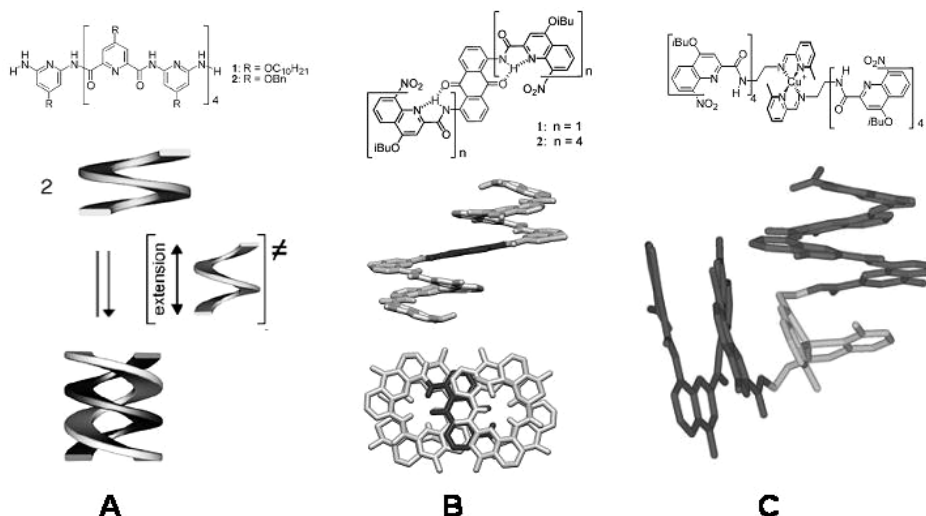
Figure 17: Peptide-based foldamers which undergo an exchange between single stranded to double (A) two types of helical handedness are introduced in a single strand (B) due to a coordination of two helical strands a continuous structure emerges of which the direction is changed by a deviation of about 90º (C).

2.5 Water soluble conjugated polymers

2.5.1 Introduction

Conjugated polymers are chains which consist of an alternating sequence of single and double bonds throughout the length of the chain, making it possible for charges created in the line of conjugation to be delocalised along the polymer giving it conducting properties. Some examples are poly-*p*-phenylene, poly-*p*-phenylenevinylene, polythiophenes, polypyrroles and polyfluorene which have very interesting electronic and spectroscopic properties. Hence, they are very well suited

for organic electronic devices like solar cells, Light Emitting Diodes, Field Effect Transistors and other photovoltaic devices. (Figure 18).[87]
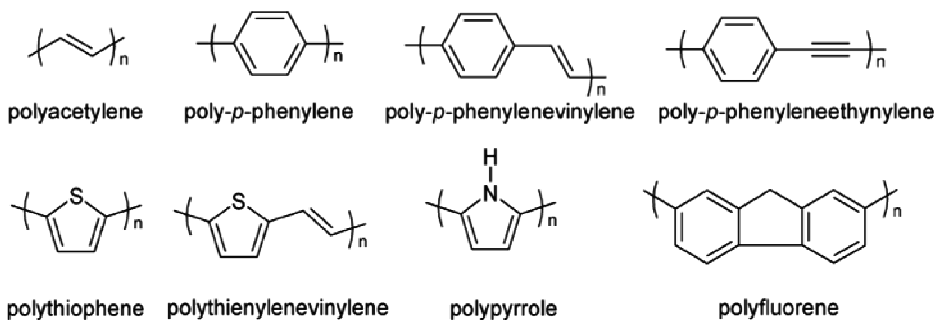
Figure 18: Examples of conjugated polymers that are available and used in molecular electronics.

It is not possible to review all conjugated polymers because it is a too extensive topic. In this section only a short overview is given of water soluble conjugated polymers. For a more complete overview the reader is referred to the reviews mentioned in ref. 89.[88]

2.5.2 Water soluble conjugated polymers

Conjugated systems are very popular because of their favourable electronic and photo-physical properties. The photo-physical properties of conjugated polymers are very sensitive to both external stimuli (temperature, interacting species, light etc.) as well as internal changes (aggregation, alignment etc.), which is also reflected in the conductive properties. This responsiveness makes them ideal for sensing and/or visualisation of biological species, relevant ions or specific domains in aqueous systems. In order to use them in such a way, they have to be water soluble.

The polymers displayed in Figure 18 have all been made water soluble by introduction of polar groups on the polymerisable monomeric unit. For polar groups, positively charged quaternary amines, neutral ethylene glycol groups and also

negatively charged deprotonated carboxylic acids or sulfonates have been used (Figure 19).[89]
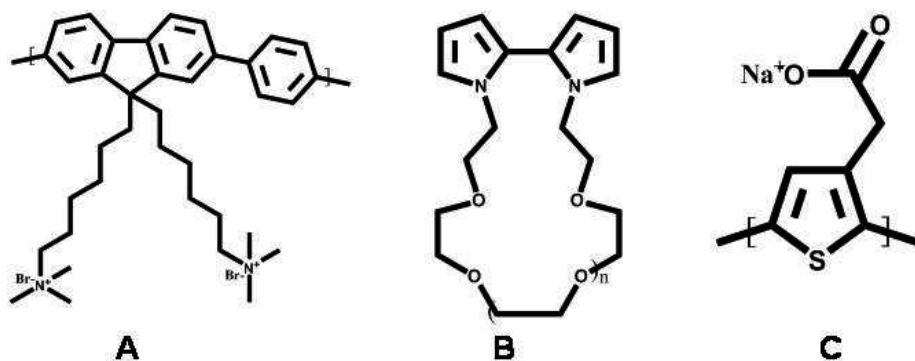
Figure 19: Monomeric species that were used for preparing water soluble conjugated polymers with A) a cationic fluorine-based polymer; B) neutral pyrrole-based polymer with crown-ethers and C) anionic deprotonated carboxylic polythiophenes based polymer.

Water soluble conjugated polymers have quite different properties than conjugated polymers in organic solvents or in the non-solute state and two aspects should be taken into account: firstly, behaviour of the polymer in water with respect to internal configuration (folding and orientation) as well as possible aggregation and secondly the photo-physical properties. The photo-physical properties are influenced not only by changes in solvent polarity but also the functional groups attached to the backbone become different in water. These changes affect the photo-physical properties of the polymer due to direct electronic interaction like electron-donation or –withdrawal which is associated by a change in colour.

The sensitivity of polymer properties in aqueous systems to changes in the environment has been exploited for the construction of sensors. Several responsive systems have been produced over the years. In the beginning mostly by playing with pH and ions that are present in the system *e.g.* by protonation of amines, deprotonation of carboxylic acids and using ion-binding groups as crown-ethers.[90] Over the last few years a trend is seen from these relatively simple detectable species

towards more elaborate structures. More bio-applicable methods are being developed and even though the previously mentioned examples are in some way also related to bio-applications, more sophisticated systems are now emerging. Detection of bio-anions like amino-acids is extended towards more complex species as for instance enzymes/proteins, DNA and even certain cells. [91,92] Detection of bio-macromolecules was achieved both on chips as well as in solution and concentrations as low as 10^{-11} moles have been detected by using zwitter-ionic polythiophenes.[93]
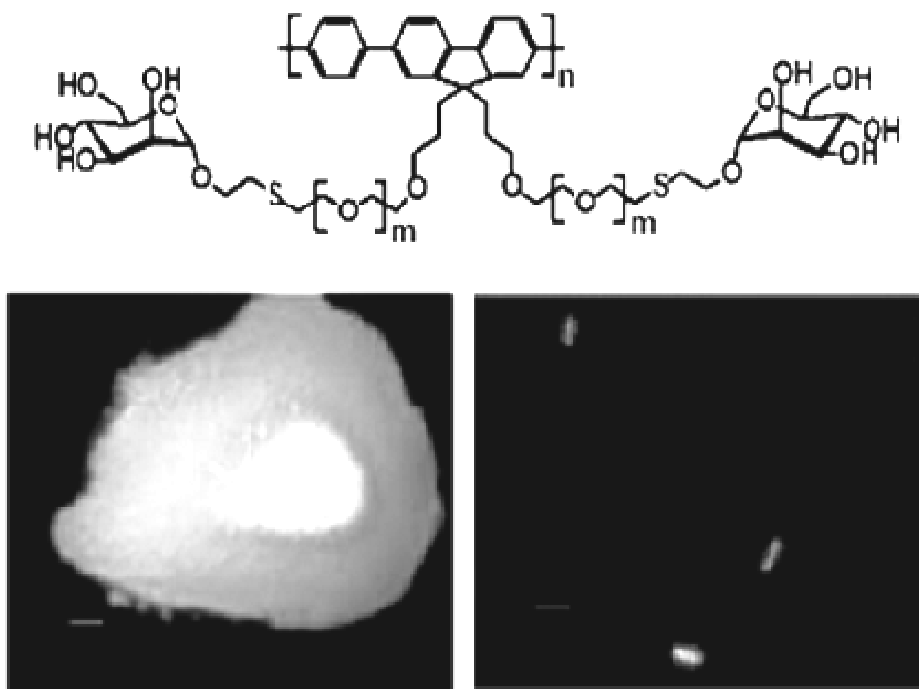
Figure 20: A) E. Coli stained with the glycol-polymer seen above.

The water soluble (and in some case water insoluble) conjugated polymers are not only important candidates for bio-sensing, but also for bio-imaging. Since the polymers were modified with a variety of functional groups they interact with

specific types of cells. The cell was then visualised by fluorescence microscopy (Figure 20).[94]

Interesting systems, as seen in Figure 20A, are still relatively unexplored compared to the small apolar molecular fluorescent probes which already produce usable and commercially available devices. However, more specificity is introduced using polymers because more variety and number of interacting groups are able to be introduced.

2.6 Conclusion

There are many different approaches which were applied towards the formation of well-defined structures and architectures. Inter-molecular self-assembly or intra-molecular folding as mentioned for amphiphiles and foldamers, respectively, are examples of these approaches. Also the addition of functions to structures is important if it is ever to be used as responsive structures for drug-delivery, bio-sensors and other applications. This responsiveness was added by introducing functional groups that are sensitive to changes of pH, ions or bulk-solvent. When used in sensors, it is important to have a good and reliable read-out. It is of no use to build a sensor if there is no way to read the changes. Therefore, conjugated molecules/polymers are very attractive, as they possess electronical and photo-physical properties. These could potentially be used to detect changes with cyclo-voltametry (CV) or fluorescence which is a convenient way to design a sensor.

The trend in current research is to cross the boundaries from one discipline to the other and combine these disciplines. This is important for new innovative research. However, in order to be able to do that, it is even more important to take a closer look at the molecules that are used for this type of research. When the appropriate molecules are not present which display properties required for different disciplines in chemistry, biology and physics, it will be much harder to cross over and combine the different disciplines. Therefore, a new type of molecular structure was designed

of which was anticipated to have novel structural properties and aggregation behaviour with a strong link to biological systems.

2.7 References

1   a) N. T. Southall, K. A. Dill and A. D. J. Haymet, *J. Phys. Chem. B*, **2002**, *106*, 521-533; b) D. Chandler, *Nature*, **2005**, *437*, 640-647.

2   D. F. Evans and H. Wennerström, *The colloidal domain*, **1999**, Wiley-VCH, *2nd ed.*.

3   P. Atkins and J. De Paula, *Atkins' Physical Chemistry*, **2006**, Oxford, *8th ed.*.

4   Bernard Valeur, *Molecular Fluorescence: Principles and Applications*, **2001**, Wiley-VCH Verlag GmbH.

5   a) M. Frindi, B. Michels, H. Levy and R. Zana, *Langmuir*, **1994**, *10*, 1140-1145; b) K. L. Herrington, E. W. Kaler, D. D. Miller, J. A. Zasadzinski and Shivkumar Chiruvolu, *J. Phys. Chem.*, **1993**, *97*, 13792-13802; c) W. Brown, R. Johnsen, P. Stilbs and B. Lindman, *J. Phys. Chem.*, **1903**, *87*, 4548-4553.

6   a) F. M. Menger, *Acc. Chem Res.*, **1979**, *12*, 111-117; b) F. M. Menger and C. A. Littau, *J. Am. Chem. Soc.*, **1993**, *115*, 10083-10090; c) R. Zana, *J. Coll. Int. Sci.*, **2002**, *248*, 203-220; d) J. N. Israelachvili, D. J. Mitchell and B. W. Ninham, *J. Chem. Soc. Faraday Trans.*, **1976**, *72*, 1525-1568; e) M. P. Pileni, *J. Phys. Chem.*, **1993**, *97*, 6961-6973.

7   G. Briganti, S. Puvvada and D. Blankschtein, *J. Phys. Chem.*, **1991**, *95*, 8989-8995.

8   Y. Marcus, *Biophys. Chem.*, **1994**, *51*, 111-127.

9   a) A. Bhattacharya, S. D. Mahanti and A. Chakrabarti, *J. Chem. Phys.*, **1998**, *108*, 10281-10293; b) A. Bhattacharya and S. D. Mahanti, *J. Phys.: Condens. Matter*, **2001**, *13*, 1413–1428; c) S. Puvvada and D. Blankschtein, *J. Phys. Chem.*, **1992**, *96*, 5567-5579; d) P. Fromherz, *Chem. Phys. Let.*, **1981**, *77*, 460-466; e) M. A. Floriano, E. Caponetti and A. Z. Panagiotopoulos, *Langmuir*, **1999**, *15*, 3143-3151.

10   R. Nagarajan and E. Ruckenstein, *Langmuir*, **1991**, *7*, 2934-2969.

11   a) A. P. Nowak, V. Breedveld, L. Pakstis, B. Ozbas, D. J. Pine, D. Pochan and T. J. Deming, *Nature*, **2002**, 424-428; b) J. A. A. W. Elemans, A. E. Rowan and R. J. M. Nolte, *J. Mater. Chem.*, **2003**, *13*, 2661-2670; c) A. T. J. Dirks, R. J. M. Nolte and J. J. L. M. Cornelissen, *Adv. Mater.*, **2008**, *20*, 3953-3957; d) D. E. Discher and A. Eisenberg, *Science*, **2002**, *9*, 967-973.

12   J.-K. Kim, E. Lee, M.-C. Kim, E. Sim and M. Lee, *J. Am. Chem. Soc.*, **2009**, *131*, 17768-17770.

13   S. Walker, M. J. Sofia, R. Kakarla, N. A. Kogan, L. Wierichs, C. B. Longley, K. Bruker, H. R. Axelrod, S. Midha, S. Babu and D. Kahne, *Proc. Natl. Acad. Sci. USA*, **1996**, *93*, 1585-1590.

14   D. W. Russel and K. D. R. Setchell, *Biorev.*, **1992**, *31*, 4737-4749.

15   E. Ros, *Artherosclerosis*, **2000**, 357 - 359.

16   A. Coelle, F. Meijide, E. R. Nunez and J. V. Tato, *J. Pharm. Sci.*, **1995**, *85*, 9-15.

17   M. Vaara, *Microbiol. Rev.*, **1992**, *56*, 395-411.

18   K. Kikuchi, E. M. Bernard, A. Sadownik, S. L. Regen and D. Armstrong, *Antimicrob. Agents and Chemotherapy*, **1997**, *41*, 1433-1438.

19   H. S. Kim, B. S. Choi, K. C. Kwon, S. O. Lee, H. J. Kwak and C. H. Lee, *Bioorg. Med. Chem.*, **2000**, *8*, 2059-2065.

20   a) K. M. Bhattarai, V. del Amo, G. Magro, A. L. Sisson, J. -B. Joos, J. P. H. Charmant, A. Kantacha and A. P. Davis, *Chem. Commun.*, **2006**, 2335-2337; b) S. N. Khan, N. -J. Cho and H. -S. Kim, *Tetrahedron. Lett.*, **2007**, *48*, 5189-5192.

21   C. Li, M. R. Lewis and P. B. Savage, *Antimicrob. Agents and Chemotherapy.*, **1999**, *43*, 1433 - 1439.

22   Q. Guan, E. J. Schmidt, S. R. Boswell, C. Li, G. W. Allman and P. B. Savage, *Org. Lett.*, **2000**, *2*, 2837-2840.

23   a) C. Ruzié, M. Krayer, T. Balasubramanian and J. S. Lindsey, *J. Org. Chem.*, **2008**, *73*, 5806-5820; b) D. K. Dogutan, M. Ptaszek and J. S. Lindsey, *J. Org. Chem.*, **2008**, *73*, 6187-6201.

24   H. Steiner, D. Hultmark, A. Engstrom, H. Bennich and H.G. Boman, *Nature*, **1981**, *292*, 246-248.

25   M. Zasloff, *Proc. Natl. Acad. Sci. USA*, **1972**, *84*, 549-5453.

26 a) G. F. Gause and M. G. Brazhnikova, *Nature*, **1944**, *154*, 703-703; b) L. S. Cardoso, M. I. Araujo, A. M. Góes, L. G. Pacífico, R. R. Oliveira and S. C. Oliveira, *Microb. Cell Fact.*, **2007**,   6:1 doi:10.1186/1475-2859-6-1; c) M. Zasloff, *Nature*, **2002**, *415*, 389-395.

27 A. Tossi, L. Sandri and A. Giangaspero, *Pept. Sci.*, **2000**, *55*, 4-30.

28 A. Zemel, A. Ben-Shaul and S. May, *J. Phys. Chem.*, **2008**, *112*, 6988-6996.

29 M. Masuda, S. Takeda, M. Sone, T. Ohki, H. Mori, Y. Kamioka and N. Mochizuki, *EMBO J.*, **2006**, *25*, 2889-2897.

30 G. K. Voeltz and W. A. Prinz, *Nat. Rev. Mol. Cell Biol.*, **2007**, *8*, 258-264.

31 G. A. Perkins and T. G. Frey, *Micron*, **2000**, *31*, 97-111.

32 a) J. R. Schnell and J. J. Chou, *Nature*, **2008**, *451*, 591-595; b) M. H. Saier Jr., *J. Membr. Biol.*, **2000**, *175*, 165-180.

33 Y. Pouny, D. Rapaport, A. Mor, P. Nicolas and Y. Shai, *Biochemistry*, **1992**, *31*, 12416 - 12423.

34 D. A. Doyle, J. M. Cabral, R. A. Pfuetzer, A. Kuo, J. M. Gulbis, S. L. Cohen, B. T. Chait and R. MacKinnon, *Science*, **1998**, *280*, 69-77.

35 K. S. Rotondi and L. M. Gierasch, *Pept. Sci.*, **2005**, *84*, 13-22.

36 H. Sakai and T. Tsukihara, *J. Biochem.*, **1998**, *124*, 1051-1059.

37 H. M. Willemen, L. C. P. M. de Smet, A. Koudijs, M. C. A. Stuart, I. G. A. M. Heikamp-de Jong, A.T.M. Marcelis and E.J.R. Sudhölter, *Angew. Chem. Int. Ed.*, **2002**, *41*, 4275-4277.

38 Y. Chen, D. M. Ho, C. R. Gottlieb, D. Kahne and M. A. Bruck, *J. Am. Chem. Soc.*, **1992**, *114*, 7319-7320.

39 U. Taotafa, D. B. McMullin, S. C. Lee, L. D. Hansen and P. B. Savage, *Org. Lett.*, **2000**, *2*, 4117-4120.

40 P. B. Savage, *Eur. J. Org. Chem.*, **2002**, 759-768.

41 H. M. Willemen, T. Vermonden, A. Koudijs, A. T. M. Marcelis and E. J. R. Sudhölter, *Coll. Surf. A: Phys. Chem. Eng. Aspects.*, **2003**, *218*, 59-64.

42 Z. Zhong, J. Yan and Y. Zhao, *Langmuir*, **2005**, *21*, 6235-6239.

43 Y. Hishikawa, R. Watanabe, K. Sada and M. Miyata, *Chirality*, **1998**, *10*, 600-618.

44 H. M. Willemen, T. Vermonden, A. T. M. Marcelis and E. J. R. Südholter, *Eur. J. Org. Chem.*, **2001**, 2329-2335.

45 H. M. Willemen, T. Vermonden, A. T. M. Marcelis and E. J. R. Südholter, *Langmuir*, **2002**, *18*, 7102-7106.

46 W-Y. Yang, J-H. Ahn, Y-S. Yoo, N-K. Oh and M. Lee, *Nat. Mater.*, **2005**, *4*, 399-402.

47 W-Y. Yang, E. Lee and M. Lee, *J. Am. Chem. Soc.*, **2006**, *128*, 3484-3485.

48 N. Reitzel, D. R. Greve, K. Kjaer, P. B. Howes, M. Jayaraman, S. Savoy, R. D. McCullough, J. T. McDevitt and T. Bjørnholm, *J. Am. Chem. Soc.*, **2000**, *122*, 5788-5800.

49 D. J. Hill, M. J. Mio, R. B. Prince, T. S. Hughes and J. S. Moore, *Chem. Rev.*, **2001**, *101*, 3893-4011.

50 R. B. Breitenkamp, L. Arnt and G. N. Tew, *Adv. Tech.*, **2005**, *16*, 189-194.

51 L. Arnt and G. N. Tew, *Langmuir*, **2003**, *19*, 2404-2408.

52 L. Arnt, K. Nüsslein and G. N. Tew, *J. Polym. Sci. Part A: Polym. Chem.*, **2004**, *42*, 3860-3864.

53 G. N. Tew, D. Clements, H. Tang, L. Arnt and R. W. Scott, *Biochimica Biophyica. Acta*, **2006**, *1758*, 1387-1392.

54 J. L. Thomas, H. You and D. A. Tirrell, *J. Am. Chem. Soc.*, **1995**, *117*, 2949-2950.

55 G. N. Tew, D. Liu, B. Chen, R. J. Doerksen, J. Kaplan, P. J. Carrol, M. L. Klein and W. F. DeGrado, *Proc. Natl. Acad. Sci. USA*, **2002**, *99*, 5110-5114.

56 D. Liu, S. Choi, B. Chen, R. J. Doerksen, D. J. Clements, J. D. Winkler, M. L. Klein and W. F. DeGrado, *Angew. Chem. Int. Ed.*, **2004**, *43*, 1158 - 1162.

57 H. Tang, T. J. Doerksen, T. V. Jones, M. L. Klein and G. N. Tew, *Chem. Biol.*, **2006**, *13*, 427-435

58 H. Tang, R. J. Doerksen and G. N. Tew, *Chem. Commun.*, **2005**, 1537-1539.

59 O. A. Matthews, A. N. Shipway and J. F. Stoddart, *Prog. Polym. Sci.*, **1998**, *23*, l-56.

60 a) F. Vögtle, S. Gestermann, R. Hesse, H. Schwierz and B. Windisch, *Prog. Polym. Sci.,* **2000**, 25, 987-1041; b) C. C. Lee, J. A. MacKay, J. M. J. Fréchet and F. C. Szoka, *Nat. Biotechol.*, **2005**, *23*, 1517-1526.

61 A. Klaikherd, B. S. Sandanaraj, D. R. Vutukuri and S. Thayumanavan, *J. Am. Chem. Soc.*, **2006**, *128*, 9231-9237.

62 K. L. Genson, J. Hoffman, J. Teng, E. R. Zubarev, D. Vaknin and V. V. Tsukruk, *Langmuir*, **2004**, *20*, 9044-9052.

63 Y. A. Fillon, J. P. Anderson and J. Chmielewski, *J. Am. Chem. Soc.*, **2005**, *127*, 11798-11803.

64 T. Hintermann and D. Seebach, *Chimia*, **1997**, *51*, 244-247.

65 E. A. Porter, X. Wang, H. S. Lee, B. Weisblum and S. H. Gellman, *Nature*, **2000**, *404*, 565.

66 a) V. Maurizot, C. Dolain, Y. Leydet, J. -M. Léger, P. Guionneau and I. Huc, *J. Am. Chem. Soc.*, **2004**, *126*, 10049-10052; b) E. R. Gillies, C. Dolain, J. -M. Léger and I. Huc, *J. Org. Chem.*, **2006**, *71*, 7931-7939.

67 Y. Hamuro, J. P. Schneider and W. F. DeGrado, *J. Am. Chem. Soc.*, **1999**, *121*, 12200-12201.

68 H. -S. Ahn, W. Cho, J. -M. Kim, B. P. Joshi, J. -W. Park, C. R. Lohani, H. Cho and K. -H. Lee, *Bioorg. Med. Chem.*, **2008**, *16*, 4127-4137.

69 P. -L. Boudreault and N. Voyer, *Org. Biomol. Chem.*, **2007**, *5*, 1459-1465.

70 D. J. Hill, M. J. Mio, R. B. Prince, T. S. Hughes and J. S. Moore, *Chem. Rev.*, **2001**, *101*, 3893-4011.

71 a) A. Dutta, S. Kar, M. G. B. Drew, P. Koley and A. Pramanik, *J. Mol. Struct.*, **2009**, *917*, 110-116; b) T. Koga, M. Higuchi, T. Kinoshita and N. Higashi, *Chem. Eur. J.*, **2006**, *12*, 1360-1367; c) W. Cai, G.-T. Wang, P. Du, R.-X. Wang, X.-K. Jiang and Z.-T. Li, *J. Am. Chem. Soc.*, **2008**, *130*, 13450-13459; d) C. Bao, B. Kauffmann, Q. Gan, K. Srinivas, H. Jiang and I. Huc, *Angew. Chem. Int. Ed.*, **2008**, *47*, 4153-4156; e) I. Huc, *Eur. J. Org. Chem.*, **2004**, 17-29; f) J. J. van Gorp, J. A. J. M. Vekemans and E. W. Meijer, *Chem. Commun.*, **2004**, 60-61; g) I. Saraogi, C. D. Incarvito and A. D. Hamilton, *Angew. Chem. Int. Ed.*, **2008**, *47*, 9691 -9694;

72 a) S. J. Wezenberg, G. A. Metselaar, A. E. Rowan, J. J. L. M. Cornelissen, D. Seebach and R. J. M. Nolte, *Chem. Eur. J.*, **2006**, *12*, 2778-2786; b) V. Maurizot, C. Dolain, Y. Leydet, J.-M. Léger, P. Guionneau and I. Huc, *J. Am. Chem. Soc.*, **2004**, *126*, 10049-10052; c) W. Cai, G.-T. Wang, Y.-X. Xu, X.-K. Jiang and Z.-T. Li, *J. Am. Chem. Soc.*, **2008**, *130*, 6936-6937; d) E. Berni, J. Garric, C. Lamit, B. Kauffmann, J.-M. Léger and I. Huc, *Chem. Commun.*, **2008**, 1968-1970; e) E. R. Gillies, F. Deiss, C. Staedel, J.-M. Schmitter and I. Huc, *Angew. Chem. Int. Ed.*, **2007**, *46*, 4081-4084; f) H. Goto, Y. Furusho and E. Yashima, *Chem. Commun.*, **2009**, 1650-1652.

73 a) K. Uemura, Y. Kumamoto and S. Kitagawa, *Chem. Eur. J.*, **2008**, *14*, 9565-9576; b) H.-J. Kim, E. Lee, H.-S. Park and M. Lee, *J. Am. Chem. Soc.*, **2007**, *129*, 10994-10995; c) M. T. Stone and J. S. Moore, *J. Am. Chem. Soc.*, **2005**, *127*, 5928-5935; d) H. Abe, N. Masuda, M. Waki, and M. Inouye, *J. Am. Chem. Soc.*, **2005**, *127*, 16189-16196.

74 a) R. M. Meudtner and S. Hecht, *Macromol. Rapid Commun.*, **2008**, *29*, 347-351; b) A. Petitjean, L. A. Cuccia, M. Schmutz, and J.-M. Lehn, *J. Org. Chem.*, **2008**, *73*, 2481-2495; c) S. Akine, T. Taniguchi and T. Nabeshima, *Tetrahedron Lett.*, **2006**, *47*, 8419-8422; d) T. Maeda, Y. Furusho, S.-I. Sakurai, J. Kumaki, K. Okoshi and E. Yashima, *J. Am. Chem. Soc.*, **2008**, *130*, 7938-7945; e) K.-J. Chang, B.-N. Kang, M.-H. Lee and K.-S. Jeong, *J. Am. Chem. Soc.*, **2005**, *127*, 12214-12215; f) S. Ghosh and S. Ramakrishnan, *Angew. Chem. Int. Ed.*, **2005**, *44*, 5441-5447; g) Z. Zhong and Y. Zhao, *J. Org. Chem.*, **2008**, *73*, 5498-5505; h) J.-H. Ryu, J. Bae and M. Lee, *Macromolecules*, **2005**, *38*, 2050-2052.

75 a) A. Petitjean, H. Nierengarten, A. van Dorsselaer and J.-M. Lehn, *Angew. Chem. Int. Ed.*, **2004**, *43*, 3695 -3699; b) R. M. Meudtner, M. Ostermeier, R. Goddard, C. Limberg and S. Hecht, *Chem. Eur. J.*, **2007**, *13*, 9834 – 9840; c) A. M. Kendhale, R. Gonnade, P. R. Rajamohanan, H.-J. Hofmann and G. J. Sanjayan, *Chem. Commun.*, **2008**, 2541-2543.

76 M. S. Gin, T. Yokozawa, R. B. Prince and J. S. Moore, *J. Am. Chem. Soc.*, **1999**, *121*, 2643-2644.

77 a) R. B. Breitenkamp, L. Arnt and G. N. Tew, *Poly. Adv. Technol.*, **2005**, *16*, 189-194; b) L. Arnt and G. N. Tew, *Langmuir*, **2003**, *19*, 2404-2408; c) L. Brunsveld, R. B. Prince, E. W. Meijer, and J. S. Moore, *Org. Lett.*, **2000**, *2*, 1525-1528.

78 H. Goto, H. Katagiri, Y. Furusho and E. Yashima, *J. Am. Chem. Soc.*, **2006**, *128*, 7176-7178.

79 A. Kahn and S. Hecht, *J. Polym. Sci.: Part A: Polym. Chem.*, **2006**, *44*, 1619-1627.

80 a) R. M. Meudtner and S. Hecht, *Angew. Chem. Int. Ed.*, **2008**, *47*, 4926-4930; b) F. Mouffouk, S. J. Higgins, S. J. Brown, N. Sedghi, B. Eccleston and S. Reeman, *Chem. Commun.*, **2004**, 2314-2315; c) R. B. Prince, S. A. Barnes and J. S. Moore, *J. Am. Chem. Soc.*, **2000**, *122*, 2758-2762.

81 A. Kahn and S. Hecht, *Chem. Eur. J.*, **2006**, *12*, 4764-4774.

82 a) R. A. Smaldone and J. S. Moore, *J. Am. Chem. Soc.*, **2007**, *129*, 5444-5450; b) R. A. Smaldone and J. S. Moore, *Chem. Eur. J.*, **2008**, *14*, 2650-2657.

83 a) A. R. Fersht, *Science*, **1998**, *280*, 541; b) O. Nureki, D. G. Vassylyev, M. Tateno, A. Shimada, T. Nakama, S. Fukai, M. Konno, T. L. Hendrickson, P. Schimmel and S. Yokoyama, *Science*, **1998**, *280*, 578.

84 a) D. Haldar, H. Jiang, J.-M. Leger and I. Huc, *Angew. Chem.*, **2006**, *118*, 5609 -5612; b) Q. Gan, C. Bao, B. Kauffmann, A. Grélard, J. Xiang, S. Liu, I. Huc and H. Jiang, *Angew. Chem.*, **2008**, *120*, 1739-1742; c) Yann Ferrand, Amol M. Kendhale, Joachim Garric, Brice Kauffmann, and Ivan Huc, *Angew. Chem.*, **2010**, 122, 1-6.

85 Victor Maurizot, Christel Dolain, Yoann Leydet, Jean-Michel Léger, Philippe Guionneau and Ivan Huc, *J. Am. Chem. Soc.*, **2004**, *126*, 10049-10052.

86 N. Delsuc, M. Hutin, V. E. Campbell, B. Kauffmann, J. R. Nitschke and Ivan Huc, *Chem. Eur. J.*, **2008**, *14*, 7140 – 7143.

87 F. J. M. Hoeben, P. Jonkheijm, E. W. Meijer and A. P. H. J. Schenning, *Chem. Rev.*, **2005**, *105*, 1491-1546.

88 a) J. Roncali, *Chem. Rev.*, **1992**, *92*, 711-738; b) J. M. Tour, *Chem. Rev.*, **1996**, *96*, 537-553; c) U. H. F. Bunz, *Chem. Rev.*, **2000**, *100*, 1605-1644 ; d) A. C. Grimsdale, K. L. Chan, R. E. Martin, P. G. Jokisz, and A. B. Holmes, *Chem. Rev.*, **2009**, *109*, 3, 897-1091; e) A. Mishra, C.-Q. Ma, and P. Bäuerle, *Chem. Rev.*, **2009**, *109*, 1141-1276; f) S. W. Thomas III, G. D. Joly and T. M. Swager, *Chem. Rev.*, **2007**, *107*, 1339-1386.

89 a) M. Monteserín, H. D. Burrows, A. J. M. Valente, R. Mallavia, R. E. Di Paolo, A. L. Maçanita and M. J. Tapia, *J. Phys. Chem. B*, **2009**, *113*, 1294-1302; b) M. Peters, M. L. Hallensleben and M. van Hooren, *J. Mater. Chem.*, **1999**, *9*, 1465-1469; c) K. Peter R. Nilsson and Per Hammarström, *Adv. Mater.*, **2008**, *20*, 2639-2645.

90 a) T. Yasuda and T. Yamamoto, *Macromolecules*, **2003**, *36*, 7513-7519; b) Y. Gao, C.-C. Wang, L. Wang and H.-L. Wang, *Langmuir* **2007**, *23*, 7760-7767; b) R. D. McCullough, P. C. Ewbank and R. S. Loewe, *J. Am. Chem. Soc.*, **1997**, *119*, 633-634; c) S. Wang, W. J. Oldham Jr., R. A. Hudack, Jr. and G. C. Bazan, *J. Am. Chem. Soc.*, **2000**, *122*, 5695-5709; d) R. Kakuchi, S. Nagata, R. Sakai, I. Otsuka, H. Nakade, T. Satoh and Toyoji Kakuchi, *Chem. Eur. J.*, **2008**, *14*, 10259-10266.

91 a) Z. Yao, C. Li and G. Shi, *Langmuir*, **2008**, *24*, 12829-12835; b) L. An, Y. Tang, F. Feng, F. He and S. Wang, *J. Mater. Chem.*, **2007**, *17*, 4147-4152.

92 a) D. Yu, Y. Zhang and B. Liu, *Macromolecules*, **2008**, *41*, 4003-4011; b) B. S. Gaylord, A. J. Heeger and G. C. Bazan, *Proc. Natl. Acad. Sci. USA*, **2002**, *99*, 10954-10957; c) C. Xue, S. Velayudham, S. Johnson, R. Saha, A. Smith, W. Brewer, P. Murthy, S. T. Bagley and H. Liu, *Chem. Eur. J.*, **2009**, *15*, 2289-2295.

93 K. Peter, R. Nilsson and O. Inganäs, *Nat. Mater.*, **2003**, *2*, 419-424.

94 a) I. Johnson, *Histochem. J.*, **1998**, *30*, 123-140; b) J. W. Lichtman and J.-A. Conchello, *Nat. Meth.*, **2005**, *2*, 910-919.

Chapter 3
Self-assembly behaviour of conjugated terthiophene surfactants in water

Abstract

Here a generic platform is presented that gives access to aggregates with different morphologies without changing the basic molecular design. The design, synthesis and aggregation behaviour of conjugated terthiophene-based surfactants is discussed in which the relation between hydrophilicity and hydrophobicity is changed due to a subtle alteration in substituents, resulting in different aggregates ranging from spherical- and elongated micelles to bilayers. The molecular design allows for further oligo- and polymerisation for the creation of new amphipathic structures. This opens the possibility to address new responsive self-assembled structures with a high degree of control over the internal structure. In total 8 new amphiphilic oligothiophenes were made and the aggregation behaviour investigated by fluorescence, DLS and Cryo-TEM, respectively. Critical micelle concentrations as low as 0.01 mM were found and different sized aggregates ranging from several nanometres up to 200 nm. Also it was discovered that the compounds possess a thermotropic phase transition and that the morphology of the aggregates can be controlled by playing on temperature.

3.1   Introduction

Conjugated polymers continue to attract much attention because of their interesting opto-electronic properties and their many applications in electronic devices.[1] For instance, polythiophenes, -fluorenes and -phenylenes based materials have frequently been applied in solar cells, field effect transistors and light emitting diodes.[2,3] Over the past decade there has also been a strongly growing interest in molecular and supramolecular electronics with nanoscale structural features, obtained by the self-assembly of molecular components.[4,5] Self-assembled electronic structures like micelles, fibres, tubes, bilayers and vesicles have been prepared from a wide variety of electronically active molecular building blocks in organic solvents[6,7,8,9,10,11] and to a limited extend also in water[12,13,14]. Alternatively, hydrophobic opto-electronic molecules have been used in combination with surfactant assemblies in *e.g.* as sensors for biological species like proteins and DNA or as a visualisation tool for membranes.[15,16,17,18] Clearly, conjugated self-assembled systems in water are of great interest because of their potential biocompatibility. However, in order to expand their scope and exploit self-assembling conjugated oligomers and polymers more efficiently, a better understanding of molecular features governing aggregate morphology is necessary, and it remains a challenge to design conjugated polymers which allow control over the aggregate morphology upon self-assembly in water.

The aim of this study was to develop conjugated oligomers, which can be programmed to self-assemble into aggregates with well-defined morphologies. Here we present amphiphilic terthiophenes as a platform for conjugated self-assembled structures. We explored the design parameters of these amphiphilic terthiophenes in detail, and studied their aggregation behaviour in aqueous solutions. We found that the aggregate morphology can be tuned by the substitution pattern of hydrophilic and hydrophobic substituents and the aggregate retains their electronic- and spectroscopic properties which will have important implications for their application

in self-assembling systems. These terthiophenes are intended to be used as building blocks for longer oligothiophenes, which will be described in the next chapter, as well as a platform for self-assembled antenna systems and sensors in biological systems (chapters 5-8).

3.2   Design of the oligothiophene surfactants

In order to develop a molecular system based on conjugated oligomers which can be programmed to self-assemble into different types of aggregates with well-defined morphologies, we have directed our attention towards differently substituted oligothiophenes. Oligothiophenes are of interest because their backbone is conjugated when coupled in an $\alpha,\omega(1,4)$-fashion, which will allow the use of their electronic properties as an intrinsic messenger for its conformation and aggregation behaviour. In addition, the rigid thiophene backbone has limited conformational freedom which is likely to provide a more regular orientation of the side chains and packing of the molecules inside the aggregates. Simultaneously, the occurrence of *trans-* and *cis-* conformations along the thiophene-thiophene bonds allows for tuning of the overall molecular shape for future longer sequences, provided that they do not consist of an even number of alternating hydrophilic and hydrophobic substituted thiophenes.[19] In this regard, of the six-membered aromatic rings, only the ortho-connected oligomers would be of interest. However, these compounds tend to be much more difficult to synthesise[20] and their self-assembly is inhibited by their strong tendency to fold.[21] In principle, any aromatic 5-membered ring would be considered as a good choice, but in this study oligothiophenes are used because their synthesis is very well established.

In order to develop a novel modular self-assembling molecular system starting from an oligothiophene backbone, we have applied several other design criteria. Obviously, the first design criterion for creating an amphiphilic compound is that at least one hydrophilic and one hydrophobic group needs to be present. Because we

would like to employ a building-block approach based on thiophene monomers in combination with high-yield cross-coupling methodologies, the second design criterion states that each thiophene can only have one substituent, which is not allowed to be on the carbons directly next to the sulphur, the so called α,ω-positions.
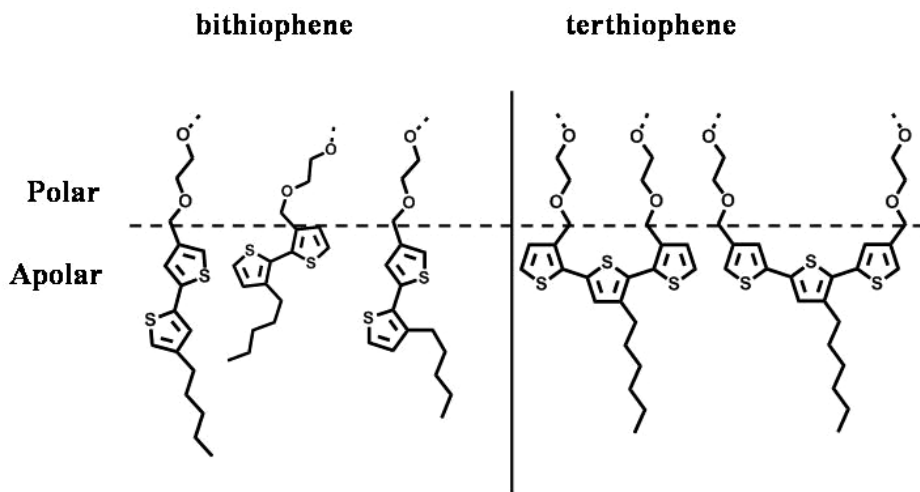
Figure 1: Possible orientations of substituted bis-thiophenes (left) and terthiophenes (right) at a polar-apolar interface.

Application of these design criteria excludes mono-thiophenes because they cannot be rendered amphiphilic with only one substituent. Also *bis*-thiophenes have not been investigated because application of the above design criteria allows only three different compounds. These *bis*-thiophenes will be less relevant as model compounds for the longer oligomers, because of the expected irregular orientation at the polar/apolar (aggregate) interface, which will be different from their longer oligomers (Figure 1). With the next oligothiophene, *i.e.* the terthiophenes, the first two criteria can be implemented without difficulty. A direct consequence of the aforementioned criteria is that an amphiphilic terthiophene is always composed of either two thiophenes substituted with a polar group and one with an apolar one or vice versa. To prevent similar orientation effects as for the *bis*-thiophenes (see Figure 1), the terthiophenes need to have a reasonable amount of symmetry *i.e.* the

two outer thiophenes are substituted with groups of the same polarity and the middle one with the inverse polarity. Using a tetra-thiophene building block would not provide any added value at this point and is more difficult to prepare because of its more extended structure.

Placing substituents on a terthiophene can result in quite a number of compounds, 24 when two types of substituents are placed in a random order. However, because the aforementioned structural design criteria were implemented, only 8 compounds remain (Figure 2). In Figure 2 it is seen how the terthiophenes have their substituents positioned and also how inverting the polar and apolar groups give similar substituted terthiophenes only with an inversed polarity.
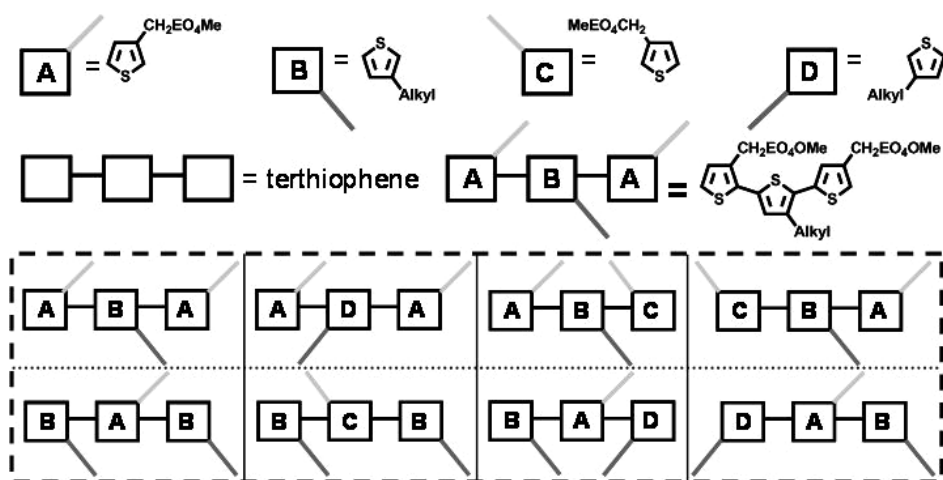
Figure 2: Possible terthiophene compounds that can be formed from 4 different mono-thiophene building-blocks by obeying the aforementioned design criteria.

Figure 2 shows eight compounds from which six were selected (ABA, BAB, ABC, BAD, CBA and DAB). The last two compounds that could be distinguished, ADA and BCB, are much alike ABA and BAB; here the difference is the substituent position on the middle thiophene.

The amphiphilic character is implemented by using hydrophobic and hydrophilic substituents. For the hydrophilic group the commonly used non-ionic tetraethylene glycol mono-methyl ether[15-20] was chosen, because it does not require additional protection-deprotection steps during the synthesis and its better solubility in organic solvents compared to ionic groups facilitates purification. Furthermore, the non-ionic character renders the final thiophene surfactants compatible with other amphiphiles regardless of their charge. The length of the hydrophilic ethylene glycol chain is not expected to have major effects on the cmc, however, at least four ethylene glycol-units are preferred to prevent the cloudpoint from dropping below room temperature.[22] For the hydrophobic substituent a hexadecyl chain was used because surfactants with a single hexadecyl chain as the hydrophobic moiety have critical micelle concentrations (cmc) ranging from millimolar concentrations for ionic surfactants down to micromolar concentrations for surfactants with an oligo-ethylene glycol head group.[32,23]

$EO_4 = (OCH_2CH_2)_4$

1-OMe: $R_2=R_4=CH_2(EO)_4OCH_3$; $R_3=C_{16}H_{33}$; $R_1=R_5=H$ (ABC)
1'-OH: $R_2=R_4=CH_2(EO)_4OH$; $R_3=C_{16}H_{33}$; $R_1=H$
2-OMe: $R_2=R_5=CH_2(EO)_4OCH_3$; $R_3=C_{16}H_{33}$; $R_1=R_4=H$ (ABA)
2-OH: $R_2=R_5=CH_2(EO)_4OH$; $R_3=C_{16}H_{33}$; $R_1=R_4=H$
3-OMe: $R_1=R_5=CH_2(EO)_4OCH_3$; $R_3=C_{16}H_{33}$; $R_1=R_5=H$ (CBA)
4: $R_3=CH_2(EO)_4OCH_3$; $R_2=R_4=C_{16}H_{33}$; $R_1=R_5=H$ (BAD)
5: $R_3=CH_2(EO)_4OCH_3$; $R_2=R_5=C_{16}H_{33}$; $R_1=R_4=H$ (BAB)
6: $R_3=CH_2(EO)_4OCH_3$; $R_1=R_5=C_{16}H_{33}$; $R_2=R_4=H$ (DAB)
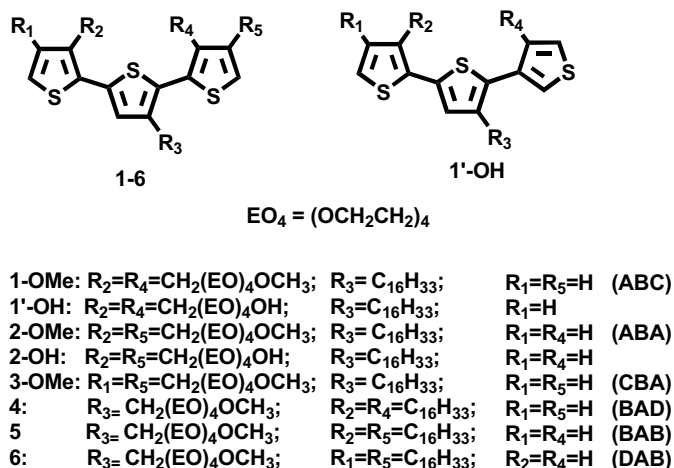
Figure 3: Overview of the amphiphilic thiophene chosen with different substitution patterns.

The structures that result from these considerations are shown in Figure 3. Going from two tetraethylene glycol tails and one C_{16}-chain (2:1) (**1-3**) to a 1:2 ratio (**4-6**),

different types of aggregates should be obtained. However, this ratio is not the only parameter which plays a role. Going from **1** to **3**, the ratio between hydrophilic and hydrophobic remains 2:1 but the positioning of the hydrophilic groups should change the effective surface they take when pointing away instead of towards one another. The same applies for the volume of the hydrophobic segments of **4-6**. This orientation should influence the aggregate morphology as well. Compound **2-OH** is the hydroxy-variation, which was prepared at an initial stage and compound **1'-OH** became accessible as well during this process and appeared to be an interesting addition. The other hydroxyl-derivatives were not pursued because of synthetic accessibility as noted above.

3.3   Synthesis of terthiophenes 1-6

The thiophene based amphiphiles have been synthesised in a modular approach using hydrophobic and a hydrophilic substituted thiophenes as building blocks. These precursors are then modified in such a way that they can be connected via a palladium catalysed cross-coupling. Here the Stille coupling was used, mainly because this method has been shown to give the best results with comparable thiophene compounds.[24]

The thiophene building blocks with the hydrophobic substituent was easily prepared in few steps starting from commercial available *3*-bromothiophene (Scheme 1). First, *3*-bromothiophene **9** was allowed to react with a Grignard reagent of *n*-bromohexadecane via a nickel (Ni(dppp)Cl$_2$) catalysed Kumada coupling resulting in *3*-hexadecylthiophene (**10**). Compound **10** was then selectively functionalised with a trimethyltin moiety on the *5*-position by *ortho*-lithiation and quenching with trimethyltinchloride to give compound **15**. Alternatively, *3*-hexadecylthiophene **10** was mono-brominated on the *2*-position by reaction with one equivalent of N-bromosuccinimide (NBS) or di-brominated on positions *2* and *5* by reaction with two equivalents of bromine (Br$_2$) to yield compounds **11** and **13**, respectively. The *2*-

bromo-*3*-hexadecylthiophene **11** underwent a halide/lithium exchange by treatment with one equivalent of *n*-butyllithium. When this was quenched with trimethyltinchloride, a trimethyltin moiety was introduced at the *2*-position (compound **12**), or by quenching with trimethylsilyl chloride (TMSCl), the *2*-position was protected with a TMS-group. This latter compound was then selectively functionalised with a trimethyltin at the *5*-position which resulted in compound **14**.
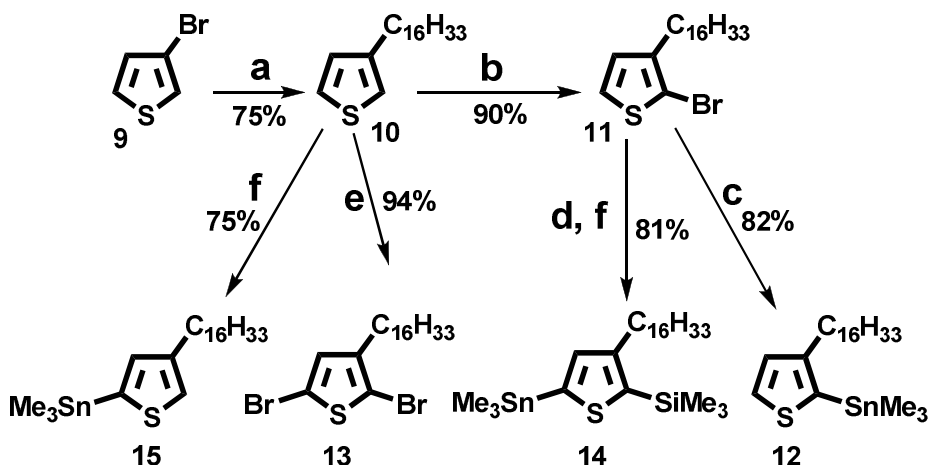
Scheme 1: Schematic overview of the synthesis of the hydrophobic part a) $C_{16}H_{33}MgBr$, Et_2O, $Ni(dppp)Cl_2$; b) NBS, DCM; c) n-BuLi, THF, -78°C, $ClSnMe_3$; d) n-BuLi, THF, -78°C, $ClSiMe_3$; e) 2 eq. Br_2, $CHCl_3$, 0°C; f) LDA, THF, -78°C, $ClSnMe_3$.

The hydrophilic thiophene building blocks were prepared starting from commercially available *3*-methylthiophene **16** (Scheme 2). *3*-Methylthiophene **16** was first brominated at the *2*-position by reaction with NBS, and subsequently at the methylene by reaction with NBS under radical-forming conditions. Then, the tetraethylene glycol monomethyl-ether was attached via a nucleophilic substitution resulting in compound **17**. Compound **18** was obtained by reaction of **17** with again NBS. Alternatively, the *2*-bromide of **17** was either transformed into a trimethylstannyl-group to give compound **19** or into a TMS-group to give compound **20**, again via halogen/lithium exchange with n-butyllithium followed by quenching

with trimethyltin chloride and TMSCl, respectively. Finally, compound **21** was synthesised by ortholithiation of **20**, followed by quenching with trimethyltin chloride.
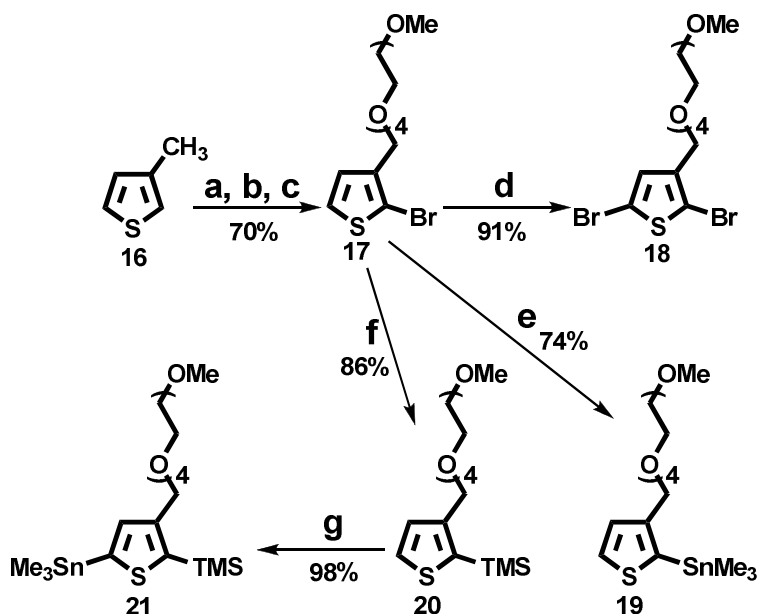
Scheme 2: Schematic overview of the synthesis of the hydrophilic parts a) NBS, AcOH; b) AIBN, NBS, benzene, reflux; c) THF, NaH, Me(OCH₂CH₂)OH, R.T.; d) NBS, DCM; e) n-BuLi, THF, -78°C, ClSnMe₃; f) n-BuLi, THF, -78°C, ClSiMe₃; g) LDA, THF, -78°C, ClSnMe₃.

From the different hydrophobic and hydrophilic substituted thiophenes, all amphiphiles (Figure 3) were prepared via a double Stille coupling (for the irregular amphiphiles **1-OMe**, **3-OMe**, **4** and **6**) or via a stepwise coupling with a bromination step in between (**2-OMe** and **5**) (Scheme 3). For the two irregular substituted structures **1-OMe** and **3-OMe**, the di-bromo compound **13** was used and allowed to react with two equivalents of either **19** or **21**, giving **1-OMe** and **3-OMe**, respectively.

The regio-regular substituted terthiophene was synthesised via a coupling of **15** with **17**, followed by a bromination and subsequently coupling with **21**. Both terthiophene **2-OMe** and **3-OMe** required a deprotection step in order to remove the TMS

protecting group. The inverted structures, **4-6** were prepared in a similar fashion by using the exact same procedures only with the reactive groups on the hydrophilic and hydrophobic structures inverted. Compounds **1'-OH** and **2-OH** were synthesised according to a similar procedure only starting with a THP-protected tetraethylene glycol, which is removed at the end. All compounds were purified using normal phase column chromatography and were characterised by ^{1}H-NMR, ^{13}C-NMR, Mass-spectrometry and analysed by HPLC with UV/ESI detection.
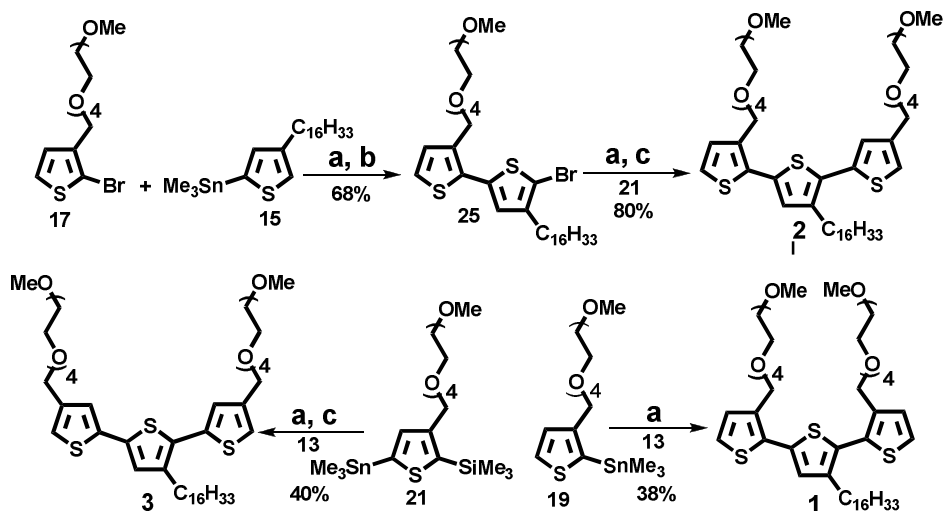
*Scheme 3: Schematic overview of the synthesis of the terthiophenes **1-3** a) Pd(PPh₃)₄, DMF, toluene, 110°C; b) NBS, DCM; c) HCl 10%, MeOH.*

3.4   Aggregation behaviour of terthiophenes 1-6

Terthiophenes **1-3** bearing two hydrophilic and only one hydrophobic group dissolved easily in water up to concentrations of 50 mM, to give transparent yellow solutions. In contrast, compounds **4-6**, which have two hydrophobic groups attached, formed turbid off-white dispersions at concentrations between 10 μM and 1 mM and precipitated at concentrations above 1 mM. These observations already indicated differences in aggregation behaviour. When looking closer at the solutions, it was

observed that solutions of **1-OMe**, **1'-OH** and **2-OMe** also were viscous at millimolar concentrations while solutions of **2-OH**, **3-OMe** and **4-6** retained a similar flow as pure water. This indicates that probably both types of compounds aggregate in water; the first type formed aggregates which interact to some extend, and the latter type formed aggregates which do not interact. Pendant-drop-surface-tension measurements revealed that compounds **1-6** are indeed surface active as was noted from a decrease of the surface tension (72 mN m^{-1} for pure water) to values around 40 mN m^{-1} and 60 mN m^{-1} at millimolar concentrations of **1-3** and **4-6**, respectively. However, the surface tension failed to stabilise during the time course of the measurements resulting in a loss of the pendant drop. Therefore, it was not possible to determine other aggregation parameters like the critical micelle concentration (cmc) by this method. Also Isothermal Titration Calorimetry (ITC) was not suitable to study the aggregation process of **1-3** because of the low enthalpies of dissociation of the aggregates, indicating an entropic aggregation process.

It is known that chromophores display changes in their photo-physical properties upon aggregation,[25] and therefore is was expected that self-assembly of **1-6** would have been accompanied by a change of the absorption and emission spectra. Remarkably, it was found that there was no significant change in the wavelength of both the absorption and emission maxima over a large concentration range from 0.005 mM to 10 mM for compounds **1-3** and 0.005 mM to 1 mM for **4-6**.

Therefore, other techniques were used first in order to investigate the aggregation behaviour. The photo-physical properties will be discussed in more detail later in the chapter.

An alternative method for determining the cmc over a wide concentration range is by measuring the scattered light intensity as a function of the concentration, because larger particles scatter light much more efficiently than small molecules. This was visualised by plotting the scattered light intensity versus the concentration, which showed a sharp increase at the cmc (Figure 4).
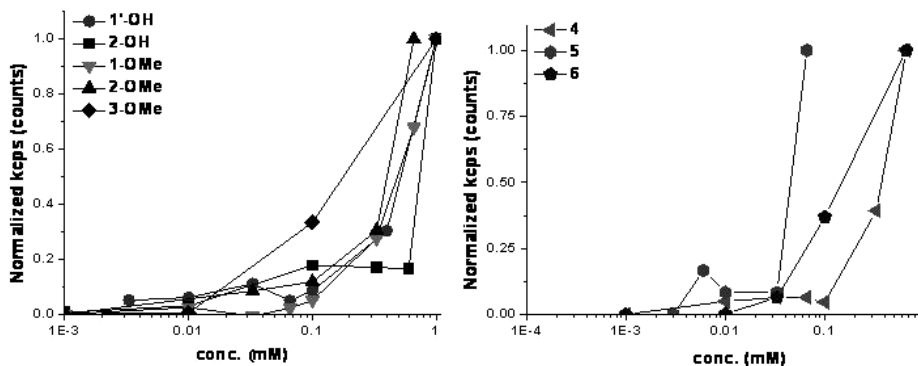
Figure 4: Concentration dependent scattering measurements of the different terthiophene amphiphiles in water at 20°C.

The cmc values determined by light scattering are summarised in Table 1. The lower cmc values of **4-6** compared to **1-3** nicely show that **4-6** are more hydrophobic in character. Separate measurements of the particles size by DLS above the cmc confirmed the formation of aggregates of **1-6** with diameters between 10 nm and 90 nm. Again, the studied compounds form two groups, with the group of **4-6** forming significantly larger aggregates than the compounds **1-3**.

Another way of determining the cmc of surfactants is by using solvochromic hydrophobic fluorescent probes like Nile Red (NR). Nile Red changes its emission properties when going from a polar environment to an apolar one by a shift in emission maximum towards shorter wavelengths, together with an increase in quantum yield.[26] In the case of thiophene surfactants **1-6**, the emission intensity of the added NR probe increased drastically at a characteristic concentration, which are in good agreement with the cmc values found by the scattering method (Table 1 and Figure 5).

Table 1   Critical Micelle and Aggregation concentrations by scattering and fluorescence

	$cmc_{scattering}$ (mM)[a]	D_h in nm (at conc.)[d]	$cmc_{NR.Em.Int.}$ (mM)[b]	$cac_{NR-EMmax}$ (mM)[c]
1-OMe	0.2	24 (1.0 mM)	0.2	<0.001
1'-OH	0.2	10 (0.4 mM)	0.2	0.01
2-OMe	0.2	16 (0.3 mM)	0.2	<0.001
2-OH	0.4	16 (1.0 mM)	0.2	0.01
3-OMe	0.2	14 (0.3 mM)	0.04	0.001
4	0.1	91 (0.1 mM)	0.01	<0.001
5	0.03	79 (0.3 mM)	0.02	<0.001
6	0.03	91 (0.1 mM)	0.01	0.03

*a) cmc determined for **1-6** by scattering (DLS); b) with change in intensity of Nile Red and c) shift in emission wavelength of Nile Red (cac) (λ_{exc} 550 nm, conc. Nile Red 1.0 μM in combination with **1-3** and 0.1 μM for **4-6**). d) The hydrodynamic diameters (D_h) obtained from DLS taken at lowest conc. with correct fitting. The error in cmc determinations is estimated to be 10%. Measurements were performed at 20°C.*

Only **3-OMe** formed an exception, and has a cmc value almost as low as those of compounds **4-6** with two alkyl chains. However, when looking at the shift of the emission maximum of NR in the presence of different concentrations of terthiophene amphiphiles, there was a discrepancy. In the presence of compounds **1-OMe** and **2-OH/OMe** the emission wavelength of NR has shifted to 620 nm and 640 nm, respectively, at concentrations as low as 0.001 mM, indicating that hydrophobic domains are already present at concentrations far below the cmc. Also for compounds **3-6** at concentrations of 0.001 mM the emission maximum of NR was between 650 and 655 nm which is a minor but significant shift in emission

wavelength compared to the NR emission maximum of 660 nm in pure water. These changes in emission wavelength of NR at much lower concentrations than the cmc values determined by scattering measurements and NR intensity are most likely due to the formation of small pre-micellar aggregates. Upon increasing the concentration of terthiophene amphiphile, a sudden change in emission wavelength was observed (Figure 5), indicating that also **3-6** formed aggregates with hydrophobic micro-domains.
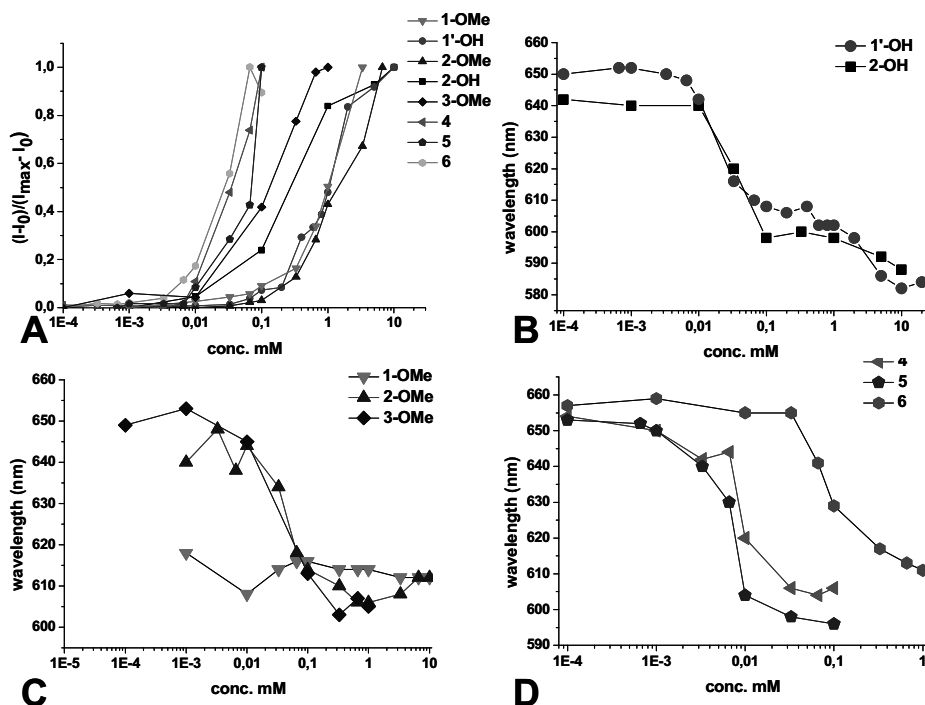
*Figure 5: Emission intensity of Nile Red in combination with different concentrations of thiophene amphiphiles to determine the cmc of isomers **1-6** at 20°C.*

3.5 Phase behaviour of the terthiophenes 1-6

Since the thiophene surfactants are non-ionic with an ethylene glycol head-group, it is expected that they display a cloudpoint (cp) or lower critical solution temperature.[27] Indeed, it was observed that transparent solutions of **1-3** at higher temperatures became turbid due to precipitation. The cp was determined for concentrations of thiophene surfactant above the cmc by measuring the light scattering intensity with increasing temperature. For compounds **4-6** the cp could not be determined by scattering experiments because the solutions were already turbid themselves. The thermotropic phase behaviour of **1-3** was investigated in more detail by micro-Differential Scanning Calorimetry (DSC). For most isomers (**1-3**) a clear exothermic transition was observed at temperatures similar to the cp temperatures found by scattering measurements (Figure 6). However, for **1'-OH** and **2-OH**, no transition was observed with DSC. The cloudpoints from scattering measurements and the DSC data are summarised in Table 2.

Table 2   Thermotropic phase behaviour of terthiophenes 1-3

No.	Cloudpoint[a] (°C)	Phase Transition DSC[b] (°C)	ΔH_{DSC}[c] (kJ mol^{-1})
1-OMe	23 (+/- 3)	9-18 / 23-27 / 28-31	2.7/ 9.9/ 15.0
1'-OH	38 (+/- 2)	none	---
2-OMe	26 (+/- 2)	12-21 / 24-29 / 29-32	2.5/ 9.5/ 15.2
2-OH	23 (+/- 2)	none	---
3-OMe	32 (+/- 2)	10-22 / 28-33 / 33-39	3.1/ 8.6/ 17.6

*a) Temperatures found by scattering for the cloudpoints, performed with 10 mM solutions and b) transitions found by micro-DSC with scan rate of 60°C/h with c) the associated enthalpy for those transitions in kJ mol^{-1}. For DSC measurements, 1.0 mM solutions were used for **1**- and **2-OMe** and 10 mM for **3-OMe**.*

For the compounds which have a hydroxyl-group at the end, an opposite trend in cp was seen when compared to the **OMe** ones. Going from the situation in which the ethylene glycol-substituents point towards each other (**1-OMe**) to the regio-regular (**2-OMe**), and pointing away from each other (**3-OMe**), an increase of the cp from 23 to 32°C was observed. In the hydroxy-end capped compounds (**1'-OH** and **2-OH**) the sterically more crowded **1'-OH** had a higher cp of 38°C and this decreased down to 23°C for the regio-regular **2-OH**. It should be noted that all determinations of the cmc and cac described before have been carried out at temperatures below the cp of the compound under investigation.
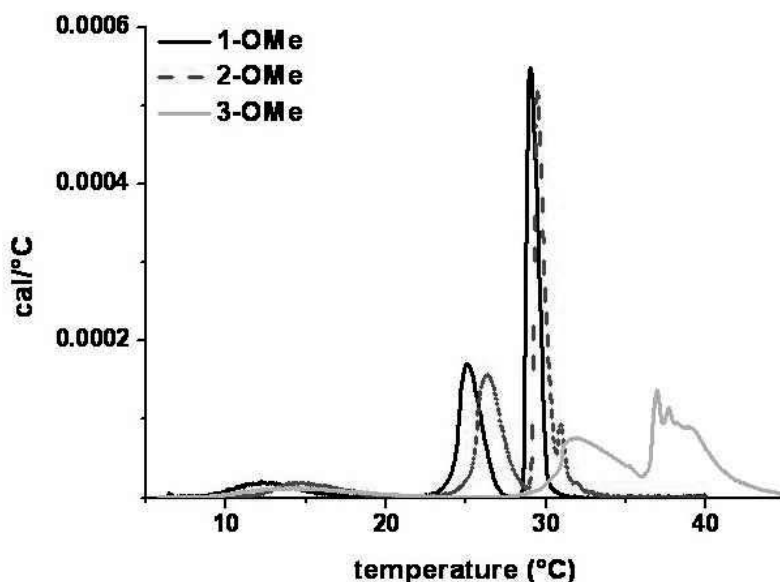
*Figure 6: DSC of the different thiophene surfactants that display a temperature effect. Concentrations used were 1.0 mM for compounds **1-OMe** and **2-OMe**, for **3-OMe** 10 mM was used and corrected for this to 1.0mM.*

Interestingly, the DSC traces for compounds **1-**, **2-** and **3-OMe** displayed beside a clear exothermic transition around the cp, also a minor exothermic transition at a lower temperature, between 12-15°C (Figure 6). The enthalpies of these transitions

have comparable values for all three compounds (Table 2). Additional measurements of the aggregate size by DLS at temperatures below and above the minor phase transition temperature, at 5 and 20°C, respectively, revealed an increase of the average aggregate size with increasing temperature for **1-OMe** and **2-OMe**, whereas the aggregate size of **3-OMe** was not affected. This was further investigated by Cryo-Transmission Electron Microscopy (cryo-TEM) which will be discussed later. One more transition was observed for **1-3-OMe** and was found at higher temperatures than the cp, but the nature of this transition was not further investigated.

3.6   Morphology of aggregates of terthiophenes 1-6

The results from fluorescence and scattering measurements, together with the observation of changes in viscosity, indicate that compounds **1-6** formed aggregates. The morphology of the aggregates in aqueous solutions of **1-6** was investigated by cryo-TEM. For all samples the concentration was at least 10 times above the cmc, and they were quenched after equilibration at 20°C. Aqueous solutions of **1-OMe** and **2-OMe** were also analysed by quenching after equilibration at 5°C because they displayed a phase transition around 12-15°C and a change in aggregate size displayed by DLS. The results of these cryo-TEM investigations are summarised in Figure 7 and Table 3.

From TEM it becomes clear that different aggregate morphologies were formed from the different compounds. Terthiophenes **2-OH** and **3-OMe** gave a mix of spherical and elongated micelles with diameters of 6-8 nm which is significant smaller than the diameters found by DLS. Cryo-TEM micrographs revealed that compounds **1-OMe**, **1'-OH** and **2-OMe** formed cylindrical micelles with a width of about 5-7 nm. The lengths are difficult to estimate but are roughly smaller than 100 nm for **1-** and larger than 100 nm for **1'-OH** and **2-OMe** (Figure 7). Also in these cases there is a large discrepancy between the sizes determined by TEM and DLS.

However, because the cylindrical micelles have a width as well as a length, it is difficult to determine a correct size using DLS since the applied model (CONTIN) to determine the hydrodynamic radius from the autocorrelation curves is only strictly valid for spherical objects.
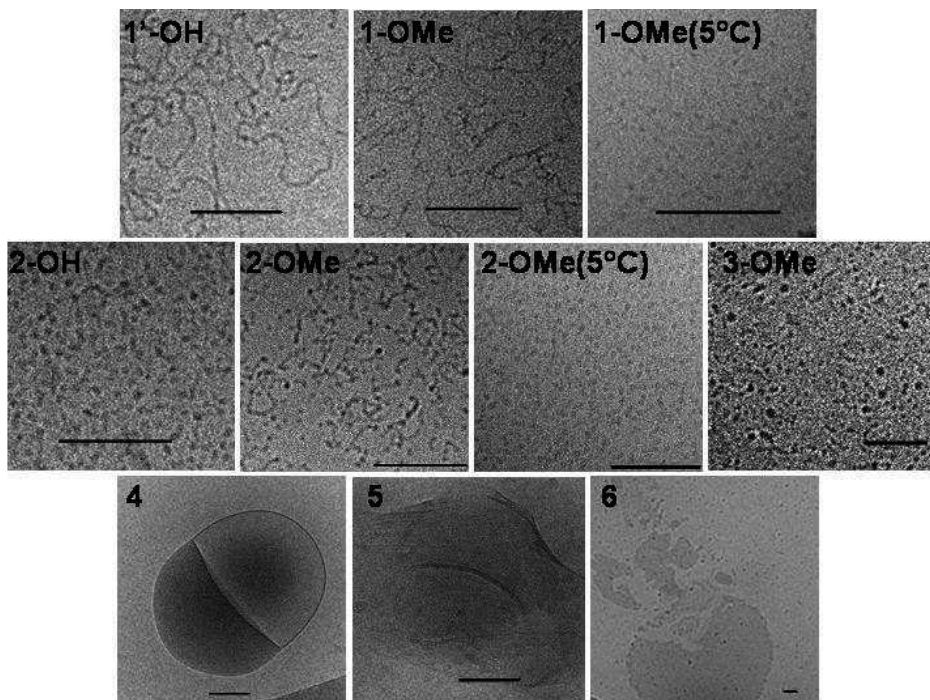
*Figure 7: Cryo-TEM of thiophene surfactants (numbers on TEM=number of compound) clearly displaying a range of different types of aggregate for the isomers of which **1-OMe** and **2-OMe** display a temperature dependency. The scale bar corresponds to 100 nm and concentrations of 10 mM were used.*

Table 3   Aggregate morphologies of terthiophenes 1-6 obtained by cryo-TEM

No.	Aggr. type (20°C)	Aggr. Size[a] (TEM) (nm) (20°C)
1-OMe	spherical micelle (5°C) / elongated micelle	5.9 (±0.7) (5°C)/ W: 4.7 (±0.4), L<100
1'-OH	elongated micelle	W: 5.5 (±0.8), L>100
2-OMe	spherical micelle (5°C) / elongated micelle	6.3 (±0.4) (5°C)/W: 7.1 (±1.0), L>100
2-OH	spherical- and elongated micelles	6.0 (±0.7)
3-OMe	mix of spherical- and elongated micelles	7.5 (±1.8)
4	bilayer	$W_{bilayer}$: 4.2 (±1.1), W_{aggr}: ~350
5	Sheet-like	W_{sheet}: 6.3 (±1.2), L_{sheet}: ~200
6	amorph. aggregate	Very distributed

*a) All solutions were in water at 10 mM concentrations and stabilised before blotting at 20°C and additionally for **1-** and **2-OMe** at 5°C. The width (W) was determined by taking the average of various positions on different aggregates within the TEM, from this the standard deviations was taken as the estimated error, L=length and is a crude estimations.*

For all these compounds, the diameter of the spherical micelles and the width of the elongated micelles are approximately twice the length of the terthiophene amphiphile along the aliphatic- and ethylene glycol chain. The differences in aggregate morphology can be rationalised in terms of the structure-shape concept.[28,31] When the two ethylene glycol groups are positioned away from each other (**3-OMe**) they occupy a larger head group surface, resulting in a decrease in the packing parameter. This decrease produces a mixture of spherical and elongated

micelles. When they are positioned towards one another (**1-OMe**) a smaller area is formed and only elongated micelles are observed.

Compounds **1-OMe** and **2-OMe** were also investigated below and above the phase transition at 15°C. It was seen that at low temperature the elongated structures have disappeared and spherical micelles were formed. This observation is in nice agreement with the DLS results, which also revealed the presence of particles with smaller diameters at low temperatures for these compounds. This type of behaviour and temperature responsiveness is known to occur for ethylene glycol based self-assembling systems. Upon increasing the temperature, the ethylene glycol head group becomes more hydrophobic due to dehydration and the overall packing parameter of the surfactant increases. The change in packing parameter is responsible for the transition from small spherical micellar aggregates to larger aggregates, *i.e* the observed elongated micelles. Even though this behaviour is known, it is peculiar that compounds **1-OH** and **2-OH** with the hydroxy-ethylene glycol chains do not show any changes with temperature while **1** and **2** with the methyl-ether terminated ethylene glycols do. Apparently the methyl-group plays a significant role in the hydration which is in line with its more hydrophobic character. Not only transitions from micelles to elongated micelles have been reported, also transitions to vesicles are known.[29]

Investigation of aqueous dispersions of the poorly soluble double alkyl-tailed terthiophenes (**4-6**) by cryo-TEM revealed that **4** and **5** give spherical and exfoliated lamellar structures, respectively. The aggregate morphologies and their dimensions are also listed in Table 3. The width of the lamella formed by **4** and **5** amounts to 4-6 nm, which is in reasonable agreement with the length of two stretched molecules of **4** or **5**. Most likely, amphiphiles **4** and **5** form bilayer type of assemblies in water. The dimensions of the aggregates found for these compounds do not concur with dimensions found by DLS. This might be due to the unstable nature of the aggregates, since they tend to precipitate, especially in the case of compound **6**. For this compound only large poorly defined structures were observed even though DLS

showed 90 nm sized aggregates. This again might be due to precipitation, during which the larger fragment quickly settled at the bottom of the sample while the smaller fragments remain longer in solution. Clearly compound **6** is not suitable for aqueous solutions and **4** and **5** are on the border. The same analogy as was used for the aggregate morphology transitions for compounds **1-3** can also be used for **4-6**. When the two alkyl chains point away from each other, the overall volume they occupy becomes larger and the amphiphile becomes more hydrophobic, and even tends to precipitate.

3.7 Photo-physical properties of terthiophenes 1-6

It was expected that the intrinsic photo-physical properties of the oligothiophenes **1-6** could be exploited to derive information about their self-assembly behaviour. Remarkably, the aggregation of **1-6** in water was not accompanied by significant changes in the wavelength of the absorption and emission maxima. It was, however, observed that the emission intensity did not increase linearly with the concentration of **1-6** and even at some point decreased, most likely due to self-quenching caused by aggregation of the compounds.[30] This fluorescence self-quenching of **1-6**, however, occurred already at much lower concentrations than the cmc-values determined with Nile Red emission intensity, but does occur at similar concentrations when compared to the concentrations where the NR emission wavelength shifts. For compounds **1-3** self-quenching started at concentration below 0.1 mM and in some cases even already below 0.001 mM. When looking at the self-quenching of compounds **4-6**, it was seen that generally it already started at lower concentrations compared to **1-3**. Most likely, the self-quenching occurring below the cmc is due to the formation of small pre-(micellar) aggregates. The formation of small pre-(micellar) aggregates has been reported before for other systems.[31] The onset of the self-quenching gives the concentration at which monomeric solubilised surfactants start to aggregate, *i.e.* the critical aggregation concentration (cac). The

cac derived from the fluorescence self-quenching curves are listed in Table 4 and these values are in nice agreement with the concentrations at which the Nile Red emission wavelength deviated from the emission wavelength in pure water (see Table 1).

Table 4: Photo-physical properties of 1-6 in chloroform and water

No.	$\lambda_{abs(H2O)}$[a] (nm)	ε_{H2O}[a] (10^3) (L mol^{-1}cm^{-1})	$\lambda_{abs(CHCl3)}$[a] (nm)	ε_{CHCl3}[a](10^3) (L mol^{-1}cm^{-1})	$\lambda_{em(H2O)}$[a] (nm)	$\lambda_{em(CHCl3)}$[a] (nm)	$\Phi_{(H2O)}$[b]	cac$_{PL}$[c] (µM)
1-OMe	327	19.9	320	21.6	478/501	439	0.06	<1
1'-OH	330	15.5	323	21.1	482/505	451	0.07	<1
2-OMe	348	16.2	338	26.2	461	444	0.05	50
2-OH	350	19.2	342	24.6	454	443	0.1	10
3-OMe	350	15.0	344	16.2	460	440	0.17	10
4	330	12.8	321	22.0	453	433	0.06	10
5	368	5.1	342	6.3	446	440	0.18	<1
6	361	15.6	353	15.3	447	443	0.12	<1

*a) Concentrations used for absorption and emission measurements are 1.0 mM for **1-3** and 0.1 mM for **4-6**. b) The quantum yield (φ_F) was determined by using 9,10-Diphenyl-anthracene as a reference. c) The concentration at which photo-luminescence self-quenching begins. Measurements were performed at 20°C.*

During the investigations of the photo-physical properties of the different amphiphiles, it was found that the absorption wavelengths and emission maxima do not shift significantly upon going from 0.005 mM to 10 mM concentrations. There are shoulders gradually appearing with increasing concentration on the red side of the maximum emission wavelength. This absence in shifts could mean that there is no exciton coupling between the chromophores inside the aggregates or that there is an exciton coupling which is also already present in pre-micellar aggregates at low

concentrations. When there is indeed an exciton coupling, a shift in absorption and emission would be visible when going from a solvent like water in which aggregation takes place to a good solvent in which the surfactants are molecularly dissolved. As can be seen in Table 4, there is a difference in absorption as well as in the emission between solutions in water and in chloroform. However, this shift could be also due to solvent polarity.

In order to investigate if solvent polarity plays a role, a range of solvents were used with different polarities. The absorption spectra of **2-OMe** (50μM) was measured in various solvents with different polarities. It was found that the absorption maxima did not change with solvent polarity upon going from moderately polar (ethanol) to an apolar solvent (chloroform), which is in contradiction with polarity as a possible cause. Therefore, the different absorption maxima of the oligothiophenes in chloroform and water are most likely due to aggregation. The reason that no changes are observed over a large concentration range for the different terthiophene amphiphiles could again be attributed to pre-micellar aggregates. This is supported by both the self-quenching data which does indicate the presence of an electronic coupling between chromophores as well as the Nile Red emission wavelength shifts indicating that aggregated states are present at micro-molar concentration and hence a fully molecularly dissolved state has never been reached in this concentration range.

Comparing the different compounds, different absorption (Figure 8, Table 4) and emission (Figure 9, Table 4) maxima were seen, even though all compounds have a similar terthiophene backbone. This difference was observed in both water as well as in chloroform and since the latter is a good solvent, preventing aggregation, these shifts are inherent to the molecular structure of the compounds.

Compound **1-OMe**, has an absorption maximum in chloroform at a relatively low wavelength of 320 nm, whereas **2-OMe** and **3-OMe** have their maxima at 338 and 344 nm, respectively. A similar trend was observed for compounds **4-6** (Figure 8 and Table 4). These differences can either be because the substituents influence the

electronic properties of the terthiophene backbone due to electron donating; or withdrawing effects. Another reason could be the twisting of the backbone towards a less planar conformation, compromising the conjugation length.

*Figure 8: Normalised absorption of all terthiophene isomers in chloroform (left) and water (right). Concentrations used are 1.0 mM for **1-3**; 0.1 mM for **4-6**.*

The substituents used here ($-CH_2(CH_2)_{14}CH_3$ and $-CH_2(OCH_2CH_2)_4OMe$) do not have strong electron donating or withdrawing character. However, because of steric interactions between the substituents, the planarity of the terthiophene is increasingly compromised going from **1** and **4** which have the substituents of similar polarity pointing towards each other and this is seen in the relatively low absorption maximum. For **2** and **5** the substituents are in the same direction and therefore hardly interact sterically. **3** and **6** have even less steric interaction since they are in opposite directions, resulting in the most planar terthiophene structure and the more red-shifted absorption maximum. These findings concur with recent studies of simple, differently methyl-substituted terthiophenes by comparing models with experimental data. It was shown that steric repulsion by groups as small as a methyl-groups is the major contributor to changes of the photo-physical properties in differently substituted terthiophenes.[32,33]
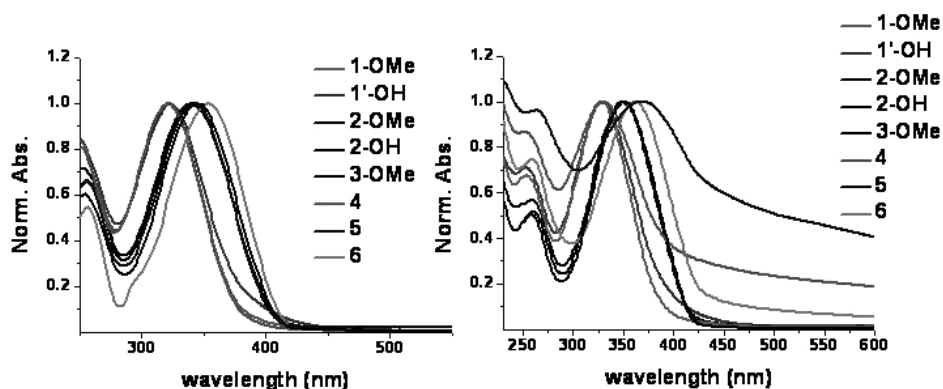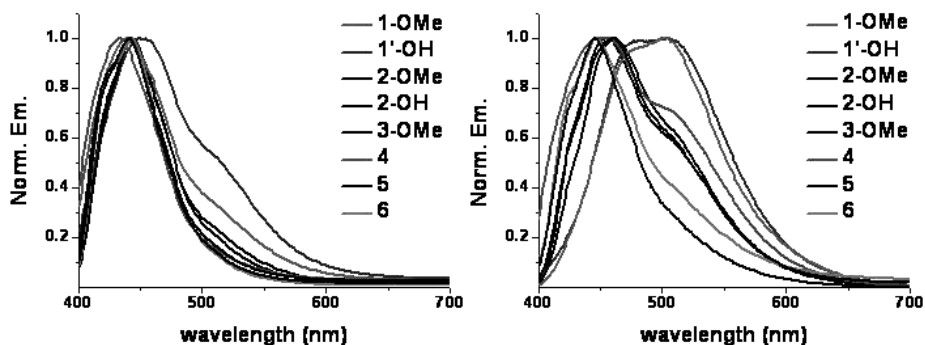
*Figure 8: Normalised emission of all thiophene surfactants in chloroform (left) and water (right). Concentrations used are 1.0 mM for **1-3**; 0.1 mM for **4-6**.*

The differences between the terthiophenes are also reflected in the emission maxima of the terthiophenes (Figure 9), though the trend was not as clear as for the absorption.

A complete overview of photo-physical values of λ_{max} and molar absorptions (ε) are given in Table 4, in water as well as in chloroform together with the fluorescence quantum yields in water.

3.8 Conclusion

A molecular system was developed which is programmed to self-assemble into different types of aggregates with various morphologies. These morphologies are based on surfactant systems which have the ability to form defined architectures upon solubilisation. It was found that different architectures could be obtained by changing the substitution pattern with ethylene glycol chains and alkyl chains on small conjugated oligothiophenes. This induces a change in overall distribution of hydrophilicity and hydrophobicity of the surfactant and in agreement with the structure-shape concept of surfactants, architectures like spherical- and elongated micelles, and bilayer structures could be formed. This aggregation takes place at low

concentration in the micro-molar regime. Due to the temperature sensitivity of ethylene glycol, the surfactant systems also display thermotropic behaviour and switching between aggregates is possible simply by changing the temperature. For longer oligomers to be prepared from these terthiophenes, compounds **2** and **5** appear to be good candidates. For **1** and **4**, the planar terthiophene structure is compromised due to steric hindrance of the substituents. This will also be the case for **3** and **6**, only then after oligomerisation. The study of the longer oligomers will be the topic of the next chapter. It is important that these structural studies are performed since it gives good insights in how to construct new systems and materials. For this we prefer that the systems are formed in pure water without any co-solvents or additives, since, with respect to possible applications, it could be of great interest, not only for molecular electronics but also for compatiblity with natural amphiphilic system. In this way, new electronic properties could be added to known natural systems. This will open a new field of biotronics, combining biology and molecular electronics in such a way that the molecular electronic active species is an integrated part of a biological system. More often it is seen that the biological systems is integrated into a molecular electronic system often referred to as an example of bioelectronics.

3.9   Experimental Section

General information

Starting materials were commercially available and were used without further purification. Synthesis of compound **10** and **17** was performed according to literature procedures (ref. 19). Aldrich silica gel Merck grade 9385 (230-400 mesh) was used for column chromatography, in combination with the Teledyne Isco CombiFlash Companion with UV-detection. All solvent used for dry reactions were purified with the use of MBRAUN Solvent purification system MB SPS-800, MilliQ-water was used in case of measurements. ^{1}H NMR-spectra were recorded on a Bruker Avance-

400 spectrometer (at 400MHz) or a Varian Inova-300 spectrometer (at 300MHz), at 25ºC. The splitting patterns are noted as follows: s (singlet), d (doublet), dd (double doublet), t (triplet), q (quartet), qt (quintet), m (multiplet) and bs (broad singlet). ^{13}C NMR spectra were recorded on a Bruker Avance-400 spectrometer (at 100 MHz) or a Varian Inova-300 spectrometer (at 75 MHz). Multiplicity was determined by Attached Proton Test (APT) and chemical shifts are given in δ (ppm) referenced to the residual protic solvent peaks. Coupling constants *J*, are given in Hz. LC-MS was performed on a SHIMADZU Liquid Chromatograph Mass Spectrometer, LCMS-2010, LC-8A pump with a diode-array detector SPD-M20. The column used here was the Xbridge Shield RP 18.5μm (4.6x150mm) with (95/5 v/v, MeOH-H$_2$O mixture as eluent). For UV/Vis measurements an AnalytikJena Specord 250 spectrometer was used equipped with a deuterium-lamp and a halogen-lamp. Quartz cuvets were used with path-lengths varying from 10mm-0.1mm. Fluorescence spectroscopy was done on a Jasco J-815 CD-spectrometer equipped with a fluorescence monochromator and detector, and an with an L-38 low wavelength filter (cut-off 380nm) placed between the sample and the detector. The cuvet used here was quartz with dimensions 3x3mm. Dynamic Light Scattering was performed on a ZetaSizer Nano series Nano-ZS by Malvern Instruments. For cryo-TEM, a few microliter of suspension was deposited on a bare 700 mesh copper grid. After blotting away the excess of liquid the grids were plunged quickly in liquid ethane. Frozen-hydrated specimens were mounted in a cryo-holder (Gatan, model 626) and observed in a Philips CM 120 electron microscope, operating at 120 KV. Micrographs were recorded under low-dose conditions on a slow-scan CCD camera (Gatan, model 794).

<div style="text-align: center;">*Experimentals*</div>

Description for synthesis of compounds 1-, 2- 3-OMe and 4-6.

2-bromo-3-hexadecylthiophene (**11**): *3*-hexadecylthiophene (**10**) (2.5 g, 8.1 mmol) was dissolved in 10 ml of chloroform. To this *N*-bromosuccinimide NBS (2.9 g, 16 mmol) was added at room temperature. It was allowed to react overnight. The reaction was quenched with 50 ml saturated sodium bicarbonate solution. Then 40 ml of chloroform was added. Organic and water phases were separated. Organic phase was washed with water and brine, dried over MgSO$_4$. Solvent was removed under vacuo. The title compound was obtained as a colourless oil which solidifies when cooled at 4ºC to a soft off-white solid in 90% yield (2.8 g, 7.3 mmol) and was not subdued to further purification. ^{1}H NMR (400 MHz, CDCl$_3$) δ$_H$: 0.88 (t, J_3 = 6.8 Hz, 3H), 1.20-1.38 (m, 26 H), 1.50-1.66 (m, 4H), 2.55 (t, J_3 = 7.8 Hz, 2H), 6.79 (d, J_3 = 5.6 Hz, 1H), 7.18 (d, J_3 = 5.6 Hz, 1H).

(3-hexadecylthiophen-2-yl)trimethylsilane (**12***): *2*-bromo-*3*-hexadecylthiophene (**11**) (10.0 g, 25.8 mmol) was dissolved in 250 ml of dry THF and cooled to -78°C. Then *n*-butyllithium (21.0 ml, 33.6 mmol, 1.6M in hexane) was added drop wise. The mixture was allowed to react at -78°C for 2h. Then TMSCl (6.6 ml, 51.6 mmol) was slowly added. The mixture was allowed to react at -78°C for additional 2h and then left overnight to slowly reach room temperature and was then quenched with water. The mixture was extracted with THF and diethyl ether. The combined organic layers were then washed with brine. The organic layer was dried over MgSO$_4$ and filtered; the solvent was removed under vacuo. The resulting slightly yellowish liquid was identified as the title compound obtained as a colourless oil which solidifies when cooled at 4ºC to a soft off-white solid in 89% yield (9.4 g, 23.0 mmol) and was used without further purification. ^{1}H NMR (400MHz, CDCl$_3$) δ$_H$:

0.35 (s, 9H), 0.88 (t, J_3 = 6.7 Hz, 3H), 1.26-1.32 (m, 26H), 1.55-1.65 (m, 2H), 2.67 (t, *J* = 7.8 Hz, 2H), 7.05 (d, J_3 = 4.7 Hz, 1H), 7.45 (d, J_3= 4.7 Hz 1H).

(3-hexadecylthiophen-2-yl)trimethylstannane (**12**):   A solution of 2.0 g (5.2 mmol) of *2*-bromo-*3*-hexadecylthiophene (**11**) in 15 ml of dry THF was cooled to -50˚C. To this 1.05 equivalent of *n*-butyllithium (3.4 ml, 1.6 M in hexane) was slowly added and the reaction mixture was stirred for 4 hours. Then 6.3 ml of a 1M solution of trimethyltinchloride in THF was added slowly to the mixture. After addition the mixture was stirred for 2 hours at -50˚C and was then allowed to slowly warm to room temperature overnight. The reaction was quenched with water. The organic and aqueous phases were separated and the organic phase was subsequently washed with water two times, then once with brine and dried over MgSO$_4$. After filtration, the solvent was removed in vacuum. The title compound was obtained as a colourless oil which solidifies when cooled at 4ºC to a soft off-white solid in 82% yield (2.5 g, 4.3 mmol) and was not subdued to further purification. ^{1}H NMR (400MHz, CDCl$_3$) δ_H: 0.37 (s, 9H), 0.85-1.00 (s, 3H), 1.20-1.40 (m, 26H), 1.50-1.70 (m, 2H), 2.62 (t, J_3 = 7.8 Hz, 2H), 7.09 (d, J_3= 4.6 Hz, 1H), 7.53 (d, J_3 = 4.7 Hz, 1H).

2,5-dibromo-3-hexadecylthiophene (**13**) : *3*-hexadecylthiophene (**10**) (1.50 g, 4.9 mmol) was dissolved in chloroform. To this Br$_2$ (1.55 g, 9.7 mmol) (2 equivalent) was added at 0 [0]C. It was allowed to react overnight. The reaction was quenched with a saturated bicarbonate solution. Then chloroform was added. Organic and aqueous phases were separated. The organic phase was washed with water and brine, dried over MgSO$_4$. Solvent was removed and the title compound was obtained in as a colourless oil which solidifies when cooled at 4ºC to a soft off-white solid a 94% yield (2.0 g, 4.6 mmol). This was used without any further purification. ^{1}H NMR (400 MHz, CDCl$_3$) δ_H: 0.87 (t, J_3 = 6.8 Hz, 3H), 1.22-1.33 (m, 25H), 1.42-1.52 (m, 2H), 2.49 (t, J_3 = 7.7 Hz, 2H), 6.77 (s, 1H).

(3-hexadecylthiophen-2-yl-trimethylsilyl-5-yl)trimethylstannane (**15**): To 100ml of THF diisopropylamine (4.2 ml, 29.7 mmol) was added. The mixture was cooled to -78°C. Then *n*-butyllithium (16.9 ml, 27.0 mmol, 1.6M in hexane) was added drop wise. The mixture was allowed to react at -78°C for 2h. Then *3*-hexadecylthiophen-*2*-yl)trimethylsilane (**12***) (9.4 g, 23.0 mmol) was added and the mixture was stirred for 4h. After this trimethyltinchloride (5.9 g, 29.7 mmol, 1M in THF) was slowly added. The mixture was allowed to react at -78°C for additional 2h and then left overnight to slowly reach room temperature and was then quenched with water. The mixture was extracted with THF and diethyl ether. The combined organic layers were then washed with brine. The organic layer was dried over $MgSO_4$ and filtered; the solvents were removed under vacuo. The resulting slightly yellowish liquid was identified as the title compound obtained as a colourless oil which solidifies when cooled at 4ºC to a soft off-white solid in 89% yield (12.4 g, 22.7mmol) and was used without further purification. ^{1}H NMR (400 MHz, $CDCl_3$) δ_H: 0.27 (s, 9H), 0.33 (s, 9H), 0.88 (t, J_3 = 6.7 Hz, 3H), 1.26-1.32 (m, 26H), 1.54-1.63 (m, 2H), 2.62 (t, J_3 = 7.8 Hz 2H), 7.03 (s, 1H). ^{13}C NMR (100 MHz, $CDCl_3$) δ_C: -8.12 (3*CH_3), 0.41 (3*CH_3), 22.54 (2*CH_2), 29.35(CH_2), 29.39 (CH_2), 29.49 (CH_2), 29.57 (CH_2), 29.60(CH_2), 29.65 (CH_2), 29.71 (CH_2), 30.29 (CH_2), 30.58 (CH_2), 31.25 (CH_2), 31.84 (CH_2), 31.94 (2*CH_2), 130.01 (CH), 135.25 (C), 142.7 (C).

1-(2,5-dibromothiophen-3-yl)-2,5,8,11,14-pentaoxapenta-decane (**18**): To a solution of *1*-(*2*-bromothiophen-*3*-yl)-*2,5,8,11,14*-pentaoxapentadecane (**17**) (0.5 g, 1.3 mmol) in 7 ml of DCM, *N*-bromosuccinimide (NBS) (0.23 g, 1.3 mmol) was added. After addition the mixture was stirred for overnight at room temperature and was then quenched with water. The mixture was extracted with DCM. The combined organic layers were then washed with a 1 M NaOH solution followed by water and brine. The organic layer was dried over $MgSO_4$ and filtered; the solvent was removed under vacuo. The resulting slightly yellowish liquid was identified as the title compound and obtained in 91% yield (0.55 g, 1.2 mmol). ^{1}H NMR (400 MHz,

CDCl$_3$) δ_H: 3.37 (s, 3H), 3.56-3.52 (m, 2H), 3.70-3.60 (m, 14H), 4.43 (s, 2H), 6.99 (s, 1H).

2-[2-(2-methoxyethoxy)ethoxy]ethyl 2-{[2-(trimethylstannyl)-3-thienyl]methoxy}ethyl ether (**19**): A solution of 2.0 g (5.2 mmol) of *1*-(*2*-bromothiophen-*3*-yl)-*2,5,8,11,14*-pentaoxapentadecane (**17**) in dry THF was cooled to -78˚C. To this 1.05 equivalent of *n*-butyllithium (3.44 ml, 1.6 M in hexane) was added slowly and the reaction mixture was stirred for 4 hours at -78˚C, during this time the colour changed to black. Then 6.37 ml of a 1 M solution of trimethyltinchloride in THF was added slowly to the mixture. After addition the mixture was stirred for 2 hours at -78˚C and was then allowed to slowly warm to room temperature overnight. The reaction was quenched with water. The organic and aqueous phases were separated and the organic phase was subsequently washed with water two times, then once with brine and dried over MgSO$_4$. After filtration and removal of solvent in vacuum, the title compound was obtained as a viscous yellow liquid in a 74% yield (1,8 g, 3.9 mmol). ^{1}H NMR (400 MHz, CDCl$_3$) δ_H: 0.36 (s, 9H), 3.37 (s, 3H), 3,65 (m, 16H), 4,5 (s, 2H), 7,17 (d, J$_3$ = 4.6 Hz, 1H), 7,54 (d, J$_3$ = 4.7 Hz, 1H).

2-[2-(2-methoxyethoxy)ethoxy]ethyl 2-{[2-(trimethylsilyl)-3-thienyl]methoxy}ethyl ether (**20**): A solution of *1*-(*2*-bromothiophen-*3*-yl)-*2,5,8,11,14*-pentaoxapentadecane (**17**) (13.0 g, 34 mmol) in 120 ml of dry THF under nitrogen atmosphere was cooled to -78°C. To this 1.05 equivalent of *n*-butyllithium (20 ml, 1.6 M in hexane) was added slowly and the reaction mixture was stirred for 3 hours. Then the reaction was quenched with trimetylsilylchloride (4.0 ml, 35.3 mmol) and stirred for an additional 3 hours at -78°C. After this the mixture was allowed to warm to room temperature slowly overnight and then quenched with water. The mixture was washed twice with water and once with brine and dried over MgSO4. After filtration and removal of solvent in vacuo, the title compound was obtained as

a yellowish oil in 86% yield (11.0 g, 29.3 mmol). The crude compound was used without further purification. ^{1}H-NMR (400 MHz, CDCl$_3$) δ_H: 0.34 (s, 9H), 3.37 (s, 3H), 3.52-3.56 (m, 2H), 3.60-3.69 (m, 14H), 4.59 (s, 2H), 7.20 (d, 1H, J$_3$= 4.9 Hz), 7.48 (d, 1H, J$_3$= 4.8Hz).

2-[2-(2-methoxyethoxy)ethoxy]ethyl2-{[2-(trimethylsilyl)-5-(trimethylstannyl)-3 thienyl]methoxy}ethyl ether (**21**): A solution of 4.0 ml diisopropylamine in 120 ml of dry THF was cooled to -78°C. To this 18.5 ml (29.6 mmol) of *n*-butyllithium was added. The mixture was then allowed to reach 0˚C and was stirred at this temperature for 10 minutes. Then it was again cooled to -78°C and 11.0 g (29.3 mmol) of **20** was added dissolved in 30 ml of dry THF and the mixture was stirred for 4 hours. Then 6 ml of trimethyltinchloride solution (5 M in THF) was added and the mixture was continues to be stirred at -78°C. After 3 hours the reaction mixture was allowed to slowly warm to room temperature overnight. The reaction was quenched with water with water and the layers were separated. The aqueous layer was extracted with diethyl ether. The combined organic layers were washed with water and then with brine. The organic phase was dried over MgSO$_4$. After filtration and removal of solvent in vacuo, the crude compound was obtained in a 98% yield (15.2 g, 28.9 mmol). This compound was used without further purification. ^{1}H-NMR (400 MHz, CDCl$_3$) δ_H: 0.34 (s, 9H), 0.35 (t, 9H, J$_{Sn}$= 29.7 Hz), 3.37 (s, 3H), 3.52-3.56 (m, 2H), 3.62-3.69 (m, 14H), 4.62 (s, 2H), 7.28 (s, 1H,).

(4-hexadecyl-3'-2,5,8,11,14-pentaoxapentadecyl-2,2'-bithiophen-5-yl)trimethylsilane(**22**):   1-(2-bromothiophen-3-yl)-2,5,8,11,14-pentaoxapentadecane (7.0 g, 18.4 mmol) was dissolved in 50 ml of dry DMF. Then palladium(tetrakis)triphenylphosphine (2.20 g, 1.9 mmol) was added to the solution. Mixture stirred for 20 min at room temperature. Then **15** (10.0 g, 18.4 mmol) solution in 50 ml of toluene was added. Temperature was raised until 110°C and left overnight. Then the solvents were removed under vacuo. The crude was purified by

column chromatography (silica gel, eluent petroleum ether/EtOAc (gradient 0-100% EtOAc) with 5% TEA) and gave the pure title compound as a yellow oil in 80% yield (8.0 g, 14.7 mmol). ^{1}H NMR (400 MHz, CDCl$_3$) δ_H: 0.37 (s, 9H), 0.88 (t, J_3= 6.7 Hz, 3H), 1.22-1.38 (m, 26H), 1.58-1.68 (m, 2H), 2.65 (t, J_3= 7.8 Hz, 2H), 3.38 (s, 3H), 3.52-3.58 (m, 2H), 3.72-3.62 (m, 14H), 4.64 (s, 2H), 7.09 (s, 1H), 7.11 (d, J_3= 5.2 Hz 1H), 7.17 (d, J_3= 5.2 Hz 1H). ^{13}C NMR (100 MHz, CDCl$_3$) δ_C: 0.01 (3*CH$_3$), 14.00 (CH$_3$), 22.52 (2*CH$_2$), 29.34(CH$_2$), 29.37 (CH$_2$), 29.50 (CH$_2$), 29.55 (CH$_2$), 29.58(CH$_2$), 29.64 (CH$_2$), 29.70 (CH$_2$), 30.27 (CH$_2$), 30.56 (CH$_2$), 58.58 (CH$_3$), 66.58 (CH$_2$), 69.20 (CH$_2$), 70.31(CH$_2$), 70.48 (4*CH$_2$), 70.49 (CH$_2$), 71.30 (CH$_2$), 123.50 (CH), 129.51 (CH), 129.52 (CH), 133.52 (C), 134.25 (C), 134.51 (C), 138.58 (C), 150.58 (C).

4-hexadecyl-3'-2,5,8,11,14-pentaoxapentadecyl-5'-(trimethylstannyl)-2,2'-bithiophen-5-yl)trimethylsilane (**23**): To 100ml of THF diisopropylamine (1.9 ml, 13.5 mmol) was added. Mixture was cooled to -78°C. Then *n*-butyllithium (8.5 ml, 13.5 mmol, 1.6M in hexane) was added drop wise and the reaction was allowed to warm to room temperature. The mixture was then cooled to -78°C and **22** (7.3 g, 13.5 mmol) dissolved in THF was added dropwise. The mixture was allowed to react at -78°C for 2h. Then trimethyltinchloride (2.7 g, 13.5 mmol, 1M in THF) was slowly added. The mixture was allowed to react at -78°C for additional 2h and then left overnight to slowly reach room temperature and was then quenched with water. The mixture was extracted with THF and diethyl ether. The combined organic layers were then washed with brine. The organic layer was dried over MgSO$_4$ and filtered; the solvents were removed under vacuo. The resulting slightly yellowish liquid was determined as the title compound obtained in 78% yield (7.0 g, 10.5 mmol) and was used without further purification.^{1}H NMR (400 MHz, CDCl$_3$) δ_H: 0.36 (s, 9H), 0.38 (s, 9H), 0.88 (t, J_3= 6.7 Hz, 3H), 1.22-1.38 (m, 26H), 1.58-1.68 (m, 2H), 2.65 (t, J_3= 7.8 Hz, 2H), 3.38 (s, 3H), 3.52-3.58 (m, 2H), 3.72-3.62 (m, 14H), 4.65 (s, 2H), 7.09 (s, 1H), 7.19 (s, 1H). ^{13}C NMR (100 MHz, CDCl$_3$) δ_C: -8.12 (3*CH$_3$), 0.41 (3*CH$_3$),

14.10 (CH$_3$), 22.52 (2*CH$_2$), 29.42 (CH$_2$), 29.50 (2*CH$_2$), 29.51(4*CH$_2$), 29.53 (5*CH$_2$), 29.54 (CH$_2$), 58.88 (CH$_3$), 66.88 (CH$_2$), 69.30 (CH$_2$), 70.41(CH$_2$), 70.58 (4*CH$_2$), 70.60 (CH$_2$), 71.98 (CH$_2$), 129.38 (CH), 133.56 (C), 135.61 (C), 136.52 (C), 138.15 (CH), 139.24 (C), 142.21 (C), 151.00 (C).

1-(4'-hexadecyl-2,2'-bithiophen-3-yl)-2,5,8,11,14-pentaoxapentadecane (**24**): A solution of 7.3 g (19.1 mmol) of 1-(2-bromothiophen-3-yl)-2,5,8,11,14-pentaoxapentadecane, 2.0 g palladium(tetrakis)triphenylphosphine in 300 ml DMF was prepared under a nitrogen atmosphere and stirred for 20 minutes. To this, 9.0 g (19.1 mmol) of **14** in 100 ml toluene was added and heated at 110°C overnight. The reaction mixture was allowed to cool to room temperature solvent was removed in vacuo. The crude was purified by column chromatography (silica gel, eluent pentane/EtOAc (1:1), Rf: 0.45) and gave the pure title compound as a yellow oil in 71% yield (8.3 g, 13.6 mmol). ^{1}H-NMR (300 MHz): 0.87 (t, 3H, J$_3$= 6.9Hz), 1.20-1.42 (m, 26H), 1.63-1.70 (m, 2H), 2.59 (t, 2H, J$_3$= 7.7Hz), 3.37 (s, 3H), 3.51-3.57 (m, H), 3.61-3.69 (m, 14H), 4.61 (s, 2H), 6.90 (s, 1H), 6.99 (d, 1H, J$_4$=1.3Hz), 7.11 (d, 1H, J$_3$= 5.2Hz), 7.17 (d, 1H, J$_3$= 5.0 Hz).

1-(5'-bromo-4'-hexadecyl-2,2'-bithiophen-3-yl)-2,5,8,11,14-pentaoxapentadecane (**25**): To a solution of 8.3 g (13.6 mmol) of **24** in 75 ml DCM, 1.0 equivalent of *N*-bromosuccinimide was added. The mixture was stirred overnight. After completion the solvent was removed in vacuo. The crude was solubilised in cold heptane and filtered over celite. After evaporation of the solvent, purification was done by column chromatography (solid silica, Pentane/EtOAc (1:1)) and gave the pure title compound as a yellow oil in 95% yield (8.9 g, 12.9 mmol). ^{1}H-NMR (300 MHz): 0.87 (t, 3H, J$_3$= 6.9 Hz), 1.20-1.42 (m, 26H), 1.63-1.70 (m, 2H), 2.55 (t, 2H, J$_3$=7.5 Hz), 3.37 (s, 3H), 3.51-3.57 (m, H), 3.61-3.69 (m, 14H), 4.56 (s, 2H), 6.86 (s, 1H), 7.10 (d, 1H, J$_3$=5.4 Hz), 7.19 (d, 1H, J$_3$= 5.1 Hz).

(**1-OMe**): A solution of 0.9 g (1.9 mmol) of **13**, 0.1 g palladium(tetrakis)triphenylphosphine in 5 ml DMF was prepared and stirred for 20 minutes. To this, 1.8 g (4.3 mmol) of **19** was added and heated at 110°C overnight. The reaction mixture was allowed to cool to room temperature and filtrated to remove any solids. To the residue an excess of water was added and this was then extracted with di-ethyl ether. The obtained organic phase was washed with brine and then dried over Na_2SO_4. After filtration and removal of solvent in vacuum the crude was purified by column chromatography (silica gel, eluent pentane/EtOAc (gradient 0-100% EtOAc)) and gave the pure title compound as a yellow oil in a 38% yield (0.66 g, 0.72 mmol). ^{1}H NMR (400 MHz, CDCl$_3$) δ_H: 0.873 (t, J$_3$= 6,7 Hz, 3H), 1.30-1.180 (m, 28 H), 2.48 (t, J$_3$= 7.7 Hz, 2H), 3.36 (s, 6H), 3.70-3.60 (m, 32H), 4.47 (s, 2H), 4.63 (s, 2H), 7.03 (s, 1H), 7,13 (d, J$_3$= 5.2 Hz, 1H) 7.18 (d, J$_3$= 3.7, 1H), 7.19 (d, J$_3$= 3.7 Hz, 1H), 7.34 (d, J$_3$= 5.3 Hz, 1H).^{13}C NMR (100 MHz, CDCl$_3$) δ_C: 14.15 (CH$_3$), 22.62 (2*CH$_2$), 28.99 (CH$_2$), 29.43 (CH$_2$), 29.49 (2*CH$_2$), 29.69(7*CH$_2$), 30.69 (CH$_2$), 31.89 (CH$_2$), 58.98 (2*CH$_3$), 66.28 (2*CH$_2$), 69.35 (2*CH$_2$), 70.50 (2*CH$_2$), 70.55 (2*CH$_2$), 70.59 (8*CH$_2$), 71.89 (2*CH$_2$), 123.91 (CH), 126.05 (CH), 128.02 (CH), 128.17 (C), 128.59 (CH), 130.51 (CH), 131.11 (C), 135.12 (C), 135.21 (C), 138.25 (2*C), 143.26 (C). (Mass: ESI) M/z-calc: 912.5; M/z-found: 935.5 (M+Na^{+}).

(**2-OMe-TMS**): A solution of 5.1 g (7.4 mmol) of **25**, 0.32 g palladium(tetrakis)triphenylphosphine in 80 ml DMF/Toluene (50/50) was prepared under a nitrogen atmosphere and stirred for 20 minutes. To this, 12.2 g (17.8 mmol) of **21** in 20 ml DMF/Toluene (50/50) was added and heated at 110°C overnight. The solvents were removed in vacuo and the crude was purified by column chromatography (silica gel, eluent heptane/EtOAc gradient 0-100% EtOAc). This gave the pure title compound in 80% yield (5.9 g, 5.9 mmol). ^{1}H-NMR (400 MHz, CDCl$_3$) δ_H: 0.37 (s, 9H), 0.88 (t, 3H, J$_3$=7.4 Hz), 1.20-1.44 (m, 26H), 1.60-1.70 (m, 2H), 2.74 (t, 2H, J$_3$=7.8 Hz), 3.37 (s, 6H), 3.54-3.63 (m, 4H), 3.66-3.76 (m, 28H),

4.56 (s, 2H), 4.62 (s, 2H), 6.99 (s, 1H), 7.12 (d, 1H, J_3=5.2 Hz), 7.18 (d, 1H, J_3=5.6 Hz), 7.21 (s, 1H).

(**2-OMe**): **2-OMe-TMS** (2.4 g, 2.3 mmol) was stirred overnight in a TBAF solution in THF. After removal of the solvent the yellow oil was dissolved in water and 100 g of a cationic ion-exchange resin (DOWEX MAC-3) was added and the suspension was stirred until the water became colourless and the resin yellow. This was then filtrated and washed several times with water to remove the TBAF. After extensive rinsing, the product was released from the resin by washing with methanol to obtain the pure title compound in quantitative yield as a yellow oil (2.6 g, 2.3 mmol). ^{1}H-NMR (400 MHz, CDCl$_3$) δ_H: 0.87 (t, 3H, J_3= 7.4Hz), 1.15-1.40 (m, 26H), 1.60-1.68 (m, 2H), 2.73 (t, 2H, J_3= 7.8 Hz), 3.37 (s, 6H), 3.54-3.63 (m, 4H), 3.66-3.76 (m, 28H), 4.55 (s, 2H), 4.64 (s, 2H), 6.99 (s, 1H), 7.08 (d, 1H, J_4=1.3 Hz), 7.12 (d, 1H, J_3= 5.2Hz), 7.19 (d, 1H, J_3=5.6Hz), 7.20 (d, 1H, J_4= 1.3Hz); ^{13}C-NMR (100 MHz, CDCl$_3$) δ_C: 13.99 (CH$_3$), 22.50 (CH$_2$), 29.10 (CH$_2$), 29.17 (CH$_2$), 30.45 (CH$_2$), 31.53 (CH$_2$), 61.56 (CH$_2$), 66.77 (CH$_2$), 68.42 (CH$_2$), 69.30 (CH$_2$), 69.33 (CH$_2$), 70.18 (CH$_2$), 70.44 (CH$_2$), 70.47 (CH$_2$), 70.50 (CH$_2$), 72.45 (CH$_2$), 122.84 (CH), 123.85 (CH), 126.04 (CH), 129.20 (CH), 130.03 (CH), 132.98 (C), 134.99 (C), 136.13 (C), 139.64 (C), 140.06 (C). (Mass: ESI) M/z-calc: 912.5; M/z-found: 935.5 (M+Na$^+$).

(**3-OMe**). A solution of 1.1 g (2.5 mmol) of **13** and palladium(tetrakis)triphenylphosphine in 5ml DMF was prepared and stirred for 20 minutes. To this, 2.6 g (5.0 mmol) of **21** was added and heated at 110˚C overnight. The solvent was removed in vacuo and redissolved in 10% HCl methanol solution and stirred for 4h. After removal of all volatile compounds in vacuo, crude was purified by column chromatography (silica gel, eluent PET 40-60/EtOAc in a gradient 0-100% EtOAc) and gave the pure title compound as a yellow oil in a 40% yield (900 mg, 1.0 mmol). ^{1}H NMR (400 MHz, CDCl$_3$) δ_H: 0.88 (t, J_3= 6.7 Hz, 3H), 1.22-1.38 (m, 26H), 1.58-1.68 (m, 2H), 2.70 (t, J_3= 8.0 Hz, 2H), 3.37 (s, 6H), 3.51-

3.56 (m, 4H), 3.62-3.70 (m, 28H), 4.52 (s, 2H), 4.55 (s, 2H), 6.98 (s, 1H), 7.07 (s, 1H), 7.09 (s, 1H), 7.11 (s, 1H), 7.18 (s, 1H). ^{13}C NMR (100 MHz, CDCl3) δ_C: 14.09 (CH$_3$), 22.65 (CH$_2$), 29.29(CH$_2$), 29.32 (CH$_2$), 29.44 (CH$_2$), 29.53 (CH$_2$), 29.57 (CH$_2$), 29.66 (CH$_2$), 30.52 (CH$_2$), 31.88 (CH$_2$), 68.48 (CH$_2$), 68.53 (CH$_2$), 69.40 (CH$_2$), 70.47 (CH$_2$), 70.57 (CH$_2$), 70.61 (CH$_2$), 71.89 (CH$_2$), 121.70 (CH), 122.74 (CH), 123.72 (CH), 125.98 (CH), 126.45 (CH), 129.59 (C), 135.01 (C), 136.37 (C), 137.67 (C), 139.75 (C), 140.22 (C), 140.27 (C).

(**4**): A solution of 0.6 g (1.3 mmol) of **18**, 0.1 g (0.1 mmol) palladium(tetrakis)triphenylphosphine in 5 ml DMF was prepared and stirred for 20 minutes. To this, 1.2 g (2.6 mmol) of **12** was added and heated at 110˚C overnight. The reaction mixture was allowed to cool to room temperature and filtrated to remove any solids. To the residue an excess of water was added and this was then extracted with di-ethyl ether. The obtained organic phase was washed with brine and then dried over Na$_2$SO$_4$. After filtration and removal of solvent in vacuum the crude was purified by column chromatography (silica gel, eluent PET 40-60/EtOAc in a gradient 0-100% EtOAc) and gave the pure title compound as a yellow oil in a 40% yield (0.85 g, 0,9 mmol).^{1}H NMR (400 MHz, CDCl$_3$) δ_H: 0.82-0.94 (m, 6H), 1.16-1.40 (m, 52H), 1.50-1.70 (m, 4H), 2.55 (t, J$_3$= 7.8 Hz, 2H), 2.77 (t, J$_3$= 7.75 Hz, 2H), 3.37 (s, 3H), 3.5-3.6 (m, 2H), 3.6-3.74 (m, 14H), 4.42 (s, 2H), 6.92 (d, J$_3$= 5.20 Hz, 1H), 6.97 (d, J$_3$= 5.2 Hz, 1H), 7.16 (d, J$_3$= 5.2 Hz, 1H), 7.17 (s, 1H), 7.31 (d, J$_3$= 5.2 Hz, 1H). ^{13}C NMR (100 MHz, CDCl$_3$) δ_C: 14.11 (2*CH$_3$), 22.52 (2*CH$_2$), 29.33(CH$_2$), 29.35 (CH$_2$), 29.50 (CH$_2$), 29.49 (CH$_2$), 29.69(11*CH$_2$), 29.71 (10*CH$_2$), 30.71 (CH$_2$), 30.83 (CH$_2$), 31.92 (CH$_2$), 59.03 (CH$_3$), 66.75 (CH$_2$), 69.40 (CH$_2$), 70.50 (CH$_2$), 70.55 (CH$_2$), 70.61 (4*CH$_2$), 71.62 (CH$_2$), 123.70 (CH), 125.81 (CH), 126.99 (CH), 128.85 (CH), 130.01 (CH), 131.12 (C), 132.15 (C), 133.52 (C), 134.41 (C), 138.02 (C), 139.72 (C), 144.01 (C). (Mass: ESI) M/z-calc: 916.6; M/z-found: 939.6 (M+Na$^+$).

(**5-TMS**) *2*-Bromo-*3*-hexadecylthiophene (**11**) (3.85 g, 9.9 mmol) was dissolved in 20 ml of toluene. Then palladium(tetrakis)triphenylphosphine (2.20 g, 1.9 mmol) was added to the solution. The mixture was stirred for 20 min at room temperature. Then **23** (7.0 g, 8.3 mmol) solution in 20 ml of toluene was added. Temperature raised until 110°C and left overnight. Then the solvents were removed under vacuo. The crude was purified by column chromatography (silica gel, eluent petroleum ether 40-60/EtOAc (gradient0-100% EtOAc)) with 5% TEA) and gave the pure title compound as a yellow oil in a 50% yield (4.0 g, 5.0 mmol). ^{1}H NMR (400 MHz, CDCl$_3$) δ_H: 0.36 (s, 9H), 0.88 (t, J$_3$= 6.7 Hz, 6H), 1.34-1.22 (m, 52H), 1.69-1.62 (m, 4H), 2.64 (t, J$_3$= 7.8 Hz, 2H), 2.77 (t, J$_3$= 7.8 Hz, 2H), 3.36 (s, 3H), 3.54-3.52 (m, 2H), 3.68-3.61 (m, 14H), 4.63 (s, 2H), 6.92 (d, J$_3$= 5.2 Hz, 1H), 7.10 (s, 1H), 7.12 (s, 1H), 7.15 (d, J$_3$= 5.2Hz, 1H).

(**5**): To 20 ml of 10% HCl solution in methanol **5-TMS** (300 mg, 0.3 mmol) was added. The mixture was allowed to react overnight at room temperature. Then solvent and HCl removed under vacou. The crude was purified by column chromatography (silica gel, petroleum ether 40-60/EtOAc (gradient0-100% EtOAc)) and gave the pure title compound in an 85% yield (250 mg, 0.26 mmol). ^{1}H NMR (400 MHz, CDCl$_3$) δ_H: 0.88 (t, J$_3$= 6.7 Hz, 6H), 1.34-1.22 (m, 52H), 1.69-1.62 (m, 4H), 2.60 (t, J$_3$= 7.6 Hz, 2H), 2.77 (t, J$_3$= 7.6 Hz, 2H), 3.37 (s, 3H), 3.54-3.52 (m, 2H), 3.69-3.61 (m, 14H), 4.61 (s, 2H), 6.92 (s, 1H), 6.92 (d, J$_3$= 5.2 Hz, 1H), 7.02 (d, J$_4$= 1.0 Hz, 1H), 7.12 (s, 1H), 7.16 (d, J$_3$= 5.2 Hz, 1H). ^{13}C NMR (100MHz, CDCl3) δ_H: 14.21 (2*CH$_3$), 22.75 (2*CH$_2$), 29.13(CH$_2$), 29.17 (CH$_2$), 29.45 (CH$_2$), 29.47 (CH$_2$), 29.68(11*CH$_2$), 29.70 (10*CH$_2$), 30.49 (CH$_2$), 30.71 (CH$_2$), 31.98 (CH$_2$), 59.00 (CH$_3$), 66.80 (CH$_2$), 69.40 (CH$_2$), 70.50 (CH$_2$), 70.55 (CH$_2$), 70.61 (4*CH$_2$), 71.91 (CH$_2$), 120.71 (CH), 127.81 (CH), 127.91 (CH), 128.51 (CH), 130.01 (CH), 134.09 (2*C), 134.49 (C), 134.99 (2*C), 139.71 (C), 143.95 (C). (Mass: ESI) M/z-calc: 916.6; M/z-found: 939.5 (M+Na$^+$).

(**6**): A solution of **18** (432 mg, 0.93 mmol), palladium(tetrakis)triphenylphosphine (50 mg, 0.04 mmol) and Cu(II)O (77 mg, 0.97 mmol) in 5 ml of dry DMF was prepared. To this **14** (964 mg, 1.90 mmol) was added. The mixture was stirred overnight at 110°C. After this, the reaction was cooled to room temperature. Formed residues were filtered off and water was added to the reaction mixture. The mixture was extracted with diethylether. The combined organic layers were then washed with brine. The organic layer was dried over $MgSO_4$ and filtered; the solvent was removed under vacuo. After filtration and removal of solvent in vacuum the crude was purified by column chromatography (silica gel, petroleum ether 40-60/EtOAc (gradient 0-100% EtOAc)) and gave the pure title compound in a 45% yield (368 mg, 0.42 mmol). ^{1}H NMR (400 MHz, $CDCl_3$) δ_H: 0.88 (t, J_3 = 6.7 Hz, 6H), 1.22-1.38 (m, 52H), 1.58-1.68 (m, 4H), 2.64-2.54 (m, 4H), 3.36 (s, 3H), 3.55-3.51 (m, 2H), 3.72-3.61 (m, 14H), 4.59 (s, 2H), 6.79 (s, 1H), 6.9 (s, 1H), 6.99 (s, 1H), 7.00 (s, 1H), 7.15 (s, 1H). ^{13}C NMR (100 MHz, CDCl3) δ_C: 14.11 (2*CH_3), 22.52 (2*CH_2), 29.23(CH_2), 29.25 (CH_2), 29.50 (CH_2), 29.51 (CH_2), 29.69(11*CH_2), 29.71 (10*CH_2), 30.49 (CH_2), 30.71 (CH_2), 31.92 (CH_2), 66.89 (CH_2), 69.41 (CH_2), 70.50 (CH_2), 70.55 (CH_2), 70.61 (4*CH_2), 71.91 (CH_2), 120.71 (CH), 123.71 (CH), 127.81 (CH), 128.51 (CH), 130.01 (CH), 134.29 (2*C), 134.49 (2*C), 134.59 (C), 139.71 (C), 143.95 (C). (Mass: ESI) M/z-calc: 916.6; M/z-found: 939.5 (M+Na^+).

Description for the synthesis of 1'-OH and 2-OH.

2-(2-(2-(2-(tetrahydro-2H-pyran-2-yloxy)ethoxy)ethoxy)ethoxy)ethanol: to an ice-cooled solution of tetra-ethylene glycol (194g, 1.0mol) and *2H*-dihydropyran (DHP) (34.4g, 0.4mol) in DCM (200ml), 5g *p*-toluenesulfonic acid was added. The mixture was stirred overnight. After this the mixture was washed with water and subsequently with brine and then dried over Na_2SO_4. After filtration the solvent was removed by evaporation in vacuo. The colourless oil was obtained in a 71% yield (80 g, 0.29 mol) and was used without further purification. ^{1}H-NMR (400MHz,

CDCl$_3$) δ$_H$: 1.38-1.58 (m, 4H), 1.64 (t, J$_3$=9.6Hz, 1H), 1.70-1.82 (m, 1H), 2.86 (bs, 1H), 3.38-3.46 (m, 2H) 3.50-3.68 (m, 14H), 3.75-3.84 (m, 2H), 4.53 (bs, 2H); ^{13}C-NMR (100MHz, CDCl$_3$) δ$_C$: 19.25 (CH$_2$), 25.24 (CH$_2$), 30.35 (CH$_2$), 61.49 (CH$_2$), 61.97 (CH$_2$), 66.45 (CH$_2$), 70.19 (CH$_2$), 70.34 (CH$_2$), 70.40 (CH$_2$), 70.42 (CH$_2$), 70.44 (CH$_2$), 72.38 (CH$_2$), 98.70 (CH).

trimethyl(3-(13-(tetrahydro-2H-pyran-2-yloxy)-2,5,8,11-tetraoxatridecyl)thiophen-2-yl)silane **(21-OTHP)**: A solution of **(17-OTHP)** (20.0 g, 43.4 mmol) in 150 ml anhydrous THF under nitrogen atmosphere was cooled to -78˚C. To this 1.05 equivalent of *n*-butyllithium (28.6 ml, 1.6 M in hexane) was added slowly and the reaction mixture was stirred for 4 hours. Then the reaction was quenched with trimetylsilylchloride (6.0 ml, 53 mmol) and stirred for an additional 2 hours at -78˚C. After this the mixture was allowed to warm to room temperature slowly overnight. The mixture was poured in water and then extracted with diethyl ether. The combined organic phases were then washed twice with water and once with brine and dried over MgSO$_4$. After filtration and removal of solvent in vacuo, the title compound was obtained in 87% yield (17.4 g, 37.7 mmol) and was used without further purification. ^{1}H-NMR (400MHz, CDCl$_3$) δ$_H$: 0.33 (s, 9H), 1.44-1.63 (m, 4H), 1.66-1.74 (m, 1H), 1.76-1.88 (m, 1H), 3.45-3.53 (m, 2H), 3.55-3.75 (m, 14H), 3.81-3.89 (m, 4H), 4.58 (s, 2H), 4.62 (bs, 1H), 7.19 (d, 1H, J$_3$=4.8Hz), 7.46 (d, 1H, J$_3$=4.4Hz). ^{13}C-NMR (100MHz, CDCl$_3$) δ$_C$: 0.25 (CH$_3$), 19.42 (CH$_2$), 25.38 (CH$_2$), 30.51 (CH$_2$), 62.13 (CH$_2$), 66.59 (CH$_2$), 68.59 (CH$_2$), 69.31 (CH$_2$), 70.48 (CH$_2$), 70.56 (CH$_2$), 70.58 (CH$_2$), 98.86 (CH), 129.54 (CH), 130.39 (CH), 137.44 (C), 146.00 (C).

trimethyl(3-(13-(tetrahydro-2H-pyran-2-yloxy)-2,5,8,11-tetraoxatridecyl)-5-(trimethylstannyl)thiophen-2-yl)silane **(21-OTHP)**: A solution of 6.5 ml diisopropylamine in 150 ml of anhydrous THF was cooled to -78˚C. To this 23.0 ml (36.5 mmol) of *n*-butyllithium (1.6 M in hexane) was added. The mixture was then

allowed to reach 0°C and was stirred at this temperature for 10 minutes. Then it was again cooled to -78°C and 16.8 g (36.5 mmol) of **(20-OTHP)** was added dissolved in 30 ml of dry THF and the mixture was stirred for 4 hours at -78°C. Then 20ml of trimethyltinchloride solution (1 M in THF) was added and the mixture was continued to be stirred at to -78°C. After 3 hours the reaction mixture was allowed to slowly warm to room temperature overnight. The reaction was quenched with water and the layers were separated. The aqueous layer was extracted with diethyl ether. The combined organic layers were washed with water and then with brine. The organic phase was dried over $MgSO_4$. After filtration and removal of solvent in vacuo, 22.5 g (36.1 mmol) of crude compound was obtained as a yellow oil. This compound was used without further purification. ^{1}H-NMR (400MHz, $CDCl_3$) δ_H: 0.34 (s, 9H), 0.35 (s, 9H), 1.47-1.65 (m, 4H), 1.67-1.76 (m, 1H), 1.78-1.88 (m, 1H), 3.46-3.54 (m, 2H), 3.57-3.71 (m, 14H), 3.82-3.91 (m, 2H), 4.62 (s, 2H), 4.63 (bs, 1H), 7.28 (s, 1H).

trimethyl(3-(13-(tetrahydro-2H-pyran-2-yloxy)-2,5,8,11-tetraoxatridecyl)-4-(trimethylstannyl)thiophen-2-yl)silane **(21'-OTHP)**: A solution of 6.5 ml diisopropylamine in 150 ml of anhydrous THF was cooled to -78°C. To this 23.0 ml (36.5 mmol) of *n*-butyllithium (1.6 M in hexane) was added. The mixture was then allowed to reach room temperature and was stirred for 10 minutes. Then 16.8 g (36.5 mmol) of **(20-OTHP)** was added dissolved in 30ml of dry THF and the mixture was stirred for 4 hours. Then 20ml of trimethyltinchloride solution (1 M in THF) was added and the mixture was continued to be stirred overnight. The reaction was quenched with water and the layers were separated. The aqueous layer was extracted with diethyl ether. The combined organic layers were washed with water and then with brine. The organic phase was dried over $MgSO_4$. After filtration and removal of solvent in vacuo, 19.8 g (31.7 mmol) of crude compound was obtained. This compound was used without further purification. ^{1}H-NMR (400MHz, $CDCl_3$) δ_H: 0.29 (s, 9H), 0.33 (s, 9H), 1.46-1.64 (m, 4H), 1.66-1.75 (m, 1H), 1.76-1.90 (m, 1H),

3.45-3.53 (m, 2H), 3.56-3.71 (m, 14H), 3.82-3.91 (m, 2H), 4.58 (s, 2H), 4.62 (bs, 1H), 7.30 (s, 1H).

(2-OTHP, TMS-protected): A solution of 5.6 g (7.4 mmol) of **(25-OTHP)**, 0.5g palladium(tetrakis)triphenylphosphine and 0.58 g (7.4 mmol) copper(II)oxide in 90 ml DMF was prepared and stirred for 20 minutes. To this, 5.0 g (8.0 mmol) of **(21-OTHP)** was added and heated at 110˚C overnight. The reaction mixture was allowed to cool to room temperature and filtrated to remove any solids. To the residue an excess of water was added and this was then extracted with di-ethyl ether. The obtained organic phase was washed with brine and then dried over Na_2SO_4. After filtration and removal of solvent in vacuo the crude was purified by column chromatography (silica gel, pentane/EtOAc (1:1)) gave the pure title compound as a yellow oil in 31% yield (2.4 g, 2.3 mmol). ^{1}H-NMR (400MHz, $CDCl_3$) δ_H:0.37 (s, 9H), 0.87 (t, 3H, J_3=6.8Hz), 1.20-1.33 (m, 26H), 1.43-1.64 (m, 7H), 1.67-1.76 (m, 2H), 1.78-1.89 (m, 2H), 2.75 (t, 2H, J_1=8.0Hz), 3.44-3.52 (m, 4H), 3.56-3.75 (m, 28H), 3.82-3.91 (m, 4H), 4.56 (s, 2H), 4.62 (bs, 2H), 4.64 (s, 2H), 6.99 (s, 1H), 7.12 (d, 2H, J_3=5.6Hz), 7.17 (d, 1H, J_3=5.2Hz), 7.21 (s, 1H).

(1'-OTHP, TMS-protected): A solution of 14.8 g (19.5 mmol) of **(25-OTHP)**, 1.5 g palladium(tetrakis)triphenylphosphine and 1.7 g (21.5 mmol) copper(II)oxide in 150 ml DMF was prepared and stirred for 20 minutes. To this, 14.5 g (23.5 mmol) of **(21'-OTHP)** was added and heated at 110˚C overnight. The reaction mixture was allowed to cool to room temperature and filtrated to remove any solids. To the residue an excess of water was added and this was then extracted with di-ethyl ether. The Obtained organic phase was washed with brine and then dried over Na_2SO_4. After filtration and removal of solvent in vacuo the crude was purified by column chromatography (silica gel, eluent: pentane/EtOAc (1:1)) and gave the pure title compound as a yellow oil in 17% yield (3.6 g, 3.4 mmol) ^{1}H-NMR (400MHz, $CDCl_3$) δ_H: 0.33 (s, 9H), 0.88 (t, 3H, J_3=6.6Hz), 1.21-1.32 (m, 26H), 1.44-1.64 (m,

7H), 1.66-1.75 (m, 2H), 1.77-1.88 (m, 2H), 2.50 (t, 2H, J_3=8.0Hz), 3.45-3.53 (m, 4H), 3.55-3.74 (m, 28H), 3.81-3.90 (m, 4H), 4.46 (s, 2H), 4.62 (bs, 2H), 4.64 (s, 2H), 7.03 (s, 1H), 7.13 (d, 1H, J_3=4.8Hz), 7.19 (d, 1H, J_3=4.8Hz), 7.29 (s, 1H).

(2-OH): **(2-OTHP)** (2.4 g, 2.3 mmol) was stirred overnight in a methanol/HCl (10%) (9:1). After removal of the solvent the yellow oil was dissolved in water and 100 g of a cationic ion-exchange resin (DOWEX MAC-3) was added and the suspension was stirred until the water became colourless and the resin yellow. This was then filtrated and washed several times with water. After extensive rinsing, the resin wash washed with methanol in order to obtain the pure title compound in quantitative yield (2.6 g, 2.3 mmol), this method of purification is not a textbook procedure and was discovered accidentally during another procedure. ^{1}H-NMR (400MHz, $CDCl_3$) δ_H: 0.88 (t, 3H, J_3=7.4Hz), 1.15-1.40 (m, 26H), 1.64 (qt, 2H, J_3=7.0Hz), 2.02 (bs, 2H), 2.73 (t, 2H, J_3=7.8Hz), 3.54-3.63 (m, 4H), 3.66-3.76 (m, 28H), 4.56 (s, 2H), 4.65 (s, 2H), 6.99 (s, 1H), 7.09 (s, 1H), 7.13 (d, 1H, J_3=5.2Hz), 7.19 (d, 1H, J_3=5.6Hz), 7.20 (s, 1H); ^{13}C-NMR (100MHz, $CDCl_3$) δ_C: 14.04 (CH_3), 22.60 (CH_2), 29.22 (CH_2), 29.27 (CH_2), 29.41 (CH_2), 29.50 (CH_2), 29.55 (CH_2), 29.57 (CH_2), 29.62 (CH_2), 30.54 (CH_2), 31.83 (CH_2), 61.61 (CH_2), 66.81 (CH_2), 68.46 (CH_2), 69.34 (CH_2), 69.37 (CH_2),70.23 (CH_2), 70.48 (CH_2), 70.52 (CH_2), 70.54 (CH_2), 72.47 (CH_2), 122.84 (CH), 123.85 (CH), 126.05 (CH), 129.22 (CH), 130.05 (CH), 131.14 (C), 133.00 (C), 133.92 (C), 135.03 (C), 136.17 (C), 139.68 (C), 140.08 (C). Purity analysed by HPLC (UV-Vis/Mass-ESI), retention time: 263 sec. M/z calc.: 884.5; Found: 902.8 (M+NH_4^+), 460.6 (M+2NH_4^+), 497.4 (M-TMS+2NH_4^+, minor), 691.5 (unknown, minor).

(1'-OH): **(1'-OTHP)** (2.4 g, 2.3 mmol) was stirred overnight in a methanol/HCl (10%) (9:1). After removal of the solvent the yellow oil was dissolved in water and 100 g of a cationic ion-exchange resin (DOWEX MAC-3) was added and the suspension was stirred until the water became colourless and the resin yellow. This

was then filtrated and washed several times with water to remove the TBAF. After extensive rinsing, the product was released from the resin by washing with methanol to obtain the pure title compound as a yellow oil in quantitative yield (3.0 g, 3.4 mmol). ^{1}H-NMR (400MHz, CDCl$_3$) δ_H: 0.88 (t, 3H, J_3=7.4Hz), 1.17-1.33 (m, 26H), 1.55 (qt, 2H, J_3=6.2Hz), 1.71 (bs, 2H), 2.49 (t, 2H, J_3=7.6Hz), 3.53-3.76 (m, 32H), 4.47 (s, 2H), 4.64 (s, 2H), 7.03 (s, 1H),   7.13 (d, 1H, J_3=5.2Hz), 7.19 (d, 1H, J_4=3.6Hz), 7.20 (d, 1H, J_4=3.6Hz), 7.34 (d, 1H, J_3=5.2Hz); ^{13}C-NMR (100MHz, CDCl$_3$) δ_C: 14.06 (CH$_3$), 22.63 (CH$_2$), 28.82 (CH$_2$) 29.30 (CH$_2$), 29.36 (CH$_2$), 29.52 (CH$_2$), 29.64 (CH$_2$), 30.64 (CH$_2$), 31.86 (CH$_2$), 61.66 (CH$_2$), 66.78 (CH$_2$), 66.89 (CH$_2$), 69.38 (CH$_2$), 69.42 (CH$_2$),70.26 (CH$_2$), 70.51 (CH$_2$), 70.57 (CH$_2$), 72.52 (CH$_2$), 123.93 (CH), 126.07 (CH), 128.04 (CH), 128.15 (C), 128.56 (CH), 130.10 (CH), 131.15 (C), 133.94 (C), 135.08 (C), 135.23 (C), 138.24 (C), 143.25 (C). Purity analysed by HPLC (UV-Vis/Mass-ESI), retention time: 263 sec. M/z calc.: 884.5; Found: 902.8 (M+NH$_4$[+]), 460.8 (M+2NH$_4$[+]), 497.4 (M-TMS+2NH$_4$[+], minor), 499.4 and 529.5 (unknown, minor).

3.10   References

1   J. M. Tour, *Acc. Chem. Res.*, **2000**, *33*, 791-804.
2   A. Mishra, C.-Q. Ma and P. Bäuerle, *Chem. Rev.*, **2009**, *109*, 1141-1276.
3   a) U. H. F. Bunz, *Chem. Rev.*, **2000**, 100, 1605-1644; b) U. Scherf and E. J. W. List, *Adv. Mater.*, **2002**, *14*, 477-487.
4   a) A. P. H. J. Schenning, A. F. M. Kilbinger, F. Biscarini, M. Cavallini, H. J. Cooper, P. J. Derrick, W. J. Feast, R. Lazzaroni, Ph. Leclère, L. A. McDonell, E. W. Meijer and S. C. J. Meskers, *J. Am. Chem. Soc.*, **2002**, *124*, 1269-1275; b) F. J. M. Hoeben, P. Jonkheijm, E. W. Meijer and A. P. H. J. Schenning, *Chem. Rev.*, **2005**, *105*, 1491-1546.
5   S. Ellinger, A. Kreyes, U. Ziener, C. Hoffmann-Richter, K. Landfester and M. Möller, *Eur. J. Org. Chem.*, **2007**, 5686-5702.
6   F. S. Schoonbeek, J. H. van Esch, B. Wegewijs, D. B. A. Rep, M. P. de Haas, T. M. Klapwijk, R. M. Kellogg and B. L. Feringa, *Angew. Chem. Int. Ed.*, **1999**, *38*, 1393-1397.
7   a) C. R. G. Grenier, W. Pisula, T. J. Joncheray, K. Müllen and J. R. Reynolds, *Angew. Chem. Int. Ed.*, **2007**, *46*, 714-717; b) Z. Chen, V. Stepanenko, V. Dehm, P. Prins, L. D. A. Siebbeles, J. Seibt, P. Marquetand, V. Engel and F. Würthner, *Chem. Eur. J.*, **2007**, *13*, 436-449.
8   a) J. P. Hill, W. Jin, A. Kosaka, T. Fukushima, H. Ichihara, T. Shimomrua, K. Ito, T. Hashizume, N. Ishii and T. Aida, *Science*, **2004**, *304*, 1481-1483; b) W. Jin, Y. Yamamoto, T. Fukushima, N. Ishii, J. Kim, K. Kato, M. Takata and T. Aida, *J. Am. Chem. Soc.*, **2008**, *130*, 9434-9440.
9   a) W.-Y. Yang, E. Lee and M. Lee, *J. Am. Chem. Soc.*, **2006**, *128*, 3484-3485; b) A. Ayaghosh and V. K. Praveen, *Acc. Chem. Res.*, **2007**, *40*, 644-656; c) S. J. George and A. Ajayaghosh, *Chem. Eur. J.*, **2005**, *11*, 3217-3227; d) A. Ajayaghosh, V. K. Praveen and C. Vijayakumar, *Chem. Soc. Rev.*, **2008**, *37*, 109-122.

10 a) K. Yoosaf, A. Belbakra, N. Armaroli, A. Llanes-Pallas and D. Bonifazi, *Chem. Commun.*, **2009**, 2830-2832; b) V. Percec, M. Glodde, T. K. Bera, Y. Miura, I. Shiyanovskaya, K. D. Singer, V. S. K. Balagurusamy, P. A. Heiney, I. Schnell, A. Rapp, H.-W. Spiess, S. D. Hudsonk and H. Duan, *Nature*, **2002**, *419*, 384-387.

11 G. Fernández, F. García and L. Sánchez, *Chem. Commun.*, **2008**, 6567–6569.

12 a) L. Jiang, R. C. Hughes and D. Y. Sasaki, *Chem. Commun.*, **2004**, 1028–1029; b) D. A. Stone, L. Hsua and S. I. Stupp, *Soft Matter*, **2009**, *5*, 1990-1993.

13 a) J.-K. Kim, E. Lee, M.-C. Kim, E. Sim and M. Lee, *J. Am. Chem. Soc.*, **2009**, *131*, 17768-17770; b) J. Locklin, J. H. Youk, T. Fulghum and R. C. Advincula, *Langmuir*, **2002**, *18*, 955-957.

14 J.-K. Kim, E. Lee, Y.-B. Lim and M. Lee, *Angew. Chem. Int. Ed.*, **2008**, *47*, 4662-4666.

15 C. Xue, S. Velayudham, S. Johnson, R. Saha, A. Smith, W. Brewer, P. Murthy, S.n T. Bagley and Haiying Liu, *Chem. Eur. J.*, **2009**, *15*, 2289-2295.

16 K. P. R. Nilsson and P. Hammarström, *Adv. Mater.*, **2008**, *20*, 2639-2645.

17 J. E. Reeve, H.A. Collins, K. De Mey, M. M. Kohl, K. J. Thorley, O. Paulsen, K. Clays and H. L. Anderson, *J. Am. Chem. Soc.*, **2009**, *131*, 2758-2759.

18 M.s Berggren and A. Richter-Dahlfors, *Adv. Mater.*, **2007**, *19*, 3201-3213.

19 T. Bjørnholm, D. R. Greve, N. Reitzel, T. Hassenkam, K. Kjaer, P. B. Howes, N. B. Larsen, J. Bøgelund, M. Jayaraman, P. C. Ewbank and R. D. McCullough, *J. Am. Chem. Soc.*, **1998**, *120*, 7643-7644.

20 A. Kahn and S. Hecht, *J. Polym. Sci. part A: Polym. Chem.*, **2005**, *44*, 1619-1627.

21 J. R. Matthews, F. Goldoni, A. P. H. J. Schenning and E. W. Meijer, *Chem. Commun.*, **2005**, 5503-5505.

22 W. L. Hinze and E. Pramauro, *Crit. Rev. Anal. Chem.*, **1993**, *24*, 133-177.

23 J. Israelachvili, *Intermolecular & Surface Forces*, **1991**, *2nd ed.*, Academic Press.

24 N. Reitzel, D. R. Greve, K. Kjaer, P. B. Howes, M. Jayaraman, S. Savoy, R. D. McCullough, J. T. McDevitt and T. Bjørnholm, *J. Am. Chem. Soc.*, **2000**, *122*, 5788-5800.

25 M. Kasha, *Radiation Research*, **1963**, *20*, 55-70.

26 M. C. A. Stuart, J. C. van de Pas and J. B. F. N. Engberts, *J. Phys. Org. Chem.*, **2005**, *18*, 929-934.

27 G. Briganti, S. Puvvada and D. Blankschtein, *J. Phys. Chem.*, **1991**, *95*, 8989-8995.

28 J. N. Israelachvilli, D. J. Mitchell and B. W. Ninham, *J. Chem. Soc. Faraday Trans.*, **1976**, *72*, 1525-1568.

29 J. N. Israelachvili, *In Physics of Amphiphiles: Micelles, Vesicles, and Microemulsions*; **1985**, Degiorgio,V.; Corti, M., Eds.; North Holland: Amsterdam.

30 B. Valeur, *Molecular Fluorescence: Principles and Applications.*, **2001** Wiley-VCH Verlag GmbH.

31 X. Cui, S. Mao, M. Liu, H. Yuan and Y. Du, *Langmuir*, **2008**, *24*, 10771-10775.

32 N. DiCsare, M. Bellette, C. Marrano, M. Leclerc and G. Durocher, *J. Phys. Chem. A*, **1999**, *103*, 795-802.

33 N. DiCsare, M. Bellette, C. Marrano, M. Leclerc and G. Durocher, *J. Phys. Chem. A*, **1999**, *103*, 803-811.

Chapter 4
Introduction of curvature in amphipathic oligothiophenes for defined aggregate formation

Abstract

Here we report upon a new concept of combining surfactant chemistry with a second structural motif which is able to influence aggregation even though the relative structure and distribution as well as the ratio of hydrophilic and hydrophobic groups remain the same. From an alternated hydrophilic/hydrophobic terthiophene, longer oligomers were prepared. Using the *cis-trans* conformation between the thiophenes, an internal molecular curvature is formed when placed in an aqueous environment due to the orientation of the polar an apolar groups. The expression of this curvature in turn influences the aggregate morphology. The aggregates that are formed are spherical and elongated in nature and display fine structures reminiscent of the thiophene molecules. The oligothiophenes aggregate at low concentrations and possess interesting spectroscopic properties due to the conjugated nature of the thiophene backbone which changes when the environment changes polarity.

4.1   Introduction

Over the past decades the self-assembly of molecular components has become a major approach for the construction of nano-structured materials and architectures with potential applications in *e.g.* biomedical materials, drug delivery and molecular devices.[1] However, the poly-dispersity in size of many self-assembling systems[2] puts serious limitations on the use of self-assembly approaches for hierarchical structure formation[3] and hampers the application of self-assembled aggregates in, for instance, optical, electronic and magnetic devices[4].

Several strategies have been developed to obtain aggregates by self-assembly of molecular components which are well defined in size and/or shape. For instance the use of small, convergent molecular components, which self-assemble through multiple cooperative, specific and directional interactions,[5] has been particularly successful to obtain a variety of nano-objects composed of a well defined number of molecular components, like capsules,[6] grids,[7] helices[8] and so on.[9] So far, these discrete assemblies have not found many applications, because the tight correlation between molecular and supramolecular structure hampers the ability to introduce functionality.

Another generic strategy to create well defined supramolecular assemblies is to make use of a repulsive interaction which increases with growing aggregate size, thereby creating a minimum at the free energy surface for a specific aggregate size. There are several factors that influence the free energy surface *e.g.* head group repulsions with some surfactants leading to spherical or rod-like micelles[1,10] and to other more exotic structures[11], the chiral twist which limits the width of the surfactant[12] and peptide ribbons[13] and steric repulsion in block-copolymers[14] leading to ordered mesophases and finite assemblies like Stupp's mushrooms[15]. All these molecular properties can be considered as manifestations of this phenomenon, and have been described in (semi-)quantitative models by *e.g.* Israelachvilli and Bates.[14,16] These models have in common that they all in some way stress the

relationship between the curvature and object dimension. However, the relationship between surfactants, peptides, and block copolymers and the local curvature of the self-assembled objects formed by them is very diffuse and hampers the rational control and design.

Clearly, the development of functional nano-devices and synthesis of mesoscopic materials using self-assembly methods would greatly benefit from novel approaches to generate nano-objects. The challenge is to develop new molecular components with a precise and versatile control of their curvature, which upon self-assembly will lead to nano-structures with well-defined shape and size, and allow the controlled spatial positioning of functional moieties.

Here we report on an amphipathic oligothiophene structure which in water is able to adopt a curvature along the thiophene backbone because of a transition from a *trans*- to a *cis*-configuration at specific positions due to reorientation of the polar and apolar side-chains. The amphipathic oligothiophenes are able to aggregate in water due to hydrophobic interactions and the obtained intrinsic molecular curvature is expected to influence the aggregate dimensions.

4.2   Design of curved amphipathic oligothiophenes

In order to obtain an amphiphilic structure with well-defined curvature we build upon amphiphilic terthiophenes shown in chapter 3, which can easily be extended to longer oligothiophenes by standard cross-coupling methodologies (Figure 1C, top structure). In Figure 1, the effect of the sequence of hydrophilic and hydrophobic thiophene residues on the folding and self-assembly of longer oligomers is depicted. The simplest structure consists of a linear sequence of hydrophilic substituted thiophenes. It has been found that such structures adopt an all *cis*-conformation between thiophene units, and nicely fold into single helices of well-defined size, which are not amphiphilic and do not aggregate any further after folding.[17]

Obviously, the dimensions of the helix are determined by the angle between the *cis*-oriented thiophenes. When an amphiphilic *bis*thiophene is taken as the monomeric structure, it can also be extended to longer structures. For an alternating sequence of hydrophilic and hydrophobic thiophene residues, the oligothiophene is expected to adopt an all-*trans* conformation, and as a result they are linear and amphipathic in nature. It was found that such thiophenes prefer to self-assemble at the air-water interface and can be used to construct Langmuir-Blodgett multi-layers.[18]
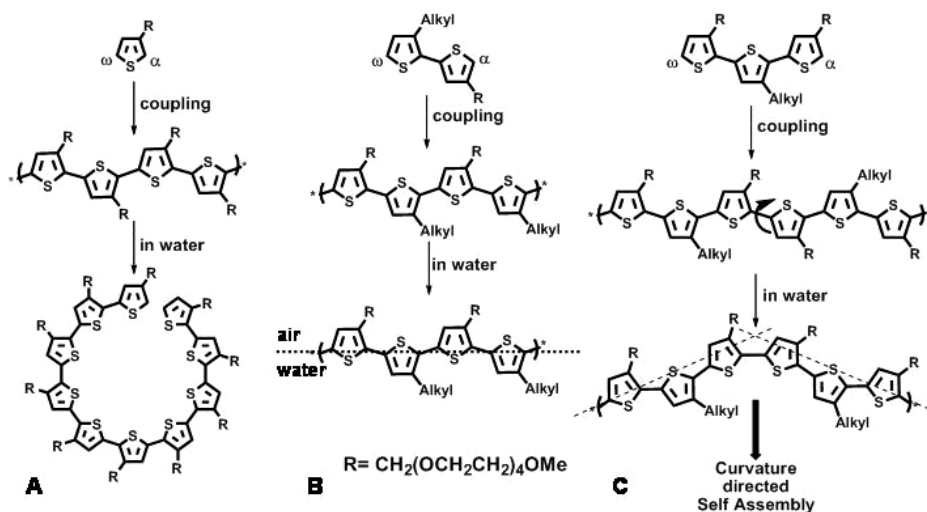

Figure 1: Different designs of conjugated oligothiophenes with different sequences of hydrophilic and/or hydrophobic substituents. When brought into an aqueous environment, they tend to organise themselves like in: A) non-amphiphilic hydrophilic substituted thiophene which folds into a helical structure with the curvature obtained from the trans to cis reorientation of the thiophene; B) an amphiphilic bis-thiophene which, upon oligomerisation, can be used to construct Langmuir-Blodgett multi-layers at the polar-apolar interface ; C) a terthiophene which is amphiphilic in nature and, due to the similar polarity of the thiophenes at the connection between the terthiophenes, a curvature is obtained, with the ability to further self-assemble due to the formed amphipathic character.

From these simple models it can be seen that the introduction of two neighbouring hydrophilic or hydrophobic thiophenes, in an otherwise alternating sequence, would introduce a *cis*-conformation in polar environments, which would result in a non-

linear or curved shape of the oligothiophene. Such oligothiophenes with a defined number of hydrophilic-hydrophilic (or hydrophobic-hydrophobic) thiophene neighbours can most conveniently be constructed for terthiophene building blocks, as depicted in Figure 1C. It is anticipated that such amphipathic oligothiophenes will be able to self-assemble in a similar fashion as surfactants. However, it is expected that the overall shape or curvature of the oligothiophene will determine the aggregate morphology, rather than the ratio between head group area and hydrophobic tail volume

It should be noted that regio-regular substituted terthiophenes like the one depicted in Figure 1C are preferred as the basic building blocks for longer oligomers, because the different reactivity of the α- and ω-positions allows the synthesis of well-defined isomers, thereby avoiding unfavourable and unwanted steric interactions which would disturb the desired *cis*- and *trans* conformations. The terthiophene itself does not possess any curvature like the longer oligomers as can be seen in Figure 2. Only coupled terthiophenes will contain *cis*-conformations, which will result in curved amphipathic molecules. Obviously, this conformational preference also driven by the different solvent affinity of the alkyl chain and ethylene glycol chain for polar and apolar solvents, and will be further enhanced by their self-assembly (Figure 2).
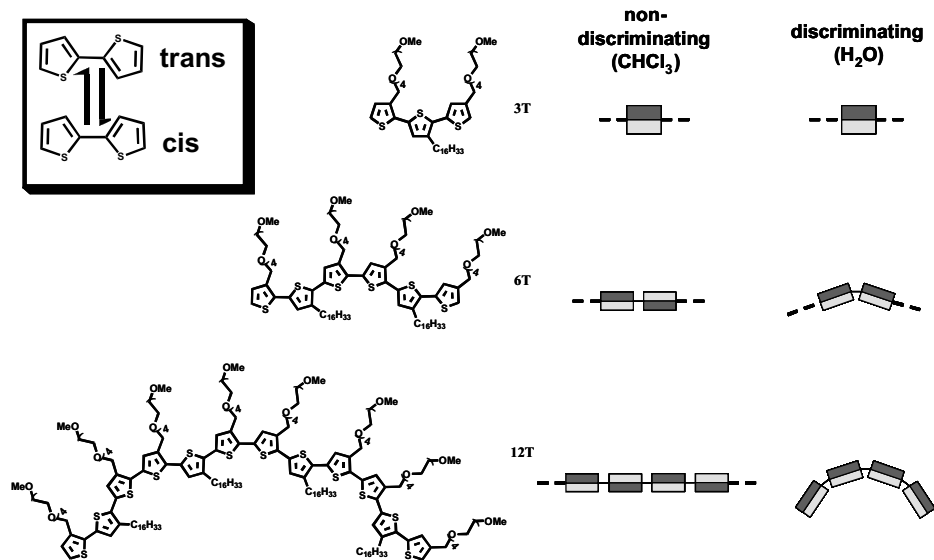
Figure 2: Molecular structures of the three different oligothiophenes (3, 6 and 10). On the right a schematic representation the curvature they obtain upon changes in environment, going from a non-discriminating to a discriminating solvent.

Based on these assumptions it is now possible to estimate the diameter directly from the molecular structure of the oligothiophenes, and from this, one can predict at least one characteristic length of the resulting supramolecular assemblies. The radii of curvature was calculated for a completely flat conformation of the oligothiophenes, with a *cis*-conformation between two identically substituted thiophenes (dihedral angle of 0°), and a *trans*-formation between non-identical substituted thiophenes (dihedral angle of 180°). From basic trigonometry one can determine the basic curvature parameters like curvature radius and cone angle from the dimensions of a partial circular shape (Figure 3A).

From the modelling, the dimensions of the chord length (**a**) and height of the arc portion (**h**) can be obtained. The radius of curvature **R** is equal to **D**/2 (**D** is the diameter) then follows directly from equation **1**.

$$2R = D = \frac{\left(h^2 + \left(\dfrac{a}{2}\right)^2\right)}{h} \qquad (1)$$

The diameter **D** was found to amount to 5.2 and 5.3 nm with cone angles of 26° and 53° for **6** and **10**, respectively. From these values it can be predicted that **6** and **10** are likely to form assemblies with at least one characteristic diameter of approximately 5 nm, with regard to the thiophene moieties, and not accounting for the oligoethylene glycol chains. For terthiophene **3**, the diameter remains undefined because the arc height portion **h** is approximately zero. Most likely, the morphology of assemblies of **3** is governed by parameters formulated in the structure-shape concept. Similar values have been obtained by application of other methods, *e.g.* fitting of the oligothiophene coordinates to a circle segment (Figure 3B-D).
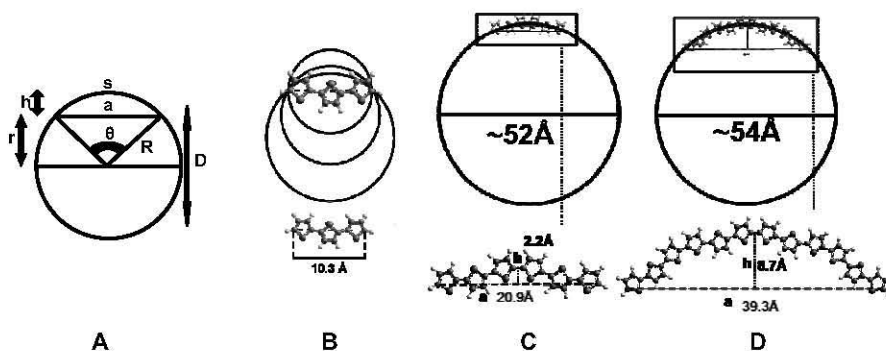

*Figure 3: A) A geometric approach to determine the diameter of the intrinsic curvature of the molecular structure. Here R is the radius, **D** is the diameters, s the arc-length, **a** is the chord length, **h** is the height of the arced portion, **r** is the height of the triangular portion and θ is the angle between the arc length and the centre of the circle. **B-D)** Fitted circle segments to the coordinates of the in which 3(A) has an infinite number of potential curvatures which are not expressed and 6(C) and 10(D) do possess a single curvature.*

4.3　　Synthesis of oligothiophenes 3, 6 and 10

The amphiphilic oligothiophenes proposed above, are based on the amphiphilic terthiophene (**3**).[14] The terthiophene **3** is alternately regio-regular substituted with a tetraethylene glycol mono-methyl ether and a C_{16}-alkyl chain, and was synthesised by the sequential addition of hydrophylic- and hydrophobic substituted thiophenes by Stille couplings. The terthiophene was then extended by homo-coupling reactions to obtain an amphipathic sexithiophene (**6**) and a dodecathiophene (**10**), respectively. The coupling was performed stepwise in order to maintain the regio-regular structural features to minimise any possible steric interactions of the side-groups which could influence the implementation of the curvature upon orientation.
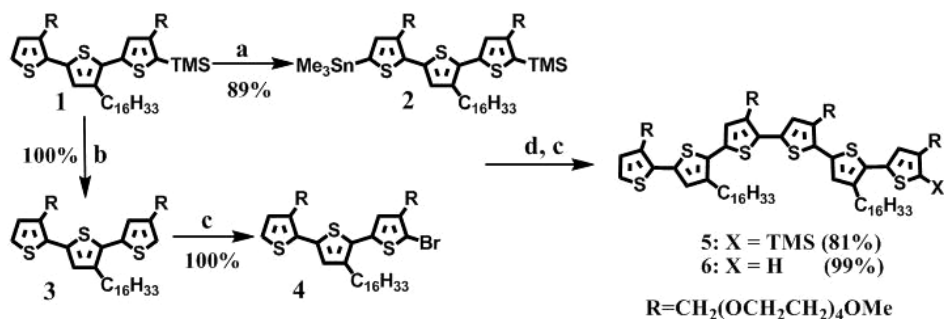

Scheme 1: Synthetic procedure for amphiphilic thiophene **6**: *a) LDA, -78°C, Me₃SnCl; b) TBAF, THF; c) NBS, DCM; d) Pd(PPh₃)₄, DMF, toluene, 110°C.*

Amphiphilic terthiophene **1**, which was TMS-protected, was the starting compound from which the higher oligomers were formed (Scheme 1). Compound **1** was regioselectively converted to stannylated (**2**) and brominated (**4**) derivatives, which could then be connected by a Stille couplings to the regioregular sexithiophene **6**. First, **1** was ortho-lithiated by reaction with LDA, followed by quenching with trimethyltinchloride, resulting in the addition of a tin-moiety on the *5'''*-position (**2**). Compound **4** was obtained in quantitative yield by first removal of the TMS-group

from **1** by reaction with TBAF to give **3**, followed by bromination on the *2*-position with NBS. A Stille coupling between **2** and **4** with Pd(PPh$_3$)$_4$ gave the TMS-protected sexithiophene **5** in 81 % yield. Deprotection of **5** was performed again with TBAF in quantitative yield resulting in **6**.

The dodecathiophene oligomer **10** was synthesised following a similar approach as for **6** (Scheme 2). Ortho-lithiation and stannylation of **5** at the *5'''''''*-position gave **7** in 82% yield and bromination of **6** afforded **8** in quantitative yield. A Stille cross-coupling of **7** and **8** gave the TMS-protected dodecamer **9**, which was directly deprotected to give **10** with an isolated yield of 14%. The isolated yield of the last coupling was significantly lower due to a combination of lower conversion and tedious purification. The compounds were purified by chromatography (normal-, reverse phase and size-exclusion (GPC)) and characterised using ^{1}H-NMR, ^{13}C-NMR, and mass spectrometry (Electron Spray Impact (-ToF)). The purity of the compounds was confirmed by GPC.
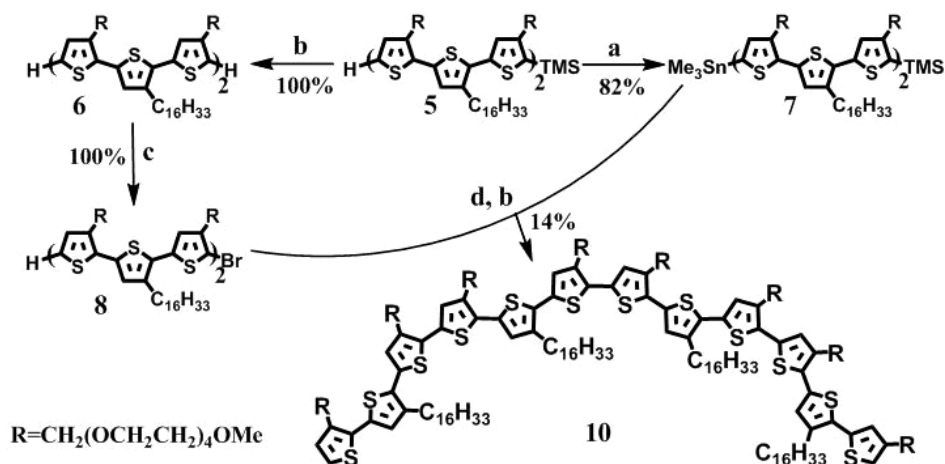
*Scheme 2: Compound **10** was synthesised by following the same approach as for **6**,: a) LDA, -78°C, Me$_3$SnCl; b) TBAF, THF; c) NBS, DCM; d) Pd(PPh$_3$)$_4$, DMF, toluene, 110°C.*

4.4 Aggregation behaviour of 3, 6 and 10 in water

The oligothiophenes **3**, **6**, and **10** were readily soluble in water. Compounds **3** and **6** could be dissolved up to at least 90 and 50 mM giving transparent yellow and orange solutions, respectively. The solution of **3** was clearly more viscous than water, while solutions of **6** retained similar flow properties as water. The longest oligomer (**10**) was at least soluble up to 10 mM and at this concentration a dark red, highly viscous solution was formed. The increased viscosities of solutions of **3** and **10**, compared to a solution of **6** and water, clearly indicate the formation of different types of aggregates.

It is well-known that chromophores display changes in their photo-physical properties upon aggregation[19] and therefore the absorption and emission properties of **3**, **6**, and **10** have been studied in more detail. Remarkably, solutions of compound **3** and **10** exhibit no significant changes in both absorption and emission wavelengths over the concentration range from 0.005 mM to 10 mM. Only solutions of **6** displayed a shift of the emission maximum with increasing concentration. Because the expected effects of aggregation on the photo-physical properties have not been observed for all three compounds, it was necessary to study the self-assembly of **3**, **6**, and **10** in more detail by other methods. The photo-physical properties will be discussed later in the chapter. Unfortunately, also surface tension measurements and isothermal titration calorimetry (ITC) were found to be unsuitable to study the self-assembly behaviour, because of surface tension instabilities and low enthalpies for dilution, respectively. The low enthalpies for dilution indicate that either self-assembly of the oligothiophene surfactants **3**, **6**, and **10** is a less cooperative process and is mainly driven by entropy effects, or that the aggregates are highly stable and remain intact on the time scale of the ITC experiments (minutes).

Table 1   cmc determination by scattering and fluorescence

	cmc$_{DLS}$ (mM)[a]	D$_h$ (nm)[b]	cmc$_{NR}$ (mM)[c]
3	0.2	18	0.2
6	0.01	9	0.2
10	0.04	18, 91, 396	n.d.

a) Determined cmc values by investigating the concentration dependent scattering by DLS. b) The hydrodynamic diameter (D$_h$) of 1.0 mM solutions of 3, 6 and 10. c) Values for cmc of 3 and 6 obtained using fluorescence in combination with Nile Red (λ$_{exci}$:550 nm) by investigating the change in emission intensity. Estimated error in cmc is about 10%. Experiments were performed at 20°C.

The self-assembly of **3**, **6**, and **10** was established more firmly by dynamic light scattering (DLS) studies (Figure 4A). From these measurements it appeared that the scattered light intensity for solutions of **3**, **6**, and **10** increased sharply at a specific concentration, which clearly indicates the formation of larger assemblies (Figure 4A). The concentration of the sharp increase of the scattering intensity was taken as the critical micelle concentration (cmc), and the resulting values are summarised in Table 1. For all compounds the cmc values are below the millimolar regime, which is slightly above other tetraethyleneglycol surfactants with a hexadecyl chain.[20] The cmc of **6** and **10**, bearing more than one hexadecyl chain, is indeed lower than the cmc of **3**, but surprisingly, the cmc of **10**, bearing four alkyl chains, is slightly higher than the cmc of compound **6** with only two alkyl chains.

The hydrodynamic diameter was investigated by DLS in separate measurements at concentrations above the cmc. It was found that all three compounds form assemblies with very different sizes. For **3**, a hydrodynamic diameter of 18 nm was found and this changes with concentration. The size is too large for a spherical micelle and an increasing diameter with increasing concentration suggests elongated micelles, which is in agreement with the observed visco-elastic properties of the solution. The hydrodynamic diameter found for **6** was 9 nm and did not show any

concentration dependency. The size would be appropriate for spherical micelles. Compound **10** displayed a polydisperse distribution of the hydrodynamic radii varying between 18 and 400 nm (see Table 1). Moreover, they strongly depend on the concentration of **10**.
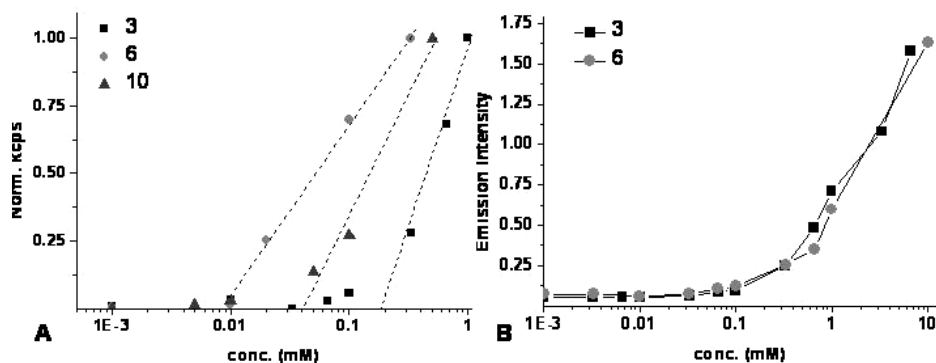

*Figure 4: A) Number of counts for aggregates at different concentration for **3**, **6** and **10**. When aggregates are formed, the counts increase drastically. This is where the cmc is depicted. B) Determination of cmc of **3** and **6** with the use of Nile Red. The concentration where the intensity drastically increases is taken as the cmc.*

The nature of the assemblies formed by **3**, **6**, and **10** was further investigated by studying the emission properties of Nile Red, which is a well known fluorescent probe for hydrophobic domains. The fluorescence intensity of Nile Red will increase when it is located in hydrophobic domains which are formed during aggregation and also the emission maximum (λ_{EM}) will shift towards the blue (λ_{NR}= 660 nm in water). The emission intensity of Nile Red showed a clear increase at concentrations around 0.2 mM for both **3** and **6** (Table 1 and Figure 4B), which for **6** is at a significantly higher concentration than the cmc value determined by light scattering. However, when looking at the shift in λ_{EM}, it was observed that, already at micromolar concentrations of oligothiophene, a significant shift has occurred towards 640 nm and 622 nm for **3** and **6**, respectively. This indicates that hydrophobic domains are already formed well below their cmc presumably due to

the formation of pre-aggregates. This was also observed in the previous chapter with different terthiophene amphiphiles. For **10**, the cmc could not be determined with Nile Red because of non-selective excitation due to overlap of the absorption spectra of Nile Red and **10**. No other fluorescent probe was found to have its excitation outside the absorption range of **10**.

The thiophene amphiphiles **3**, **6** and **10** have oligoethylene glycol moieties as hydrophylic groups, and therefore they might exhibit a lower critical solution temperature (LCST) or cloudpoint (cp).[21] It was found that oligothiophene surfactants **3** and **6** exhibit a well-defined cloudpoint of 26°C and 38°C, respectively, while for compound **10** no cloudpoint was observed between 5 and 90°C. Previous differential scanning calorimetry (DSC) and transmission electron microscopy (TEM) studies revealed that compound **3** exhibits a morphological transition from spherical micelles to elongated micelles between 12-15°C. This type of transition was not found for compound **6** and **10**.

4.5 Morphology of 3, 6 and 10 assemblies in water

The values of the hydrodynamic diameter listed in Table 1 and the differences in visco-elastic properties of solutions of **3**-**10** already suggested that their assemblies have different properties. In order to elucidate these different properties, the morphologies of the aggregates of **3**-**10** were investigated using cryo-TEM. For all cryo-TEM studies described below, samples were prepared by quenching 10 mM solutions of **3**, **6** and **10** from 20°C, *i.e.* well above the critical micelle concentration and well below the cloudpoint. The diameters of the different aggregate morphologies were determined by measuring one hundred different positions on several aggregates and several electron-micrographs, from which the average was taken.

The cryo-TEM studies revealed that the amphiphilic oligothiophenes **3**, **6**, and **10** clearly formed different morphologies upon self-assembly in water (Figure 5). For

compound **3,** elongated micelles were observed with a diameter of 7.1±1.0 nm, and a contour length of about 100-150 nm (Figure 5A, B). This latter value is a crude estimate since the structures are coiling and overlap in the micrograph at these relatively high concentrations. The presence of elongated micelles explains the visco-elastic properties of the solution, and also concurs with the previously mentioned DLS measurements.
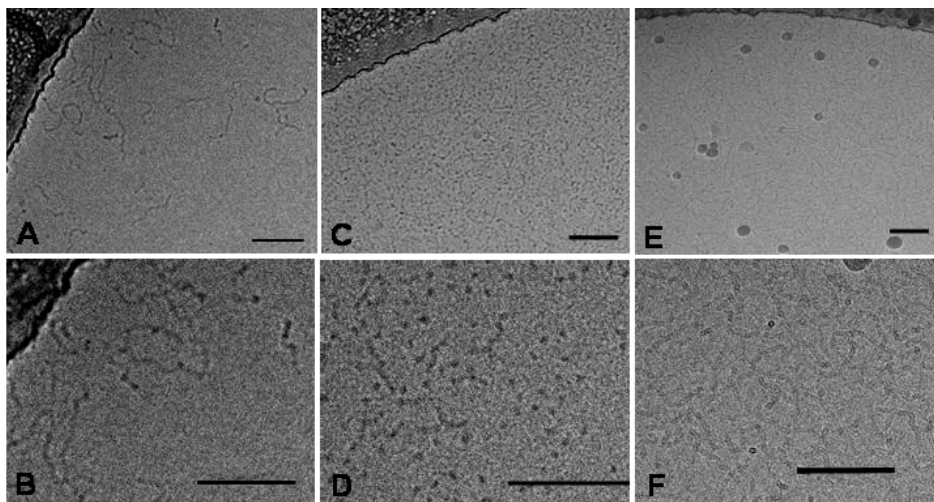
Figure 5: Cryo-Transmission Electron Micrographs of 3 showing elongated micelles (A and B), 6 showing clustered spherical aggregates (C and D), and 10 showing tubular elongated micelles (E and F), the scale bar notes 100 nm.

The TEM images of compound **6** displayed spherical micelles with a diameter of about 7.4±0.9 nm (Figure 5C, D). This is smaller than the hydrodynamic diameter of 9 nm measured by DLS, but this latter value also includes the hydration shell. When looking carefully, the aggregates tend to cluster a bit into an elongated fashion with the individual spherical structures still visible.

The cryo-TEM images of solutions of compound **10** displayed dense network of cylindrical micelles, which is in excellent agreement with the observed viscoelastic properties of the solutions. The diameter of the cylindrical micelles of **10** amounted

to 5.4±0.8 nm, but the contour length could not be determined due to extreme overlap of the structures (Figure 5E, F). These observations nicely explain the poly-dispersity as observed by DLS.
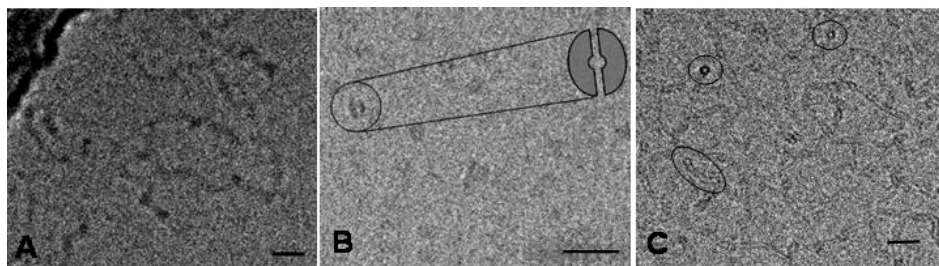

*Figure 6: Cryo-Transmission Electron Micrographs, highly magnified in order to show the contrast differences and displaying a difference fine structure in the aggregates (circled in black; B and C) between **3** (A), **6** (B) and **10** (C). Scale bar depicts 20 nm.*

Even though at first sight the aggregate morphologies are similar to comparable aggregate morphologies formed by other more common surfactants, when taking a closer look at the fine structure, some striking features emerged (Figure 6). The aggregates formed by compound **3** looks just like what one would expect from an elongated micelle: an elongated structure with a homogeneous filling and a darkening at the ends due to a higher density of surfactants. When enlarging the structures of **6**, it became visible that the contrast is not equally distributed throughout the aggregate. In the middle there is a clear spot which has less contrast and it appears as if there is a structure of increased density at the edges. Similar contrast differences were observed for the aggregates of **10**. For these structures, the contrast was higher along the long edges of the elongated structure, and also many circular structures with strongly enhanced contrast at the edges were visible. These elongated and circular structures are most likely the longitudinal and cross-sections of a tubular, perhaps intertwined, structure, respectively (Figure 7). At this point it is not known what the origins of the fine structure are, but but this is currently under investigation.

The observed diameters of aggregates of **3**, **6**, and **10** deviate significantly. For **3** and **6** the diameter determined by cryo-TEM amounted to 7.1 and 7.4 nm, respectively. For compound **6** this is a significant deviation from the diameter of 5 nm expected from its diameter of curvature. When taking into account the dimensions of the surfactant concerning the area (σ) and the width (δ) of the surfactant, compounds **3** and **6** can also be described by a conventional packing[1,22] with an approximate diameter calculated according to eq. **2**.

$$D = \frac{4\sigma}{\delta} \qquad (2)$$

It should be noted that here the assumption is made that the side chains are in their fully extended state which is not accurate for most systems bearing long flexible chains. It was found that for **3** and **6** the diameter approximated by eq. 2 amount to 8.0 nm and 8.4 nm, respectively. Within 10-15% error margin, the values are the same as the measured values and also show that indeed **6** should have a slightly larger diameter than **3**. When the same determination of diameter is applied to compound **10**, a diameter of 8.4 nm was found, the same as for **6**. However, experimentally the diameter was about 35% smaller, 5.4 nm.

The findings suggest that the morphology of **10** does not follow conventional packing. Normal micelle forming surfactants are said to have a cone shaped molecular structure while the amphiphiles used here are flat. This will influence already the molecular packing inside the aggregates. Since the different oligomers are of similar design with an equal ratio of hydrophilic and hydrophobic groups, one would normally expect that similar aggregate morphologies should be formed. It can be concluded from this that the curvature also influences the packing of the surfactants since this is the main difference between the structures shown here.

The molecular curvature is located along the oligothiophene backbone and the diameter of this circular structure is 5.4 nm. However, the aliphatic chains are also about 2.0 nm in length. This means that only a cross section of 4.0 nm can be filled

inside the hydrophobic domain of the micellar structure. This would result in an empty space upon aggregation which is not desired and as a result the system finds another type of packing. Some possible packing of the oligothiophene surfactants are depicted in Figure 7.
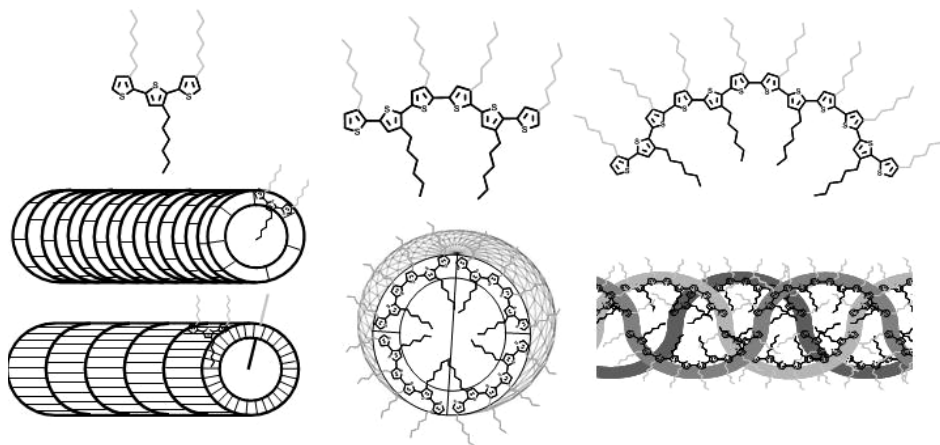

Figure 7: Suggested packing of compounds 3, 6 and 10 in their aggregated form in water. Elongated micelles with either a face-to-face or edge-to-edge packing and spherical micelles are observed for 3 and 6, respectively. For 10 a different kind of packing is suggested, more intertwined which causes the reduced diameter and explains the fine structure observed in Figure 6C.

Here **3** can potentially pack in two ways, either with the thiophene backbone parallel or perpendicular to the length of the elongated micelle. Compound **6** is spherical in nature and therefore will pack in such a way that the surface curvature of the aggregate extends in two directions in the same structure. The surfactants are oriented in a certain angle with respect to each other to obtain the spherical structure. For **10**, a completely different approach is necessary in order to obtain the condensed diameter. Intertwining of the curved surfactant is a way that they can form aggregates with a significant smaller diameter than initially was predicted. This intertwining is also a possible cause of the fine structure which was presented in Figure 6C.

4.6   Photo-physical properties of 3, 6 and 10

It was expected that the intrinsic photo-physical properties of the oligothiophenes **3**, **6** and **10** could be exploited to derive information about their self-assembly behaviour. As already noted above, the aggregation of **3** and **10** in water, however, was not accompanied by significant changes of the absorption and emission maxima[23]. Solutions of compound **6** displayed a clear shift of the emission maxima of 51 nm towards the blue, upon increasing the concentration above 0.03 mM (Figure 8A).
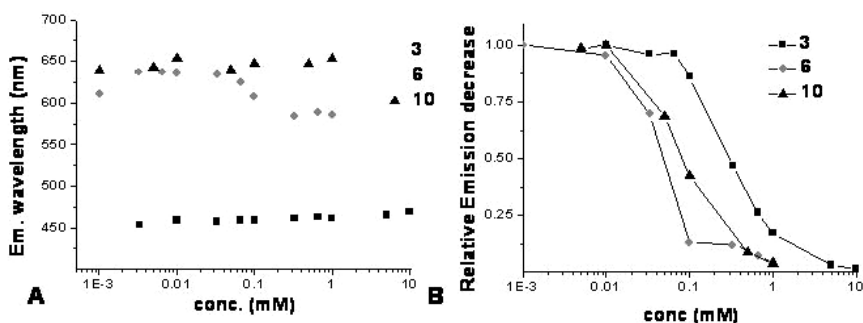

*Figure 8: **A**) Emission wavelength maxima of **3**, **6** and **10** with increasing concentration, displaying no shift for **3** and **10**, however, for **6** a shift is seen around 0.03 mM. **B**) Photoluminescence self-quenching (PL) of **3**, **6**, and **10** with increasing concentration measured for the intensity at the emission maximum. All measurements were performed at 20°C.*

This found concentration is in nice agreement with the cmc determined by DLS. It was, however, observed that the emission intensity did not increase linearly with the concentration of **3**, **6**, and **10** and even at some point decreased, most likely due to self-quenching caused by aggregation of the compounds.[24] This fluorescence self-quenching occurred already at much lower concentrations than the cmc-values determined with Nile Red and light scattering, but does occur at similar concentrations when compared to the concentrations where the NR emission

wavelength shifts (for **3** and **6**). For compounds **3**, **6,** and **10** self-quenching started at concentrations of 0.1, 0.01 and 0.01 mM, respectively (Figure 8B and Table 2). Most likely, the self-quenching occurring below the cmc is due to the formation of small pre-micellar aggregates. The formation of these aggregates has been reported before for other systems.[15,25] The onset of the self-quenching gives information about the concentration at which monomeric surfactants in solution start to aggregate, *i.e.* the critical aggregation concentration (cac).

Table 2   Photo-physical properties of 3, 6 and 10 in water and chloroform

	Abs.[a] λ_{max}(nm)	Em.[a] λ_{max}(nm)	ε[a](10^3) (L mol^{-1} cm^{-1})	Abs.[a*] λ_{max}(nm)	Em.[a*] λ_{max}(nm)	ε[a*](10^3) (L mol^{-1} cm^{-1})	ΔE Abs.[b] (eV) (CHCl$_3$-H$_2$O)	cac$_{PL}$[c] (mM)
3	348	461	16.2	337	444	26.2	0.11	0.1
6	423	572	35.7	404	523	35.0	0.14	0.01
10	454	645	69.4	426	564	77.6	0.17	0.01

*a) Concentrations used were 1.0 mM for **3T** and 0.1 mM for **6T** and **12T**. Listed are the λ_{max} for absorption as well as emission and the molar absorption coefficient (ε) in water and chloroform*. b) Also listed is the energy difference in eV of the λ_{max} for absorption between both solvents to depict the amount of created disorder between a discriminating to a non-discriminating solvent. c) The concentration at which the photo-luminescence (PL) deviates from linearity with increasing concentration. Estimated error in cac is about 10%. All measurements were performed at 20°C.*

Water is a discriminating solvent for the amphiphiles since one part does not want to dissolve and the other one does. This makes the groups orient, which influences the position of the thiophenes and the planarity. When both types of chains (aliphatic and hydrophilic) extend to opposite sides, the thiophenes will be planar and, in the case of **6** and **10**, also curved. In a non-discriminating solvent both chains are soluble and therefore, even though the all *trans*-configuration would be preferred, will have some more rotational freedom between the thiophene-thiophene bonds. The

difference in rigid curved conformation and all *trans*-conformation with more rotational freedom was seen in the photo-physical properties since the conformation is directly related to the conjugation length and this is observed in the absorption. When a discriminating solvent (H_2O) and a non-discriminating solvent ($CHCl_3$) are compared, it is seen that there is a shift in the absorption towards the blue which can be interpreted as a reduction in conjugation length. This was also reflected in the emission where a similar trend was observed (Table 2, Figure 9).
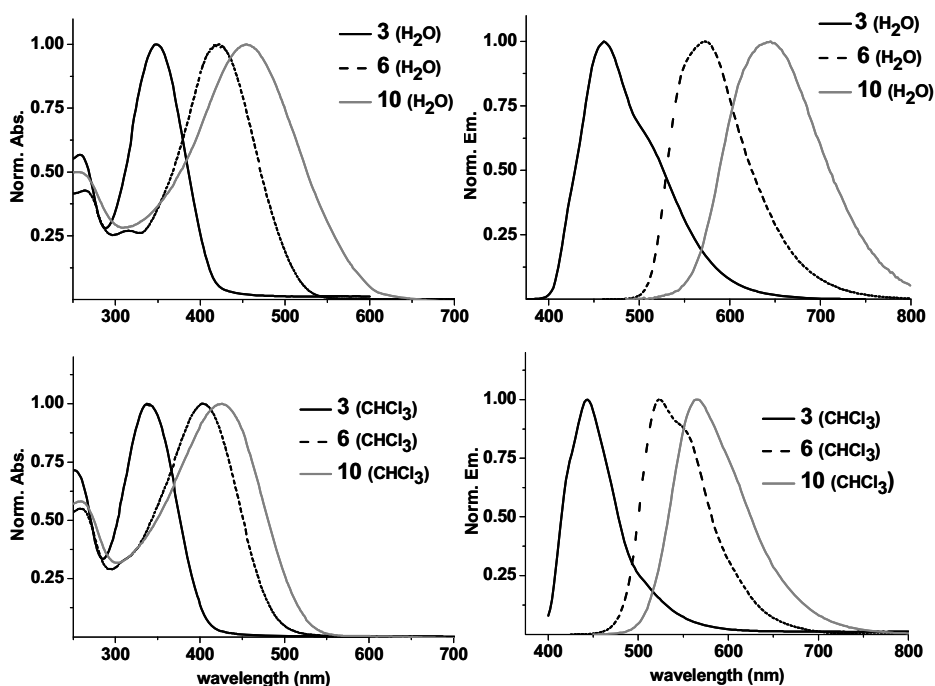

*Figure 9: Absorption (left) and emission (right)) spectra in water (top) and chloroform (bottom). Spectra were taken at concentrations of 1.0 mM for **3** and 0.1 mM for **6** and **10**. Large blue shifts are observed when compared between water and chloroform. The values for the λ_{max} of emission and absorption are listed in Table 3. Measurements were performed at 20°C.*

The amount of energy that is related to this change in conjugation becomes apparent when the relative energy of the main absorption signal (LUMO) between the two

solvents is calculated. It was seen that the difference in energy between water and chloroform becomes greater with increasing number of thiophenes, suggesting that **10**, in water, obtains a higher degree of stabilisation than **6** and likewise between **6** and **3**. This is what can be expected in line with the proposed conformational changes.

4.7   Conclusion

In this study intrinsically curved amphipathic oligothiophenes and non-curved amphiphilic oligothiophene have been investigated for their aggregation bahavior and morphology in water. A successful attempt was made in synthesising an amphipathic curved series of conjugated oligothiophenes in which the sequence and ratio of hydrophilic and hydrophobic groups was kept constant. It was found that the morphology depends on the length of the oligmers, The structure-morphology relationship of **3** and **6** could be described by conventional packing theory, but the diameter for aggregates of **10** deviated significantly from predicted diameters. This different behaviour of **10** can be interpreted as a more pronounced expression of the intrinsic curvature of this dodecathiophene.

These observations demonstrate that it is possible to control the aggregation morphology of simple amphipathic oligothiophenes by implementation of an additional structural motif namely, the curvature. Currently it is under investigation whether this can be extended, thereby developing a new approach on predicting and designing aggregate morphologies with specific diameters derived from the intrinsic molecular curvature. This class of conjugated curved amphipathic molecules have potential functions in aqueous electronic devices as sensors and light harvesting systems but also they would be compatible with biological systems like living cells as will become clear from the following chapters.

4.8 Experimental Section

General information

Starting materials were commercially available and were used without further purification. Starting compound **1** and **3** were synthesised in the previous chapter. Aldrich silica gel Merck grade 9385 (230-400 mesh) was used for column chromatography, in combination with the Teledyne Isco CombiFlash Companion with UV-detection. All solvent used for dry reactions were purified with the use of MBRAUN Solvent purification system MB SPS-800. MilliQ-water and spectroscopic grade solvents were used for measurements. ^{1}H NMR-spectra were recorded on a Bruker Avance-400 spectrometer (at 400MHz) or a Varian Inova-300 spectrometer (at 300MHz), at 25ºC. The splitting patterns are noted as follows: s (singlet), d (doublet), dd (double doublet), t (triplet), q (quartet), qt (quintet), m (multiplet) and bs (broad singlet). ^{13}C NMR spectra were recorded on a Bruker Avance-400 spectrometer (at 100 MHz) or a Varian Inova-300 spectrometer (at 75 MHz). Multiplicity was determined by Attached Proton Test (APT) and chemical shifts are given in δ (ppm) referenced to the residual protic solvent peaks. Coupling constants *J*, are given in Hz. GPC was performed on a Waters Gel Permeation Chromatography machine, LC-8A pump with a Waters dual λ absorbance detector (detection wavelength set on 254 and 360 nm). The column used here was the reprogel PS-GPC 500, 5μm particle size dimensions 300x30mm for preparative with a 6 ml/min flow and 2.5 ml injection volume, for analytical the same column with dimensions 30x8mm was used with a flow of 1 ml/min (THF) with 50μl injection volume. Surface Tension measurements were done on a setup by KRÜSS FM40 Easy Drop, consisting of a syringe pump and a CCD camera, at ambient temperature. Isothermal Titration Calorimetry was done on a Microcal VP-ITC micro-calorimeter apparatus at 20ºC. For UV/Vis measurements an AnalytikJena Specord 250 spectrometer was used equipped with a deuterium-lamp and a halogen-lamp. Quartz cuvets were used with path-lengths varying from 10mm-0.1mm.

Fluorescence spectroscopy was done on a Jasco J-815 CD-spectrometer equipped with a fluorescence monochromator and detector, and an L-38 low wavelength filter (cut-off 380nm) placed between the sample and the detector. The cuvet used here was quartz with dimensions 3x3mm. Dynamic Light Scattering was performed on a ZetaSizer Nano series Nano-ZS by Malvern Instruments.

Experimentals

Compound **2**: A solution of 0.5 ml diisopropylamine in 20 ml of anhydrous THF was cooled to -78˚C. To this 1.75 ml (2.8 mmol) of *n*-butyllithium (1.6 M in hexane) was added. The mixture was then allowed to reach 0˚C and was stirred at this temperature for 10 minutes. Then it was again cooled to -78˚C and 2.6 g (2.6 mmol) of **1** was added dissolved in 30 ml of dry THF and the mixture was stirred for 4 hours at -78˚C. Then 5 ml of trimethyltinchloride solution (1 M in THF) was added and the mixture was continued to be stirred at to -78˚C. After 3 hours the reaction mixture was allowed to slowly warm to room temperature overnight. The mixture was quenched with water and extracted with DCM. The organic phase was dried over $MgSO_4$ and the solvent was removed in vacuo. The title compound was obtained as a yellow oil in 89% yield (2.7 g, 2.4 mmol). This compound was used without further purification. ^{1}H-NMR (400MHz, $CDCl_3$) δ_H: 0.37 (s, 9H), 0.38 (t, 9H, J_{Sn}=24.0Hz), 0.88 (t, 3H, J_3=7.4Hz), 1.15-1.40 (m, 26H), 1.60-1.68 (m, 2H), 2.75 (t, 2H, J_3=7.8Hz), 3.37 (s, 6H), 3.54-3.63 (m, 4H), 3.66-3.76 (m, 28H), 4.56 (s, 2H), 4.64 (s, 2H), 6.98 (s, 1H), 7.18 (s, 1H,), 7.20 (s, 1H)

Compound **3**: Compound **1** (2.6 g, 2.6 mmol) was stirred overnight in 10 ml THF with added, 10 ml of a 1.0 M TBAF solution in THF. After removal of the solvent the yellow oil was dissolved in water and about 100 g of cationic ion-exchange resin (DOWEX MAC-3) was added and the suspension was stirred until the water became colourless and the resin yellow. This was then filtrated and washed several times

with water to remove the TBAF. After extensive rinsing, the product was released from the resin by washing with methanol to obtain the pure title compound as a yellow oil in quantitative yield (2.4 g, 2.6 mmol). ^{1}H-NMR (400MHz, CDCl$_3$) δ$_H$: 0.87 (t, 3H, J$_3$=7.4Hz), 1.15-1.40 (m, 26H), 1.60-1.68 (m, 2H), 2.73 (t, 2H, J$_3$=7.8Hz), 3.37 (s, 6H), 3.54-3.63 (m, 4H), 3.66-3.76 (m, 28H), 4.55 (s, 2H), 4.64 (s, 2H), 6.99 (s, 1H), 7.08 (d, 1H, J$_4$=1.3Hz), 7.12 (d, 1H, J$_3$=5.2Hz), 7.19 (d, 1H, J$_3$=5.6Hz), 7.20 (d, 1H, J$_4$=1.3Hz); ^{13}C-NMR (100MHz, CDCl$_3$) δ$_C$: 13.99 (CH$_3$), 22.50 (CH$_2$), 29.10 (CH$_2$), 29.17 (CH$_2$), 30.45 (CH$_2$), 31.53 (CH$_2$), 61.56 (CH$_2$), 66.77 (CH$_2$), 68.42 (CH$_2$), 69.30 (CH$_2$), 69.33 (CH$_2$), 70.18 (CH$_2$), 70.44 (CH$_2$), 70.47 (CH$_2$), 70.50 (CH$_2$), 72.45 (CH$_2$), 122.84 (CH), 123.85 (CH), 126.04 (CH), 129.20 (CH), 130.03 (CH), 132.98 (C), 134.99 (C), 136.13 (C), 139.64 (C), 140.06 (C). Purity analysed by GPC (UV-Vis), retention time: 507 sec. Exact mass calc. C$_{48}$H$_{314}$O$_{40}$S$_{12}$: 912.49 (mono-isotopic); Found M/z: 935.5(M+Na^{+}).

Compound **4**: To a solution of 2.4 g (2.6 mmol) of **3** in 100 ml DCM, *N*-bromosuccinimide (0.5 g, 2.8 mmol) was added. The mixture was stirred overnight, followed by removal of the solvent in vacuo. The crude product was dissolved in cold heptane and filtered over celite. After evaporation of the heptane, the pure title compound was obtained as a yellow oil in quantitative yield (2.6 g, 2.6 mmol). ^{1}H-NMR (400 MHz, CDCl$_3$) δ$_H$: 0.87 (t, 3H, J$_3$= 7.4Hz), 1.15-1.40 (m, 26H), 1.60-1.68 (m, 2H), 2.67 (t, 2H, J$_3$= 8.0 Hz), 3.34 (s, 6H), 3.49-3.54 (m, 4H), 3.58-3.68 (m, 28H), 4.48 (s, 2H), 4.60 (s, 2H), 6.97 (s, 1H), 6.99 (s), 7.10 (d, 1H, J$_3$= 5.2Hz), 7.17 (d, 1H, J$_3$=5.2Hz).

Compound **5**: A solution of 2.4 g (2.4 mmol) of **4**, 1.0 g palladium(tetrakis)triphenylphosphine in DMF/toluene (50/50) was prepared under a nitrogen atmosphere and stirred for 20 minutes. To this, 2.7 g (2.4 mmol) of **2** in DMF/toluene (50/50) was added and heated at 110˚C overnight. The solvent of the reaction mixture was removed in vacuo and the crude product was purified by

column chromatography (reverse phase C_{18}-silica, flushing with acetonitrile removes impurities, flushing with DCM gives pure compound). This gave the pure title compound as a red oil in 81% yield (3.6 g, 1.9 mmol). ^{1}H-NMR (400MHz, CDCl$_3$) δ_H: 0.36 (s, 9H), 0.85 (t, 6H, J_3=7.4Hz), 1.15-1.40 (m, 52H), 1.60-1.68 (m, 4H), 2.75 (m, 4H, J_3=7.8Hz), 3.32-3.38 (m, 12H), 3.54-3.63 (m, 8H), 3.66-3.76 (m, 56H), 4.55 (s, 2H), 4.64 (bs, 6H), 6.99 (s, 1H), 7.03 (s, 1H), 7.11 (d, 1H, J_3=5.2Hz), 7.15 (s, 1H), 7.17 (d, 1H, J_3=5.2Hz), 7.19 (s, 1H), 7.21 (s, 1H)

Compound **6**: Compound **5** (0.74 g, 0.39 mmol) was stirred overnight in 10 ml THF with added, 0.5 ml of a 1.0 M TBAF solution in THF. After removal of the solvent the red oil was dissolved in water and about 100 g of cationic ion-exchange resin (DOWEX MAC-3) was added and the suspension was stirred until the water became colourless and the resin red. This was then filtrated and washed several times with water to remove the TBAF. After extensive rinsing, the product was released from the resin by washing with THF to obtain the pure title compound as a red oil in quantitative yield (0.71 g, 0.39 mmol). ^{1}H-NMR (400MHz, CDCl$_3$) δ_H: 0.87 (t, 6H, J_3=7.4Hz), 1.15-1.40 (m, 52H), 1.60-1.68 (m, 4H), 2.75 (m, 4H, J_3=7.8Hz), 3.32-3.38 (m, 12H), 3.54-3.63 (m, 8H), 3.66-3.76 (m, 56H), 4.55 (s, 2H), 4.63 (s, 2H), 4.64 (bs, 4H), 7.00 (s, 1H), 7.04 (s, 1H), 7.09 (s, 1H) , 7.13 (d, 1H, J_3=5.2Hz), 7.15 (s, 1H), 7.18 (d, 1H, J_3=5.2Hz), 7.20 (bs, 2H); ^{13}C-NMR (75MHz, CDCl$_3$) δ_C: 14.06 (CH$_3$), 22.62 (CH$_2$), (CH$_3$), 29.30 (CH$_2$), 29.61 (CH$_2$), 29.66 (CH$_2$), 31.86 (CH$_2$), 66.88 (CH$_2$), 68.52 (CH$_2$), 69.42 (CH$_2$), 69.55 (CH$_2$), 70.54 (CH$_2$), 70.59 (CH$_2$), 71.87 (CH$_2$), 122.89 (CH), 123.94 (CH), 126.10 (CH), 128.52 (CH), 129.35 (CH), 130.12 (CH), 130.69 (C), 131.52 (C), 132.52 (C), 132.87 (C), 133.23 (C), 133.28 (C), 133.83 (C), 134.15 (C), 134.64 (C), 135.22 (C), 135.58 (C), 135.66 (C), 136.11 (C), 139.83 (C), 140.30 (C), 140.40 (C); Purity analysed by GPC (UV-Vis), retention time: 485 sec. Exact mass calc. $C_{96}H_{158}O_{20}S_6$: 1822.97 (mono-isotopic); Found M/z: 930.2 $(M+2NH_4^+)^{2+}$; 932.5 $(M+Na^++NH_4^+)^{2+}$.

Compound **7**: A solution of 0.15 ml diisopropylamine in 5 ml of anhydrous THF was cooled to -78˚C. To this 0.22 ml (0.35 mmol) of *n*-butyllithium (1.6 M in hexane) was added. The mixture was then allowed to reach 0˚C and was stirred at this temperature for 10 minutes. Then it was again cooled to -78˚C and 0.66 g (0.35 mmol) of **5** dissolved in 10 ml of dry THF was added and the mixture was stirred for 4 hours at -78˚C. Then 0.5 ml of trimethyltinchloride solution (1 M in THF) was added and the mixture was continued to be stirred at to -78˚C. After 3 hours the reaction mixture was allowed to slowly warm to room temperature overnight. The mixture was quenched with water and extracted with DCM. The organic phase was dried over $MgSO_4$ and the solvent was removed in vacuo. The title compound was obtained as a red oil in 82% yield 0.58 g (0.28 mmol). This compound was used without further purification. ^{1}H-NMR (300MHz, $CDCl_3$) δ_H: 0.36 (s, 9H), 0.38 (s, 9H), 0.85 (t, 6H, J_3=7.4Hz), 1.15-1.40 (m, 52H), 1.60-1.68 (m, 4H), 2.78 (m, 4H, J_3=7.8Hz), 3.32-3.38 (m, 12H), 3.54-3.63 (m, 8H), 3.66-3.76 (m, 56H), 4.57 (s, 2H), 4.64 (bs, 6H), 7.03 (s, 1H), 7.08 (s, 1H), 7.16 (s, 1H), 7.19 (d, 1H, J_3=5.2Hz), 7.21 (s, 1H), 7.22 (s, 1H).

Compound **8**: To a solution of 0.69 g (0.38 mmol) of **6** in 10 ml DCM, *N*-bromosuccinimide (0.07 g, 0.4 mmol) was added. The mixture was stirred overnight. After completion the solvent was removed in vacuo. The crude was solubilised in cold heptane and filtered over celite. After the evaporation of heptane, the title compound was obtained in quantitative yield as a red oil (0.72 g, 0.38 mmol) was obtained. ^{1}H-NMR (400MHz, $CDCl_3$) δ_H: 0.85 (t, 6H, J_3=7.4Hz), 1.15-1.40 (m, 52H), 1.60-1.68 (m, 4H), 2.75 (m, 4H, J_3=7.8Hz), 3.32-3.38 (m, 12H), 3.54-3.63 (m, 8H), 3.66-3.76 (m, 56H), 4.55 (s, 2H), 4.64 (bs, 6H), 7.01 (s, 1H), 7.02 (s, 1H), 7.04 (s, 1H), 7.17 (d, 1H, J_3=5.2Hz), 7.18 (s, 1H), 7.21 (d, 1H, J_3=5.2Hz), 7.22 (s, 1H).

Compound **10**: A solution of 0.70 g (0.37 mmol) of **8**, 0.2 g palladium(tetrakis)triphenylphosphine in DMF/toluene (50/50) was prepared under a

nitrogen atmosphere and stirred for 20 minutes. To this solution 0.58 g (0.28 mmol) of **7** in DMF/toluene (50/50) was added and heated at 110˚C overnight. The solvent of the reaction mixture was removed in vacuo and the crude was purified by column chromatography (reverse phase C_{18}-silica, flushing with acetonitrile removes impurities, flushing with DCM gives mixture of compounds, i.e. compound **9**, starting materials and side-products. It was chosen first to remove the TMS-group and then continue purification in order to minimise number of possible compounds.

To this extend 1.3 g of crude **9** was stirred overnight in a TBAF solution in THF. After removal of the solvent the dark red oil was dissolved in water and a cationic ion-exchange resin (DOWEX MAC-3) was added and the suspension was stirred until the water became colourless and the resin red. This was then filtrated and washed several times with water to remove the TBAF. After extensive rinsing, the product was released from the resin by washing with THF to obtain 1.0 g crude product as a dark red oil after removal of the solvent. The crude product was purified by GPC (Repro-Gel PS, 5μm. 500Å, THF), which allows isolation of the title compound as a dark red oil, in 14% yield (150 mg, 0.04 mmol). ^{1}H-NMR (400MHz, CDCl$_3$) δ$_H$: 0.87 (t, 12H, J_3=7.4Hz), 1.15-1.40 (m, 104H), 1.60-1.68 (m, 8H), 2.79 (bs, 8H, J_3=7.8Hz), 3.32-3.38 (m, 24H), 3.54-3.63 (m, 16H), 3.66-3.76 (m, 112H), 4.56 (s, 2H), 4.61-4.69 (bs, 14H), 7.01 (s, 1H), 7.05 (s, 1H), 7.07 (s, 1H), 7.09 (s, 1H) , 7.14 (d, 1H, J_3=5.2Hz), 7.16-7.24 (overlapping thiophene protons, 9H); ^{13}C-NMR (75MHz, CDCl$_3$) δ$_C$: 14.06 (CH$_3$), 22.62 (CH$_2$), (CH$_3$), 29.30 (CH$_2$), 29.61 (CH$_2$), 29.66 (CH$_2$), 31.86 (CH$_2$), 66.88 (CH$_2$), 68.52 (CH$_2$), 69.42 (CH$_2$), 69.55 (CH$_2$), 70.54 (CH$_2$), 70.59 (CH$_2$), 71.87 (CH$_2$), 128-142 (clusters of overlapping signals of 14 CH and 34 C); Purity analysed by GPC (UV-Vis), retention time: 438 sec. ESI-TOF, Exact mass calc. $C_{192}H_{314}O_{40}S_{12}$; 3643.92 (mono-isotopic) Found: 1844.9081 $(M+2Na^+)^{2+}$ 1237.6293 $(M+3Na^+)^{3+}$, calculated from this gives Mw: 3643.8 (mono-isotopic).

4.9   Reference

1   a) I. W. Hamley and V. Castelletto, *Angew. Chem. Int. Ed.*, **2007**, *46*, 4442-4455; b) A. J. Kirby, P. Camilleri, J. B. F. N. Engberts, M. C. Feiters, R. J. M. Nolte, O. Söderman, M. Bergsma, P. C. Bell, M. L. Fielden, C. L. García Rodríguez, P. Guédat, A. Kremer, C. McGregor, C. Perrin, G. Ronsin and M. C. P. van Eijk, *Angew. Chem. Int. Ed.*, **2003**, *42*, 1448-1457; c) I. W. Hamley, *Angew. Chem. Int. Ed.*, **2003**, *42*, 1692-1712.

2   J. N. Israelachvili, *In Physics of Amphiphiles: Micelles, Vesicles, and Microemulsions*; **1985,** Degiorgio,V.; Corti, M., Eds.; North Holland: Amsterdam.

3   a) A. Aggeli, I. A. Nyrkova, M. Bell, R. Harding, L. Carrick, T. C. B. McLeish, A. N. Semenov and N. Boden, *Proc. Natl. Acad. Sci. USA*, **2001**, *98*, *21*, 11857-11862; b) B. Pokroy, S. H. Kang, L. Mahadevan, J. Aizenberg, *Science*, **2009**, *323*, 237-240; c) Y. He, T. Ye, M. Su, C. Zhang, A. E. Ribbe, W. Jiang and C. Mao, *Nature*, **2008**, *452*, 198-202.

4   a) S. Günes, H. Neugebauer and N. Serdar Sariciftci, *Chem. Rev.*, **2007**, 107, 1324-1338; b) A. A. Argun, P.-H. Aubert, B. C. Thompson, I. Schwendeman, C. L. Gaupp, J. Hwang, N. J. Pinto, D. B. Tanner, A. G. MacDiarmid and J. R. Reynolds, *Chem. Mater.*, **2004**, *16*, 4401-4412; c) G. Zotti, B. Vercelli and A. Berlin, *Acc. Chem. Res.*, **2008**, *41*, 1098-1109.

5   a) J. M. Kang, J. Rebek, *Nature*, 1996, *382*, 239-241; b) M. C. Calama, P. Timmerman, D. N. Reinhoudt, *Angew. Chem. Int. Ed.*, **2000**, *39*, 755-756.

6   a) L. R. MacGillivray, J. L. Atwood, *Nature*, **1997**, *389*, 469-472; b) J. M. Rivera, T. Martin, J. Rebek, *Science*, **1998**, *279*, 1021-1023; c) J. Rebek, *Angew. Chem. Int Ed.*, **2005**, *44*, 2068-2078.

7   M. Ruben, J. Rojo, F. J. Romero-Salguero, L. H. Uppadine, and J.-M. Lehn, *Angew. Chem. Int. Ed.*, **2004**, *43*, 3644-3662.

8   a) E. D. Sone, E. R. Zubarev, and S. I. Stupp, *Angew. Chem. Int. Ed.*, **2002**, *41*, 1705-1709; b) P. G. A. Janssen, J. Vandenbergh, J. L. J. van Dongen, E. W. Meijer and A. P. H. J. Schenning, *J. Am. Chem. Soc.*, **2007**, *129*, 6078–6079.

9   H. Dietz, S. M. Douglas and W. M. Shih, *Science*, **2009**, *325*, 725-730.

10   J. N. Israelachvili and H. Wennertröm, *J. Phys. Chem.*, **1992**, *96*, 520-531.

11   a) J. P. Hill, W. Jin, A. Kosaka, T. Fukushima, H. Ichihara, T. Shimomrua, K. Ito, T. Hashizume, N. Ishii and T. Aida, *Science*, **2004**, *304*, 1481-1483; b) W.-Y. Yang, E. Lee, and M. Lee, *J. Am. Chem. Soc.*, **2006**, *128*, 3484-3485; c) J.-K. Kim, E. Lee, M.-C. Kim, E. Sim and M. Lee, *J. Am. Chem. Soc.*, **2009**, *131*, 17768-17770; d) V. Percec, C. H. Ahn, G. Ungar, D. J. P. Yeardley, M. Moller, S. S. Sheiko, *Nature***, 1998,** *391***,** 161-164; e) S. D. Hudson, H.-T. Jung, V. Percec, W.-D. Cho, G. Johansson, G. Ungar, V. S. K. Balagurusamy, *Science*, **1997**, *278*, 449-452.

12   a) R. Oda, I. Huc, M. Schmutz, S. J. Candau and F. C. MacKintosh, *Nature*, **1999**, *399*, 566-569; b) A. Brizard, C. Aimé, T. Labrot, I. Huc, D. Berthier, F. Artzner, B. Desbat and R. Oda, *J. Am. Chem. Soc.*, **2007**, *129*, 3754-3762.

13   a) A. Aggeli, M. Bell, N. Boden, J. N. Keen, P. F. Knowles, T. C. B. McLeish, M Pitkeathly and S. E. Radford, *Nature*, **1997**, *386*, 259-262; b) J. D. Hartgerink, E. Beniash, S. I. Stupp, *Science*, **2001**, *294*, 1684-1688; c) H. Dong, S. E. Paramonov and J. D. Hartgerink, *J. Am. Chem. Soc.*, **2008**, *130*, 13691-13695; d) S. E. Paramonov, H.-W. Jun and J. D. Hartgerink, *J. Am. Chem. Soc.*, **2006**, *128*, 7291-7298.

14   a) M. W. Matsen and F. S. Bates, *J. Chem. Phys.*, 1997, *106*, 2436-2448; b) M. W. Matsen and F. S. Bates, *Macromolecules*, **1996**, *29*, 7641-7644.

15   S. I. Stupp, V. LeBonheur, K. Walker, L. S. Li, K. E. Huggins, M. Keser and A. Amstutz, *Science*, **1997**, *276*, 384-389.

16   J. N. Israelachvilli, D. J. Mitchell and B. W. Ninham, *J. Chem. Soc. Faraday Trans.*, **1976**, *72*, 1525-1568.

17   J. R. Matthews, F. Goldoni, A. P. H. J. Schenning and E. W. Meijer, *Chem. Commun.*, **2005**, 5503-5505.

18   N. Reitzel, D. R. Greve, K. Kjaer, P. B. Howes, M. Jayaraman, S. Savoy, R. D. McCullough, J. T. McDevitt and T. Bjørnholm, *J. Am. Chem. Soc.*, **2000**, *122*, 5788-5800.

19   M. Kasha, *Radiation Research*, **1963**, *20*, 55-70.

20   W. L. Hinze and E. Pramauro, *Crit. Rev. Anal. Chem.*, **1993**, *24*, 133-177.

21   L. Qiao and A.J. Easteal, *Coll. Polym. Sci.*, **1998**, *276*, 313-320.
22   a) R. Nagarajan, *Langmuir*, **2002**, *18*, 31-38; b) Michal Borkovec, *Adv. Coll. Interface Sci.*, **1992**, *37*, 195-217.
23   The shifts that were seen were in the order of 10-15 nm towards the red and this occurred gradually, suggesting inter-filter effects. For **3** a shoulder did appear at higher concentrations.
24   B. Valeur, *Molecular Fluorescence: Principles and Applications*, **2001**, Wiley-VCH Verlag GmbH.
25   X. Cui, S. Mao, M. Liu, H. Yuan and Y. Du, *Langmuir*, **2008**, *24*, 10771-10775.

Chapter 5

Amphiphilic conjugated thiophenes for self-assembling antenna systems in water

Abstract

Newly developed conjugated terthiophene surfactants are able to aggregate in water and to act as a host for hydrophobic chromophores, creating a multiple donor/single acceptor energy transfer (ET) system by self-assembly. These structures display a high Energy Transfer efficiency and are very easy to create.

5.1 Introduction

The transfer of excitation energy in the light harvesting complexes of the photosynthetic system is one of the most important physical processes for life.[1] Photonic energy can be absorbed by chromophores and due to this absorption an electron is promoted from the ground state to the excited state. When this electron falls back to the ground state in the simplest case this energy is expressed again as photonic energy of lower energy content due to some loss of energy because of relaxation (Figure 1A).
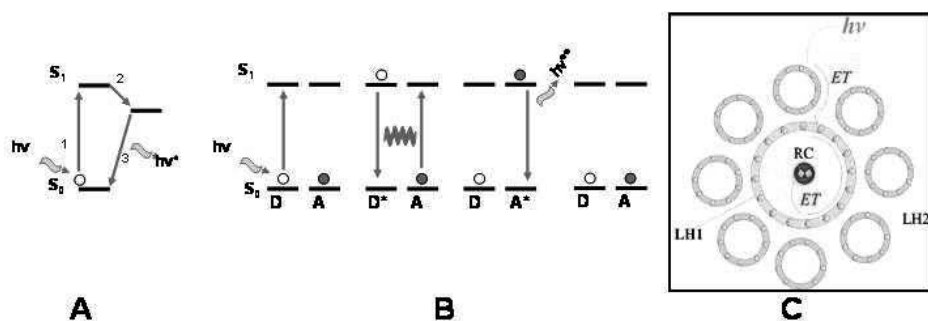

Figure 1: A) The normal decay of an electron promoted to the excited (1) state by irradiation with photonic energy, followed by relaxation (2), and going back to the ground state expelling the excess energy as a photon of different energy (3); B) After excitation of a donor molecule, the energy is used to excite an electron of an acceptor by resonance energy transfer. This in turn will emit a photon of different energy when it falls to its ground state; C) an illustration of a natural light harvesting complex which is able to absorb, transport and transform photonic energy,

It is also possible that photonic energy is absorbed by one chromophore and due to overlapping energy-levels, energy is transferred by oscillation to the next chromophore which is in close enough proximity. This couple is called a donor-

acceptor couple, where the donor (**D**) chromophore absorbs the energy and donates it to the acceptor (**A**) chromophore. After transfer from the donor to the acceptor, the energy will be released again (Figure 1B) either as photonic energy, as energy to initiate chemical reactions (e.g. charge separation), or as non-radiative decay . In the light harvesting complexes multiple donor molecules like chlorophyll are used to absorb light and to transfer excitation energy to a central acceptor molecule via Förster Resonance Energy Transfer (FRET) (Figure 1C).[2]

Over the past decade a variety of interesting model systems have been designed and studied to mimic the natural light harvesting antenna system, that part which is able to act as a receiver for light, and gain insight into the underlying physical principles.[3-7] For instance, dendrimers consisting of several donors covalently attached to a central acceptor core have been found to display the antennae effect[3] which is one of the key features that make natural light harvesting systems so successful. Even though this covalent strategy has produced a number of interesting systems,[4,5] changing the donors and/or acceptor in such covalent systems remains cumbersome.

The self-assembly of donors and acceptors is an attractive alternative to covalent approaches because of its versatility and flexibility, and moreover, also the natural light harvesting systems are formed completely by self-assembly. Several examples of self-assembled multiple donor-acceptor systems have been reported,[6] however, these systems are either still based on covalently connected donors, or only display an antenna effect in some cases.[7] Convenient self-assembling systems in water are surfactant systems. Surfactant self-assembly in combination with ET has often been used for vesicle fusion experiments and co-assembly of chromophores to change or investigate their spectroscopic properties, only hardly ever as an antenna system.[8] Therefore, it remains the challenge to create light harvesting antenna systems that are completely formed through self-assembly of multiple donors and an acceptor in water.

5.2 Using oligothiophenes as a light harvesting system in combination with small hydrophobic dye molecules

In our pursuit to develop water-soluble curved conjugated amphipathic molecules, a fully self-assembled antenna- ET-system was discovered. The amphiphilic conjugated terthiophenes, discussed in chapter 3 are able to self-assemble into micelles in water and can be turned into an ET-system by incorporation of suitable hydrophobic acceptor molecules into the hydrophobic micellar interior. A variety of hydrophobic acceptor molecules can be hosted in the hydrophobic micellar core, leading to stable water-soluble self-assembled ET-systems solely composed of donor and acceptor molecules (Figure 2). In the case of Nile Red as an acceptor, the system displays an antenna effect and overall a very efficient ET within the assemblies.
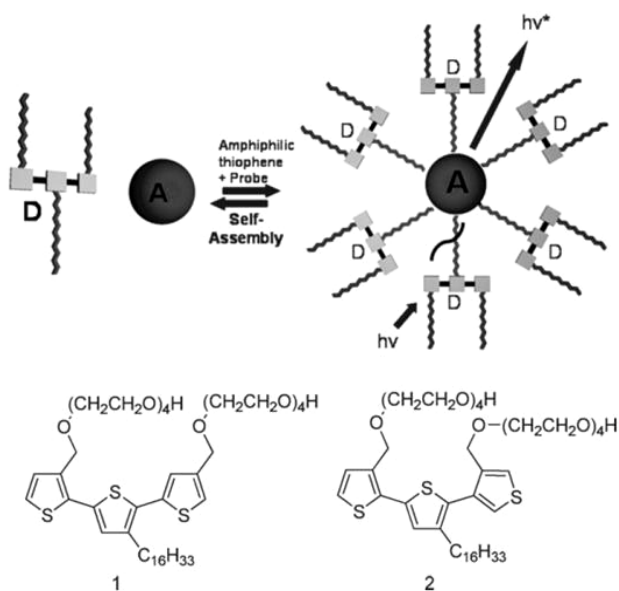

*Figure 2: Schematic representation of the ET-system that is formed from the donor (**D**) thiophene amphiphiles (**1** and **2**) and the hydrophobic acceptors (**A**).*

The amphiphilic terthiophenes reported before have complementary spectroscopic properties with hydrophobic molecules like porphyrins and Nile Red. The synthesis and aggregation behaviour of the used amphiphilic terthiophenes **1** and **2** was discussed in chapter 3 (there abbreviated as **2**-OH and **1**'-OH, respectively).

Terthiophenes **1** and **2** are soluble in water up to concentrations of at least 50 mM to give transparent yellow solutions. Turbidity measurements revealed that the surfactants have a cloud point of 23±1 ^{o}C and 38±2 ^{o}C for compound **1** and **2**, respectively, which is typical for non-ionic oligoethyleneglycol based surfactants.[9] Dynamic light scattering confirmed the formation of micellar aggregates above 1.0 mM (20 ^{o}C) with diameters of 6±2 nm (spherical) for **1** and 21±5 nm for **2** (elongated). This was visualised by cryo-transmission electron microscopy.

The terthiophene isomers described used here have their absorption maximum at 350 and 330 nm, and emission maxima 455 nm and 470 nm for **1** and **2**, respectively. For these and similar compounds it is known that aggregation can affect the electronic properties of chromophores due to electronic coupling between transition dipole moments.[10] The absorption and emission maxima of thiophene amphiphiles **1** and **2** do not shift and the intensities increase linearly with the concentration up to 1.0 mM. However, above 1.0 mM the absorption spectra of isomer **1** do not follow the Lambert-Beer law, whereas the emission intensities of both **1** and **2** deviate from linearity with increasing concentration, indicating that self-assembly occurs. The above data agrees with the formation of micellar aggregates of **1** and **2** in which there is a small electronic coupling between the terthiophene groups at concentrations above 1.0 mM, whereas the pretransition at 0.1 mM should be ascribed to the formation of small pre-micellar aggregates with no significant electronic interactions between the chromophores. The optical properties of the micelles are summarised in table 1. Observed lifetimes, and quantum yields are close to previously published data

on terthiophene analogues. [11]

Micelles of **1** and **2** are in fact aqueous assemblies of multiple chromophores, and therefore they are of potential interest for the construction of self-assembled ET- and antenna systems. A straightforward approach towards such systems would be co-assembly with an acceptor molecule by entrapment of the acceptor in the hydrophobic core. Suitable hydrophobic acceptor molecules are for instance tetraphenylporphyrin (TPP) and Nile Red (NR), because their absorption spectra (λ_{max}(TPP) = 421 nm, and λ_{max}(Nile Red) = 550 nm) nicely overlap with the emission spectra of **1** and **2** (Figure 3).
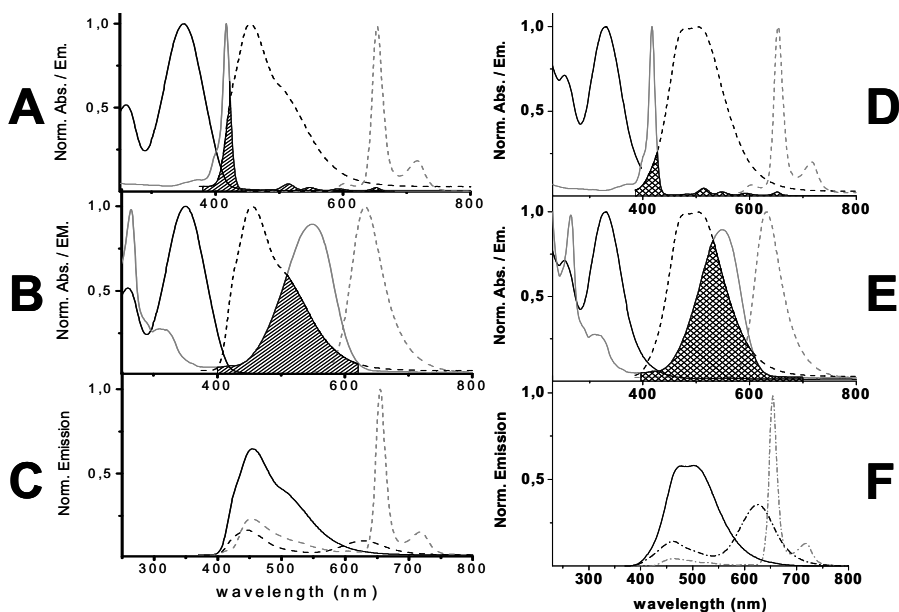

*Figure 3: Norm. Abs. (solid) and Em. (dashed) of **1** (A) and **2** (D) (black) ($\lambda_{max}=\lambda_{exc}$: 350 nm, λ_{em}: 455 nm (**1**) λ_{max}:330 nm, λ_{em}: 470 nm(**2**)) in water and TPP (grey) (λ_{max}: 421 nm, λ_{em}: 655 nm) in THF, showing the overlap integral; Norm. Abs. (solid) and Em. (dashed) of **1** (B) and **2** (E) (black) in water and NR (grey) (λ_{max}: 550 nm, λ_{em}: 632 nm) in EtOH, showing the overlap integral; Norm. Em. of micelle sol. of **1** (C) and **2** (F) (solid black) (1.0 mM), (λ_{em}:455 nm) without and with 50μM acceptor (NR (dashed black), TPP (dashed grey).*

Nile Red is a well-known fluorescence probe for hydrophobic micro-environments.[12] Addition of Nile Red to an aqueous solution of **1** or **2** leads to a pronounced blue shift and an increase of the intensity of the Nile Red emission. The emission maxima of Nile Red above the CMC of **1** and **2** are comparable to the emission found when Nile Red is solubilised in *t*-butanol, indicating the formation of hydrophobic domains in micelles of **1** and **2** in which Nile Red resides. Also the otherwise water-insoluble TPP can be solubilised in water by **1** or **2** above the CMC up to a molar ratio of 1:4 (TPP: **1** or **2**)**.** Apparently, both Nile Red and TPP can efficiently be accommodated by isomer **1** and **2** in their hydrophobic micro-environment, which directly places donor and acceptor in close proximity.

It was found that when **1** or **2** were combined with the hydrophobic chromophores as acceptors an ET-system in water could be formed, based solely on self-assembly of donors and acceptor due to hydrophobic interactions. To 1.0 mM solutions of amphiphilic thiophenes **1** or **2** different quantities of TPP or Nile Red were added to give acceptor concentrations of 0 to 250 μM. It was observed that the emission of **1** and **2** is increasingly quenched by the addition of increasing amounts of TPP and Nile Red as indicated by χ, until a plateau is reached at a molar ratio of **1** or **2** to TPP of about 20:1 (Figure 4).

The quantum efficiencies are 66% and 92% for combinations **1**/TPP and **2**/TPP, respectively. Simultaneously an increase of the emission intensity of TPP is observed. These results indicate that there is efficient ET from the thiophenes to the porphyrin. The large overlap of the excitation spectrum with the absorption spectra of the thiophenes, and the similarity of the TPP emission maxima by direct excitation of TPP or via the thiophenes confirms this conclusion and exclude the formation of excimers and ground state interaction of **1** or **2** with TPP.
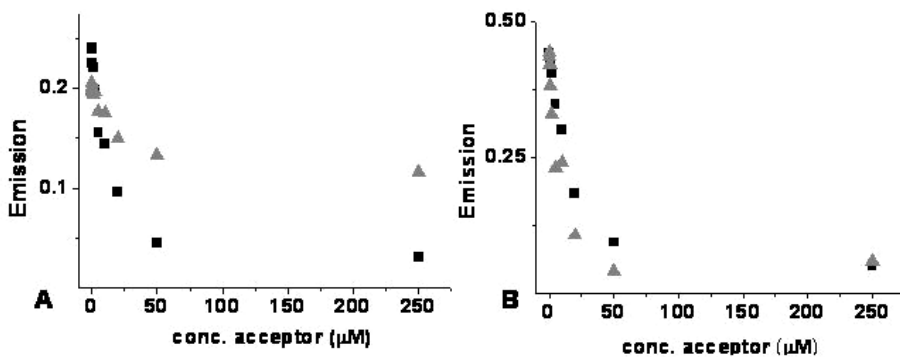
Figure 4: The decrease in thiophene emission of 1 (A) and 2 (B) both 1.0 mM with increasing probe concentration (triangle=Nile Red, square=TPP).

Table 1: Photophysical properties of thiophenes and mixtures in water

Donor (D)	τ_D (ps)[b]	φ_F[c]	k_F (10^9 s^{-1})	k_{NR} (10^9 s^{-1})
Isomer **1**	95	0.10	1.1	9.5
Isomer **2**	125	0.07	0.56	7.4
D/A mix (20:1)	$\chi(I_{DA}/I_D)$	k_{ET} (10^{10} s^{-1})[a]	φ_{ET}	
1+Nile Red	0.25	3.2	0.75	
1+TPP	0.34	2.0	0.66	
2+Nile Red	0.39	1.3	0.61	
2+TPP	0.13	8.9	0.92	

*a) k_{ET} was determined using $1/(\chi\tau_D)-1/(\tau_D)$ were χ is the ratio in emission of **D/A** (1mM:50µM) and **D** (λ_{ex} : 350 nm and λ_{em} : 454nm for isomer **1**, λ_{ex} : 330 nm and λ_{em} : 482 nm for isomer **2**). b) Lifetimes τ_D were measured (λ_{ex} : 407 nm) and c) the quantum yield (φ_F) was determined by using 9,10-Diphenyl-anthracene as a reference.*

Similar observations were made upon the incorporation of Nile Red in micelles of **1** or **2**, concluding that also the Nile Red/thiophene combinations display efficient ET. The emission intensity of Nile Red by ET is 20 and 12 times higher by excitation of **1** and **2**, respectively, than when Nile Red is directly excited at 550 nm under the same conditions (Figure 5). Apparently, the micellar assembly acts as a light absorbing antenna in which the presence of multiple thiophene donors increase the absorption cross section and therefore this increase is seen.
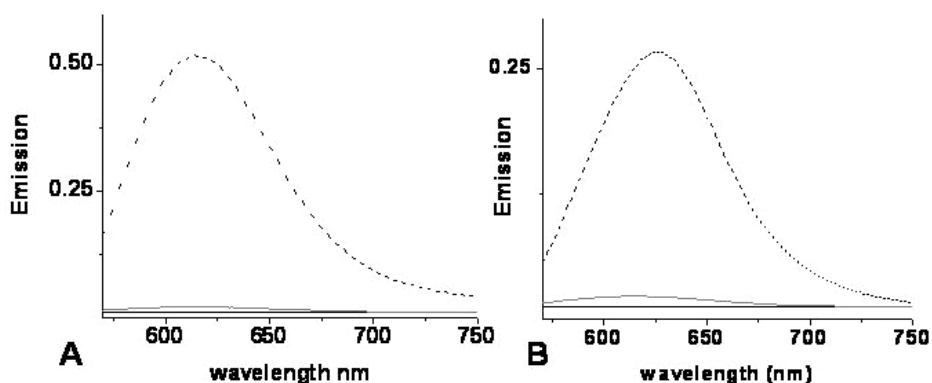

*Figure 5: When **1** (A) or **2** (B) is combined with Nile Red, it is observed that there is a large increase in Em. Intensity of NR, 20 and 10 times more, respectively, via ET (dashed black) than via direct excitation of NR (solid grey). The contribution of thiophene emission excited at λ_{exc} of Nile Red is negligible (solid black).*

When considering the absorption of TPP in the micelles, a 7 nm red shift is observed for the absorption while for TPP normally a blue shift is observed with decreasing polarity which indicates that there is a small coupling between donor and acceptor. A similar interaction is seen in the combination with Nile Red, the emission maximum shifts to the red (~20 nm) and that of the thiophene to the blue (~5 nm). This may be due to a ground-state coupling between donor and

acceptor, and presumably ET proceeds via the Förster mechanism considering that $k_{ET}>k_{NR}$.

5.3 Conclusion

In conclusion, the developed conjugated terthiophene surfactants that aggregate into micellar type assemblies at low concentrations can be used as a host for hydrophobic molecules. This is especially interesting when the hydrophobic molecule is a chromophore with spectral overlapping between the emission of the micelle and the absorption of the hydrophobic chromophore. In that case ET can take place between the donor aggregate and the acceptors as seen here with the combination of the terthiophenes with Nile Red and tetraphenylporphyrin. This approach gives access to new antenna systems which are completely formed by self-assembly of small molecular components and can easily be modified by varying the hydrophobic acceptor.

5.4 Methods

Samples were prepared by combining the correct amounts for the appropriate ratios from a stock solution of thiophene in chloroform and a stock solution of probe molecule in chloroform. The solvent was then removed and the film was re-suspended in milliQ-water. Nile Red was obtained from Sigma Aldrich without any purification, TPP was synthesised according to literature procedures. For UV/Vis measurements an AnalytikJena Specord 250 spectrometer was used equipped with a deuterium-lamp and a halogen-lamp. Quartz cuvets were used with path-lengths varying from 1.0mm-0.1mm. Fluorescence spectroscopy was done on a Jasco J-815 CD-spectrometer equipped with a fluorescence monochromator and detector, and an L-38 low wavelength filter (cut-off 380nm) placed between the sample and the detector. The cuvet used here was quartz with dimensions 3x3mm. Dynamic Light

Scattering was performed on a ZetaSizer Nano series Nano-ZS by Malvern Instruments. For determination of the luminescene lifetimes a LifeSpecs-ps (Edinburgh instruments) was used with excitation pulses of 70 ps at 405 nm.

5.5 References

1   a) C. J. Law, A. W. Roszak, J. Southall, A. T. Gardiner, N. W. Isaacs and R. J. Cogdell, *Mol. Membr. Biol.*, **2004**, *21*, 183; b) N. Armaroli and V. Balzani, *Angew. Chem. In. Ed.* **2007**, *46*, 52-66.

2   a) M. Ghirotti, C. Chiorboli, C. -C. You, F. Würthner, and F. Scandola, *J. Phys. Chem. A*, **2008**, *112*, 3376-3385; b) C. Devadoss, P. Bharathi, and J. S. Moore, *J. Am. Chem. Soc.*, **1996**, *118*, 9635-9644; c) J.-S. Hsiao, B. P. Krueger, R. W.Wagner, T. E. Johnson, J. K. Delaney, D. C. Mauzerall, G. R. Fleming, J. S. Lindsey, D. F. Bocian and R. J. Donohoe, *J. Am. Chem. Soc.* **1996**, *118*, 11181-11193; d) J. Hofkens, M. Maus, T. Gensch, T. Vosch, M. Corlet, F. Köhn, A. Herrmann, K. Müllen and F. De Schryver, *J. Am. Chem. Soc.*, **2000**, *122*, 9278-9288.

3   a) S. L. Gilat, A. Adronov and J. M. J. Fréchet, *J. Org. Chem.*, **1999**, *64*, 7474; b) A. Adronov, S. L. Gilat, J. M. J. Fréchet, K. Ohta, F. V. R. Neuwahl and G. R. Fleming, *J. Am. Chem. Soc.* **2000**, *122*, 1175-1185; U. Hahn, M. Gorka, F. Vögtle, V. Vicinelli, P. Ceroni, M. Maestri and V. Balzani, *Angew. Chem. In. Ed.* **2002**, *41*, 3595-3598; C. Giansante, P. Veroni, V. Balzani and F. Vögtle, *Angew. Chem. In. Ed.* **2008**, *47*, 5422-5425.

4   J. H. Hurenkamp, W. R. Browne, R. Augulis, A. Pugžlys, P. H. M. van Loosdrecht, J. H. van Esch and B. L. Feringa, *Org. Biomol. Chem.*, **2007**, *5*, 3354–3362.

5   L. Jullien, J. Canceill, B. Valeur, E. Bardez, J. -P. Lefèvre, J. -M. Lehn, V. Marchi-Artzner and R. Pansu, *J. Am. Chem. Soc.* **1996**, *118*, 5432-5442.

6   a) A. Ajayaghosh, V.K. Praveen and C. Vijayakumar *Chem. Soc. Rev.*, **2008**, *37*, 109-122; b) C. Röger, Y. Miloslavina, D. Brunner, A. R. Holzwarth and F. Würthner, *J. Am. Chem. Soc.*, **2008**, *130*, 5929-5939; c) T. Shu, J. Wu, L. Chen, T. Yi, F. Li and C. Huang, *J. Mater. Chem.*, **2008**, *18*, 886-893. d) J. Larsen, F. Puntoriero, T. Pascher, N. McClenaghan, S. Campagna, E. Åkesson and V. Sundström, *ChemPhysChem*, **2007**, *8*, 2643-2651; e) F. J. M. Hoeben, L. M. Herz, C. Daniel, P. Jonkheijm, A. P. H. J. Schenning, C. Silva, S. C. J. Meskers, D. Beljonne, R. T. Phillips, R. H. Friend and E. W. Meijer, *Angew. Chem. Int. Ed.*, **2004**, *43*, 1976-1979. g) M. J. Ahrens, L. E. Sinks, B. Rybtchinski, W. H. Liu, B. A. Jones, J. M. Giaimo, A. V. Gusev, A. J. Goshe, D. M. Tiede and M. R. Wasielewski, *J. Am. Chem. Soc.* **2004**, *126*, 8284-8294; i) R. F. Kelly, R. H. Goldsmith and M. R. Wasielewski, *J. Am. Chem. Soc.*, **2007**, *129*, 6384-6385.

7   A. Ajayaghosh, V. K. P., Chakkooth Vijayakumar and S. J. George, *Angew. Chem. Int. Ed,*. **2007**, *46*, 6260 –6265.

8   a) S. Bhosale, A. L. Sisson, N. Sakai and S. Matile, *Org. Biomol. Chem.*, **2006**, *4*, 3031-3039; b) N. Nagata, Y. Kuramochi and Y. Kobuke, *J. Am. Chem. Soc.*, **2009**, *131*, 10-11.

9   L. Qiao and A.J. Easteal, *Coll. Polym. Sci.*, **1998**, *276*, 313-320.

10 M. Kasha, *Radiation Research*, **1963**, *20*, 55-70.

11 a) D. Grebner, M Helbig and S Rentsch, *J. Phys. Chem.*, **1995**, *99*, 16991-16998; b) R. S. Becker, J. Seixas de Melo, A. L. Maanita and F. Elisei, *J. Phys. Chem.*, **1996**, *100*, 18683-18695.

12 M. C. A. Stuart, J. C. van de Pas and J. B. F. N. Engberts, *J. Phys. Org. Chem.*, **2005**, *18*, 929-934.

Chapter 6
Highly efficient Energy Transfer in water-soluble mixed aggregated oligothiophenes

Abstract

The creation of synthetic self-assembled antenna systems in water which display features like light harvesting, energy transport and creation of a reactive centre is still a challenge. In this work energy transfer processes in self-assembled elongated micellar aggregates in water composed of amphiphilic terthiophenes (**3T**) doped with a sexithiophene equivalent (**6T**) were studied. The mixed aggregates have sizes ranging from 80 nm to 210 nm depending on the **3T** concentration as is concluded on basis of TEM and DLS measurements. From the analysis of optical absorption and (time-resolved) fluorescence measurements on these self-assembled donor-acceptor systems, quantum efficiencies for energy transfer from **3T** to **6T** up to 98% were found. The origin of this high quantum efficiency became clear from titration experiments and Stern-Volmer plots, which revealed that apart from direct energy transfer also migration of excitation energy over the **3T** units occurred.

6.1   Introduction

The transfer of excitation energy in light harvesting complexes of the photosynthetic system is one the most important photo-physical processes for life.[1] In this complex multiple chlorophyll molecules absorb light and transfer the excitation energy to a central acceptor system where it is further processed to yield a charge separated state.[2] Due to energy transfer the absorbed energy is able to move over the light harvesting chromophores (LH2) until the appropriate energy-sink is reached (LH1) to which the energy is transferred.[3] These energy transfer (ET) processes occur on a timescale of 0.5-1 picoseconds, making this process very efficient.

Many attempts to create analogues energy donor acceptor systems have been made. Successful systems are e.g. based on dendrimers[4] or on self-assembled systems.[5,6] However, creating a system capable of transporting the energy over an array of molecules and of funnelling it towards a central energy acceptor, like in the natural photosynthetic system is still a challenge. Funnelling of excitation energy towards an energy acceptor within a completely self-assembled array has been reported[7] and in order to create a biocompatible system we extend those studies by using self-assembling (SA) water soluble chromophores.

To realise efficient long-range dipole-dipole ET in these kinds of systems a number of requirements are of importance including the luminescence yield (Φ_D) of the energy donor (**D**), the absorption coefficient (ε_A) of the acceptor (**A**) and the mutual arrangement of their transition dipole moments.[8] For dipole-dipole ET this orientation effect is expressed in the orientation parameter, κ. This parameter can vary from 4 for collinear orientated dipole moments to zero for orthogonally orientated dipoles. Apart from this, for efficient ET, there must be considerable spectral overlap (J) between the emission of the **D** and the absorption of the **A**.[8] All these parameters, together with Avagadro's number (N_A) and the refractive index (n) determine the critical distance for long-range dipole-dipole ET or so called Förster radius (R_0) i.e. the distance at which ET and natural decay given by k_d are equally

probable.

$$R_0^6 = \frac{9000(\ln 10)\kappa^2 \phi_D^0}{128\pi^5 N_A n^4} J \qquad (1)$$

The rate constant for ET (k_{ET}) is then given by eq. **2**.

$$k_{ET} = k_d \left(\frac{R_0}{r}\right)^6 \qquad (2)$$

Here r is the distance between the transition dipole moments of both chromophores and k_d is the rate constant for fluorescence decay of **D** without added **A**.

In this paper the transport of excitation energy in aqueous media as observed in nature is studied by using a terthiophene (**3T**) as **D**, and a sexithiophene (**6T**) as **A**. (see Figure 1 for molecular structures). These compounds contain hydrophilic tetraethylene glycol and hydrophobic aliphatic substituents, which make them amphiphilic enabling them to self-assemble in water due to hydrophobic effects, and form mixed aggregates because of their similar chemical nature. In addition, the large spectral overlap between the absorption of the **6T** and the emission of the **3T** make efficient ET feasible. The aggregates were studied by TEM, dynamic light scattering (DLS) and optical spectroscopy.

6.2   Self-assembling behaviour of 3T and 6T

Both oligomers are very well soluble in water and concentrations up to 50 mM for **6T** and 90 mM for **3T** could be realised. The critical micelle concentration (cmc) for **3T** and **6T** are 0.2 mM and 0.01 mM, respectively. However, it was also found that there is a form of pre-aggregation below the cmc, based on fluorescence measurements in combination with Nile Red, which showed the presence of

hydrophobic domains being formed at concentrations as low as 0.001 mM. Cryo-TEM images as shown in Figure 1 of **3T** and **6T** demonstrate that in water the compounds form elongated and spherical micellar structures, respectively, with a diameter (*d*) of about 7 nm. At high concentrations the **3T** aggregates can reach lengths up to 210 nm. Due to this non-spherical shape of the **3T** aggregates, the dimensions of the SA structures cannot directly be determined using DLS and is also difficult from TEM due to overlap of the aggregates. Therefore the results from DLS were used in combination with the TEM data to retrieve an approximation for the length-concentration dependence. Perrin's formula relates the hydrodynamic radius (R_H) of freely rotating rod-like micelles from DLS to the contour length (*L*) and diameter (*d*) of the elongated micelles[9] given by **3**.

$$R_H = \frac{\dfrac{L}{2}\sqrt{1-\dfrac{3}{2}\left(\dfrac{d}{L}\right)^2}}{\ln\left(\dfrac{1+\sqrt{1-\dfrac{3}{2}\left(\dfrac{d}{L}\right)^2}}{\dfrac{d}{L}\sqrt{\dfrac{3}{2}}}\right)} \qquad \textbf{(3)}$$

By using this relation, values of *L* are determined for different concentrations **3T**, while *d* was assumed to be constant (7 nm from TEM). The calculated values of *L* are plotted in Figure 1C versus the concentration of **3T**. Clearly, increasing the **3T** concentration results in a linear increase of the length of the elongated micelles. This corresponds reasonable well with estimated contour lengths from TEM, even though this is difficult to estimate correctly.
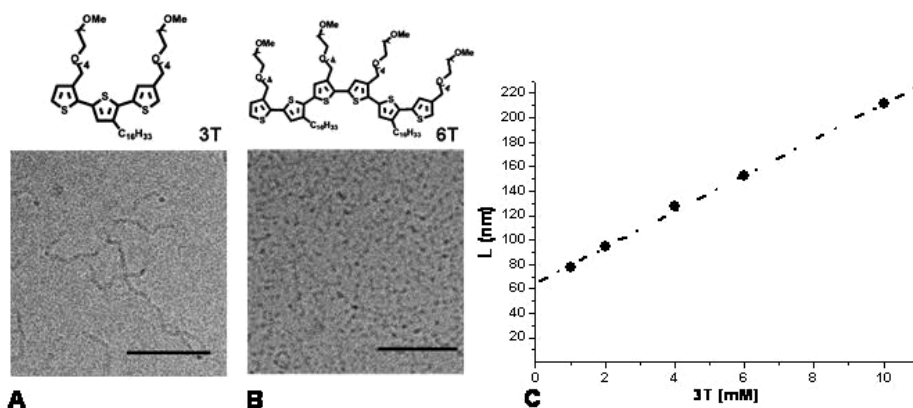
*Figure 1: A) Molecular structures of **3T** and **6T** and B) cryo-TEM micrographs of aqueous solutions of **3T** at 1 mM and **6T** at 10 mM concentrations. The scale bar represents 100 nm; C) The modelled change of the elongated micelle contour length L of **3T** with increasing concentration.*

6.3   Energy transfer in 3T/6T mixed aggregates

The absorption and emission spectra of pure solutions of **3T** and **6T** are given in Figure 2. From these spectra absorption maxima of 348 nm and 423 nm and emission maxima of 461 and 572 nm were found for **3T** and **6T**, respectively. The molar absorption coefficients amount to 16×10^3 and 36×10^3 L mol^{-1} cm^{-1} for **3T** and **6T**, respectively. The patterned area depicts the substantial overlap between the emission of **3T** and the absorption of **6T**.
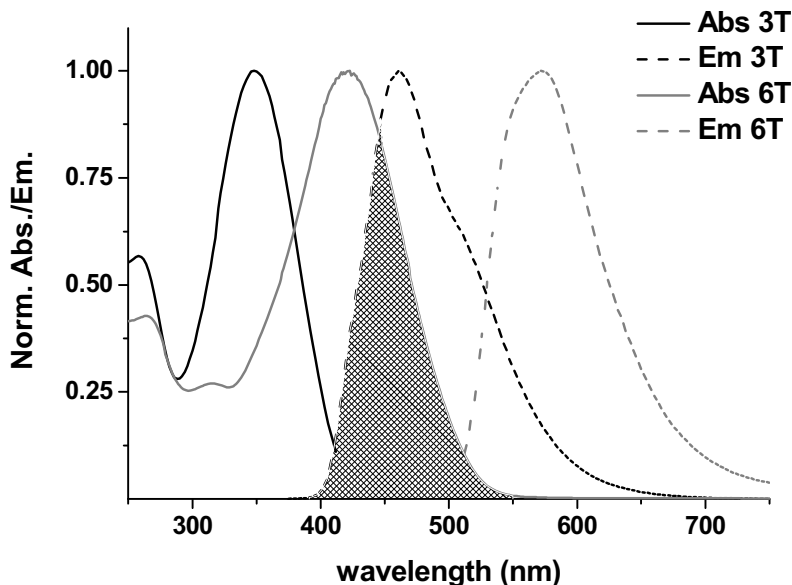
*Figure 2: Absorption and emission of both **3T** (λ_{exc}: 348 nm) (10 mM in water) and **6T** (λ_{exc}:423 nm) (0.7 mM in water). Patterned area is the spectral overlap between the absorption **6T** and emission of **3T**.*

Figure 3A shows the absorption spectrum of a **3T**:**6T** mixed aggregate in a 50:1 molar ratio including the spectra of the corresponding pure materials with the same concentration. The spectrum of the mixed aggregate can be reconstituted by the pure **3T** and **6T** spectra indicating that there are no ground state interactions. To examine if ET occurs in mixed **3T**:**6T** aggregates, luminescence spectra on excitation of the **D** were recorded for a number of different molar ratios **3T**:**6T** while keeping the **3T** concentration constant at 1 mM (Figure 3B). From the luminescence spectra shown in Figure 3 it is apparent that the emission of **3T** is gradually quenched and in a 10:1 ratio, the **3T** emission is almost completely quenched. This would normally not be possible since the cmc depicts the concentration of amphiphiles which are not

aggregated and hence, would not take part in the ET process. However, the complete quenching here is possible due to the formation of pre-aggregates. This was strengthened by the observation that, though with lower efficiency, energy transfer also occurs (data not shown). In addition to the decrease in **3T** emission, a strong increase was seen in **6T** emission, which was hardly observed without **3T**, indicating that energy transfer from **3T** to **6T** occurs.
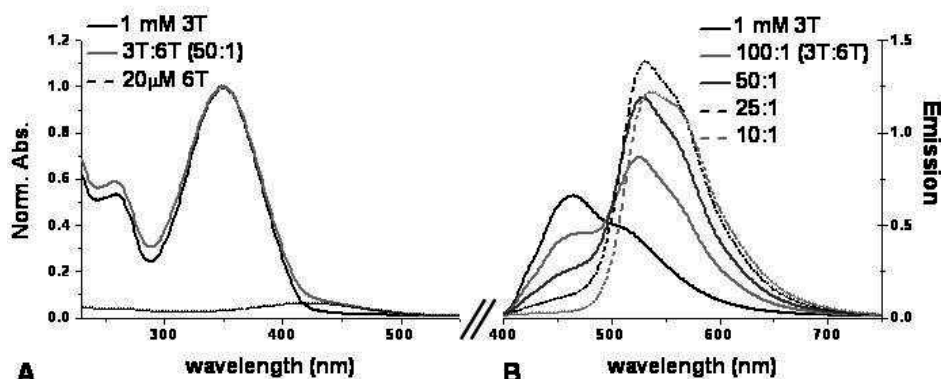

*Figure 3: A) Absorption of **3T** and **6T** separately and combined (50:1 **3T/6T** ratio); B) decreasing emission of **3T** (λ_{exc}: 348 nm) with increasing amount of **6T** with.*

Fluorescence lifetime measurements confirmed the ET process by displaying a decreasing fluorescent lifetime of the **3T** detected at 460 nm on increasing the **6T** concentration. The observed lifetimes are collected in Table 1. By using the known lifetime and quantum yield of **3T**, the rate constant and efficiency for ET from **3T** to **6T** could be determined for the mixed aggregates with different molar ratios. The fluorescence lifetimes were fitted bi-exponential and displayed in all cases one dominant lifetime with 3-5% residual contribution of a second longer fluorescent lifetime.

<div align="center">**Table 1: ET parameters for mixed aggregates of 3T and 6T**</div>

Donor (D)	τ_D (ps)[a]	φ_F[b]	k_F (10^8 s^{-1})	k_{NR} (10^9 s^{-1})[c]
3T	97	0.05	5.2	9.8
D/A (**3T/6T**)		$\chi(I_{DA}/I_D)$ Donor: 1mM/ 10mM	k_{ET} (10^{10} s^{-1})[d] 1mM/ 10mM	φ_{ET} 1mM/ 10mM
100:1	86	0.67/ 0.57	0.5/ 0.8	0.33/ 0.43
50:1	69	0.38/ 0.21	1.7/ 3.8	0.62/ 0.78
25:1	61	0.17/ 0.10	4.9/ 9.5	0.82/ 0.90
10:1	32	0.04/ 0.04	25.9/ 57.0	0.96/ 0.98

*a) Fluorescent lifetimes τ_D were measured at 1 mM concentrations of **3T** (λ_{ex} : 407 nm; monitored at λ_{mon} 460 nm); b) the quantum yield (φ_F) was determined by using 9,10-diphenyl-anthracene as a reference[8]; c) k_{NR} is the non-radiative decay rate constant and was calculated with the use of the quantum efficiency; d) k_{ET} was determined using $k_{ET} = ((1/(\chi\tau_D))-(1/\tau_D))$ were χ is the ratio in emission of D/A and D and τ_D the fluorescence lifetime of **3T**.*

6.4   ET properties of 3T/6T mixed aggregates at different concentrations

Upon inspecting the parameters more closely, it was found that energy transfer from **3T** to **6T** was more efficient at 10 mM than at 1 mM concentration of **3T** (Table 1). It was shown above that the concentration has primarily an effect on the length of the elongated micelles, which increased with increasing **3T** concentration.

To investigate the effect of the length of the SA aggregate on the ET process similar optical experiments were carried out with the same molar ratios. However the **3T** concentration was increased to 10 mM. The observed rate constants and efficiencies

for ET are added in Table 1. From the values for φ mentioned in Table 1 it is concluded that at higher **3T** concentrations, which lead to longer elongated micelles, the ET process is enhanced. To examine this effect in more detail the φ for ET in SA mixed aggregates was measured by changing the **3T** concentration between 1 and 10 mM, while keeping the molar ratio **3T**:**6T** constant at 20:1.
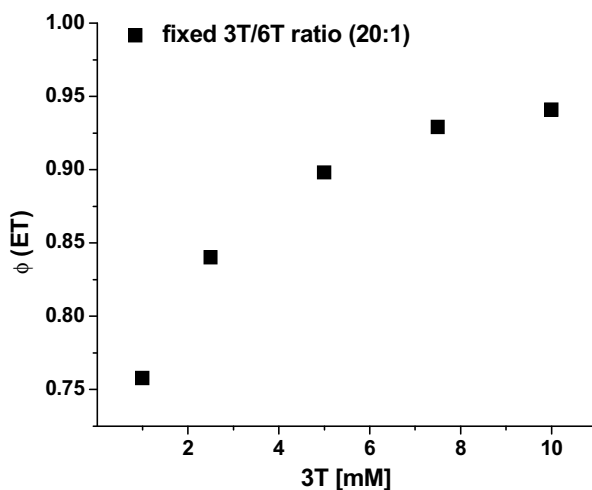

Figure 4: The efficiency depending on the concentration determined by a dilution series with a fixed 3T/6T ratio of 20:1.

Figure 4 shows the φ found for ET versus the concentration of **3T** of the SA mixed aggregate. A clear enhancement of the efficiency is observed as the length of the aggregate increases.

An explanation for the increased ET efficiency for increasing concentration originates from the growth of the aggregates. As was seen from the modelled relationship shown in Figure 1, a ten-fold increase in concentration results in an average increase in length by a factor of 3 of the elongated micelle which is logical since there are probably several of molecules per cross section of the aggregate resulting in a relatively smaller increase in length with increasing concentration.

This growth results in a better distribution of **6T** molecules over the **3T** aggregates with less chance of an aggregate not containing an acceptor. Less non-occupied aggregates by the **A** would be more efficient and hence contributes to higher energy transfer efficiency.

At this point in time it is not clear what exactly causes the increased efficiency of energy transfer and it is still under investigation whether it is due to the dimensions of the aggregate, the distribution of the **A** or due to the distribution of **3T** molecules over different states (aggregated, pre-aggregated or non-aggregated).

6.5   Fluorescence decay pathways in 3T/6T mixed aggregates

In order to examine the quenching process in more detail the results obtained from the luminescence experiments were analysed by plotting I_0/I (I_0 is the emission intensity without **A**, I is the intensity with **A**) versus the concentration of **A** (**6T**). Clearly a non-linear increase was found as function of the **A** concentration. Furthermore, the values found for τ_0/τ versus the **6T** concentration were added in Figure 5, which display a linear increase with the **6T** concentration. The discrepancies between the slopes of I_0/I and of τ_0/τ and the nonlinearity of the I_0/I curves reveal that in addition to dynamic processes also static quenching processes contribute.
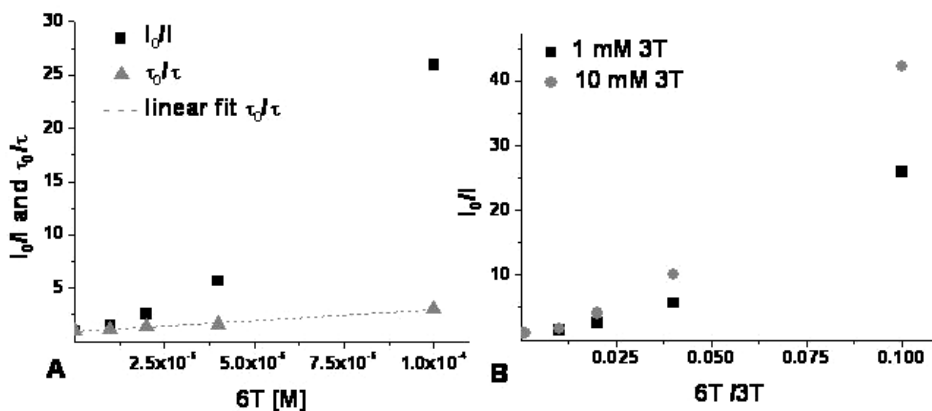
*Figure 5: **A)** Stern-Volmer plot which shows a non-linear increase in I_0/I vs. the [**6**] and hence a non-uniform value for the quenching rate constant. **B)** The relative non-uniformity of the components in the energy transport compared between a short (1 mM) and a long (10 mM) aggregate.*

It should be noted that the actual lifetime of the **3T** molecules within the aggregate might be significantly smaller, because in our fluorescence lifetime experiments **3T** molecules are present in different aggregated states. Therefore, the luminescence measurements yield only an upper limit of the actual **3T** lifetimes within the mixed aggregates and the slope of the τ_0/τ dependence is not analysed in more detail and cannot be used for further analysis even though the linear relationship is still clearly present. When looking at the absorption and emission of **3T**, it is observed that there is a small overlap between the two. This overlap means that, apart from direct ET from the **3T** molecules to a **6T** molecule, it is also possible that first ET between **3T** molecules occurs followed by ET to a **6T** molecule. These different processes will result in a non-uniform value for the quenching rate constant, explaining the non-linearity observed in the Stern-Volmer plot of Figure 5.

Table 2: Calculated k_{ET} between different chromophores inside the aggregate

molecules[a] involved in ET	$\kappa^{2\ b}$	R_0 (**nm**)	r^c (**nm**)	k_{ET} (**s^{-1}**)
D$_1$ A	1.0	3.7	5	1.7×10^9
D$_2$ A	1.4	3.9	4.6	3.9×10^9
D$_3$ A	2.5	4.3	3.5	3.4×10^{10}
D$_4$ A	3.6	4.6	1.9	2.0×10^{12}
D$_n$ D$_{n\pm1}$	3.6	1.9	1.9	8.8×10^9

*a) The ET between species as depicted in Figure 6. b) For the above calculations it is supposed that the transition dipole moment is along the direction of the terthiophene or sexithiophene moiety.[10] Furthermore, we assume that the angles and distance between an **D** and an **A** do not change during the ET process. c) The distance is calculated based on the assumption that the **3T** molecules organise in regular cylindrical shape, with a distance of 5 nm between the opposite chromophores.*

From the initial increase in ET efficiency with increasing concentration of **6T** at a fixed concentration of **3T**, it was calculated that up to forty-three **3T** molecules are being quenched by one **6T** (determined at 10 mM **3T**). To evaluate to what extent ET between **3T** and **6T** molecule occurs and to what extent ET between neighbouring **3T** molecules takes place, we calculated the Forster distance and rate constants for various cases[8], see Table 2 and Figure 6. For the arrangement of the **3T** and **6T** molecules at opposite positions of the micelle, k_{ET} amounts to 1.7×10^9 s^{-1}. Decreasing the distance between **D** and **A** leads to larger rate constants up to 2×10^{12} s^{-1} for neighbouring **3T** and **6T** molecules. For energy transfer between two neighbouring **3T** molecules, the overlap integral decreases by two orders of magnitude (from 2.1×10^{14} for the overlap between **3T/6T** down to 2.1×10^{12} M^{-1}cm^{-1}nm^4 for **3T/3T**). However, the high value of κ^2 and the short inter-molecular

distance makes this **3T-3T** ET process as fast as ET between D_1 and **A** or between D_2 with **A** (compare entry 5 with entry 1 and 2 in Table 2). Because of the much higher occurrence of **3T-3T** than **3T-6T** contacts, and as well as the calculated rate constants, it can be concluded that it is very likely that both ET processes *i.e.* **3T-3T** and **3T** to **6T** are taking place.
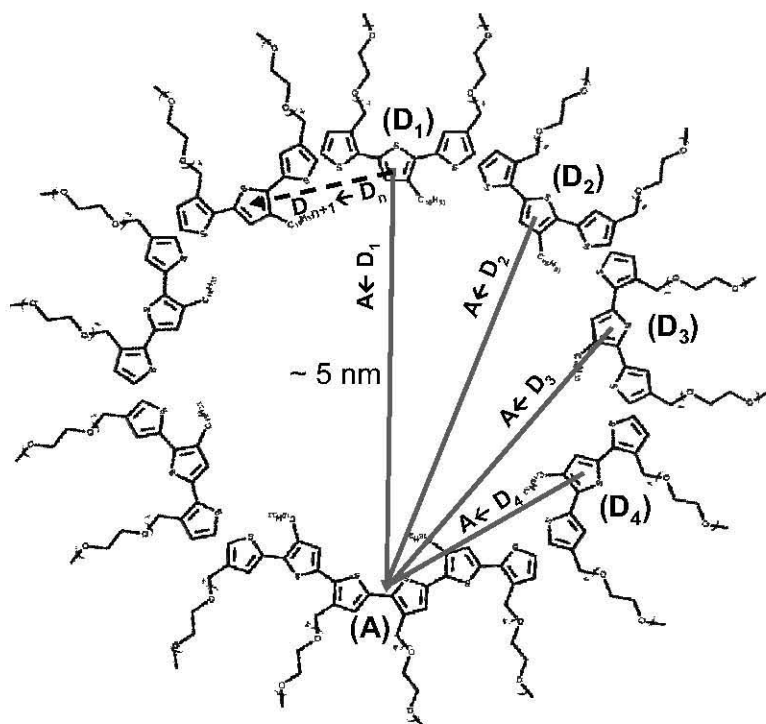

*Figure 6: A schematic representation of the proposed orientation between **D** (3T) with respect to each other and between different **D** and the **A** (6T) with a total distance between two oppositely positioned chromophores of about 5 nm, based on previous work.*

Additional support for the migration of the exciton was also obtained by investigating the quenching volume (V_q) which shows an enlarged volume of

quenching with respect to the determined Förster distances (Table 2). The V_q is the volume around the **A** that is being quenched and can be calculated form equation **4**.[11]

$$\frac{I_0}{I} = e^{V_q N_a [A]} \qquad \textbf{(4)}$$

When $\ln(I_0/I)$ is plotted against the [**A**] (Figure 7), the slope divided by N_a (Avagadro's number) gives V_q (dm^3).
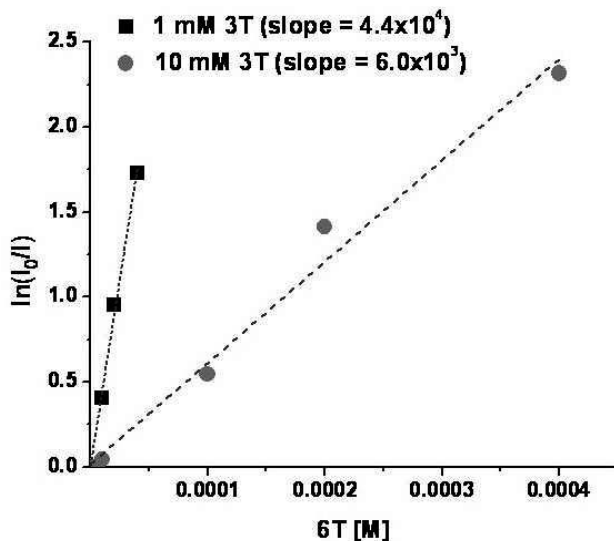

*Figure 7: plot of ln(I$_0$/I) vs. [**6T**] as a measure to determine the quenching volume (V$_q$) for a series of 1 mM **3T** solutions and of 10 mM solutions.*

Assuming that the volume is spherical symmetric, the distance r_q where quenching is still possible can be determined and was found to be about 26 and 13 nm for 1 mM and 10 mM, respectively. It is said that there should be no quenching of **D** by **A** beyond 1.5 times the Förster distance (R_0, ranging from 1.9-4.6 nm, see Table 2),

which would mean that the maximum distance for quenching should be about 7 nm.[11] (about 3-7.5 nm). From calculations, the distance of quenching on average is extended by at least 8 to 21 nm, depending of the concentration of **3T**. This distance is probably a gross underestimation, since there is not a spherical but a more linear distribution of **3T** molecules inside the aggregate.
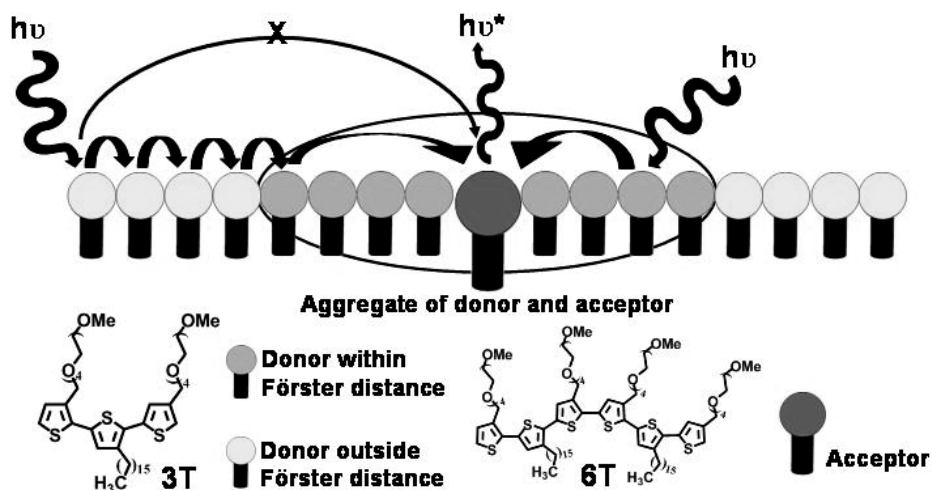

*Figure 8: Schematic representation of **6T** inside the **3T** aggregate and the mechanisms of energy transport, on the right an energy transfer according to the Förster mechanism and on the left the excited state is transported between neighbouring donors until it is within the Förster distance which then follows the mechanism presented on the right.*

Our findings clearly show that the exciton, created on a **3T** molecule, can take part in two types of ET processes in mixed **3T-6T** aggregates. Either the excited state on the **3T** is close enough to the **A** leading to direct resonant ET to the **A** takes place, or the **D** and **A** are too far from each other for direct ET to occur and the energy is transferred to a neighbouring **3T** molecule. This process is repeated until the exciton

is close enough the have again direct ET with the **A**. A schematic representation of the system is given in Figure 8.

6.6   Conclusion

This work demonstrates that water-soluble self-assembling energy transfer systems could be obtained by simple mixing of amphiphilic ter- and sexithiophenes. Nearly complete quenching of the emission of the **3T** energy donor was found. Although migration of excitation energy has been observed intra-molecular in conjugated polymers[10] and inter-molecular in crystals[11], it remains a rare phenomenon in self-assembled systems[7] and to the best of our knowledge has not yet been observed in aqueous self-assembling systems. It was found that the excitation energy is transported along the elongated micelle until it reaches the **A**. Stern-Volmer analysis showed that different processes take part in the quenching and hence ET process. According to the calculated k_{ET}, that for **3T** molecules which are more than 3.5 nm removed from the **6T**, that it is more likely that ET takes place between **3T** molecules than between the excited **3T** and **6T** molecules. These findings were supported by the enlarged quenching sphere of the **A** and it was found that the distance of quenching is larger than theoretically possible according to the spectroscopic overlap. The rate of energy transfer and the transport of the exciton along the aggregates come close to the speeds observed in natural photonic transport systems. The approach of using electronically active components like thiophenes in combination with the driving forces that make amphiphilic systems incredibly versatile, has proven to have serious potential in the development of new materials, which due to the amphiphilic character may also be applied in biological systems.

6.7   Methods

Samples were prepared by combining the correct amounts for the appropriate ratios from stock solutions of terthiophene and sexithiophene in milliQ-water. The synthesis of the ter- and sexithiophene was described in chapter 3 and 4, respectively. For UV/Vis measurements an AnalytikJena Specord 250 spectrometer was used equipped with a deuterium-lamp and a halogen-lamp. Quartz cuvets were used with path-lengths varying from 1.0mm-0.1mm. Fluorescence spectroscopy was done on a Jasco J-815 CD-spectrometer equipped with a fluorescence monochromator and detector, and an L-38 low wavelength filter (cut-off 380nm) placed between the sample and the detector. The cuvet used here was quartz with dimensions 3x3mm. Dynamic Light Scattering was performed on a ZetaSizer Nano series Nano-ZS by Malvern Instruments. For determination of the luminescence lifetimes a LifeSpecs-ps (Edinburgh instruments) was used with excitation pulses of 70 ps at 405 nm.

For cryo-TEM, a few microliter of suspension was deposited on a bare 700 mesh copper grid. After blotting away the excess of liquid the grids were plunged quickly in liquid ethane. Frozen-hydrated specimens were mounted in a cryo-holder (Gatan, model 626) and observed in a Philips CM 120 electron microscope, operating at 120 KV. Micrographs were recorded under low-dose conditions on a slow-scan CCD camera (Gatan, model 794).

6.8   References

1   a) C. J. Law, A. W. Roszak, J. Southall, A. T. Gardiner, N. W. Isaacs and R. J. Cogdell, *Mol. Membr. Biol.*, **2004**, *21*, 183; b) N. Armaroli and V. Balzani, *Angew. Chem. In. Ed.* **2007**, *46*, 52-66.

2   a) M. Ghirotti, C. Chiorboli, C. -C. You, F. Würthner and F. Scandola, *J. Phys. Chem. A*, **2008**, *112*, 3376-3385; b) C. Devadoss, P. Bharathi and J. S. Moore, *J. Am. Chem. Soc.*, **1996**, *118*, 9635-9644; c) J.-S. Hsiao, B. P. Krueger, R. W. Wagner, T. E. Johnson, J. K. Delaney, D. C. Mauzerall, G. R. Fleming, J. S. Lindsey, D. F. Bocian and R. J. Donohoe, *J. Am. Chem. Soc.* **1996**, *118*, 11181-11193; d) J. Hofkens, M. Maus, T. Gensch, T. Vosch, M. Corlet, F. Köhn, A. Herrmann, K. Müllen and F. De Schryver, *J. Am. Chem. Soc.*, **2000**, *122*, 9278-9288.

3   V. Sundstrom and T. Pullerits, *J. Phys. Chem. B*, **1999**, *103*, 2327-2346.

4   a) S. L. Gilat, A. Adronov and J. M. J. Fréchet, *J. Org. Chem.*, **1999**, *64*, 7474.; b) A. Adronov, S. L. Gilat, J. M. J. Fréchet, K. Ohta, F. V. R. Neuwahl and G. R. Fleming, *J. Am. Chem. Soc.* **2000**, *122*, 1175-1185; U. Hahn, M. Gorka, F. Vögtle, V. Vicinelli, P. Ceroni, M. Maestri and V. Balzani, *Angew. Chem. In. Ed.*, **2002**, *41*, 3595-3598; C. Giansante, P. Veroni, V. Balzani and F. Vögtle, *Angew. Chem. In. Ed.,* **2008**, 47, 5422-5425.

5   a) A. Ajayaghosh, S. J. George and V. K. Praveen, *Angew. Chem. Int. Ed.,* **2003**, *42*, 332; (b) K. Sugiyasu, N. Fujita and S. Shinkai, *Angew. Chem. Int. Ed.,* **2004**, *43*, 1229; c) C. Tan, E. Atas, J. G. Müller, M. R. Pinto, V. D. Kleiman and K. S. Schanze, *J. Am. Chem. Soc.* **2004**, *126*, 13685-13694; d) P. van Rijn, T. J. Savenije, M. C. A. Stuart and J. H. van Esch, *Chem. Commun.*, **2009**, 2163-2165.

6   a) S. Bhosale, A. L. Sisson, N. Sakai and S. Matile, *Org. Biomol. Chem.*, **2006**, *4*, 3031-3039; b) D. Gust, T. A. Moore and A. L. Moore*, Acc. Chem. Res.*, **2001**, *34*, 40-48.

7   a) F. J. M. Hoeben, L. M. Herz, C. Daniel, P. Jonkheijm, A. P. H. J. Schenning, C. Silva, S. C. J. Meskers, D. Beljonne, R. T. Phillips, R. H. Friend and E. W. Meijer, *Angew. Chem. Int. Ed.*, **2004**, *43*, 1976-1979; b) A. Del Guerzo, A. G. L. Olive, J. Reicjwagen, H. Hopf and J.-P. Desvergne, *J. Am. Chem. Soc.*, **2005**, *127*, 17984-17985; c) H. Lin, R. Camacho, Y. Tian, T. E. Kaiser, F. Würthner and I. G. Scheblykin, *Nano Lett.*, **2010**, *10*, 620-626; d) X. Zhang, Z.-K. Chen and K. Ping Loh, *J. Am. Chem. Soc.*, **2009**, *131*, 7210-7211; f) J. G. Müller, E. Atas, C. Tan, K. S. Schanze and V. D. Kleinman, *J. Am. Chem. Soc.*, **2006**, *128*, 4007-4016.

8   a) J. R. Lakowicz, *Principles of Fluorescence Spectroscopy*, **2006**, *3rd ed.*, Springer; b) B. Valeur, *Molecular Fluorescence: Principles and Applications*, **2001** Wiley-VCH Verlag GmbH.

9   a) A. G. Denkova, E. Mendes and M.-O. Coppens, *J. Phys. Chem. B*, **2008**, *112*, 793-801; b) A. G. Denkova, E. Mendes and M.-O. Coppens, *J. Phys. Chem. B*, **2009**, *113*, 989-996; c) W. Eimer and R. Pecora, *J. Chem. Phys.*, **1991**, *94*, 2324-2329; d) J. Wilcoxon and J. M. Schurr, *Biopolymers*, **1983**, *22*, 849-867; e) A. K. Wright and J. E. Baxter, *Biophys. J.*, **1976**, *16*, 931-938.

10   E. E. Nesterov, Z. Zhu and T. M. Swager, *J. Am. Chem. Soc.*, **2005**, *127*, 10083-10088.

11   O. D. Jurchescu, J. Baas and T. T. M. Palstra, *Appl. Phys. Lett.,* **2004**, *84*, 3061-3063; b) H. Yoshikawa, K. Sasaki and H. Masuhara, *J. Phys. Chem. B*, **2000**, *104*, 3429-3437.

Chapter 7
Photo-induced charge separation in self-assembled PCBM/amphipathic oligothiophene aggregates in water

Abstract

In this study it has been demonstrated that the amphipathic sexithiophene, discussed in chapter 4, and PCBM can be used as a self-assembled antenna system which displays photo-induced charge separation with an efficient electron transfer occurring with a high quantum yield up to 95%. The solubilisation of up to 1 mM PCBM in water was achieved with the use of an amphipathic conjugated sexithiophene (**6T**) and by that bringing two photo-/electro-chemical active moieties in close proximity by self-assembly. A decrease in luminescence of the **6T** was observed with increasing the PCBM concentration and charge separation was confirmed with light-induced electron spin resonance spectra showing signatures of the **6T** radical cation and of the PCBM radical anion. Preparing aqueous charge transfer systems with the appropriate energy levels is of great interest for self-assembled organic photo-electro chemical cells for producing energy rich compounds with the use of sunlight.

7.1   Introduction

Using sunlight as an alternative source of energy is already receiving vast amounts of attention ever since the first silicon solar cells were produced.[1] Since silicon cells are costly to prepare and mechanically fragile, over the years alternatives have been found by chemists in the form of films prepared from organic molecules for solar cells based on conjugated polymers and fullerene derivatives being more flexible and less costly.[2,3] In chapter 5 and 6 antenna systems have been discussed which were able to absorb (5) and transport (6) photonic energy and due to energy transfer from the donor aggregate to a second chromophore, the acceptor, the energy was released as a photon of different energy than would be observed without the acceptor. In this chapter a different use of this energy is discussed. As mentioned in chapter 5, absorbed photonic energy can also be released as heat (in non-radiative decay) or the energy is used to obtain a charge separated state. A charge separated state can be obtained when a donor and acceptor are in close proximity of each other and the corresponding LUMO (lowest unoccupied molecular orbital) of the donor is higher in energy than that of the acceptor (Figure 1). When an electron is transferred from the HOMO (highest occupied molecular orbital) of the donor to the LUMO by excitation, it is possible that the electron is transferred from the LUMO of the donor to the LUMO of acceptor. This results in the formation of charges since the donor has lost one electron and the acceptor gained one electron. This loss and gain of one electron not only allows for the creation of charges but also since the electron is no longer paired, a radical is formed. Therefore the donor will become a radical cation and the acceptor a radical anion (Figure 1). This is a form of oxidative electron transfer. It is also possible to transfer an electron from the HOMO of the acceptor to the half empty HOMO of the excited donor. This occurs when the HOMO/LUMO levels of the acceptor are higher in energy and is referred to as reductive electron transfer.
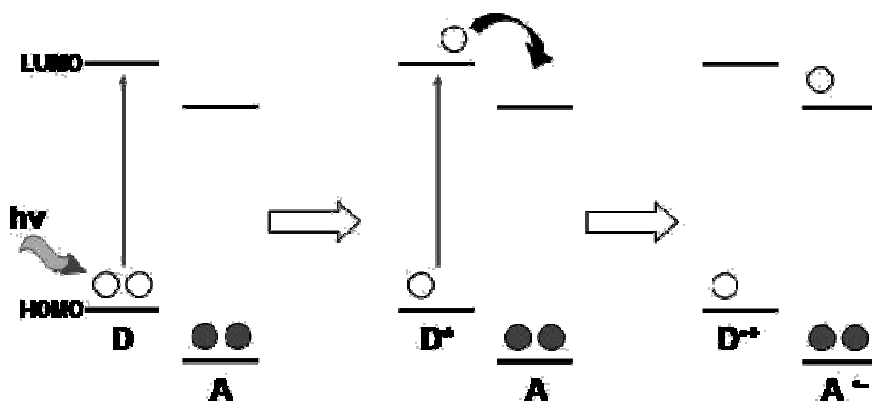
Figure 1: Upon excitation the electron is transported from the HOMO to the LUMO within the donor. This is then able to transfer to the LUMO of the acceptor but only if that is equal or lower in energy than the LUMO of the donor. When electron transfer occurs, it results in a donor radical cation and an acceptor radical anion.

Harvesting sunlight for using the energy is noble. However, it should be transformed into a usable form and the mentioned formation of a charge separated state is one way. This charge separated state can be used for the production of energy rich compounds and for producing electricity.[3,4] Nature does this efficiently by inducing chemical reactions with the energy of sunlight by transforming e.g. ADP (Adenosine diphosphate**)** into the energy rich ATP (Adenosine-5'-triphosphate)[5] and photovoltaic cells are able to produce a charge separated state which can be transported and allows for a current to be formed[3]. It is still a challenge to have a light harvesting antenna system with controllable dimensions and morphology which is able to produce an active/reactive state like is found in photovoltaic cell and in nature. Previously, covalently bound conjugated oligomers with fullerenes have been intensively studied. Interestingly, for substituted oligo phenyl-vinylene-C60 compounds it was found that on excitation of the oligomer a two step process took place: First energy transfer from the oligomer to the PCBM, followed by an electron transfer step, albeit this last step only occurred in polar media.[6]

Here a self-assembled antenna system in water was prepared which utilises the harvested photonic energy to induce a charge separated state. This was achieved with the use of self-assembled amphipathic sexithiophene (**6T**) aggregates in water which was described in chapter 4, in combination with PCBM (Figure 2).
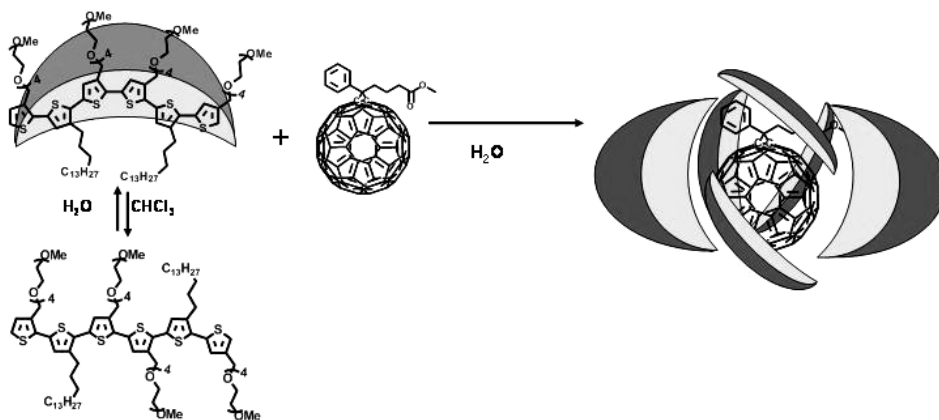

Figure 2: schematic representation of the assembly of the curved donor and spherical acceptor (thiophene/PCBM) aggregate surrounded by water, in which the hydrophobic cavity acts as a host for the hydrophobic PCBM.

The solubilisation of large concentrations of fullerene-derivatives in water has been done with conventional surfactants[7] without any additional functionality or by chemical modification of the fullerene with hydrophilic moieties like polymers, sugars or charged groups.[8] In chapter 4 it was discussed that the amphipathic sexithiophenes are able to aggregate due to hydrophobic effects in water and produce small micellar aggregates. These aggregates contain a hydrophobic cavity which is excellent for solubilising hydrophobic compounds, such as porphyrins and other hydrophobic moieties as seen in chapter 5.[9] Since oligothiophenes are redox and optically active compounds, combining it with a hydrophobic electronically interesting compound like PCBM produces exciting self-assembled donor-acceptor

systems. In this way the donor (**6T**) and the acceptor (PCBM) are located together at the nanometre-scale in a polar medium (Figure 2). The polar medium and the energy of the LUMO-levels (sexithiophene: 2.6eV(from lit.)[10], PCBM: 3.8eV(from lit.)[3], both with respect to vacuum), should favour oxidative electron transfer between the donor (**6T**) and acceptor (PCBM). The aggregates were studied by optical techniques and dynamic light scattering (DLS). Additionally, light-induced electron spin resonance (LESR) measurements were carried out to confirm the charge transfer process.

7.2   A   sexithiophene/PCBM   self-assembled   antenna system in water which is able to form a charge separated state

In water PCBM is insoluble; however when PCBM was added to a solution of **6T** of concentrations above the critical micelle concentration (cmc), small amounts were able to dissolve. In order to achieve higher solubility the PCBM doped **6T** aggregates were made by preparing a mixed film of **6T** with the appropriate amount of PCBM in chloroform, followed by re-suspension of the film in water. This procedure proved more successful in obtaining high solubility of PCBM in water. The maximum solubility of PCBM in a 5.0 mM **6T** solution was 1.0 mM (ratio of 5:1). The solutions were stable for weeks and even the ratio of 5:1 was still transparent without precipitation for more than a week. Also a highly saturated solution was made by preparing a mixed film of PCBM and **6T** in a 1:1 ratio. After re-suspending the film in water, the formed suspension was filtered to remove excess PCBM (ratio of ~2.5:1 calculated according to the fitted quenching curve). The solution was only stable for a few days. While determining the aggregate size by dynamic light scattering (DLS), it was observed that the solubilisation is paired with an increase in the overall hydrodynamic diameter going from 9 nm initially without PCBM to 24 nm when a high loading of PCBM is added. This suggests that PCBM influences the aggregate size and that at high ratios of PCBM, more than one

PCBM molecules can reside inside the hydrophobic domain of the aggregate. It can be assumed that the PCBM is taken up inside the hydrophobic domains of the aggregate since quenching of the emission of **6T** was observed upon introducing PCBM indicating there is transfer of energy or charge and that indeed they are in close proximity of each other.

When electronically active species are brought in close proximity of one another, this can result in altered photo-physical properties. Figure 3 (left) shows the absorption of **6T** (λ_{max}: 423nm) and PCBM alone, and of a 5:1 ratio **6T**:PCBM (λ_{max}: 415nm) mixed system. It becomes clear that there is a small shift in **6T** absorption wavelength towards the blue of about 8 nm, which might indicate small ground-state coupling. Upon introduction of PCBM into the **6T** aggregates the **6T** emission (λ_{max}: 582nm) also displayed a small shift in emission maximum towards the blue of about 6 nm for the 5:1 ratio (576nm) (Figure 3, right), again indicating that, though small, electronic interactions are present. For the luminescence experiments, 5.0 mM solutions of **6T** were titrated with PCBM, in order to obtain molecular ratios from 200:1 (**6T**: PCBM) to a 5:1 ratio (Figure 3). It was observed that the emission of **6T** was increasingly quenched with increasing PCBM concentration. This quenching can be attributed to energy transfer or charge transfer from the **6T** to the PCBM or to two consecutive steps, consisting of energy transfer followed by charge transfer. In view of the close proximity of donor and acceptor energy transfer as well as charge transfer is possible. The overlap integral between the emission spectrum of the donor (**6T**) and the absorption spectrum of the acceptor (PCBM) is relatively small, and in combination with the low quantum yield for radiative emission of **6T**, energy transfer is less likely to occur. Charge transfer, however, is much more likely to occur, because the relative positions of the LUMO energy levels of both compounds involved as mentioned before, provide a substantial driving force for charge transfer from the excited **6T** to the PCBM, which would lead to the **6T** radical cation and a PCBM radical anion.
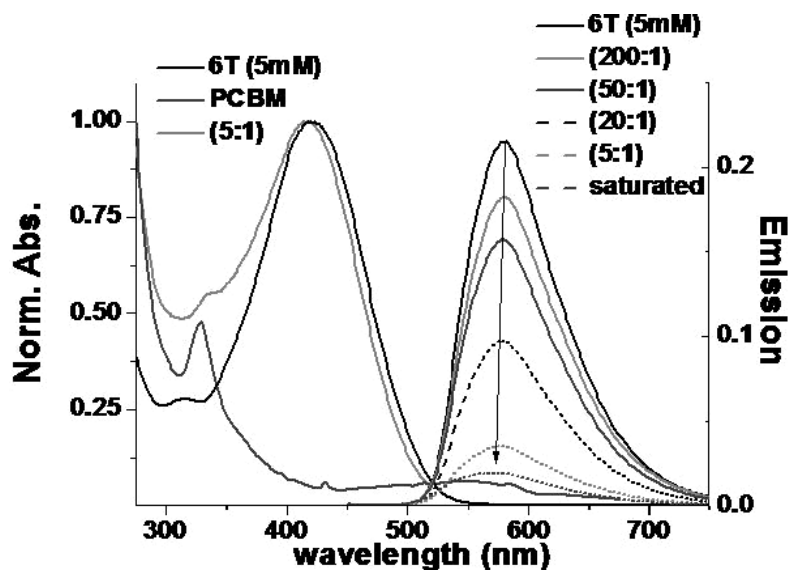
*Figure 3: On the left, normalised absorption spectra of sexithiophene (water), PCBM (THF) and the combination of the two in a 5:1 ratio (water). On the right, **6T** fluorescence (λ_{ex}:425 nm, λ_{em}:580 nm) in the presence of increasing amounts of PCBM in water.*

Further evidence for charge transfer in these systems came from additional studies of the emission of the PCBM. When a 1 mM solution of PCBM in chloroform was excited at 425nm and the emission investigated, it was found that there was an appreciable emission between 470 and 650 nm with the emission maxima at 555 nm. When a 5mM aqueous solution of **6T** was irradiated which also contains 1 mM of PCBM (5:1 ratio), no emission corresponding to the PCBM was observed which would be visible since the emission of **6T** is mostly quenched. From this observation we can conclude that though energy transfer cannot be excluded, the absence of PCBM emission, demonstrates that a charge transfer step is involved (Figure 4).
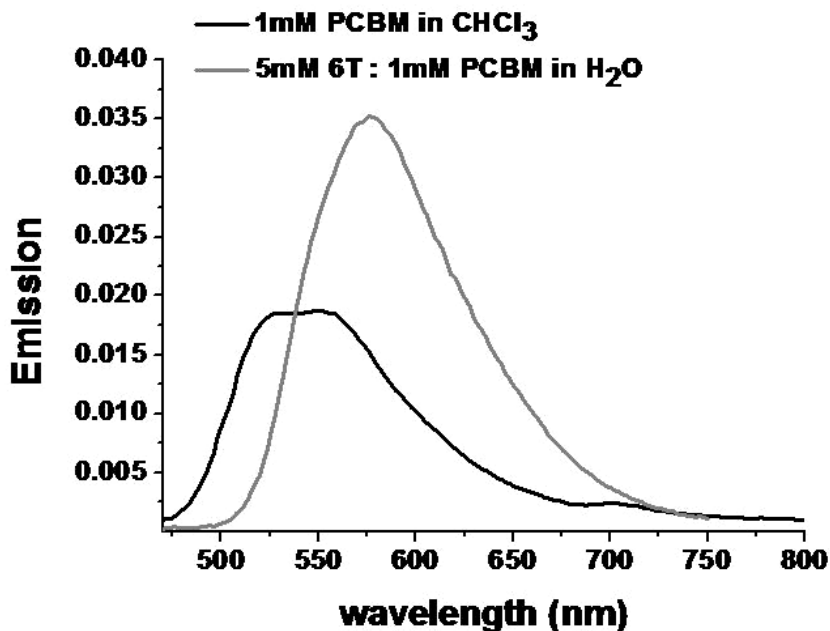
Figure 4: The emission spectrum of a 1 mM solution of PCBM in chloroform emitted between 450 and 650 nm with the maximum around 550nm. The emission of PCBM was not detected in the 5:1 aqueous sexithiophene (5mM) : PCBM (1mM) system, where also 1 mM PCBM is present in an apolar environment. This indicates that charge separation occurs which is a non-radiative process in the case of PCBM.

To verify if indeed charge transfer from **6T** to a PCBM molecule occurs, light induced electron spin resonance experiments (LESR) were carried out. To this end an aqueous solution with a ratio of 5:1 was transferred into a quartz ESR tube and cooled down to 100 K. The spectrum recorded in the dark did not give any appreciable signal. On continuous illumination of the sample at 488 nm the ESR spectrum clearly demonstrates the presence of unpaired electron spins. The shape of the light spectrum can be reconstituted by two separate contributions consisting of the derivative of a Gaussian and of a Lorentzian line shape, which are both added in Figure 5. In using this approach it was assumed that both g tensors were isotropic.

The Gaussian transition at g = 2.0018 can be attributed to the formation of a radical cation on the **6T** and the Lorentzian transition at g = 2.0001 is attributed to the PCBM radical anion.[11]
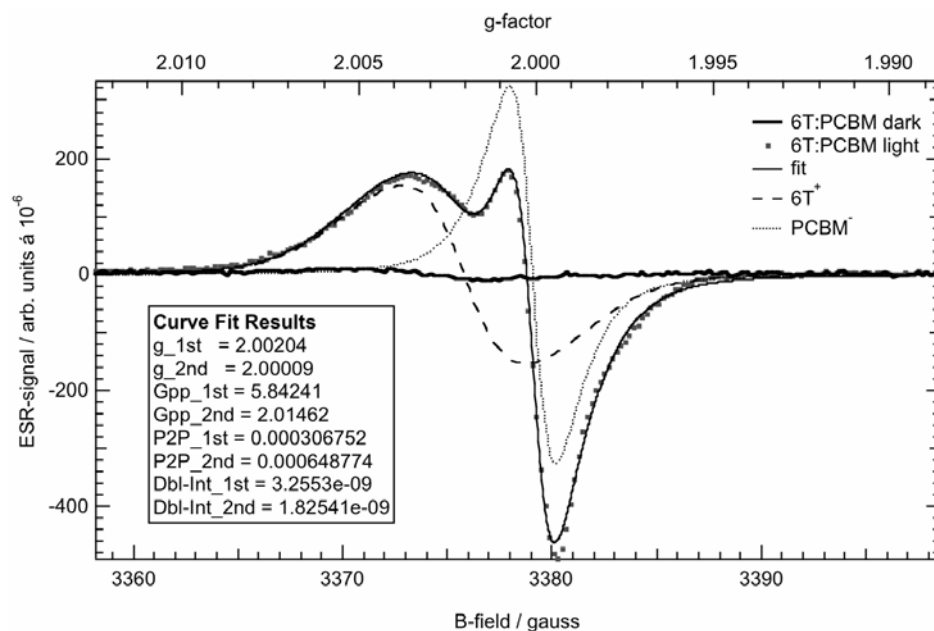

Figure 5: X-band ESR spectra of the 6T:PCBM aggregates (5:1) at 100K recorded on excitation at 488 nm. The fit is based on a summation of a Gaussian and a Lorentzian lineshape with parameters as indicated.

Typically, a Gaussian line shape is related to inhomogeneous broadening, which can be explained by the rather randomly orientated **6T** molecules within the micellar aggregate. On varying the microwave power it was observed that the relative contributions of both transitions change, indicating that the spins involved are uncoupled, similar as has been concluded previously for composite systems of substituted poly-thiophenes and fullerenes.[12] For the **6T** radical cation the peak to peak distance amounts to 7.5 Gauss, similar as has been reported for amorphous oligothiophenes[12], and which indicates the presence of an isotropic system of the **6T**

molecules. This concurs with a micellar structure. Examination by LESR of pure **6T** aggregates without PCBM in frozen water showed that on prolonged illumination also **6T** radical cations are formed. This can be rationalised by assuming that **6T*** is energetically able to reduce the surrounding water molecules yielding the corresponding **6T** radical cation. In contrast, PCBM molecules in an apolar environment (dry film) do not give an appreciable LESR signal as also has been reported previously.[12] In conclusion; the LESR measurements confirm that on visible illumination light-induced charge transfer from the **6T** to the PCBM occurs.

From the quenching and the corresponding fluorescence lifetime measurements, the electron transfer parameters were determined and collected in Table 1. A quantum efficiency of 95% for charge transfer was found for the saturated system (~2.5:1) and 86% for the 5:1 ratio. There is a high driving force for charge transfer and the process is very efficient. From equations **1**, **2** and **3**, in combination with the fluorescence lifetime τ_D and fluorescence quantum yield (φ_F) of 0.03 (determined by using 9,10-diphenyl-anthracene as a reference), the different fluorescence rate constants k_{LUM} (luminescence rate constant), k_{NR} (non-radiative decay constant) and k_{CT} (charge transfer rate constant) can be determined.

$$\phi_F = k_{LUM}\tau_D^0 \qquad (1)$$

$$\tau_D^0 = \frac{1}{k_{LUM} + k_{NR}} \qquad (2)$$

$$k_{CT} = \frac{1}{\chi\tau_D} - \frac{1}{\tau_D} \qquad (3)$$

Here χ is the ratio of the emission of the donor between **D/A**-complex and **D**.

When looking at the rate for luminescence (k_{LUM}: 0.21 ns^{-1}) of the thiophene system it is seen that the non-radiative decay (k_{NR}: 7.0 ns^{-1}) is much faster than the k_{LUM}. The k_{NR} was calculated using a, However, when PCBM is added the rate of charge

transfer, (k_{CT}) (listed in Table 1) becomes faster than the k_{NR}, demonstrating that the energy and/or charge transfer process is very efficient.

Table 1: Charge transfer properties of 6T aggregates and PCBM in water

Composition **D/A**	τ_D in (**ps**)[a]	Emission Int.	$X(I_{DA}/I_D)$	Φ_{ct} [b]	k_{ct} (s[-1])[c] 10^9
D 5.0mM	146 (τ^0_D)	0.22	1	- - -	- - -
D:A 200:1	147	0.18	0,85	0.15	1.24
D:A 50:1	146	0.16	0,73	0.27	2.51
D:A 20:1	124	0.10	0,45	0.55	8.33
D:A 5:1	80	0.04	0,16	0.86	41.1
D:A saturated	76	0.02	0,09	0.95	126.0

*a) Lifetimes τ_D were measured (λ_{ex} : 407 nm, monitored at 560 nm). b) The charge transfer efficiency was calculated using $\Phi_{Ct} = k_{ct}/(k_{ct} + k_{lum} + k_{nr})$. c) k_{CT} was determined using $k_{CT} = 1/(\chi\tau_D)-1/(\tau_D)$ were χ is the ratio in emission of **D/A** and **D**, where **D** (donor)= sexithiophene and **A** (acceptor)= PCBM with τ_D as the fluorescence lifetime of **D** without A.*

7.3 Association of PCBM with sexithiophene aggregates in water

The gradually enhanced quenching of the fluorescence upon increasing PCBM concentration is more closely investigated by plotting the I_0/I versus concentration of PCBM. Here, I_0 is the initial fluorescence without PCBM and I the fluorescence obtained with the **6T**/PCBM systems, a Stern-Volmer plot is obtained with a linear relationship between the **6T** fluorescence and PCBM concentration (Figure 6).
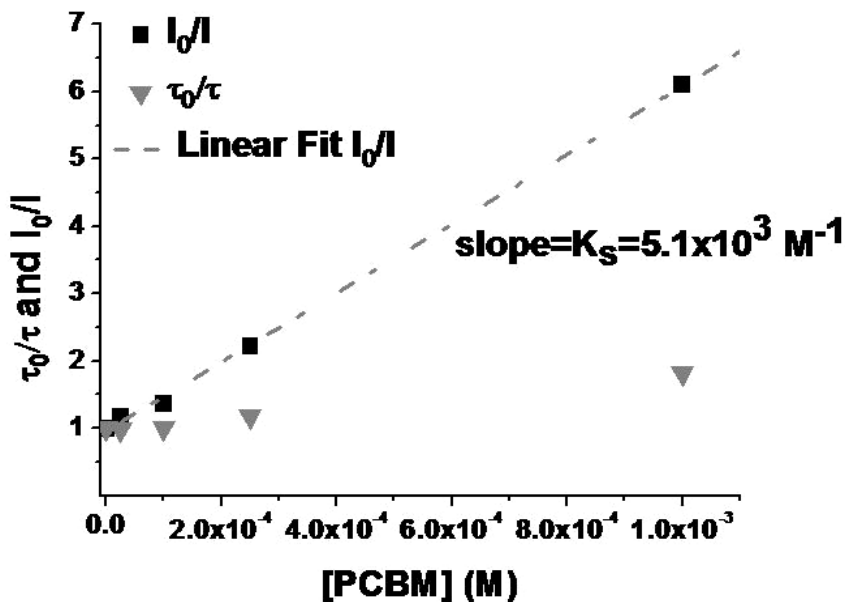
Figure 6: Stern-Volmer plot of change in fluorescence (I_0/I) versus the quencher concentration (square). Also plotted is τ/τ_0 versus the quencher concentration (triangle) showing that at higher PCBM concentrations dynamic quenching plays a minor role (τ/τ_0 increasing).

If assumed that the quenching is static, then by using the relation:

$$I_0 / I = 1 + K_{SV}[Q] \qquad (4)$$

where Q is the quencher concentration, the association constant K_s can be determined.[13] This was found to be $5.1 \cdot 10^3$ (± 100) M^{-1}. This value does not correspond to the molecular association between a PCBM molecule and a sexithiophene amphiphile and probably also not the association of PCBM with an aggregate of sexithiophenes because of the pour solubility of PCBM (in order to determine the association constant an equilibrium between PCBM in solution and

inside the aggregate is needed, due to the low solubility in water, this equilibrium is negligable). Therefore the association value found is probably between a **6T** in solution and an aggregate of **6T** which holds PCBM and is able to quench the bound **6T**. The linear relation between I/I_0 *vs.* the PCBM concentration in the Stern-Volmer plot indicates that the quencher is located at a position where it is at the same distance from all **6T** donors. This suggests that the PCBM molecules are indeed located in the centre of the **6T** aggregates.

The quenching was found to be only static in a limited PCBM range. When τ/τ_0 is plotted versus the quencher concentration, a constant value of unity should be observed if the quenching is static, meaning that there is no change in the fluorescence lifetime. However, at high PCBM concentrations a deviation from unity is observed, indicating dynamic quenching. This is generally attributed to diffusion based motion of the excited molecule or of the quencher. In view of the lifetimes of the excited state of less than 100 ps the diffusion length is however limited. Therefore we tentatively attribute the cause of the dynamic quenching to energy migration of the excited state over the closely packed **6T** molecules in the large aggregates. This is possible due to the overlap between the absorption and emission of **6T**. Even though this is a small overlap, still Förster resonance energy transfer is possible. The contribution of this type of quenching is only minor, since the I_0/I (static quenching) shows a linear relationship and when there is an appreciable contribution of dynamic quenching this would deviate from linearity.

7.4 Potential application in photo-chemical devices

We have shown that it is possible to have a self-assembled system from amphipathic sexithiophenes which has a high affinity for PCBM, shown by Stern-Volmer calculations. This sexithiophene/PCBM combination displays charge separation when irradiated with photonic energy. This creates a sexithiophene radical cation and a PCBM radical anion. From the energy levels of PCBM and sexithiophene, this

system has a potential application in producing energy rich compounds with the use of sunlight. Looking at the HOMO-LUMO levels of PCBM and sexithiophene (Figure 7) it shows what was experimentally already proven, that electron transfer is possible from the thiophene to the PCBM. However examining the energies needed for the splitting of water, it would be feasible in the future to do water-splitting with this self assembled-antenna system (Figure 7).
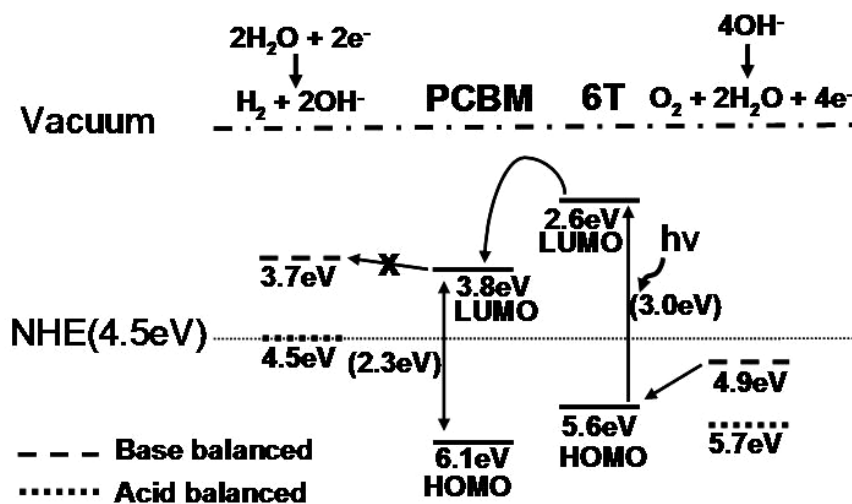

*Figure 7: Schematic representation of the energy level diagram for the conversion of water into H_2 and O_2 by light in combination with PCBM and **6T**, where the limiting factor is the reduction of water by PCBM.*

Combining electronically active species in water by self-assembly using hydrophobic interactions offers a new route towards practical devices e.g. hydrogen cells. Just as in solar cells there is a transition in the use of materials and instead of using metal-oxides[14] for these hydrogen cells, organic compounds attract more attention.[15,16] Also the way of preparation shifts more towards self-assembled systems of functional molecules for solar harvesting.[8,17] This because self-assembling systems offer great potential for the facile fabrication of all kinds of structures including photo-electro chemical cells since.

7.5 Conclusion

It was shown that it is possible to use a photo-responsive conjugated thiophene surfactant (**6T**) to solubilise an otherwise insoluble electro- and photochemical active compound like PCBM, in water up to 1.0 mM concentrations. The encapsulation of PCBM by the surfactant is associated to the hydrophobic domains of the aggregates and the interaction between thiophene and PCBM was displayed by quenching of fluorescence of the **6T** and PCBM, which indicates that charge transfer takes place. Luminescence quenching efficiencies of up to 95% have been found, demonstrating efficient charge transfer between **6T** and PCBM. LESR measurements confirm the light-induced charge separation between the **6T** and PCBM molecules.

7.6 Methods

Samples were prepared by combining the correct amounts for the appropriate ratios from a stock solution of sexithiophene in chloroform and a stock solution of PCBM in chloroform. The solvent was then removed and the film was re-suspended in milliQ-water. PCBM was obtained from Sigma Aldrich without any purification. For UV/Vis measurements an AnalytikJena Specord 250 spectrometer was used equipped with a deuterium-lamp and a halogen-lamp. Quartz cuvets were used with path-lengths varying from 1.0mm-0.1mm. Fluorescence spectroscopy was done on a Jasco J-815 CD-spectrometer equipped with a fluorescence monochromator and detector. The cuvet used here was quartz with dimensions 3x3mm. Dynamic Light Scattering was performed on a ZetaSizer Nano series Nano-ZS by Malvern Instruments. For determination of the luminescene lifetimes a LifeSpecs-ps (Edinburgh instruments) was used with excitation pulses of 70 ps at 405 nm.

LESR spectra are recorded using a modified X-band spectrometer (Bruker, ER200D) with an optically accessible microwave cavity (Bruker, ST4102). For illumination an Ar Ion laser (Melles Griot, 43SE) yielding 488 nm with an intensity

of 10 milliwatt entering the cavity was used. Spectra were recorded using 100 KHz field modulation of 2 Gauss. Solutions containing **6T**:PCBM in 5:1 ratio were transferred into a quartz ESR tube and cooled down to 100 K using a He flow cryostat (Oxford)

7.7 References

1   M. Grätzel, *Chemistry Letters*, **2005**, *34*, 8-13.
2   G. Yu, J. Gao, J. C. Hummelen, F. Wudl and A. J. Heeger, *Science*, **1995**, *270*, 1789-1791.
3   a) C. J. Brabec, N. S. Saricitifi and J. C. Hummelen, *Adv. Funct. Mater.*, **2001**, *11*, 1, 15-26; b) G. Dennler, M. C. Scharber and C. J. Brabec, *Adv. Mater.*, **2009**, *21*, 1323-1338.
4   a) M. Woodhousea and B. A. Parkinson, *Chem. Soc. Rev.*, **2009**, *38*, 197-210; b) M. Grätzel, *Nature*, **2001**, *414*, 338-344; c) O. Khaselev and J. A. Turner, *Science*, **1998**, *280*, 425-427.
5   a) C. J. Law, A. W. Roszak, J. Southall, A. T. Gardiner, N. W. Isaacs and R. J. Cogdell, *Mol. Membr. Biol.*, **2004**, *21*, 183; b) N. Armaroli and V. Balzani, *Angew. Chem. In. Ed.,* **2007**, *46*, 52-66.
6   P. A. van Hal, R. A. J. Janssen, G. Lanzani, G. Cerullo, M. Zavelani-Rossi and S. De Silvestri, *Phys. Rev. B*, **2001**, *64*, 7, 075206.
7   a) Ksenija Kogej and Bart Goderis, *J. Phys. Chem. C*, **2007**, 111, 2892-2900; b) Hongguang Li and Jingcheng Hao, *J. Phys. Chem. B*, **2007**, *111*, 7719-7724
8   a) H. Kato, C. Böttcher and A. Hirsch, *Eur. J. Org. Chem.*, **2007**, 2659-2666; b) Annamaria Quaranta, Y. Zhang, S. Filippone, J. Yang, P. Sinaÿ, A. Rassat, R. Edge, S. Navaratnam, D. J. McGarvey, E. J. Land , M. Brettreich, A. Hirsch and R. V. Bensasson, *Chemical Physics*, **2006**, *325*, 397-403; c) S. K. Teoh, P. Ravi, S. Dai and K. C. Tam, *J. Phys. Chem. B*, **2005**, *109*, 4431-4438; d) C. Burger, J. Hao, Q. Ying, H. Isobe, M. Sawamura, E. Nakamura and B. Chu, *J. Coll. Interface Sci.*, **2004** *275*, 632–641; e) P. Brough, D. Bonifazi and M. Prato, *Tetrahedron*, **2006**, *62*, 2110-2114; f) R. Charvet, D.-L. Jiang and T. Aida, *Chem. Commun.*,**2004**, 2664-2665.
9   P. van Rijn, T. J. Savenije, M. C. A. Stuart and J. H. van Esch, *Chem. Commun.*, **2009**, 2163–2165.
10 M. Grobosch and M. Knupfer, *Org. Electronics*, **2008**, *9*, 767-774.
11 a) V. Dyakonov, G. Zoriniants, M. Scharber, C. J. Brabec, R. A. J. Janssen, J. C. Hummelen and N. S. Sariciftci, *Phys. Rev. B*, **1999**, *59*, 12, 8019-8025; b) K. Marumoto, N. Takeuchi, T. Ozaki and S. Kuroda, *Synthetic Metals*, **2002**, *129*, 3, 239-247.
12 K. Kanemoto, K. Furukawa, N. Negishi, Y. Aso and T. Otsubo, *Phys. Rev. B*, **2007**, *76*, 15, 155205.
13 J. R. Lakowicz, *Principles of Fluorescence Spectroscopy*, **2006**, *3rd ed.*, Springer.
14 a) K. Rajeshwar, *J. Appl. Electrochem*, **2007**, *37*, 765-787; b) R. Asahi, T. Morikawa, T. Ohwaki, K. Aoki and Y. Taga, *Science*, **2001**, *293*, 269-271.
15 a) H. Imahori, *J. Phys. Chem. B*, **2004**, *108*, 6130-6143 ; b) H. Imahori, K. Mitamura, Y. Shibano, T. Umeyama, Y. Matano, K. Yoshida, S. Isoda, Y. Araki and O. Ito, *J. Phys. Chem. B*, **2006**, *110*, 11399-11405 ; c) R. Marczak, V. Sgobba, W. Kutner, S. Gadde, F. D'Souza and D. M. Guldi, *Langmuir*, **2007**, *23*, 1917-1923.
16 T. Abe, K. Nagai, S. Kabutomori, M. Kaneko, A. Tajiri, and T. Norimatsu, *Angew. Chem. Int. Ed.*, **2006**, *45*, 2778-2781.
17 a) A. Ajayaghosh, V. K. Praveen, C. Vijayakumar and S. J. George, *Angew. Chem. Int. Ed.*, **2007**, *46*, 6260-6265; b) S. Bhosale, A. L. Sisson, N. Sakai and S. Matile, *Org. Biomol. Chem.*, **2006**, *4*, 3031-3039; c) G. De Luca, A. Romeo, V. Villari, N. Micali, I. Foltran, E. Foresti, I. G. Lesci, N. Roveri, T. Zuccheri, and L. M. Scolaro, *J. Am. Chem. Soc.*, **2009**, *131*, 6920-6921.

Chapter 8
Amphipathic curved oligothiophenes as a tool for detecting membrane curvatures and imaging of membranes in living cells

Abstract

In this report we describe the use of curved conjugated amphipathic oligothiophenes to specifically target and detect strongly curved bilayer membranes in synthetic phospholipid vesicles and living cells. These curved amphipathic oligothiophenes were found to bind at micromolar concentrations to phospholipid bilayer membranes, with a preference for more strongly curved membranes. Differently curved membranes changed the emission properties of the membrane-bound oligothiophenes in the form of a blue shift and an increased quantum yield with increasing curvature. These changes in photo-physical properties were found to be of practical use for the targeting and fluorescence staining of organelles with highly curved membranes in living cells.

8.1 Introduction

Cellular bilayer membranes are constantly changing shape and surface curvature due to all kinds of processes like division, vesicle trafficking and movement.[1] Since all these processes are related to membrane curvature, it is important to be able to sense and target the different curvature. Being able target these membrane curvatures, helps to gain more insights in these processes and to develop diagnostic tools for membrane curvature related processes. The surface curvature in cellular membranes is implemented by scaffolding by specific membrane-bound proteins, for instance endophilins and epsins which can be found in different organisms.[2-6] They are able to bind through interactions between amphipathic helical domains which are located at the rims of a protein which has an overall banana shaped structure or curved domain (BAR-domain). There are several types of domains that are able to recognise and induce membrane curvature[3] and it is known that these domains play a key role in the bending and recognition.

Recently it was shown that proteins like endophilin-A1, containing BAR-domains, are able to induce a curvature of the membrane[4] and that these domains are able to recognise the curvature which is accompanied by an increase in binding affinity.[5,6] This affinity results in an increased local concentration proteins containing curved amphipathic domains as seen in BAR-domains and amphipathic α-helices.[4,7]

There are also examples in which there are structural deformations in the protein itself when presented to different curved membranes e.g. BAR domain proteins, epsins, and annexin B12.[8,9] For annexin B12, this conformational change was utilized as a sensor and structural changes in the protein with differently curved membranes was investigated with Electron Paramagnetic Resonance (EPR) and Circular Dichroism (CD).[9] Probing, sensing and visualization of membranes, organelles (ER, Golgi etc.) and cellular events or detecting certain biological active compounds like proteins has been investigated numerous times.[10,11] However, the

sensing moiety is always a natural occurring structure which often lacks powerful sensing tools in particular fluorescence. This can be added chemically to a membrane native protein and in this way stain and visualize the target membrane, however, this targeting is not based on the curvature but instead on the affinity for specific membrane-bound proteins.[16] Curvature sensing in membranes is also becoming increasingly important to gain insights in processes in which membrane interactions play an important role as well as to detect the formation and movement of small vesicles.[2-8] So far these experiments can only be done *in vitro* and with synthetic phospholipid membranes, in which the addressed membranes are always present with a relative high mono-dispersity in curvature e.g. extruded vesicles. In order to improve curvature sensing, a more general approach should be realized that not only allows for a qualitative curvature determination but is also able to be used as a direct visualization tool in confocal fluorescent microscopy studies and which can tolerate highly disperse membrane systems like a cell.

Here we report on a fully synthetic approach to target and detect highly curved lipid bilayer membranes by using fluorescent amphipathic conjugated oligothiophenes. These linear amphipathic oligothiophenes consist of hydrophilic and hydrophobic thiophene residues, which sequence has been designed to adopt a well-defined curved conformation upon exposure to a hydrophilic-hydrophobic interface. The curved conformation has a relatively large hydrophobic surface area, which is a key component for interaction with other amphiphilic systems like phospholipid membranes (Figure 1).[12] It was found that these amphipathic oligothiophenes bind preferably to small vesicles (30 nm), which is accompanied by large changes of the fluorescence properties. These features were exploited for the labelling of specific membranes in living Mel JuSo cells.
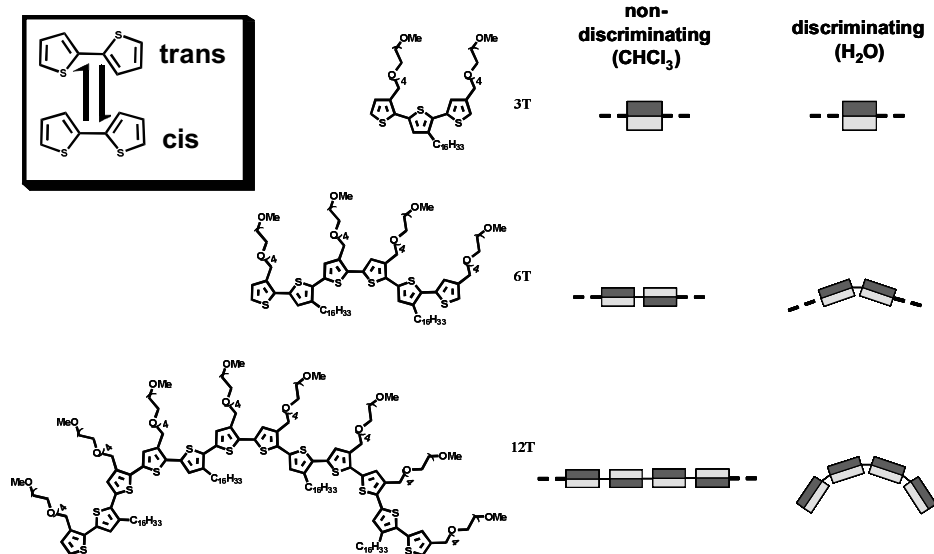
Figure 1: Molecular structures of the amphiphilic oligothiophenes. When placed in different media, apolar (chloroform) and polar (water), the overall molecular conformation changes due to reorientation of the aliphatic and ethylene glycol chains.

8.2 Incorporation of oligothiophenes into synthetic phospholipid bilayers

Liposomes and cell membranes are formed by hydrophobic interactions between phospholipids. Because the oligothiophenes described here also make use of this driving force for self-assembly, it was investigated whether these amphipathic oligothiophenes were compatible with these types of membranes. For these experiments we used three different oligothiophenes, which varied in length from 3 to 12 consecutively coupled thiophenes (**3T**, **6T**, **12T**). Previous investigations revealed that **6T** and **12T** can adopt a curved conformation in a polar environment due to orientation of the hydrophilic and hydrophobic substituents (Figure 1). In a

polar environment oligothiophenes **6T** and **12T** have an internal radius of curvature of about 2.5 nm. This radius depicts a full circle along the thiophene backbone.[10] In contrast, the terthiophene **3T** is a linear molecule without any apparent curvature and therefore is considered as good reference compound. The synthesis of these molecules was described in previous work.[10] It was found that all amphiphilic oligothiophenes aggregate into elongated- and spherical micellar type aggregates and were able to absorb and emit photonic energy (λ_{max} Absorption: 348 nm (**3T**), 423 nm (**6T**), 454 nm (**12T**); λ_{max} Emission: 461 nm (**3T**), 572 nm (**6T**), 645 nm (**12T**)). To investigate whether these oligothiophenes incorporate into membranes, we mixed the oligothiophenes with giant multi-lamellar vesicles (GMV). Fluorescence microscopy revealed that the bilayer membranes became fluorescent upon addition of the oligothiophenes (Figure 2). These observations clearly indicate that the thiophenes are able to bind to the lipid bilayer membrane of giant liposomes.
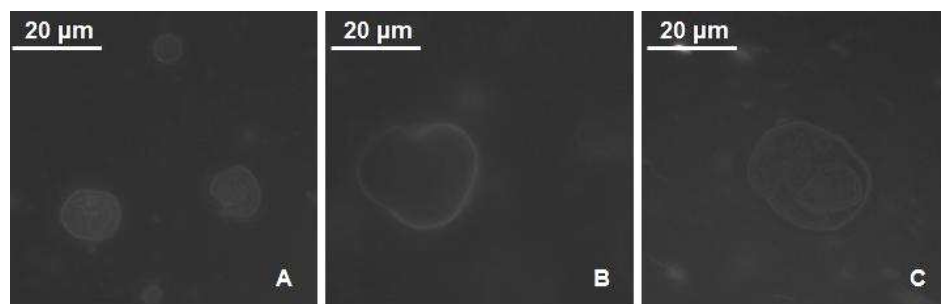

Figure 2: Incorporation of the different oligothiophenes in 10 mM DOPC Giant Multi-Lamellar Vesicles, visualized by fluorescence microscopy; A) 3T (10μM); B) 6T (10μM) and C) 12T (10μM) in buffer (HEPES/NaCl, 125mM/135mM at pH 7.2) at room temperature.

The binding of thiophenes to lipid bilayer membranes was further investigated by differential scanning calorimetry (DSC). Addition of oligothiophenes to extruded 400 nm DMPC vesicles in a lipid/thiophene ratio of 250:1 resulted in a change in the lipid phase transition. These changes of the main transition were less drastic for **6T**

and **12T** than for **3T** (Figure 3). A drastic shift and broadening of the main transition was observed when **3T** was introduced, a minor loss of the splitting[13] and broadening of the main transition for **6T** and a small shift in the main transition to lower temperatures for **12T**. For all compounds, upon introducing them to the vesicles, the pre-transition disappeared, also indicating incorporation.[14] Both the fluorescence microscopy and DSC indicate that compounds **3T**, **6T** and **12T** readily incorporate into lipid bilayers by mixing at room temperature.
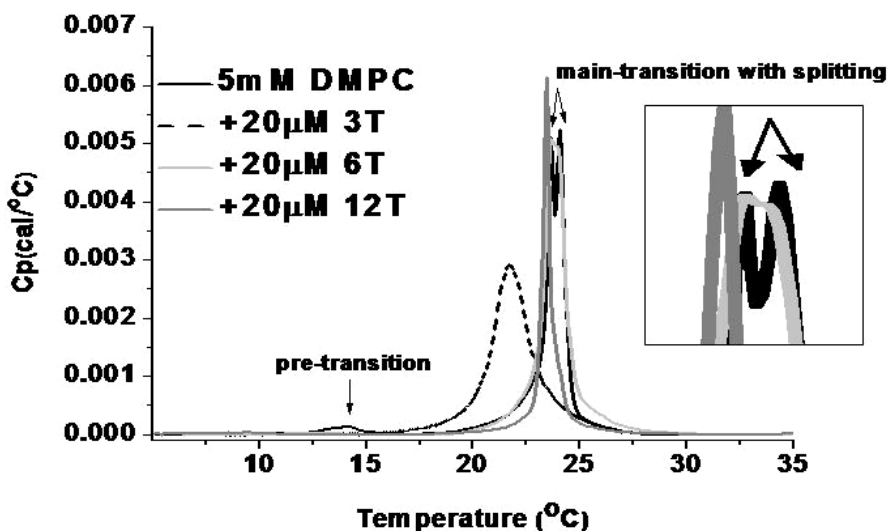
*Figure 3: DSC heating curves with scan rate 60ºC/h of pure DMPC (5.0 mM) and mixtures of DMPC (5.0 mM) in a 250:1 ratio with **3T**, **6T** and **12T** in HEPES/NaCl, 125mM/135mM at pH 7.2.*

Preliminary experiments revealed a significant stronger increase of the emission intensity of **12T** in the presence of small vesicles compared to large vesicles. To investigate this phenomenon in more detail, different sized uni-lamellar liposomes were prepared by extrusion of a liposome suspension over a poly-carbonate filter with pore sizes of 1000, 100 and 50 nm, respectively. According to Dynamic Light Scattering (DLS) the average diameters that were obtained were 400, 80 and 50 nm,

respectively. Smaller vesicles with a diameter of 20 nm were prepared by sonication of 50 nm sized liposomes. When 0.005 mM of oligothiophene was added, being below the critical aggregation concentration of the oligothiophenes, to four differently sized vesicles of in buffer, it became clear that the emission properties of the oligothiophenes depended on the vesicles size (Figure 4 and 5).

The changes in emission could be determined by the naked eye. When the samples were placed on a regular UV-lamp (366 nm irradiation), difference in colour was seen for **6T** and **12T**. For **3T**, no apparent colour difference was observed (Figure 4).
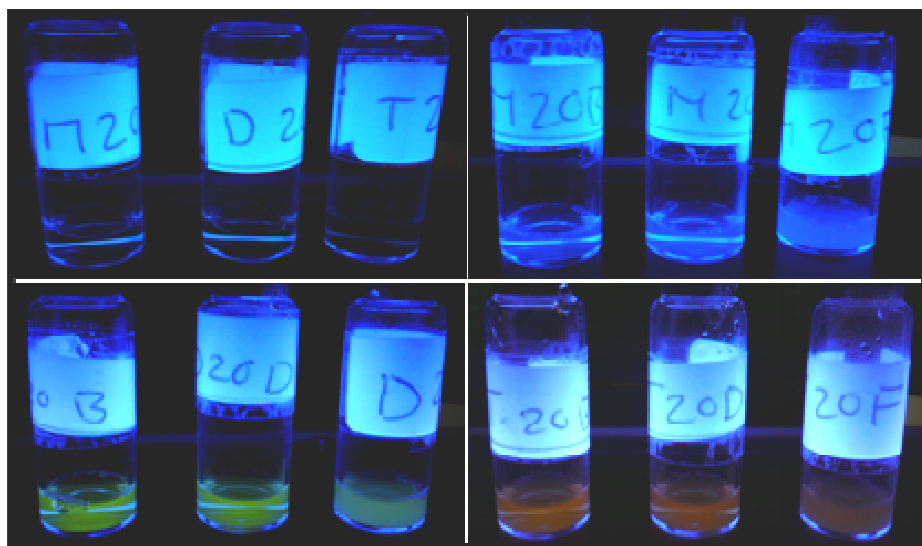

Figure 4: photographs of: 3T, 6T and 12T, respectively, in water at 0.005 mM (top-left), 3T (0.005 mM) in combination with DMPC vesicles (10 mM) at 30°C with diameters of 50, 100, 1000 nm, respectively (top-right); the same only with 6T (0.005 mM) (bottom-left) and for 12T (0.005 mM) (bottom-right).

The observations made by eye, were also quantified using fluorescence spectroscopy. For the **12T** it was observed that the changes in emission depended on the size of the vesicles which were added, i.e. the emission maximum showed an

increasing blue shift and an increased emission intensity with decreasing vesicle diameter as can be seen in Figure 5.
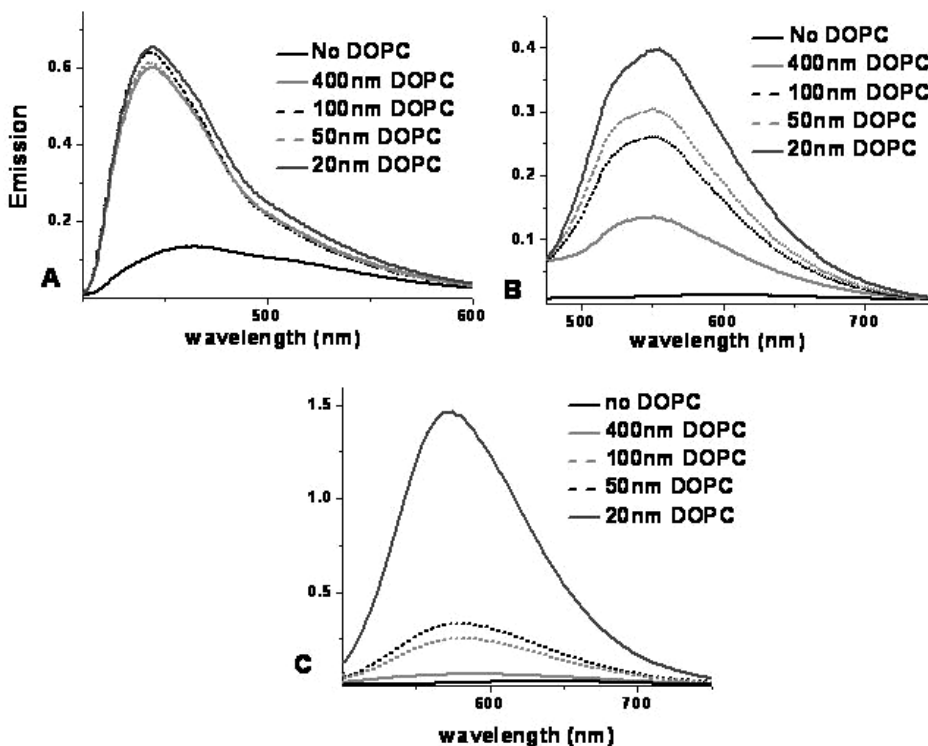

*Figure 5: The dependency of the fluorescent properties of incorporated **3T** (A), **6T** (B) and **12T** (C) at 0.005 mM concentrations into different sized DOPC vesicles at 10mM concentrations in buffer (HEPES/NaCl, 125mM/135mM at pH 7.2) at 20ºC. Excitation of the mixture was done at 350, 425 and 450 nm for **3T**, **6T** and **12T**, respectively.*

The size dependency of the emission properties was also observed for **6T** which showed less pronounced differences for vesicles of different sizes. Hardly any influence of the liposome size was seen for the emission properties of **3T**, even though it is significantly different compared to a pure solution of **3T** in buffer (Figure 5). Blue shifted emission maxima and increased quantum were observed

previously when the oligothiophenes were dissolved in a more apolar medium such as chloroform compared to water. It suggests that the changes in fluorescence are caused by interactions with the vesicles and influenced by the size of the vesicles.

The experiment was repeated for **12T** with different lipids in order to investigate if the changes were a general phenomenon or limited to a certain type of lipid. For this purpose differently sized vesicles of DMPC and DOPS were used. DMPC lipid bilayers have a phase transition of the packing of the aliphatic tails at 23 ºC compared to -20 ºC for DOPC lipid bilayers. By using DOPS the head group changes and thereby changing the surface charge of the vesicle while keeping the hydrophobic domain constant. It was seen that for DMPC and DOPS also a difference in emission is present when different sized vesicles were used in combination with **12T** (Figure 6). This reproducibility of changes in emission for different sized vesicles for different lipids shows that it is a general sensing tool and even though the exact values differ between lipids, the trend is clearly present, though only a limited number of lipids have been used.

The difference in emission intensity between the different sizes in DMPC is smaller than compared to the DOPC and DOPS combinations with **12T** (Figure 6). It should be noted that all measurements were performed above the lipid phase transition temperature in order to make sure the incorporation is not due to defects in the lipid membrane. For DMPC this is at 23°C and therefore the measurements were performed at 30°C. For DOPC and DOPS the phase transition is at -20 and -11°C, respectively and therefore these measurements were performed at 20°C. When a similar sample of DOPC was investigated at 20°C as well as 30°C, it was observed that at higher temperatures the emission intensity was significantly higher. This phenomenon is most likely due to higher incorporation at elevated temperature and is currently under a more detailed investigation.
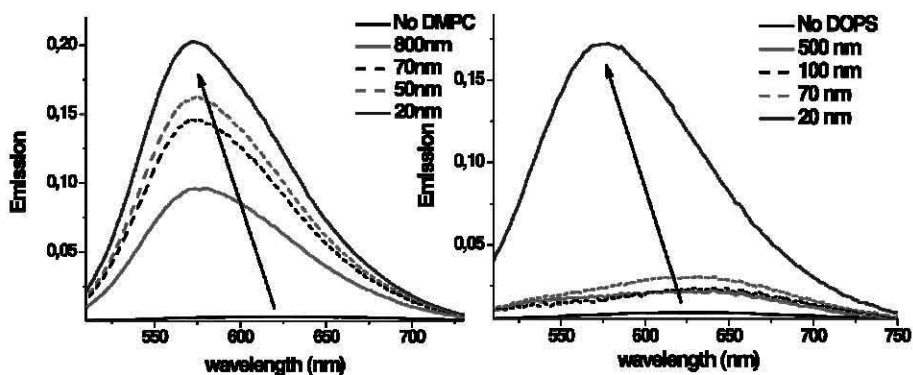
Figure 6: The dependency of the fluorescent properties of incorporated 12T at 0.005 mM concentration in buffer (HEPES/NaCl, 125mM/135mM at pH 7.2) into different sized DMPC (1.0 mM, 30°C)(left) and DOPS (10 mM, 20°C)(right) vesicles. It was seen that, even though the values differ, the general trend is the same as observed for DOPC. Excitation of the mixtures was done at 450 nm.

The fluorescence experiments clearly showed that the emission properties of **6T** and **12T** depended on the size of the vesicles they are bound to. One possible explanation for this observation is that the incorporation of **12T** into vesicles with smaller diameter is more efficient, because the local curvature of smaller vesicles is more comparable to the intrinsic curvature of the thiophene-backbone. In order to investigate whether the oligothiophenes have a preference for binding to small or large vesicles, three types of experiments were performed. First a titration experiment was done taking a fixed amount of thiophene and adding various amounts of differently sized vesicles. The association constant for binding of the oligothiophenes to the vesicles could be estimated from initial slope of the Stern-Volmer plots, to avoid saturation effects (Figure 7).
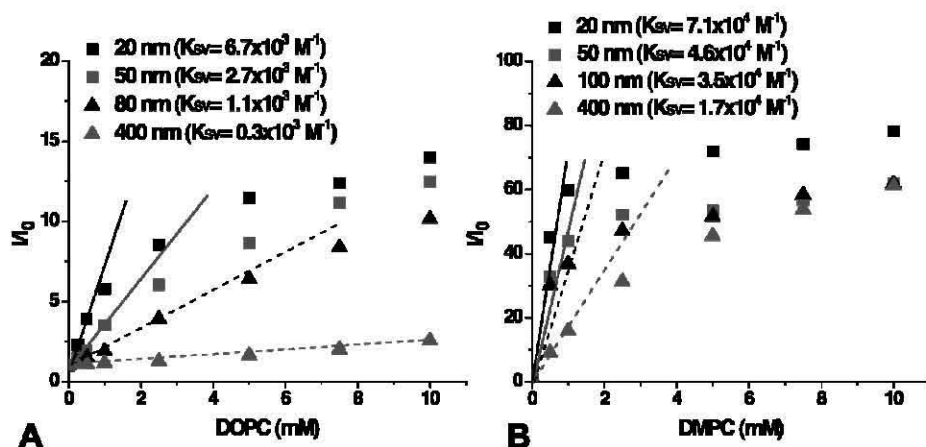
*Figure 7: Stern-Volmer type titration of different sized vesicles with various concentrations of A) DOPC and B) DMPC to 0.005 mM **12T**. Measurements were performed in buffer (HEPES/NaCl, 125mM/135mM at pH 7.2) at 20°C for the DOPC mixtures and 30°C for DMPC. Lines depict an estimate for the K_{SV} which is a measure for the association for **12T** with the different vesicles (in M^{-1}).*

From the data in Figure 7, it became clear that with smaller sized vesicles the association constant (K_{SV}, M^{-1}) increased. This trend was found for both DOPC and DMPC, in which the latter displayed K_{SV}'s which were 10 times higher. The measurements for DMPC were performed at higher temperature which could explain this difference, however, at this stage the exact origin of this increased K_{SV} is not known.

From the same titration experiment, also the wavelength of the emission maximum can be used and plotted against the amount of lipid being added to the **12T** solution (Figure 8). The emission wavelength dependence on the concentration for the different vesicles sizes followed the same trend of the association constants determined above, although less pronounced. Interestingly, for DOPC vesicles of different size the emission wavelengths reached different plateau values depending on the vesicle size. For DMPC the plateau value is reached already at low

concentrations. Also fewer changes are observed in the maximum emission wavelength with respect to different vesicle sizes. These observations can be explained by the higher affinities for DMPC as mentioned with respect to the Stern-Volmer plots in Figure 7.
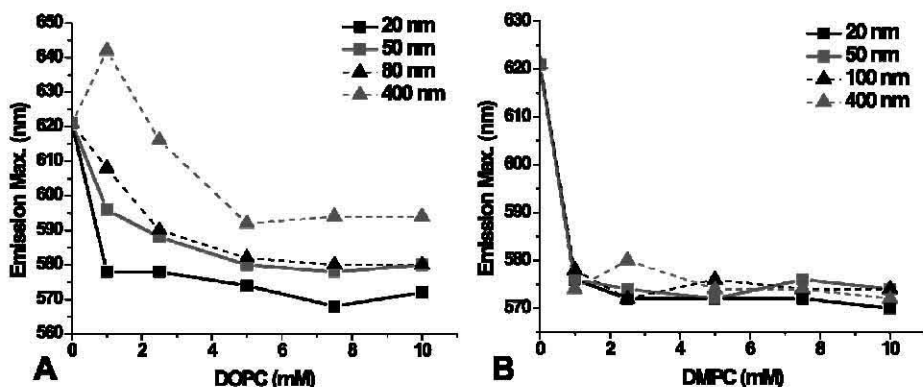

*Figure 8: Maximum emission wavelength analyzed as a function of lipid concentration with various vesicle sizes of **A**) DOPC and **B**) DMPC to 0.005 mM* **12T**. *Measurements were performed in buffer (HEPES/NaCl, 125mM/135mM at pH 7.2) at 20°C for the DOPC mixtures and 30°C for DMPC. Excitation was done at 450 nm.*

Secondly, competition experiments were performed in which the emission spectra of different vesicle mixtures were compared to investigate selectivity and dynamics of the mixtures (Figure 9). Therefore we incubated a 10 mM solution of 400 nm vesicles with **12**T and then diluted it with an equal amount of 20 nm vesicles. The same experiment was done visa versa. The emission was compared with vesicles solutions which were only diluted with HEPES-buffer in order to have comparable overall concentrations. The dilution of the, with 400 nm incubated, thiophene solution with an equal amount of 20 nm vesicle solution, displayed changes in emission that would be expected for incorporation into the smaller vesicles. Diluting the thiophene solution incubated with 20 nm vesicles with 400 nm sized vesicles did

not lead to changes in the emission which indicates that there is no incorporation into larger vesicles once they are associated to the 20 nm vesicles. These results indicate that the process of incorporation is dynamic and that the **12T** preferably binds to smaller vesicles.
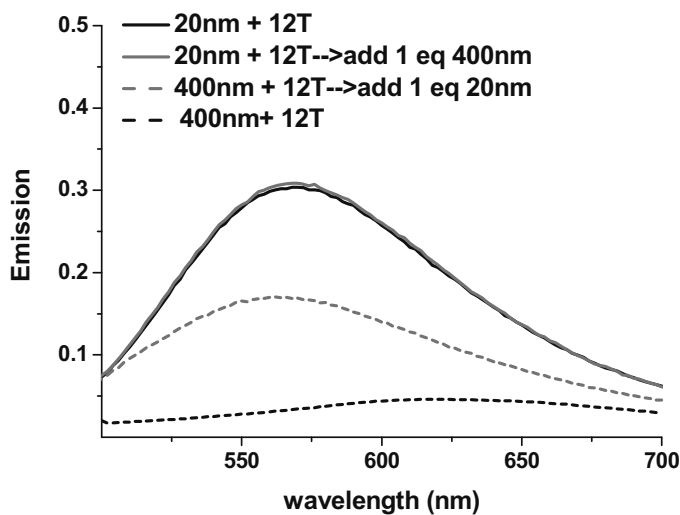

*Figure 9: Competition experiments by mixing 0.005 mM **12T**, incubated with either 20 nm or 400 nm DOPC vesicles (1.0 mM) to which, after incubation, the other vesicle size is added. Measurements were performed in buffer (HEPES/NaCl, 125mM/135mM at pH 7.2) at 20ºC. Excitation of the mixtures was done at 450 nm.*

A third type of experiment confirmed the findings when the enthalpic effects were investigated using Isothermal Titration Calorimetry (ITC), titrating a fixed amount of **12T** to a 3.3 mM solution of either large vesicles (400 nm) or small vesicles (20 nm). The determined heat effect of incorporation was much larger for the smaller vesicles. The enthalpy effect of the titration of the thiophene into a solution of large vesicles was comparable to titration of thiophene into buffer without liposomes. These measurements were rather qualitative and should be investigated in a more quantitative fashion in order to obtain the values for energy associated to binding of the thiophene to the vesicles.

The incorporation of molecules inside a lipid membrane influences the composition of the membrane and, as mentioned before, the phase transition. The small vesicles did not display altered shapes or deformations visualized by cryo-TEM (data not shown).

8.3 Using the altered emission properties of 12T as a curvature sensor

As mentioned, the emission properties of **12**T alter with respect to emission maximum, emission intensity and fluorescence lifetimes, when differently curved membranes are presented.

When the shift in emission wavelength is investigated with respect to the different sizes, it was found that for DOPC vesicles a clear changing was trend was observed, unlike for DMPC which did not show this clear changing trend (Figure 10A).

When investigating the fluorescence lifetimes of the pure **12T** in buffer, compared to incubated solutions of **12T** with different sized vesicles, it was observed that the fluorescence lifetimes (τ) increased with smaller vesicle size. A change in fluorescence lifetimes can be expected when there is also a change in intensity, since the fluorescence lifetime is associated to the rate of decay (radiative (k_R) as well as non-radiative (k_{NR}) $\tau = 1/(k_R+k_{NR})$) which in turn relates to the number of emitted photons per unit time. The change in association can be related in this case to the loss in non-radiative decay (k_{NR}), hence the increase in intensity, making k_R+k_{NR} smaller and therefore τ larger. This change in lifetime with the vesicle diameter could be useful in determining curvature by fluorescence lifetimes.
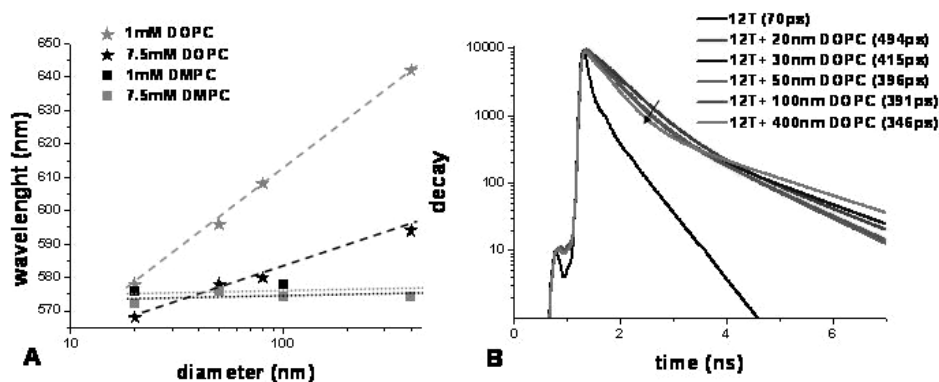
*Figure 10: A) The shift in emission wavelength versus the diameter of DOPC and DMPC vesicles both at 1.0 and 7.5 mM concentrations in buffer (HEPES/NaCl, 125mM/135mM at pH 7.2) at 20ºC for DOPC and 30ºC for DMPC. The lines are added to guide the eye. **B**) Changes in fluorescence lifetimes of **12T** with different sized DOPC vesicle under similar conditions as for the other experiments, correlating size and fluorescence lifetimes.*

At this point there is no clear model to explain the observed changes, even though for the DOPC vesicles a direct relationship was found between the vesicle diameter and the shift in emission maximum. For the fluorescence lifetimes it is more difficult to say what the exact relationship is, however, there is potential in using it for read-out of curvature.

8.4   Incorporation of oligothiophenes into living cells

One system that is composed of diversely shaped membranes is the cell. The cell has a large relatively non-curved outer membrane and inside there are many organelles which are composed of partly curved and partly lamellar structures.[3] As there is a strong preference of the oligothiophenes for certain shaped bilayers and coupled to changes in the photo-physical properties for the phopholipid bilayers it was

envisioned that cellular membranes could also be visualized with these compounds. The oligothiophenes were added to Mel JuSo cells to a final concentration of 10μM (Figure 11). The smaller non-curved terthiophene stained most of the membranes inside the cell and also the outer membrane could be visualized (Figure 11). Introducing fluorescent-labelled phospholipids in a similar way also displayed membrane staining (NBD-PE, Exc.: 405 nm, Em. Detection: 430-710 nm). The staining properties of the fluorescent-labelled phospholipid were comparable with that of the terthiophene, **3T**. These compounds non-specifically stained all the membranes. However, while the terthiophene and fluorescent phospholipid a-specifically stained membranes, the curved sexithiophene and dodecathiophene only stained the membranes found around the nucleus. Here the more curved membranes are likely targeted like the ER, mitochondria and the lysosomes as specific ER, lyso- or mito-trackers showed identical localization (data not shown). The preference for these membranes is based on curvature and non-specific hydrophobic interactions which is unique for a synthetic derived system. Staining of the specific membranes is usually done by attaching a chromophore to a peptide sequence which is complementary to a native-membrane protein binding attaches the chromophore to the membrane and can then be detected by fluorescence microscopy.[15] Handling and visualization of the cells with the oligothiophenes is comparable to commercially available markers. The incorporation was found to be by diffusion processes across the membrane and visualization could commence already after a few minutes. It was observed, especially for **6T**, that different membranes were stained over a period of time. Directly after addition, first the outer membrane was seen and slowly the inner membranes were stained. The pictures in Figure 11 were taken after incubation overnight. There was no indication that the membranes were harmed in any way (Figure 11). Even after prolonged exposure, the cell showed healthy and continued growing (data not shown) which means that there is no direct antibiotic properties associated with the amphipathic oligothiophenes as seen for other amphipathic structures in nature.[16]
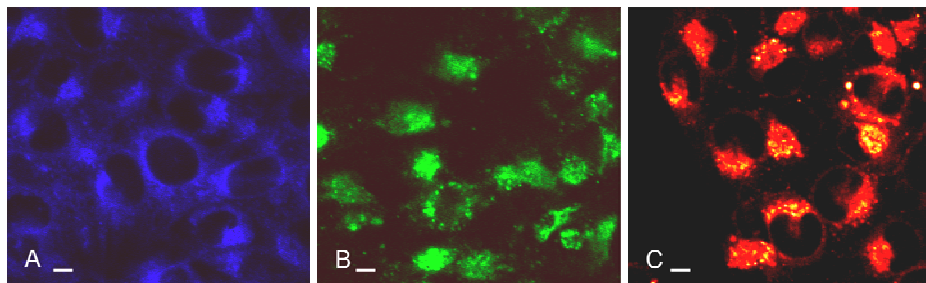
*Figure 11: Confocal fluorescent microscopy images of Mel JuSo cells in HEPES-buffer incubated with oligothiophene in an overall concentration of 0.01 mM. Visualization of the membranes is possible when **A**) terthiophene (Exc.: 405 nm, Em detect.: 430-500 nm), **B**) sexithiophene (Exc.: 488 nm, Em detect.: 520-650 nm) or **C**) dodecathiophene (Exc.: 488 nm, Em detect.: 520-650 nm) was added (bar 10 μm).*

From comparing the obtained fluorescent images with commercial markers that stain the ER, mitochondria or lysosomes, the images correspond best with the lysosome-marker and ER-marker.

From the individual cells, fluorescence spectral measurements were done in order to investigate whether it is possible to derive some information from this. It was found that both **6T** and **12T** displayed a large shift with respect to the pure form. This indicates that they reside in highly curved membranes (Figure 12). For **3T** large shifts were not observed, this was seen in a similar range as for the pure solutions of **3T**. This was to be expected from our findings with the synthetic bilayers.
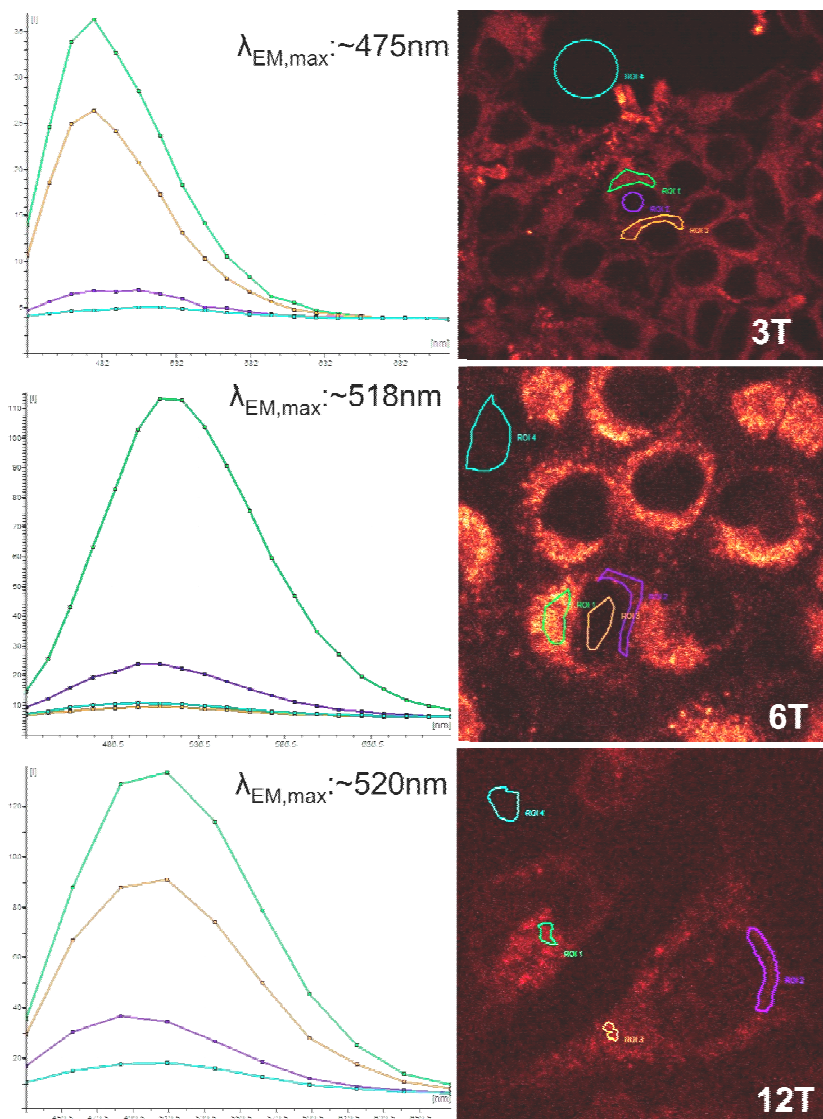
*Figure 12: Emission of parts of the cell which were incubated with **3T**, **6T** and **12T**. **6T** and **12T** display large shifts with respect to their pure solutions. **3T** does not display any shift. This was also observed for the experiments with synthetic bilayers.*

These shifts observed in the cell were confirmed by investigating bulk-cells with incubated thiophene. A large quantity (approx. 10^7 cells ml^{-1}) of cells was incubated with **3T**, **6T** and **12T**, respectively. These cells were then isolated by centrifugation and washed two times with buffer according to the same procedure. The washed cells were then re-suspended in buffer and an emission spectrum of the bulk was taken (Figure 13).
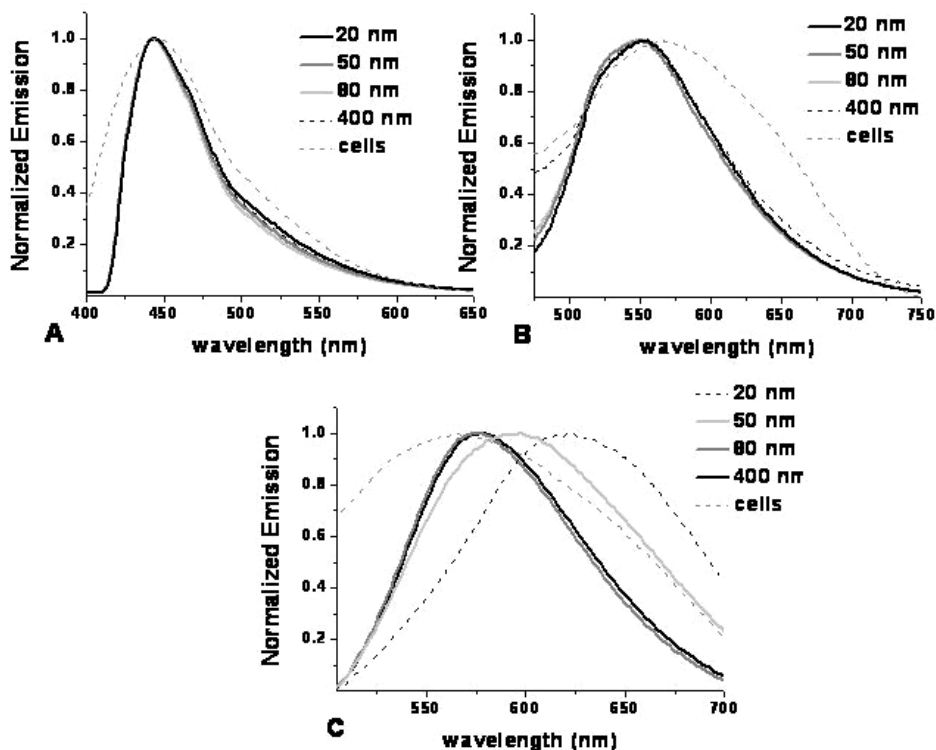

*Figure 13: The emission of **3T** (A), **6T** (B) and **12T** (C) incorporated inside cells compared to the different DOPC vesicles sizes (normalized spectra from Figure 4). Excitation was done at 350, 425 and 450 nm for **A**, **B** and **C** respectively.*

The shifts that were observed were smaller than what was seen for the individual cells. However, they were almost the same as what was seen for the small vesicles.

This similarity in emission indicates that also inside the cell, the curved thiophenes prefer the more curved membranes.

A large body of intracellular membranes can be detected for the sexithiophene by collecting the emitted photons over a broad range (500-650 nm). However, it was found that by narrowing the bandwidth we could visualize different membranes. When this detection was divided in two regions 550-600 and 600-650 nm different regions of the cell became visible (Figure 14). When the lower wavelengths were analyzed the part of the cell where the lysosomes reside, were observed. If the emission at higher wavelengths were analyzed the rim around the nucleus became visible. These are more stretched elongated membranes, while the other visible membranes correspond to the more curved membranes. This coincides with the findings in different sized liposomes where the more curved liposomes (smaller diameter) display a shift in the emission wavelength. It is therefore possible to visualize different parts of the cell by a single chromophore simple by varying the detection range. Unfortunately this was not reproducible and currently further investigation is being done to isolate the exact conditions where this is observed.
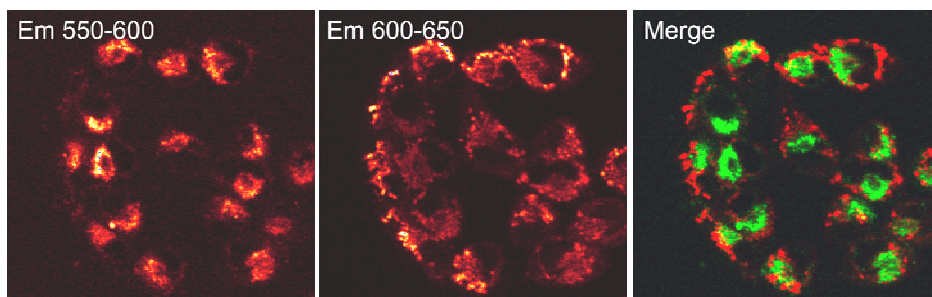

Figure 14: Mel JuSo cells with sexithiophene excitation at 488nm, detection left between 550-600nm (green) and right between 600-650nm (red). The overlay shows two different regions which are illuminated by the same compound and detected in the same system.

Overall the use of the curved thiophenes is a mild way of visualization of membranes inside the cell. It was found that after addition of the thiophenes, the division of the cells was unaffected and showed healthy behaviour. After division again a similar staining was observed in all cells, meaning that during the division the thiophenes are still distributed evenly. For imaging a variety of wavelengths could be used to excite the thiophenes ranging from 405 to 514 nm for the **6T** as well as the **12T**. It is advantageous that the excitation is in the visible range since ultra violet light is toxic for the cells. Also the large Stokes-shift of the thiophenes is advantage because this prevents quenching by re-absorption of the emitted photons which would make imaging more difficult. The visualization of the membranes by the thiophenes tolerated various conditions, including fixation of the cells by cold methanol as well as NBF (Neutral Buffer Formalin). The different conditions in which the visualization can take place is advantage for many different fields of biological research: cell biology (cells remain healthy), histology (under fixating conditions) and currently we are optimizing the systems in order to have a tool which can detect membranes under numerous conditions and for a variety of applications in biology, biochemistry and medical research.

8.5   Conclusion

The oligothiophenes described here show different photo-physical properties depending on the shape of the membrane in which it resides. Depending on the curvature of the vesicles the oligothiophenes emit light in a range visible to the naked eye. A more quantitative read-out is obtained by fluorescence measurements, since the spectroscopic properties like emission maximum, intensity and lifetimes are related to the molecular structure. Not only overall curvatures of mono-disperse systems presented here can be quantified but also non-isolated membranes located intracellular, display different kinds of curvatures. Incorporation into the membrane allows visualization of this membrane and local fluorescent lifetime measurements

by confocal fluorescent microscopy would give information on local membrane curvature. Visualization of biological systems and the processes that takes place with the use of synthetic molecular probes is still an interesting and important field of research and would be interesting for various fields of research in biology, biochemistry and medical research.[17] Currently the systems is being optimized in order to probe biological processes in which small vesicle transport plays an important role and extend the curvature detection to visualize cellular processes in which the membrane curvature is of key interest.

8.6   Methods

Vesicle solutions were prepared in a 10mM aqueous HEPES-buffer, containing 135mM sodium chloride. This was done by preparing a thin lipid-film and subsequently hydration followed by extrusion over carbonate nanopore filters. Pore sizes of 1000, 100, 50 and 30 nm were used. The smaller vesicles were prepared by sonication of extruded 50 nm vesicles. The incorporation of the thiophenes into the bilayers was done by adding the correct amount of thiophene from a stock solution to the prepared vesicle solutions. Fluorescence spectroscopy was done on a Jasco J-815 CD-spectrometer. The cuvet used here was quartz with dimensions 3x3mm. Dynamic Light Scattering was performed on a ZetaSizer Nano series Nano-ZS by Malvern Instruments. For determination of the luminescence lifetimes a LifeSpecs-ps (Edinburgh instruments) was used with excitation pulses of 70 ps at 405 nm. For cryo-TEM, a few microliter of suspension was deposited on a bare 700 mesh copper grid. After blotting away the excess of liquid the grids were plunged quickly in liquid ethane. Frozen-hydrated specimens were mounted in a cryo-holder (Gatan, model 626) and observed in a Philips CM 120 electron microscope, operating at 120 KV. Micrographs were recorded under low-dose conditions on a slow-scan CCD camera (Gatan, model 794). The visualization of the GMV was performed on a Zeiss

axiovert 100M, microscope equipped with a fluorescence-setup of Zeiss AttoArc 2, HBO 100W light source and a AxioCam ICc30 CCD-camera. For Cell culture and imaging, Mel JuSo fibroblast were cultured on 24mm coverslips (Thermo Scientific) in Iscove's modified Dulbecco's medium (IMDM, Gibco) supplemented with 10% fetal calf serum and penicillin-streptomycin-L-glutamine and incubated at 5% CO_2. The oligothiophenes where pre-incubated for one to 72hours without affecting the cell viability. Confocal images where obtained using a Leica SP2 confocal microscope with a 63x objective. Note that images were taken in glow-over-under mode.

8.7   References

1   R. Parthasarathy and J. T. Groves, *Soft matter*, **2007**, *3*, 24-33.
2   H. T. McMahon and J. L. Gallop, *Nature*, **2005**, *438*, 590-596.
3   M. A. Lemmon, *Nat. Rev. Mol. Cell Biol.*, **2008**, *9*, 99-111.
4   a) K. Farsad and P. De Camilli, *Curr. Opin. Cell Biol.,* **2003***, 15***,** 372-381; b) J. Zimmerberg and M. M. Kozlov, *Nat. Rev. Mol. Cell Biol.,* **2006***, 7*, 9-19.
5   G. K. Voeltz and W. A. Prinz, *Nat. Rev. Mol. Cell Biol.*, **2007**, *8*, 258-264
6   B. J. Peter, H. M. Kent, I. G. Mills, Y. Vallis, P. Jonathan, G. Butler, P. R. Evans and H. T. McMahon, *Science*, **2004**, *303*, 495-499.
7   a) G. Drin, J.-F. Casella, R. Gautier, T. Boehmer, T. U. Schwartz and B. Antonny, *Nat. Struct. Mol. Biol.*, **2007**, *14*, 138-146; b) R. B. Cornell and S.G. Taneva, *Curr. Prot. Pept. Sci.*, **2006**, *7*, 539-552.
8   a) J. L. Gallop, C. C. Jao, H. M. Kent, P. J. Butler, P. R. Evans, R. Langen and H. T. McMahon, *EMBO J.*, **2006**, *25*, 2898-2910; b) M. Masuda, S. Takeda, M. Sone, T. Ohki, H. Mori, Y. Kamioka and N. Mochizuki, *EMBO J.*, **2006**, *25*, 2889-2897; c) M. G. Ford, I. G. Mills, B. J. Peter, Y. Vallis, G. J. Praefcke, P. R. Evans and H. T. McMahon, *Nature*, **2002**, *419*, 361-366
9   T. Fischer, L. Lu, H. T. Haigler and R. Langen, *J. Biol. Chem.*, **2007**, *282*, 9996-10004.
10   a) J. Hu, Y. Shibata, C. Voss, T. Shemesh, Z. Li, M. Coughlin, M. M. Kozlov, T. A. Rapoport, W. A. Prinz, *Science*, **2008**, *319*, 1247-1250; b) B. Mesmin, G. Drin, S. Levi, M. Rawet, D. Cassel, J. Bigay and B. Antonny, *Biochemistry*, **2007**, *46*, 1779-1790; c) R. Aloya, A. Shirvan, H. Grimberg, A. Reshef, G. Levin, D. Kidron, A. Cohen and I. Ziv, *Apoptosis*, **2006**, *11*, 2089-2101.
11   a) K. Kim, M. Lee, H. Park, J.-H. Kim, S. Kim, H. Chung, K. Choi, I.-S. Kim, B. L. Seong and I. C. Kwon, *J. Am. Chem. Soc.,* **2006**, *128*, 3490-3491; b) S. M. Butterfield, T. Miyatake and S. Matile, *Angew. Chem. Int. Ed.,* **2009**, *48*, 325-328; c) K. Welsher, Z. Liu, D. Daranciang and H. Dai, *Nano Lett.*, **2008**, *8*, 586-590.
12   a) J. A. McNew, *Chem. Rev.,* **2008**, *108*, 1669-1686; b) A. Zemel, A. Ben-Shaul and S. May, *J. Phys. Chem. B*, **2008**, *112*, 6988-6996;
13   Splitting of the main transition is known in uni-lamellar membranes which still contain a fraction of multi-lamellar membranes. H. Heerklotz and J. Seelig, *Biophys. J.*, **2002**, *82*, 1445-1452.
14   R. J. Malcolmson, J. Higinbotham, P. H. Beswick, P. O. Privat and L. Saunier, *J. Membr. Sci.*, **1997**, *123*, 243-253.
15   a) M. Chalfie, Y. Tu, G. Euskirchen, W. W. Ward and D. C. Prasher, *Science*, **1994**, *263*, 802-805; b) R. Rizutto, M. Brini, P. Pizzo, M. Murgia and T. Pozzan, *Curr. Biol.*, **1995**, *5*, 635-642.
16   a) H. Steiner, D. Hultmark, A. Engstrom, H. Bennich and H.G. Boman, *Nature*, **1981**, *292*, 246-248; b) G. F. Gause and M. G. Brazhnikova, *Nature*, **1944**, *154*, 703-703; c) L. S. Cardoso, M. I. Araujo, A. M.

Góes, L. G. Pacífico, R. R. Oliveira and S. C.Oliveira, *Microb. Cell Fact.*, **2007**, 6:1 doi:10.1186/1475-2859-6-1; d) M. Zasloff, *Nature*, **2002**, *415*, 389-395.

17   a) S. Ikeda, T. Kubota, M. Yuki and A. Okamoto, *Angew. Chem. Int. Ed.,* **2009**, *48*, 6480-6484; b) C. Dyrager, A. Friberg, K. Dahlén, M. Fridén-Saxin, K. Börjesson, L. M. Wilhelmsson, M. Smedh, M. Grøtli and K. Luthman, *Chem. Eur. J.,* **2009**, *15*, 9417-9423; c) V. Sharma and D. S. Lawrence, *Angew. Chem. Int. Ed.,* **2009**, *48*, 7290-7293.

Concluding Remarks

In this thesis-work we made an attempt to implement an additional structural motif, namely curvature, in an amphiphilic framework. This is seen in nature but has not yet been utilised in a synthetic system. We have shown that from a simple starting point already different self-assembled structures can be obtained with the use of amphiphilic terthiophenes of which the positions of the substituents were systematically altered. In order to actually achieve the molecular curvature one of the "basic" terthiophene structures was oligomerised. Making use of the cis-trans isomerisation of the oligothiophene and the inter-conversion of a linear array in the trans-form to a non-linear/curved array in the cis-form, curved amphipathic oligothiophenes were produced. The driving force for the inter-conversion of the trans- to cis-form is the reorientation of the hydrophilic and hydrophobic substituents in a polar medium like water.

The newly formed amphiphilic and amphipathic oligothiophenes were not only extensively investigated with respect to aggregation behaviour in water and their photo-physical properties but also for potential applications. It was found that they are very well suited to be used in self-assembled light harvesting systems which displays not only transfer of energy but also is able to transport energy and even create a reactive centre. All these aspects combined make it an attractive mimic for the natural light harvesting systems. Since the oligothiophenes display a curvature, it was decided to investigate the compatibility with other curved systems like phospholipid-vesicles. It was found that the closer the diameter of this vesicle is to the intrinsic diameter (curvature) of the oligothiophene the better the incorporation. The incorporation was accompanied with changes in fluorescent properties, making it an indicator or probe for curved surfaces. This was extended to natural system like living cells. It was also found that the differently curved molecules target different types of membranes. This can be visualised by fluorescence confocal microscopy

and could be used as a membrane staining agent. It is now currently under investigation whether it can also be used to visualise membrane/vesicle formation in biological processes.

The overall research was quite successful, even though at first we hoped to achieve longer oligomers which would form helical structures and create a whole library of these. This was not feasible in this time span, luckily the shorter molecules already displayed interesting properties. In fact, even more than was discussed in this thesis. Patterning of surfaces, three dimensional curved structures, interaction with carbon nanotubes and mixing oppositely curved systems are all still under investigation.

In order to address the initial idea of creating more defined structures and a more transparent correlation between aggregate morphology and molecular structure by introducing a curvature is not unambiguously shown. We did manage to show that conventional packing theory of surfactants can be circumvented because of the curvature but actually making complex structures of differently curved systems and combining these systems in order to gain structural control and complexity was not achieved. To prove this control over aggregation phenomena, quite a lot of additional research has to be performed and compounds to be synthesised. However, the prognosis is that in the near future, mixed curvature in a single molecular system will be achieved and this will be of great interest in investigating self-assembling curved systems.

Samenvatting

### Gekromde Amfipathische Oligothiophenen:

Kromming gestuurde zelf-assemblage met applicaties in energy overdracht systemen en detectie van membraankromming in levende cellen

De basis van het onderzoek gepresenteerd in dit stukje geschreven werk is iets waar iedereen, hoe divers ook, mee te maken heeft, namelijk het samenkomen van moleculen in water door hydrofobe interacties. Dit wordt gedaan met zogenaamde amphifiele moleculen, ook wel surfactanten genaamd. Deze moleculen heten amphifiel vanwege hun karakter, ze bestaan namelijk uit een deel dat graag in water oplost en een deel die dat niet wil, en worden surfactant genoemd omdat ze actief interacties aangaan met oppervlakten (surfaces), bijvoorbeeld het water-lucht grensvlak. Wanneer de surfactanten in water worden gebracht zullen deze zich tegelijk gedeeltelijk willen oplossen en zich gedeeltelijk van het water willen scheiden, zoals olie dat doet in water (fasescheiding) (Figuur 1, links). De hydrofobe gedeeltes van de moleculen komen dan samen zodat deze niet meer in contact staan met het water, maar de hydrofiele delen van de moleculen willen wel in water zijn en gaan daarom richting het water staan. Dit heeft als gevolg dat op heel kleine schaal een fasescheiding ontstaat, waarbij zeer kleine domeinen van enkele nanometers dik (1 nanometer is 10^{-9} meter) worden gevormd die aan de buitenkant gestabiliseerd worden door de hydrofiele delen van de surfactanten (Figuur 1, rechts).

De eigenschappen van surfactanten kennen veel verschillende toepassingen, zo worden ze bijvoorbeeld gebruikt voor het wassen van kleren; vetten en vuil dat niet in water wil oplossen, kan wel worden opgelost in het hydrofobe gedeelte van de structuren. Ook kunnen ze gebruikt worden voor het stabiliseren van oppervlakten (vandaar de naam surfactant = oppervlakte actieve stof), voorbeelden daarvan zijn: het maken van een zeepbel bij bellen blazen of het maken van emulsies, een stabiele

fasescheiding op micrometer schaal (1 micrometer is 10^{-6} meter), in bijvoorbeeld voedsel. Ditzelfde type molecuul komt ook in het menselijk lichaam voor, de zogenaamde phospholipide, en vormt daar de basis voor alle celmembranen. In dit onderzoek zijn nieuwe type surfactanten ontworpen en gemaakt. Deze zijn vervaardigd door middel van chemische synthese, wat vergelijkbaar is met het spelen met lego. Door verschillende bouwstenen te combineren kunnen moleculen vervaardigd worden met diverse eigenschappen. In dit geval is het een molecuul met een hydrofiel deel en een hydrofoob deel. Het aardige is echter dat er twee additionele structuur eigenschappen aan toegevoegd zijn, namelijk een kromming en elektronische eigenschappen.
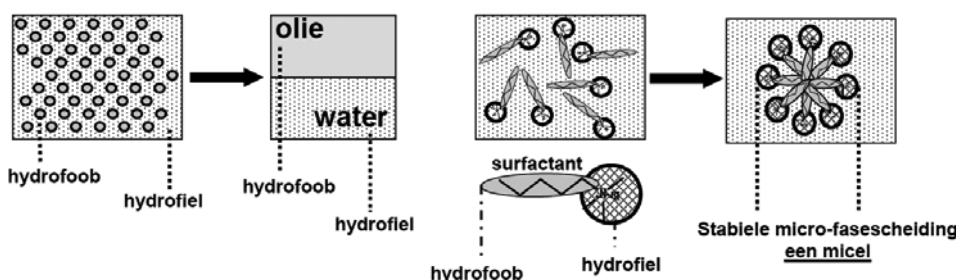

Figuur 1: Links een voorbeeld van het gedrag van kleine oliedruppels in water; er ontstaat een twee fasesysteem. Rechts gebeurt hetzelfde proces maar dit maal met surfactanten.

De kromming is toegevoegd om de wijze waarop de surfactanten in water samenkomen, te beïnvloeden dan wel te sturen. Het is te vergelijken met het bouwen van een huis; wanneer een huis gemaakt wordt van normale bakstenen zal het huis een vorm aannemen die overeenkomt met de vorm van de baksteen, dus meestal rechthoekig/vierkant (Figuur 2). Echter, wanneer bakstenen worden genomen die anders van vorm zijn, beïnvloedt dit ook de vorm van het huis wat kan resulteren in architectonische hoogstandjes (Figuur 2). Van dit principe is ook uitgegaan bij het vervaardigen van de nieuwe surfactanten. Een normaal surfactant ziet er schematisch

uit als een kleine hydrofiele groep met een lange hydrofobe staart eraan (Figuur 2). De structuur die in dit onderzoek naar voren komt, heeft een verdeling van de hydrofiele en hydrofobe gedeeltes over de lengteas van het molecuul en heeft als geheel een gekromde/gebogen contour as (Figuur 2). Ook met deze vreemd gevormde surfactanten, proberen we architectonische hoogstandjes te maken op moleculaire schaal. Tevens is het streven om een relatie te leggen tussen de vorm van het gebruikte surfactant en de architectuur die het vormt.

normale baksteen **gehoekte baksteen** **normale surfactant** **gekromde surfactant**
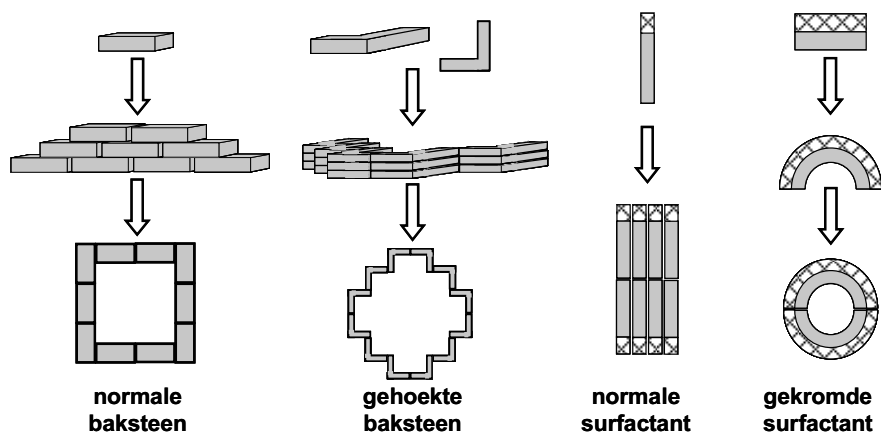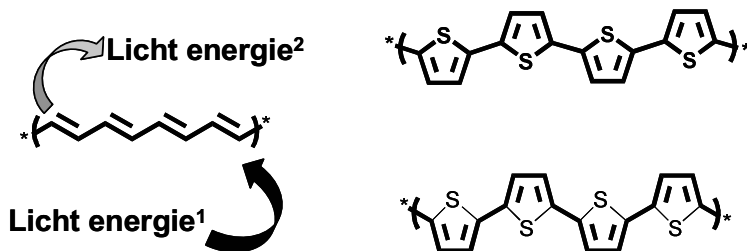
Figuur 2: Schematische weergave van de wijze waarop het gebruik van verschillende type bouwmaterialen de vorm van de gebouwde structuur beïnvloedt. Rechts wordt hetzelfde principe weergegeven alleen vormen ditmaal de moleculen de bouwstenen.

Naast een kromming is ook een elektronisch actieve structuur component geïmplementeerd in het ontwerp. Dit is gedaan door een molecuul te synthetiseren waarin een sequentie van alternerende enkele en dubbele bindingen aanwezig is, ook wel conjugatie genoemd (Figuur 3, links). Deze conjugatie maakt dat het molecuul bijvoorbeeld licht kan absorberen van bepaalde energie en deze opgenomen energie ook weer kan uitstralen, wat gezien wordt als fluorescentie. Het licht dat wordt afgegeven, heeft een lagere energie-inhoud en is daardoor anders van kleur. De

moleculen die in dit onderzoek een centrale rol hebben gespeeld, zijn weergegeven in Figuur 3, rechtsboven, daaronder is aangegeven waar de alternerende sequenties van dubbele en enkele bindingen zich bevinden.

Het aardige van deze ingevoegde conjugatie in de moleculaire structuur is dat de eigenschappen ervan, om licht te absorberen en uit te zenden, erg gevoelig zijn voor veranderingen in de omgeving van het molecuul. Daarbij kan gedacht worden aan oplosmiddel (een polair oplosmiddel als water kan andere interacties hebben met het molecuul dan bijvoorbeeld een apolair oplosmiddel zoals olie), het bij elkaar komen van identieke moleculen van gelijke type (aggregatie, hierdoor komen de moleculen zo dicht bij elkaar dat ze elkaar kunnen "voelen", wat de eigenschappen beïnvloed van de elektronische eigenschappen) of het complexeren van andere actieve componenten met complementerende elektronische eigenschappen waardoor interessante systemen ontstaan (twee moleculen die verschillend zijn en erg dicht bij elkaar komen kunnen elkaar ook "voelen" en daardoor soms met elkaar "communiceren"). De conjugatie kan door de enorme gevoeligheid gebruikt worden als interne boodschapper, wat er met het molecuul gebeurt.

Figuur 3: Schematische weergave van de opbouw van geconjugeerde moleculen waarin zich een alternerende sequentie bevindt van enkele en dubbele bindingen. Rechts staat het molecuul beschreven dat de basis vormt voor dit promotiewerk.

Aan wetenschappelijk onderzoek moet tegenwoordig altijd een functie ten grondslag liggen. Onderzoek enkel met als doel de nieuwsgierigheid te bevredigen door te

onderzoeken hoe iets in elkaar steekt zonder enige vorm van geldelijk gewin, is in de hedendaagse maatschappij niet meer mogelijk. Voor het in dit werk beschreven moleculen zijn verschillende (mogelijke) toepassingen gevonden, waardoor het onderzoek ook tegenover de economen van de bevolking weer gerechtvaardigd is. In de hoofdstukken 5 t/m 7 is de genoemde conjugatie van de gesynthetiseerde moleculen samen gebracht met andere elektronisch actieve componenten in water. Doordat de gesynthetiseerde surfactanten, zoals in Figuur 1 beschreven, micro-fasescheiding vertonen in water kunnen hydrofobe moleculen worden opgelost, zoals dat ook gedaan wordt met zepen. De gebruikte hydrofobe moleculen hebben complementerende elektronische eigenschappen aan die van de gebruikte surfactanten. De twee componenten worden op basis van de micro-fasescheiding bij elkaar gebracht en beïnvloeden op die manier elkanders elektronische eigenschappen. Dit wordt vervolgens gebruikt om licht, bijvoorbeeld zonlicht, door de surfactant op te laten nemen en daarna door te geven aan de component die zich in de omsloten micro-fasescheiding bevindt. Deze component kan vervolgens andere energie afgeven in de vorm van licht of de energie gebruiken om ladingen te vormen, afhankelijk van de gekozen hydrofobe component. Dit soort processen is bijvoorbeeld bekend van planten, waarbij het fotosynthese wordt genoemd, en wordt vandaag de dag gebruikt in organische zonnecellen en brandstof (waterstof) cellen.

De verbindingen kunnen daarnaast ook gebruikt worden voor het herkennen en visualiseren van membranen (hoofdstuk 8). Daarbij moet gedacht worden aan celmembranen en aan membranen van organellen binnen een cel. Deze membranen hebben allen een andere kromming die op basis van de gekromde structuur van de gesynthetiseerde surfactanten kunnen worden herkend en gebonden. Dezelfde elektronische eigenschappen, zoals eerder beschreven, liggen daaraan ten grondslag; doordat de verbindingen een ander type licht kunnen uitzenden dan ze opnemen, kunnen membranen worden gezien en worden gediscrimineerd. Ontdekt is namelijk dat verschillend gekromde membranen de eigenschappen van de surfactanten dusdanig veranderden dat, door detectie van de verschillende energieën die het licht

bezit, de verschillende membranen apart konden worden gedetecteerd. Dit principe heeft allerlei potentiële toepassingen binnen de biochemische en medische wetenschap omdat hiermee allerlei biologische processen gevolgd zouden kunnen worden. Deze toepassingen worden in de toekomst onderzocht en maken zelfs een reële kans om geëxploiteerd te worden.

Patrick van Rijn

Summary

Curved Amphipathic Oligothiophenes:

Curvature directed S.A. with applications in energy transfer systems and membrane curvature detection in living cells

The basis for the research presented in this research is something which everyone is familiar to often without realising it, namely, the coalescence of small molecules in water by due to hydrophobic interactions. This coalescence in water happens with small molecules called, amphiphiles, also named surfactants. They are called amphiphile because of their character, part of the molecule can dissolve in water and the other part is largely insoluble. The other name, surfactants, is given because they have actively go to at polar-apolar interfaces, e.g. air-water interfaces. When surfactants are placed in water, they will partly want to dissolve and partly want to phase-separate, like oil does in water (Figure 1, left). The hydrophobic parts of the molecules will gather together in order to minimise their contact with water, however, the hydrophilic parts of the molecules will be positioned in such a way the it is still in contact with the water. As a consequence, a phase separation will occur on a very small scale, where the formed domains are only several nanometres thick (1 nanometre is 10^{-9} metre) and are stabilised on the outside by the hydrophilic groups oriented towards the water (Figure 1, right).

The properties of surfactants have many different applications; they are being used as detergents for washing; fats and dirts which are not soluble in water can be taken-up by the hydrophobic domains which form upon the coalescence in water. Also surfactants are used to stabilise polar-apolar interfaces, examples of these are making soap bubbles or in the preparation of emulsions, a stable micro-phase separation (1 micrometer is 10^{-6} meter) in e.g. foods. A similar type of molecule also appears in the human body, the so called phospholipid, and forms the basis for all the cell membranes. In this research, new types of surfactants have been designed

and prepared by means of chemical synthesis, which can be compared of building a structure with Lego building blocks. By combining different building blocks, molecules with different properties can be formed. Here, hydrophobic and hydrophilic building blocks have been combined. The interesting part is that two additional properties have been added to these structures, namely, curvature and electronic properties.
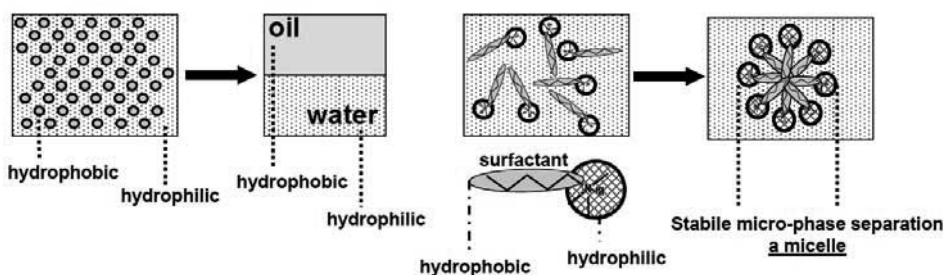

Figure 1: Left is an example of the behaviour of small oil droplets in water; in the end two phases are formed. Right, represents a similar process with surfactants.

The curvature is added to influence the behaviour of the coalescence of the surfactants in water and to direct it. One could compare it to building a house; when a house is prepared from normal bricks the house will have an appearance that is inherent to the shape of the brick, usually rectangular/square (Figure 2). However, when the bricks are differently shaped, it will influence the shape/structure of the house and can result in very architectonically interesting pieces (Figure 2). This principle is also being used in the creation of new types of surfactants. A conventional surfactant has a hydrophilic head group and a long hydrophobic tail (Figure 2). In this research the newly prepared surfactants have a different distribution of the hydrophilic and hydrophobic groups, namely, along the length axis of the molecule and the length axis has an overall curved structure (Figure 2). Also with these curved surfactants we attempted to prepare architectonically

interesting structures and try to formulate a relationship between the molecular curved structure of the surfactants and the shape of the aggregates they form.

normale baksteen   **gehoekte baksteen**   **normale surfactant**   **gekromde surfactant**
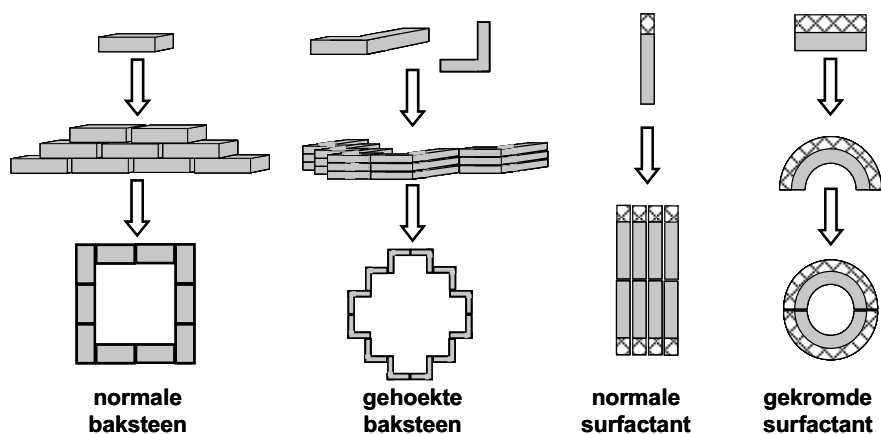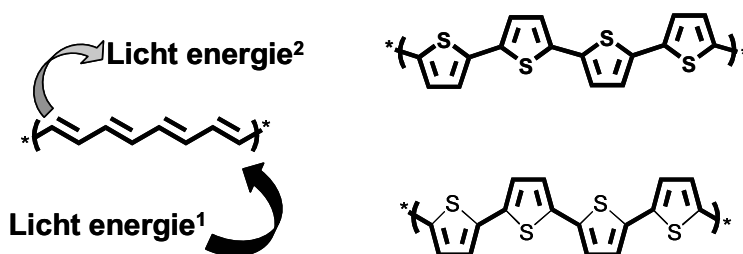
Figure 2: A schematic representation of the way different types of building blocks influence the build structure. Left is an example using differently shaped bricks, right the structure variation in the surfactant structure used in this research.

In addition to the curvature, another property is added in the form an electronically active component. These electronic properties were added by synthesising a surfactant which has alternating sequence of single and double bonds which is called conjugation (Figure 3, left). This conjugation makes it possible for the molecule e.g. to absorb light of a certain energy and in turn release the energy also in the form of light, a process called fluorescence. The light which is being released has lower energy content and therefore the light id of a different colour. The molecule that played a central role in this research is shown in Figure 3; top structure on the right, and also it is shown where the exact alternating sequence of single and double bonds is located.

The interesting aspect of the implemented conjugation in the molecular structure is that the electronic properties are very sensitive towards changes in the surroundings of the molecule. One can think of changes in the solvent (polar solvents like water

have different interactions with the molecule than apolar surroundings like oil). Also when molecules come together in the solvent due to aggregation as shown in the case for surfactants, the molecules are able to 'sense' each other, and also then the electronic properties are affected. The sensing between molecules can also occur when other electronically active components are being added, especially when they have complementary electronic properties and are then able to communicate with each other. So the conjugation can be used in general as an internal messenger for the state in which the molecule is in.

Figuur 3: On the left a schematic representation of a simple conjugated sequenche in which alternating single and double bonds are present. On the right the basic type of molecule which was used in this research.

These days, when scientific research is being performed, direct functions and applications have tob e kept in mind in order to justify the spend research funding. It is no longer possible to investigate solely out of curiosity and commercialisation of the findings is always an important aspect. For the presented structures in this work several (potential) applications have been found which justifies the research in the eyes of the economists of the population. In chapters 5-7, the mentioned conjugation has been used in combination with other electronically active species. Because of the micro-phase separation in water, as shown in Figure 1, hydrophobic electronically active species can be complexed inside the surfactant structures like soap takes up grease. The used hydrophobic electronically active components have complementary

electronically active properties and can therefore communicate with the electronically active surfactants and were used for absorbing light (which could potentially be sunlight) transport this energy and convert it in a similar way that is for photo-synthesis, the way plant use sunlight to produce energy and what present day is being used to produce (organic) solar- and fuel cells.

The compounds presented in this thesis were also used to recognise and visualise phospholipid membranes (Chapter 8). This visualisation is for cell membranes as well as membranes of organelles inside the cell. The membrane were able to be recognised by their curvature in combination with the curvature of the conjugated surfactants and the quantification and visualisation depend on the changes in the electronic properties of the surfactants. It was found that in differently curved membranes, the compounds emit a different type of light, which allows for discrimination of membranes by detecting different coloured lights. This principle has all kinds of possible applications within biochemistry and (bio-)medical sciences for the tracking of vesicles and membranes in biological processes. These applications will be part of a future study and have serious potential of being commercialised.

Patrick van Rijn

Summary

Dankwoord

Het is tijd, het is gebeurd. Ik ben aangekomen bij het, wat waarschijnlijk het meest gelezen stuk is van dit proefschrift en dat is terecht in mijn ogen. Het onderzoek dat ik heb mogen doen in de afgelopen 4 jaar en 4 maanden is als je het goed bekijkt even belangrijk geweest als de mensen met wie ik heb mogen samenwerken.

Jan, als mijn promotor was jou visie een goede en inspirerende leidraad in het onderzoek en waren er altijd opbeurende woorden bij mislukte syntheses (gepaard met: 'neem een biertje en ga morgen weer verder'), mijn dank daarvoor.

Naast de visie van mijn promotor heb ik het geluk gehad de goede personen in de buurt te hebben gehad. Allereerst Tom, bedankt voor de initiële bijdrage aan het eerste artikel, de artikelen die daarop volgen(den) en de inzichten in hoe om te gaan met photo-physica. Marc bedankt voor de Cryo-TEMs, door het dagje meekijken heb ik een nog groter respect gekregen voor de techniek. Marcel en Eric, bedankt voor jullie advies en de metingen m.b.t. interactie met cellen. Marcel het was erg leuk om ook eens i.p.v. aan het catan bord en de bar, met jou aan de confocal plaats te nemen. Eduardo, I would like to thank you for introducing new insights in DLS and physical chemistry. Also I would like to thank our collaborators: Prof. Paolo Samorì and Luc Piot for investigating surface patterning with STM and Prof. Ehud Keinan and Doron Pappo for combining the thiophenes with corannulenes. The topics haven't had the success yet we hoped for but I hope the work will continue with my successor.

Minstens zo belangrijk als het onderzoek zijn de mensen met wie ik deze dagelijkse worsteling heb meegemaakt want uiteindelijk zitten we allemaal in hetzelfde schuitje. Aurélie ('petit cherie'), Job ('son') en Christophe ('de belg') we hebben gedurende de tijd veel vreugde en teleurstellingen gedeeld. Jullie zijn allen geweldig en ik heb naast de wetenschappelijke discussies (meestal onder het genot van bier) dan ook altijd veel plezier beleefd aan onze streken, grappen en grollen. Daarvoor mijn dank, ik wens jullie allen succes en geluk toe.

Daarnaast hebben we uiteraard de grappen en grollen niet alleen met elkaar uitgehaald maar ook met onze collega's (lees medegedupeerde). Christian ('italian stallion'), Ahson, Dainius (my worthy successor), Lars, Krishna, Aernout, Mohan, Marta ('double wodka'), Judith, Iwona and Daniella, you were all at some point the subject of pranks and practical jokes, I assure you it was done with the utmost respect and admiration. I thank you all for the special times we spend in and on occasion, outside of the lab. I wish you all the best in the future.

Also I want to thank Sid (*aka* "Lord Sith"), you were a good master-student and it is a pity that we could not convince you to stay as a PhD.

Christian Pester, vielen Dank für das sprachliche Korrigieren meiner Thesis.

Daarnaast wil ik ook de vaste wetenschappelijke staf bedanken voor hun gezelligheid en inbreng tijdens koffiepauzes, borrels, wetenschappelijke discussies en voor hun advies; Louis, Wolter, Rienk en Ger, bedankt.

Mieke en Louw, bedankt dat jullie er waren om ons wegwijs te maken in het begin toen we in Delft aankwamen en voor alles wat daarna kwam.

Van de BOC groep wil ik ook iedereen bedanken. Jullie waren zo aardig om ons vanaf het begin al welkom te heten en de groepen hebben dan ook veelvuldig samen de ECAST onveilig gemaakt. In het bijzonder wil ik een paar namen eruit pikken; Daniel, Jeroen, Frank, Kristina, Remco en Maria maar ook alle anderen van de groep.

In de vroege dagen in Groningen heb ik ook veel gehad aan vroegere groepsgenoten en afdelingsgenoten: Joost, Jaap, Niek, Jochem, Wesley, bedankt voor jullie hulp en gezelligheid.

Naast de mensen in mijn dagelijks labbestaan heb ik ook enorm veel steun gehad aan de mensen die niet dagelijks bij mij in het lab hebben gestaan. Twee inspiratie bronnen zijn geweest, de collega's Stroppen. Boelo, we waren al begonnen om ideeën samen te voegen zodat we mooi onderzoek kunnen gaan doen en ik hoop dan ook dat dit ook ooit gaat lukken. Richard, mochten we ooit bevindingen doen die geld opleveren dan ben je de eerste die het hoort om winst te komen maken en ons in

boekenbonnen uit te betalen. Het is dan ook een eer om jullie als paranimfen te mogen hebben.

Tevens wil ik de vrienden bedanken die ik al ken vanaf het begin van de studie chemie en van wie menigeen zich in hetzelfde promotie-schuitje bevinden. Wouter (Trp), Hendrie (3), Alex, Behnam, Gert Jan en Niels, de catanavonden, BBQs en de gezamelijke reisjes om elkaar op te zoeken overal en nergens waren altijd een feest en gezamenlijk klagen over de gang van zaken binnen de academie, begeleider en andere promotiezaken was altijd een steuntje in de rug.

Als laatste wil ik graag mijn naasten bedanken; mijn ouders, mijn broer en familie waaronder mijn schoonouders, voor de steun en toeverlaat waaronder de allergrootste steun en toeverlaat mijn vriendin. Laura, chemie in de vorm van een 'zeep-maak-cursus' i.c.m. jou assertiviteit heeft ons samengebracht. Ik heb het niet altijd willen laten zien maar zoals je hebt gemerkt waren er wat tijden van stress en bij jou vond ik altijd een troostende schouder. Jij betekend meer voor mij dan chemie ooit kan doen, ondanks dat het misschien niet altijd bleek uit de hoeveelheid tijd die ik op het lab was i.p.v. thuis.

't is mooi west…
P.

Dankwoord

Curriculum Vitae

Patrick van Rijn was born in Delfzijl (Netherlands) on the 21st of April 1981. He received his high school education from *Ommelander college* in Appingedam and obtained his degree in 1999 after which he studied chemistry at the *University of Groningen* (Netherlands). During his studies he obtained research experience in the group of Prof. dr. Ben L. Feringa and Dr. Jan H. van Esch on 'Molecular switches' (Bachelor research; 2002), in the group of Dr. Jan H. van Esch on 'Amphipatic molecules with controllable curvature' (Master research; 2004-2005) and in the group of Dr. Wilhelm T.S. Huck together with Dr. Omar Azzaroni on 'Poly electrolyte polymer brushes' (Internship, *University of Cambridge*, U.K.; 2005). After obtaining his degree in 2005, he continued his master research as a PhD in the group of Prof. Dr. Jan. H. van Esch in Groningen and was continued at *Delft University of Technology* from March 2007 when the group moved there. Currently he is expanding his research experience at the *Rheinisch-Westfälische Technische Hochschule* (RWTH) in Aachen in the group of Prof. Alexander Böker on Tobacco Mosaic Virus-polymer hybrid materials for functional membranes and materials.

Articles:

"Mechanically-induced Generation of Counterions inside Surface Grafted Charged Macromolecular Films: Towards Enhanced Mechanotransduction in Artificial Systems"**:** O. Azzaroni, B., Trappmann, P. van Rijn, F. Zhou, B. Kong, W. T. S. Huck*, Angew. Chem. Int. Ed.* **2006**, 45, *7440-7443*.

"Dynamic chirality, chirality transfer and aggregation behaviour of dithienylethene switches", Jaap J.D. de Jong, Patrick van Rijn, Theodora D. Tiemersma-Wegeman, Linda N. Lucas,Wesley R. Browne, Richard M. Kellogg, Kingo Uchida, Jan H. van Esch, Ben L. Feringa, *Tetrahedron,* **2008**, *64*, 8324-8335. (*special issue: 2007 Tetrahedron Prize for Creativity in Organic Chemistry. Synthetic NanoSystems and NanoMachinery. Professor Sir Fraser Stoddart*)

"Amphiphilic conjugated thiophenes for self- assembling antenna systems in water": Patrick van Rijn, Tom J. Savenije, Marc C. A. Stuart and Jan H. van Esch, *Chem. Commun.*, **2009**, *2163 - 2165*   (*highlighted in RSC special issue: "A celebration of Supramolecular Chemistry"*)

"Synthesis and Self-Assembly of a Novel Multisegment Amphiphile Leading to Microdomain Separation", Job Boekhoven, Patrick van Rijn, Aurélie M. A. Brizard, Marc C. A. Stuart and Jan H. van Esch. *Accepted to Chemical Communications.*

"Liposomes with Conjugates of a Calix[4]arene and a Gd-DOTA Derivative on the Outside Surface; an Efficient Potential Contrast Agent for Magnetic Resonance Imaging", Daniel T. Schühle, Patrick van Rijn, Sophie Laurent, Luce Vander Elst, Robert N. Muller, Marc C. A. Stuart, Jürgen Schatz, Joop A. Peters. *Accepted to Chemical Communications.*

"Self-assembly of conjugated thiophene surfactants in water", Patrick van Rijn, Danius Janeliunas, Aurélie M. A. Brizard, Marc C. A. Stuart and Jan H. van Esch. *Submitted.*

"Self-assembly of curved amphipathic oligothiophenes for defined aggregate formation", Patrick van Rijn, Aurélie M. A. Brizard, Marc. C. A. Stuart, Ger M. C. Koper and Jan H. van Esch. *Submitted.*

"Highly efficient Energy Transfer in water-soluble mixed aggregated oligothiophenes": <u>Patrick van Rijn</u>, Tom J. Savenije, Eduardo Mendes, Marc C. A. Stuart and Jan H. van Esch. *Manuscript in preparation.*

"Photo-induced charge separation in self-assembled PCBM/amphipathic oligothiophene aggregates in water": <u>Patrick van Rijn</u>, Tom J. Savenije and Jan H. van Esch. *Manuscript in preparation.*

"Amphipathic curved oligothiophene as a tool for detecting membrane curvatures by multi-chromatic fluorescent output in living cells": <u>Patrick van Rijn</u>, Marcel A. Raspe, Marc C. A. Stuart, Eric A. J. Reits and Jan H. van Esch. *Manuscript in preparation.*

Patents:
"Amphipathic curved oligothiophene as a tool for detecting membrane curvatures in biological processes in living cells": Jan H. van Esch, <u>Patrick van Rijn</u>, Marcel A. Raspe, Eric A. J. Reits. *Patent application procedure in progress.*

Conference contribution:
- Lunteren, Netherlands, Design and Synthesis, Structure and Reactivity and Biomolecular Chemistry, October **2006**, poster-presentation, "Conjugated amphiphilic surfactants for functional nano-devices".

- Wageningen, Netherlands, NanoNed Flagship meeting "Bionanosystems", December **2006**, oral presentation, "Folding and Self-Assembly of Foldamers: *towards the understanding of structure-control*".

- Harz, Germany, joined workweek meeting with the group of Prof. dr. Stefan Hecht (Max Planck institut, Muelheim), January **2007**, oral presentation, "Folding and Self-Assembly of Foldamers: *towards the understanding of structure-control*".

- Eindhoven, Netherlands, NanoNed Flagship meeting "Bionanosystems", June **2007**, oral presentation, "Self-assembled thiophene surfactants: *A possible application using fluorescence*".

- Boston, USA, American Chemical Society Meeting & Exposition, August, **2007**, poster presentation, "Amphiphilic conjugated molecules for functional nano-architectures".

- Lunteren, Netherlands, Design and Synthesis, Structure and Reactivity and Biomolecular Chemistry, October **2007**, poster presentation, "Conjugated amphiphilic surfactants for functional nano-architectures".

- Graz, Austria, July **2008**, Functional Pi-systems, poster presentation, "Conjugated amphiphilic surfactants for functional nano-architectures".

- Delft, Netherlands, October **2008**, DelftChemTech colloquium, oral presentation, "Size and Shape control with Self-Assembly: *New approach for defined functional aggregates*".

- Lunteren, Design and Synthesis, Structure and Reactivity and Biomolecular Chemistry, October **2008**, oral presentation, "Conjugated amphiphilic surfactants for functional nano-architectures".

- Lunteren, Design and Synthesis, Structure and Reactivity and Biomolecular Chemistry, October **2009**, poster presentation, "Exploiting the electronic properties of self-assembling oligothiophenes for efficient energy and charge transfer systems in water".

- Delft, Netherlands, November **2009**, NanoMina-Ned, poster presentation, "Size and Shape control with Self-Assembly: "Exploiting the electronic properties of self-assembling oligothiophenes for efficient energy and charge transfer systems in water".